



# **Model based sustainable production of biomethane**

Herstellung von Biomethan aus landwirtschaftlichen Quellen nach Kriterien der  
Ökoeffizienz

Von der Fakultät für Mathematik und Naturwissenschaften der Carl von Ossietzky  
Universität Oldenburg zur Erlangung des Grades eines

Doktors der Naturwissenschaften

angenommene Dissertation

von

Herrn Piotr Biernacki

geboren am 20. Mai 1985 in Wroclaw (Polen)

Oldenburg 2014

Gutachter: Prof. Dr. Axel Brehm

Zweitgutachter: Prof. Dr. Michael Wark

Tag der Disputation: 24. November 2014

**To my family**

Ich versichere hiermit, dass ich die vorliegende Doktorarbeit selbstständig und ohne unzulässige fremde Hilfe erbracht habe. Ich habe keine anderen als die angegebene Quellen und Hilfsmittel verwendet.

BIERNAUKI, PIOTR  
Name, Vorname

2829 127  
Matrikelnummer

EMDEN, 03.11.2019  
Ort, Datum

  
Unterschrift

Diese Dissertation wurde im Rahmen des vom Bundesministerium für Bildung und Forschung (BMBF) geförderten Projektes „*Herstellung von Biomethan aus landwirtschaftlichen Quellen nach Kriterien der Ökoeffizienz*“ (FKZ 17N1710) erstellt. Die Verantwortung für den Inhalt liegt beim Autor.

## Acknowledgement

At this point I would like to kindly thank Prof. Dr. Axel Brehm and Prof. Dr. Sven Steinigeweg for being my supervisors, for their time, support, and guidance, without which this project would not be completed.

Prof. h. c. Dr. Jürgen Reiner Rarey, who kindly accepted to review my dissertation.

Support from Dr. Frank Uhlenhut, Dipl. Ing. Ingo Stein, Dipl. Ing. Wilfried Paul, Dipl. Ing. Manfred Becker is greatly appreciated.

Discussions with Prof. Dr. Axel Borchert, Prof. Dr. Michael Schlaak, Prof. Dr. Eike Siefert, M. Sc. Preseela Satpathy and M. Sc. Christian Rojas from EUTEC Institute, Hochschule Emden/Leer are highly valued.

Work with students like M.Sc. Dirk Stolz, Dipl. Ing. S. Röefzaad and others was also fun and help, but at the same time delivering supervising experience, is here acknowledged.

Mrs. Manuela Beyer from EWE Wittmund Biogas Power Plant with her whole team, is also acknowledged for their time, support, and providing me with substrates. I would also like to thank ME. Michael Ogurek from ifak e.V. Magdeburg, and Dr. Konrad Koch from Institute of Water Quality Control at Technische Universität München for kind assistance.

## Table of contents

Acknowledgement .....	6
Index of tables .....	11
Index of figures.....	13
List of symbols.....	16
I. Summary.....	22
II. Zusammenfassung in deutscher Sprache .....	23
III. Podsumowanie w języku polskim.....	24
1) Introduction .....	26
2) Outline of the work .....	28
3) Literature review.....	30
3.1. Biomethane .....	30
3.1.1. Anaerobic digestion and methane formation .....	30
3.1.1.1. History.....	30
3.1.1.2. Anaerobic digestion process .....	32
3.1.1.2.1. Bioreactions.....	32
3.1.1.2.2. Biochemistry .....	34
3.1.1.3. Substrates.....	35
3.1.1.4. Composition .....	37
3.1.1.5. Gas upgrading.....	39
3.1.1.5.1. Carbon dioxide removal.....	42
3.1.1.5.2. 2-(Ethylamino)ethanol.....	47
3.1.1.6. Potential.....	48
3.2. Biochemical modelling of the anaerobic digestion .....	49
3.2.1. Anaerobic Digestion Model No. 1 (ADM1).....	49
3.2.1.1. Modifications to the model (ADM1xp).....	53
3.2.1.2. Kinetic constants' describing disintegration and hydrolysis's phase.....	54
3.2.2. Literature review on the ADM1's usage .....	56
3.3. Thermodynamic modelling of gas solubility .....	58

3.3.1.	Vapour-liquid phase equilibrium.....	58
3.3.2.	Physical solubility.....	61
3.3.3.	Chemical solubility .....	62
3.3.4.	The Peng-Robinson Equation of State.....	66
3.3.5.	The electrolyte Non Random Two Liquid (eNRTL) model .....	68
3.3.6.	Literature review on the eNRTL's usage .....	75
4.	Materials and methods .....	77
4.1.	Optimisation of biogas power plants through process simulation.....	77
4.1.1.	Experimental set-up.....	77
4.1.1.1.	Characterization of complex substrates.....	77
4.1.1.2.	Biogas potential measurement .....	78
4.1.2.	Continuous fermentation.....	80
4.1.2.1.	Characterization of the inoculum and substrate.....	80
4.1.2.2.	Batch experiments .....	81
4.1.2.3.	Continuous fermentation .....	81
4.1.3.	Industrial size biogas power plant .....	82
4.1.4.	Mathematical modelling and simulation .....	84
4.1.4.1.	Simulation's software .....	84
4.1.4.2.	Transferability of the experimental results to the ADM1 .....	84
4.1.4.3.	Parameters used in the modelling .....	86
4.1.4.4.	Determination of the kinetic constants.....	86
4.1.4.5.	Optimization tool .....	86
4.1.4.6.	Optimization procedure .....	87
4.1.4.7.	Determination of the common constants .....	87
4.2.	Experimental study and thermodynamic modelling of carbon dioxide absorption capturing method .....	88
4.2.1.	Experimental set-up.....	88
4.2.1.1.	Materials and solutions.....	88
4.2.1.2.	Development of a new experimental apparatus.....	89

4.2.1.3.	Measuring procedure .....	90
4.2.1.4.	Solubility calculation .....	91
4.2.2.	Thermodynamic modelling solubility .....	92
4.2.2.1.	Pure component parameters .....	92
4.2.2.2.	Binary interaction parameters.....	93
4.2.2.3.	Determined parameters.....	93
4.2.2.4.	Physical solubility .....	94
4.2.2.5.	Chemical solubility .....	94
4.2.2.6.	Reaction kinetics .....	96
4.3.	Sustainability assessment of the biomethane production .....	97
4.3.1.	Analysed system.....	98
4.3.2.	Model used in this research .....	98
4.3.3.	Pure component properties.....	98
4.3.4.	Case study.....	99
4.3.5.	Process design .....	99
5.	Results.....	100
5.1.	<i>“Application of Anaerobic Digestion Model No.1 for describing anaerobic digestion of grass, maize, green weed silage, and industrial glycerine”</i> .....	100
5.1.1.	Characterization of the reactors initial state .....	100
5.1.2.	Characterization of the complex substrates .....	100
5.1.3.	Batch experiments and simulation .....	102
5.1.4.	Sensitivity analysis.....	105
5.2.	<i>“Application of Anaerobic Digestion Model No. 1 for describing an existing biogas power plant”</i> .....	107
5.2.1.	Characterization of the reactors initial state and an existing biogas power plant 107	
5.2.2.	Analysis of the substrates used .....	107
5.2.3.	Batch results with the common hydrolysis constants .....	108
5.2.4.	Application of the common hydrolysis constants .....	113
5.2.5.	Industrial size biogas power plant simulation .....	113

5.3.	<i>“Continuous mesophilic anaerobic digestion of manure and rape oilcake - modelling with ADM1”</i>	117
5.3.1.	Substrate composition	117
5.3.2.	Batch fermentation	119
5.3.3.	Continuous fermentation and simulation	121
5.4.	<i>“Experimental Measurements and Thermodynamic Modelling of biogas upgrading process with use of 2-(Ethylamino)ethanol”</i>	124
5.4.1.	Experimental results	124
5.4.1.1.	Assessment of the apparatus precision	124
5.4.1.2.	Solvent characteristics	125
5.4.1.2.1.	Density	125
5.4.1.2.2.	Mixtures liquid heat capacity	125
5.4.1.3.	Results of the solubility measurements	126
5.4.2.	Thermodynamic modelling	128
5.4.2.1.	Carbamate stability parameters	128
5.4.2.2.	Heat capacity parameters	128
5.4.2.3.	NRTL’s interaction binary parameters	130
5.5.	<i>“Sustainability assessment of the biomethane production”</i>	132
5.5.1.	Ecological assessment	132
5.5.2.	Social analysis	133
5.5.3.	Economical evaluation of the biomethane upgrading facility	136
6.	Conclusion and Recommendations	138
7.	Recommendations for future work	141
8.	References	142
9.	Appendix	162
9.1.	Appendix A	162
9.2.	Appendix B	168
9.3.	Appendix C	171
9.4.	Appendix D	194

## Index of tables

Table 1 Specification of biogas power plants in Germany in year 2000 (Deublein & Steinhauser, 2011).	31
Table 2. Pure component properties (Thermodynamics Research Center, 2014).	37
Table 3. General properties of biogas (Deublein & Steinhauser, 2011).	37
Table 4. Content and effect of typical impurities (Deublein & Steinhauser, 2011).	38
Table 5. Desulfurization techniques (Deublein & Steinhauser, 2011).	41
Table 6. <i>Biogas qualities required for different applications in Europe</i> (Deublein & Steinhauser, 2011; Franke, 2007; Keicher, et al., 2004; Keicher, et al., 2006; Reher, 2003; Schmack & Nusko, 2006)	43
Table 7. Biogas upgrading methods (Deublein & Steinhauser, 2011).	44
Table 8. Solubility of different gases in water in different temperatures (Deublein & Steinhauser, 2011).	45
Table 9. Kinetic constant values found in the literature for mesophilic digestion of different substrates.	55
Table 10. Theoretical oxygen demand (ThOD) of different fractions [45].	84
Table 11. Degradability rate and methane content of analysed substrates [160].	86
Table 12. Coefficients for Henry's constant (Aspen Technology Inc., 2008).	92
Table 13. Binary interaction parameters for water and carbon dioxide (Chen & Evans, 1986).	93
Table 14. Equilibrium constants for reactions 90, 93-97 (without 94).	96
Table 15. The pre-exponential factor ( $k$ ) and activation energy ( $E$ ) parameters for reduced power law.	97
Table 16. Characteristics of the examined substrates.	101
Table 17. Optimized disintegration and hydrolysis kinetic constants according to the downhill simplex methods algorithm from Nelder and Mead (Nelder & Mead, 1965).	102
Table 18. Correlation between literature and calculated values for methane content.	105
Table 19. Characteristics of the examined substrates.	108
Table 20. Optimized disintegration and hydrolysis kinetic constants according to the downhill simplex methods algorithm from Nelder and Mead (Nelder & Mead, 1965).	109
Table 21. Optimized disintegration kinetic constants, for CHC approach, according to the downhill simplex methods algorithm from Nelder and Mead (Nelder & Mead, 1965).	109
Table 22. Characteristics of inoculum obtained from EWE Wittmund Biogas Power Plant (EWE Biogas GmbH & Co. KG., 2011) used for continuous fermentation.	117

Table 23. Characteristics of substrates used for continuous fermentation. ....	117
Table 24. Parameters used in the modelling.....	118
Table 25. Optimized disintegration kinetic constants, according to the downhill simplex methods algorithm from Nelder and Mead (Nelder & Mead, 1965). ....	120
Table 26. CO <sub>2</sub> solubility in 2-(Ethylamino)ethanol (EAE).....	127
Table 27. Temperature dependent coefficients of ideal gas heat capacity equation (CPIG). .....	129
Table 28. NRTL's binary interaction parameters obtained with use of ASPEN Plus® V8.0 Data Regression System (DRS). ....	130
Table 29. Marine biodegradability and ecotoxicity of 10 amines(Eide-Haugmo, et al., 2012). .....	133
Table 30. Hazardous substances' safety. ....	134
Table 31. Calculation results of the EWE Wittmund biogas' upgrading. ....	137

## Index of figures

Figure 1. Ensiling conservation method (St-Pierre, 2013).....	37
Figure 2. Typical chemical absorption plant.....	47
Figure 3. Conversion processes occurring during the anaerobic digestion (Schoen, 2009). .	50
Figure 4. Biochemical processes included in Anaerobic Digestion Model No. 1 (Batstone, et al., 2002). .....	53
Figure 5. <i>PT</i> - diagram, representing triple point, and change phase curves (Gmehling, et al., 2012).....	59
Figure 6. Carbon dioxide solubility in methanol ( - physical absorption) and 30 mass %aqueous monoethanolamine solution ( - chemical absorption) at $T = 313.15K$ (DDBST GmbH, 2014; Gmehling, et al., 2012) .....	63
Figure 7. Like-ion repulsion and electroneutrality assumption (Gmehling, et al., 2012).....	72
Figure 8. Weender analysis with van Soest extension (Koch, et al., 2010). .....	78
Figure 9. ANKOM wireless gas production system. ....	79
Figure 10. Water baths used for conducting anaerobic digestion experiments. ....	80
Figure 11, Continuous fermentation lab-scale plant.....	82
Figure 12. EWE Wittmund Biogas Power Plant (EWE Biogas GmbH & Co. KG., 2011). .....	83
Figure 13. Apparatus for measuring gas solubility. ....	90
Figure 14. Measuring procedure presented base on pressure change in the 2nd reactor. ....	91
Figure 15. Structure of the sustainability assessment applied in this research.....	97
Figure 16. Comparison of the experimental cumulative biogas production from grass silage to simulation results, where the ADM1 default values for disintegration and hydrolysis kinetic constants were used.....	103
Figure 17. Comparison of the experimental cumulative biogas production from maize silage to simulation results, where the ADM1 default values for disintegration and hydrolysis kinetic constants were used.....	103
Figure 18. Comparison of the experimental cumulative biogas production from green weed silage to simulation results, where the ADM1 default values for disintegration and hydrolysis kinetic constants were used.....	104
Figure 19. Comparison of the experimental cumulative biogas production from industrial glycerin to simulation results, where the ADM1 default values for disintegration and hydrolysis kinetic constants were used.....	104
Figure 20. Disintegration ( $k_{dis}$ ) and hydrolysis ( $k_{hyd}$ ) kinetic constants sensitivity analysis for maize silage, where the lowest error represents the best correlation between simulated and experimental results. ....	106

Figure 21. Two-point charts representing the proceedings of the optimization tool, where the starting points were chosen to be a boundary values. ....	106
Figure 22. Comparison of the experimental cumulative biogas production from grass silage to simulation results, where the “IHC” indicates individually determined all kinetic constants, whereas the common hydrolysis phase constants and an individual determined kinetic constant for disintegration are used for “CHC” . ....	110
Figure 23. Comparison of the experimental cumulative biogas production from maize silage to simulation results, where the “IHC” indicates individually determined all kinetic constants, whereas the common hydrolysis phase constants and an individual determined kinetic constant for disintegration are used for “CHC” . ....	110
Figure 24. Comparison of the experimental cumulative biogas production from industrial glycerine to simulation results, where the “IHC” indicates individually determined all kinetic constants, whereas the common hydrolysis phase constants and an individual determined kinetic constant for disintegration are used for “CHC” . ....	111
Figure 25. Comparison of the experimental cumulative biogas production from green weed silage to simulation results, where the “IHC” indicates individually determined all kinetic constants, whereas the common hydrolysis phase constants and an individual determined kinetic constant for disintegration are used for “CHC” . ....	111
Figure 26. Comparison of the experimental cumulative biogas production from organic waste (food waste) to simulation results, where the “IHC” indicates individually determined all kinetic constants, whereas the common hydrolysis phase constants and an individual determined kinetic constant for disintegration are used for “CHC” . ....	112
Figure 27. Comparison of the experimental cumulative biogas production from cattle manure to simulation results, where the “IHC” indicates individually determined all kinetic constants, whereas the common hydrolysis phase constants and an individual determined kinetic constant for disintegration are used for “CHC” . ....	112
Figure 28. Validation of determined common hydrolysis constants for chicken manure. ....	113
Figure 29. The model of EWE Wittmund Biogas Power Plant (EWE Biogas GmbH & Co. KG., 2011) prepared in SIMBA ® simulation software (ifak system GmbH, 2005) by Rojas et al. (Rojas, et al., 2010) and modified for this research. ....	115
Figure 30. Assessment of the simulation results against the industrial size EWE Wittmund Biogas Power Plant (EWE Biogas GmbH & Co. KG., 2011), where the “IHC” indicates individually determined all kinetic constants, whereas the common hydrolysis phase constants and an individual determined kinetic constant for disintegration are used for “CHC” . ....	116
Figure 31. Assessment of the methane content in biogas from the industrial size EWE Wittmund Biogas Power Plant (EWE Biogas GmbH & Co. KG., 2011), and in two	

simulation methods, where the “IHC” indicates individually determined all kinetic constants, whereas the common hydrolysis phase constants and an individual determined kinetic constant for disintegration are used for “CHC” .	116
Figure 32. Experimental batch anaerobic digestion and simulation of rapeseed oilcake. ....	119
Figure 33. Experimental batch anaerobic digestion and simulation of rapeseed oilcake. ....	120
Figure 34. Total biogas production during the continuous fermentation. ....	122
Figure 35. Organic loading rate and mass fraction of organic dry mass in the digested sludge. ....	122
Figure 36. Methane content in the biogas formed. ....	123
Figure 37. The pH and FOS/TAC ratio of the reactor’s effluent. ....	123
Figure 38. Concentration of the ammonium in the effluent. ....	124
Figure 39. Comparison of the experimental results to the literature found at Dortmund Data Bank (DDBST GmbH, 2014) on solubility of CO <sub>2</sub> in water at a temperature of 19.8°C, pressure range of 5 up to 12 bar. ....	125
Figure 40. Experimental results of pure compound and mixture’s liquid heat capacity, compared to the literature results. ....	126
Figure 41. Modelling mixture’s liquid heat capacity, and comparison to the experimental results. ....	130
Figure 42. Modelling CO <sub>2</sub> absorption in aqueous 2-(Ethylamino)ethanol solutions at 293 K, and comparison to the experimental results. ....	131
Figure 43. Modelling CO <sub>2</sub> absorption in aqueous 2-(Ethylamino)ethanol solutions at 313.15 K, and comparison to the experimental results. ....	131
Figure 44. Modelling CO <sub>2</sub> absorption in aqueous 2-(Ethylamino)ethanol solutions at 333.15 K, and comparison to the experimental results. ....	132

## List of symbols

$a$	Attractive parameter in cubic equations of state	$\text{J m}^3 \text{ mol}^{-2}$
$a_i$	Stoichiometric coefficient of components $i$ in the reaction equation, used for reduced power law expression	
$a_{ij}, b_{ij}, c_{ij}, d_{ij}$	Binary or group interaction parameter in local composition model (NRTL)	
$A, B, C, \dots$	Constants in pure component property correlations	
$ADF$	Acid detergent fibre in the Weender analyse with van Soest extension	% DM
$ADL$	Acid detergent lignin in the Weender analyse with van Soest extension	% DM
$A_m$	Parameter in Debye-Hueckel equation	$\text{kg}^{0.5} \text{ mol}^{0.5}$
$A_\phi$	Parameter in Pitzer-Debye-Hückel term	
$b$	Repulsive parameter in cubic equations of state	$\text{m}^3 \text{ mol}^{-1}$
$c$	Volume concentration	$\text{mol m}^{-3}$
$c_i(r)$	Volume concentration of ionic species in a volume element at distance $r$ from the centre	$\text{mol m}^{-3}$
$c_i^{(0)}$	Volume concentration of ionic species	$\text{mol m}^{-3}$
$d$	degradability rate of organic mass	mass %
$D$	Temperature dependent dielectric constant	
$DM$	Dry mass	mass %
$e$	Elementary charge $e = 1.602189 \cdot 10^{-19} \text{ C}$	C

$E$	Activation energy in reduced power law expression	cal mol <sup>-1</sup>
$f$	Stoichiometric f-factors describing disintegration phase in the Anaerobic Digestion Model No. 1	kg <sub>COD</sub> kg <sub>COD</sub> <sup>-1</sup>
$f_i$	Fugacity of component $i$	Pa
$f_P$	Decayed biomass factor in the Anaerobic Digestion Model No. 1	
$g$	Specific Gibbs energy	J mol <sup>-1</sup>
$g^l$	The specific Gibbs energy of boiling liquid	J mol <sup>-1</sup>
$g^v$	The specific Gibbs energy of saturated vapour	J mol <sup>-1</sup>
$H_{ij}$	Henry constant of component $i$ in solvent $j$	PA
$I_n$	Inhibition, e.g. hydrogen inhibition on acetate groups etc.	
$k$	Boltzmann's constant; $k = 1.38048 \cdot 10^{-23}$	J K <sup>-1</sup>
$k_p$	Pre-exponential factor in reduced power law expression	$\frac{\left(\frac{\text{kgmole} \cdot \text{K}^{-n}}{\text{sec} \cdot \text{m}^3}\right)}{\left(\frac{\text{kgmole}}{\text{m}^3}\right)}$
$k_{Dis}$	Kinetic constant describing disintegration phase in the Anaerobic Digestion Model No. 1	d <sup>-1</sup>
$k_{hyd\_Ch}$	Kinetic constant describing hydrolysis phase of the carbohydrates in the Anaerobic Digestion Model No. 1	d <sup>-1</sup>
$k_{hyd\_Pr}$	Kinetic constant describing hydrolysis phase of the proteins in the Anaerobic Digestion Model No. 1	d <sup>-1</sup>
$k_{hyd\_Li}$	Kinetic constant describing hydrolysis phase of the lipids in the Anaerobic Digestion Model No. 1	d <sup>-1</sup>

$k_L$	Dynamic gas-liquid transfer coefficient	$d^{-1}$
$k_m$	Maximum specific uptake	$kg_{COD_{Sc}} kg_{COD_X}^{-1} d^{-1}$
$K$	Chemical equilibrium constant	
$K_{H,CO_2}$	Henry's law equilibrium constant	$kmol m^{-3} bar^{-1}$
$K_S$	Half saturation coefficient	$kg_{COD} m^{-3}$
$I$	Ionic strength	$mol kg^{-1}$
$n_i$	Number of moles of component $i$	$mol$
$N_A$	Avogadro's number	
	$N_A = 6.023 \cdot 10^{23}$	
$NDF$	Neutral detergent fibre in the Weender analyse with van Soest extension	% DM
$NfE$	Nitrogen free extracts in the Weender analyse with van Soest extension	% DM
$oDM$	Organic dry mass	% DM
$p_i$	Partial pressure of component $i$	bar
$P$	Total pressure	Pa
$P_i^s$	Vapour pressure of component $i$	Pa
$Q$	Flow	$m^3 d^{-1}$
$q$	Vapour fraction	
$r_i$	Ionic radius	
	$r_{\neq} = 3 \cdot 10^{-10} m$	
$R$	Universal gas constant	$J mol^{-1} K^{-1}$

$$R = 8.314471 \text{ J mol}^{-1} \text{ K}^{-1} = 1.98721 \text{ cal mol}^{-1} \text{ K}^{-1}$$

<i>RF</i>	Raw fibre content in the Weender analyse	% DM
<i>RL</i>	Raw lipid content in the Weender analyse	% DM
<i>RP</i>	Raw protein content in the Weender analyse	% DM
<i>S</i>	Entropy	J K <sup>-1</sup>
<i>S<sub>Aa</sub></i>	Amino acids fraction in the Anaerobic Digestion Model No. 1	kg <sub>COD</sub> m <sup>-3</sup>
<i>S<sub>C</sub></i>	Substrate concentration	kg <sub>COD<sub>Sc</sub></sub> m <sup>-3</sup>
<i>S<sub>Fa</sub></i>	Long chain fatty acids fraction in the Anaerobic Digestion Model No. 1	kg <sub>COD</sub> m <sup>-3</sup>
<i>S<sub>gas,i</sub></i>	Gas concentration	kmol m <sup>-3</sup>
<i>S<sub>i</sub></i>	Component concentration	kg <sub>COD</sub> m <sup>-3</sup>
<i>S<sub>NH4</sub></i>	Fraction describing ammonium ions in the Anaerobic Digestion Model No. 1	kg N m <sup>-3</sup>
<i>S<sub>Su</sub></i>	Monosaccharides fraction in the Anaerobic Digestion Model No. 1	kg <sub>COD</sub> m <sup>-3</sup>
<i>T</i>	Absolute temperature	K
<i>ThOD</i>	Theoretical oxygen demand	kg <sub>O2</sub> kg <sub>DM</sub> <sup>-1</sup>
<i>v</i>	Specific volume	m <sup>3</sup> mol <sup>-1</sup>
<i>V</i>	Volume	m <sup>3</sup>
<i>V<sub>lig</sub></i>	Volume of the reactor	m <sup>3</sup>
<i>VS</i>	Volatile solids	g L <sup>-1</sup>
<i>w</i>	Weighting factor in objective functions	
<i>x<sub>i</sub></i>	Mole fraction of component <i>i</i> in the liquid phase	

$X$	Substrate specific biomass concentration	$\text{kg}_{\text{COD}_X} \text{m}^{-3}$
$X_C$	Composite fraction in the Anaerobic Digestion Model No. 1	$\text{kg}_{\text{COD}} \text{m}^{-3}$
$X_{Ch}$	Carbohydrates fraction of the Anaerobic Digestion Model No. 1	$\text{kg}_{\text{COD}} \text{m}^{-3}$
$X_i$	Inert fraction in the Anaerobic Digestion Model No. 1	$\text{kg}_{\text{COD}} \text{m}^{-3}$
$X_p$	Inert decay products fraction in the Anaerobic Digestion Model No. 1	$\text{kg}_{\text{COD}} \text{m}^{-3}$
$X_{Pr}$	Protein fraction in the Anaerobic Digestion Model No. 1	$\text{kg}_{\text{COD}} \text{m}^{-3}$
$X_{Li}$	Lipids fraction in the Anaerobic Digestion Model No. 1	$\text{kg}_{\text{COD}} \text{m}^{-3}$
$y_i$	Mole fraction of component $i$ in the vapour phase	
$z$	Compressibility factor	
$z_i$	Charge of ion $i$	C
$\alpha_{ij}$	Nonrandomness parameter in the NRTL equation	
$\gamma_i$	Activity coefficient of component $i$	
$\Delta_{Born} g^E$	Born term for regarding the dielectricity constant of the solvent	$\text{J mol}^{-1}$
$\Delta g_f^0$	Standard Gibbs energy of formation	$\text{J mol}^{-1}$
$\Delta g_R^0$	Standard Gibbs energy of reaction	$\text{J mol}^{-1}$
$\Delta G_f'$	Gibbs free energy	$\text{kJ mol}^{-1}$
$\varepsilon$	Relative dielectricity constant	$\text{A}^2 \text{s}^4 \text{kg}^{-1} \text{m}^{-3}$

$\Theta_{ij}$	Local concentration of species $i$ around species $j$	
$\mu_i$	Chemical potential of component $i$	$\text{J mol}^{-1}$
$\nu_i$	Stoichiometric coefficient of component $i$	
$\rho$	Substrate uptake	$\text{kg}_{\text{COD\_Sc}} \text{m}^{-3} \text{d}^{-1}$
$\rho_j$	Kinetic rate for process $j$	$\text{kg}_{\text{COD}} \text{m}^{-3} \text{d}^{-1}$
$\rho_{T,i}$	Kinetic transfer rate	$\text{kmol m}^{-3} \text{d}^{-1}$
$\tau_{ij}$	Temperature dependent binary interaction parameter in the NRTL equation	
$\varphi_i$	Fugacity coefficient of component $i$	
$\varphi^{el}(r)$	The electric potential at distance $r$ from the centre	$\text{V}$
$\omega$	Acentric factor	

## I. Summary

Renewable energy sources became significant topic of research over last years, due to increased interest in environmental issues. As an already identified solution to directly substitute e.g. natural gas is biomethane, obtained through anaerobic digestion of biomass. Therefore the main intention of this dissertation was to evaluate sustainable production of biomethane. Biogas production, together with its upgrading was represented via mathematical modelling, thus enabling designing of an optimal plant, considering sustainability aspects. To achieve this goal, widely acknowledged models like Anaerobic Digestion Model No.1 (ADM1), describing anaerobic digestion, and electrolyte Non-Random Two Liquid Model (eNRTL), for gas purification, were utilized. In addition to that, experimental data on batch anaerobic digestion of different substrates like manures (cattle and chicken), organic waste, industrial glycerine, silages (green weed, maize, grass) rapeseed oilcake were obtained. Following this, the continuous fermentation of cattle manure and rapeseed oilcake was performed to verify models applicability. Moreover, experimental data of carbon dioxide solubility (chemical and physical absorption) in 2-(Ethylamino)ethanol (CAS: 110-73-6) were measured with use of apparatus developed for this dissertation. The experimental results were used to determine kinetic constants describing disintegration and hydrolysis phases, together with binary energy interaction parameters for ADM1 and eNRTL respectively. Subsequently, ADM1 with updated parameters was proved to successfully describe anaerobic digestion occurring at existing, industrial scale EWE Biogas Power Plant (2 reactors, each 3 500 m<sup>3</sup>). This plant was theoretically optimized later in this research to biomethane power plant with the use of mathematical modelling, and additionally the economical, social and ecological criteria were used to search for the optimal alkanolamine applied for biogas upgrading. As a consequence, 2-(Ethylamino)ethanol (EAE), together with monoethanolamine (MEA) were identified as a sustainable reagents for carbon dioxide capture. Finally, a model based optimization of biomethane power plants with use of mathematical modelling was successfully achieved, in accordance with the sustainability requirements.

## II. Zusammenfassung in deutscher Sprache

Innerhalb der letzten Jahre sind erneuerbare Energiequellen zu einem wichtigen Themenfeld der Forschung geworden. Nicht zuletzt ist dies auf das zunehmende Interesse an umweltrelevanten Fragestellungen im Kontext zur Endlichkeit fossiler Energiequellen und der mit deren Verbrauch verbundenen CO<sub>2</sub>-Problematik zurückzuführen. Eine als Stand der Technik zu bezeichnende Lösung zur Reduzierung des fossilen Energieverbrauchs ist es, Erdgas durch Biomethane zu ersetzen. Angelehnt an diesen Themenkomplex war das Ziel dieser Dissertation war die „*ökoeffiziente Herstellung von Biomethan*“. Hierbei wurden die Biogasproduktion sowie die Biogasaufbereitung mit Hilfe von mathematischer Modellierung dargestellt. Auf dieser Grundlage wurde unter Berücksichtigung von Nachhaltigkeitsaspekten das Anlagenkonzept von Biogasanlagen verbessert. Verwendet wurden dabei das in der Forschung anerkannte Anaerobic Digestion Model Nr. 1 (ADM1) zur Beschreibung der anaeroben Vergärung sowie das electrolyte non-random two liquid Modell (eNRTL) für die Gasreinigung. Darüber hinaus wurden auf Grundlage von Batchversuchen experimentelle Daten zur Vergärung von Rindergülle, Hühnermist, organischen Abfällen, Industrieglycerin, grüner Rübensilage, Maissilage, Grassilage und Rapsölkuchen erhoben und ausgewertet. Diese und die Ergebnisse einer kontinuierlichen Fermentation von Rindergülle und Rapsölkuchen wurden dazu genutzt das mathematische Modell zu validieren. Zusätzlich wurden Experimente zur Löslichkeit (chemische und physikalische Absorption) von Kohlendioxid in einer wässrigen Lösung von 2-(Ethylamino)ethanol (CAS: 110-73-6) durchgeführt. Die Apparatur zur Durchführung dieser Experimente wurde eigens für diese Dissertation entwickelt und gebaut. Auf Basis dieser Ergebnisse wurden die kinetischen Konstanten der Hydrolyse und Desintegration in ADM1 adaptiert sowie die binary interaction energy parameters des eNRTL-Modells bestimmt. Des Weiteren konnte nachgewiesen werden, dass das adaptierte ADM1 Modell dazu in der Lage ist die anaerobe Vergärung einer Biogasanlage im Industriemaßstab (2 Reaktoren mit je 3.500 m<sup>3</sup>, EWE) abzubilden. Diese Biogasanlage wurde im weiteren Verlauf modellbasiert und unter Berücksichtigung von ökonomischen, sozialen und ökologischen Aspekten bei der Evaluierung des idealen Alkanolamins zur Gasaufbereitung optimiert. Auf Grundlage dieser Ergebnisse konnte schließlich ein Modell zur Optimierung von Biogasanlagen erstellt werden, mit dessen Hilfe die nachhaltige Erzeugung von Biogas verbessert wird. Als Konsequenz wurden 2-(Ethylamino)ethanol (EAE) und Monoethanolamin (MEA) als nachhaltiges Absorptionsmittel zur Abtrennung von CO<sub>2</sub> aus Biogas identifiziert. Auf Grundlage der Ergebnisse konnte schließlich eine modellbasierte Optimierung einer Biogasanlage erreicht werden, sowie Richtlinien zur nachhaltigen Weiterentwicklung entworfen werden.

### III. Podsumowanie w języku polskim

Odnawialne źródła energii stały się znaczącym tematem badań w ciągu ostatnich lat, ze względu na wzrost zainteresowania kwestiami środowiskowymi. Jednym z zidentyfikowanych już rozwiązań, dzięki którym można bezpośrednio zastąpić np. gaz ziemny, jest uzyskiwany w procesie beztlenowej fermentacji biomasy bio-metan. Mając to na uwadze, celem pracy doktorskiej było przygotowanie i analiza „*eko-wydajnych zakładów produkcji bio-metanu*”, gdzie produkcja jest prowadzona z jednej strony zgodnie z założeniami zrównoważonego rozwoju, a z drugiej, jej wydajność jest zoptymalizowana poprzez symulacje oparte na matematycznych modelach. Żeby sprostać postawionemu celowi, zostały wykorzystane dwa powszechnie uznane i zaakceptowane modele matematyczne: Anaerobic Digestion Model No. 1 (ADM1) oraz electrolyte Non-Random Two Liquid Model (eNRTL). Model ADM1 opisuje formowanie biogazu, natomiast model eNRTL jest wykorzystany przy ulepszaniu biogazu do bio-metanu.

W ramach niniejszej pracy doświadczalnie został przeanalizowany beztlenowy rozkład w systemie wsadowym (batch) różnych popularnych substratów, takich jak: gnojowica (kurza, krowia), organiczne odpady, przemysłowa gliceryna, kiszonka (kukurydziana, z trawy, z zielonego zboża). Dodatkowo została przeprowadzona ciągła fermentacja gnojowicy krowiej z wtyłokami rzepakowymi w celu weryfikacji modelu matematycznego. Dane eksperymentalne rozpuszczalności dwutlenku węgla (chemiczna oraz fizyczna absorpcja) w wodnych roztworach 2-(Ethylamino) etanolu (CAS 110-73-6) zostały wyznaczone przez wykorzystanie urządzeń pomiarowych zaprojektowanych i skonstruowanych w ramach prowadzonych badań. Dane eksperymentalne z beztlenowego rozkładu substratów zostały wykorzystane do optymalizacji modelu ADM1, gdzie stałe kinetyczne, opisujące fazę dezintegracji oraz fazę hydrolizy węglowodanów, białek i tłuszczu, zostały zaktualizowane. Dane eksperymentalne dotyczące absorpcji dwutlenku węgla, zostały wykorzystane do wyznaczenia *binary energy interaction parameters* niezbędnych dla modelu eNRTL.

Następnie wykazano, że ADM1 z zaktualizowanymi parametrami, jest w stanie dobrze przedstawić beztlenowy rozkład zachodzący w istniejącej biogazowni (EWE Biogas Power Plant, Wittmund, Dolna Saksonia, Niemcy) o przemysłowych rozmiarach (2 reaktory fermentacyjne o objętości 3 500 m<sup>3</sup>). W dalszej części badań, optymalizacja biogazowni EWE Biogas Power Plant do zakładu wytwarzania bio-metanu została przeprowadzona przy użyciu matematycznej symulacji. Jako metoda ulepszania biogazu do bio-metanu została wybrana chemiczna absorpcja z wykorzystaniem związków amin. Wybór związków amin został przeprowadzony na podstawie kryteriów ekonomicznych, społecznych oraz ekologicznych zgodnych z założeniami i wytycznymi polityki zrównoważonego rozwoju. W

konsekwencji, 2-(etyloamino) etanol (EAE), wraz z monoetanolaminą (MEA) zostały zidentyfikowane jako wydajne reagenty do usuwania dwutlenku węgla z biogazu. Podsumowując, optymalizacja zakładów wytwarzania bio-metanu przy wykorzystaniu matematycznego modelowania jest możliwa do osiągnięcia, z zachowaniem wytycznych polityki zrównoważonego rozwoju.

## 1) **Introduction**

The mathematical modelling is intended to precisely predict behaviour of a system, concurrently significantly reducing amount of experiments necessary prior to accurate description of the system like e.g. phase equilibrium or anaerobic digestion (Gmehling, et al., 2012; Eladawy, 2005). If an experimental approach was the only method possible for describing a 10-component system at a constant pressure in 10 mol% - steps, and assuming that 10 data points were to be acquired per working day, the required 92378 data points for precise description of the system, will be acquired in ~37 years (Gmehling, et al., 2012; Novak, et al., 1987). As a consequence the mathematical modelling, an efficient method for finding the optimal configuration of a plant, is gaining the appreciation among engineers. Therefore a new experimental data, determination of parameters' values, models' optimizations, along with further proving of the mathematical modelling against existing plants is required for precise and efficient application of the numerical simulations (Gmehling, et al., 2012; Eladawy, 2005; Novak, et al., 1987; Austgen, 1989; Schoen, 2009).

Renewable energy sources became significant topic of research over last years, due to increased interest in environmental issues. An already identified solution to directly substitute natural gas or liquefied petroleum gas is biogas, since it can be further upgraded to become clean vehicle fuel, send to the gas grid or can be directly utilized in combined heat and power units (CHP). Substrates used for biogas production through anaerobic digestion, like manures and organic wastes, are an additional advantage of biogas application over conventional energy sources, since biogas production is also a waste treatment technology. Taking under consideration all benefits coming from biogas production, it is not a surprise that number of biogas plants is growing. Moreover, biogas upgrading is achieved with different techniques like pressure swing adsorption, water scrubbing or amine washing, which are applied to remove carbon dioxide, and allow maximal methane slippage (Deublein & Steinhauser, 2011; Weiland, 2006). Since amine scrubbing is the most technically and commercially mature method, which can be easily retrofitted to an existing plant (Kohl & Nielsen, 1997), and according to Rochelle (Rochelle, 2009) in 2030 it probably will be the dominant method applied for coal-fired power plants, amine scrubbing was selected for this research.

As a consequence, there is a need of a tool for precise design of biomethane plants, ensuring an optimal usage of available substrates, along with identifying potential of optimization of existing biogas power plants to biomethane plants, and ensuring optimal biogas upgrading. Consequently, a reliable simulation model, based on bio-chemical

fundamentals is necessary for predicting biogas formation and a thermodynamic model is required for correct representation of vapour – liquid phase equilibrium, necessary for accurate calculation of gas solubility. In order to ensure that a model is useful also for plant operators, a widely accepted model should be the basis of model development. The primary goal is to improve a model already applied in practice with respect to the reliable calculation of digester dynamics for a wide range of substrates. Therefore it was decided to make use of a common model and to analyse the agreement between experimental and calculated data. This analysis shows capabilities and limitations of an established model and gives information about necessary improvements. In the current study, a reliable model for anaerobic digestion of different substrates and their mixtures was developed based on the Anaerobic Digestion Model No. 1 (ADM1) developed in 2002 by International Water Association's (IWA) Task Group (Batstone, et al., 2002). It was shown that ADM1 was capable of describing biogas production rate and composition without major changes to the model structure. Nevertheless, improvement of parameters was necessary since the initial biomass disintegration and hydrolysis phase was not reflected adequately for different substrates.

On the other side, for correct description of the carbon capture with amines scrubbing physical and chemical solubility needs to be considered. In the research physical solubility is calculated with use of the activity coefficients calculated with electrolyte-Non Random Two Liquid Model (eNRTL) (Chen & Evans, 1986), because of its common applicability for other alkanolamines. On the other hand, chemical absorption is represented via chemical equilibria together with reaction kinetics and mass transfer developed within this research in accordance to literature (Austgen, 1989). In addition to that, as an alkanolamine applied for carbon dioxide removal 2-(Ethylamino)ethanol (EAE; CAS: 110-73-6) is proved, which is an interesting alternative to commonly employed amines, due to its features like lower corrosion rate (in comparison to MEA), and the most substrate for its' production may be bio-ethanol(Mimura, et al., 1995; Mimura, et al., 1997; Mimura, et al., 1998; Suda, et al., 1996; Sutar, et al., 2012). On the top of that, the ecological, social and economical efficiency of biogas upgrading is exercised, and the result confirmed EAE as an interesting alternative.

## 2) **Outline of the work**

The dissertation "*Model based sustainable production of biomethane*" consists of 9 chapters. Following introduction (chapter 1) and outline of this dissertation (chapter 2), the literature overview necessary for understanding the concept and work completed upon this research is prepared (chapter 3). Subsequently is presented methodology applied in this research, along with materials utilized (chapter 4). Outcome of this dissertation is explained and discussed in chapter 5, which structure's is adjusted to the scientific publications. Finally the dissertation is summarized in chapter 6. Results of this dissertation were presented to the scientific community via publications, and oral or poster presentations on conferences summarized below:

- **Scientific publications:**

- P. Biernacki, S. Steinigeweg, A. Borchert, E. Siefert, F. Uhlentut, I. Stein and M. Wichern, "Modellbasierte Optimierung von Biogasanlagen," in Biogas Innovationskongress., Osnabrueck, 2011. ISBN 978-3-9813776-1-3.
- P. Biernacki, S. Steinigeweg, A. Borchert and F. Uhlentut, "Application of Anaerobic Digestion Model No. 1 for describing anaerobic digestion of grass, maize, green weed silage, and industrial glycerine," *Bioresource Technology*, vol. 127, pp. 188-194, 2013.
- P. Biernacki, S. Steinigeweg, A. Borchert, F. Uhlentut and I. Stein, "Model based optimization of biomethane plants," in International Conference of Agricultural Engineering, CIGR-AgENG, Valencia, 2012. ISBN-10: 84-615-9928-4.
- P. Biernacki, S. Steinigeweg, A. Borchert, F. Uhlentut and A. Brehm, "Application of Anaerobic Digestion Model No. 1 for describing existing biogas power plant," *Biomass & Bioenergy*, vol. 39, no. 2, pp. 405-409, 2013.
- S. Jablonski, P. Biernacki, S. Steinigeweg and M. Lukaszewicz, "Continuous mesophilic anaerobic digestion of manure and rape oilcake - modelling with ADM1," Submitted to *Bioresource Technology*.
- P. Biernacki, S. Steinigeweg, W. Paul and A. Brehm, "Experimental Measurements and Thermodynamic Modelling of Carbon Dioxide Capture with use of 2-(Ethylamino)Ethanol," Submitted to *Journal of Chemical Engineering Data*.
- P. Biernacki, S. Steinigeweg, W. Paul and A. Brehm, "Eco-efficient production of biomethane," Submitted to *Industrial & Engineering Chemistry Research Journal*.

- **Oral presentations:**

- P. Biernacki, S. Steinigeweg, A. Borchert, F. Uhlenhut and A. Brehm, "Model based optimization of biomethane plants," in SIMBA-Treffen und Biogas-Workshop, Leipzig, 2013.
- P. Biernacki, S. Steinigeweg, A. Borchert and F. Uhlenhut, "Modellbasierte Optimierung von Biomethaneanlagen," in Fachseminar BIOGAS-Analytik, Emden, 2013.
- P. Biernacki, S. Steinigeweg, A. Borchert and F. Uhlenhut, "Model based optimization of biomethane plants," in International Conference of Agricultural Engineering CIGR-AgEng, Valencia, 2013.
- P. Biernacki, S. Steinigeweg, A. Borchert and F. Uhlenhut, "Model based optimization of biomethane plants," in Achema, Frankfurt am Main, 2012.
- P. Biernacki, S. Steinigeweg, A. Borchert, E. Siefert, F. Uhlenhut, I. Stein and M. Wichern, "Modellbasierte Optimierung von Biogasanlagen," in Biogas Innovationsskongress, Osnabrueck, 2011.

- **Poster presentations:**

- P. Biernacki, S. Steinigeweg, A. Borchert and F. Uhlenhut, "Model based optimization of biomethane plants," in Achema, Frankfurt am Main, 2012.
- P. Biernacki, S. Steinigeweg, A. Borchert and F. Uhlenhut, "Model based optimization of biomethane plants," in BioGas World, Berlin, 2012.
- P. Biernacki, S. Steinigeweg, A. Borchert, E. Siefert and I. Uhlenhut, "Model based optimization of the biogas power plants," in 8th European Congress of Chemical Engineering 7 1st European Congress of Applied Biotechnology, Berlin, 2011.
- P. Biernacki, S. Steinigeweg, A. Borchert, E. Siefert, F. Uhlenhut, I. Stein and M. Wichern, "Modellbasierte Optimierung von Biogasanlagen," in Biogas Innovationsskongress, Osnabrueck, 2011.

### 3) **Literature review**

#### 3.1. **Biomethane**

In the following chapter anaerobic digestion process resulting in methane formation is explained, together with substrates and key parameters for biogas production. Also explanation of the biochemical modelling of the anaerobic digestion of organic matter is included.

##### 3.1.1. **Anaerobic digestion and methane formation**

In nature organic material is decomposed by metabolically active microorganisms in a humid atmosphere to simpler matter. If the breakdown is occurring without presence of air, so called anaerobic digestion is occurring, methane is created and released. This naturally occurring process was examined by Alessandro Volta in 1776, when the collected gas (marsh gas) from Lake Como proved to create explosive mixtures with air, and its' quantity depends on the decomposition process. Currently anaerobic digestion is also industrially applied process to produce drink and food (fermentation), but also at the waste water treatment plants or biogas power plants. At the biogas power plants not only methane is formatted, but also other gases like carbon dioxide, hydrogen sulfide, ammonia, and hydrogen. As a consequence the formed gas was called biogas, and the methane achieved after purification is called biomethane ( $\geq 96$  volume % of  $\text{CH}_4$ ) (Deublein & Steinhauser, 2011) .

##### 3.1.1.1. **History**

Glimmering light coming from the bottom of swamps, described by roman scholar Pliny around 50 BC is recognized as a first record concerning methane formation. Following work of Van Helmont (17<sup>th</sup> century), Volta (1776), Faraday, Dalton, Henry and Davy (around 1800), the final methane structure was described by Avogadro in 1821. Year 1884 was important for biogas history, since then horse dung collected from the streets of Paris was used by Louis Pasteur and his student Gavon for fermentation in 35°C to obtain 100l of methane from 1m<sup>3</sup> of substrate. He proposed to use biogas for lighting streets of Paris. This idea was followed in Exeter in England, where in 1897 gas obtained from wastewater treatment plant was used for street lamps. Since this moment further development of biogas was directly linked to progress in wastewater treatment technology (Deublein & Steinhauser, 2011). In 1923 in Germany for this first time biogas was sold to the public gas works (Imhoff, 1980), and it was followed in Europe. In addition to that, before the Second World War first combined heat and power (CHP) units were utilizing biogas, where energy was already used for wastewater treatment plants, and heat was delivered to houses (Deublein & Steinhauser, 2011). In the

1930s agriculture waste was also identified as a substrate for biogas power plants, first in United States by Buswell, who covered the whole gas requirement of a small town Urbana (Illinois). Afterwards in Algeria small domestic biogas plants were constructed to satisfy farmhouses' energy needs by Ducellier and Isman. In 1947 Imhoff analysed biogas potential from excrements. Finally in year 1950 first industrial scale biogas power plant was commissioned in Celle, Germany, where the cylindrical fermenters developed earlier in Darmstadt were used. As a result about 50 biogas power plants were constructed in Germany. However, around year 1955 the biogas boom was stopped by low oil prices, and the fact that more mineral fertilizer was used despite natural fertilizer from biogas power plants. As a consequence almost all plants were shut down. Dependence of biogas' profitability on oil prices began a new wave of interest in this technology in 1970s during oil crisis. In the 1990s due to disposal acts in Europe, anaerobic digestion of waste became again interesting topic, often promoted by the government. In Germany the Law of Renewable Energies effective since year 2000, which clearly regulated subsidization of the biogas power plants resulted in outstanding amount of plants installed, as presented in table 1 (Deublein & Steinhauser, 2011). Due to the increase also in averaged nominal power of plants to 500 kW in year 2008 (Hoelker, 2008), whereas the largest plants deliver more than 10 MW, an amendment to the Law of Renewable Energies in 2009 was established to promote small biogas power plants (150 kW), due to issues connected to feeding big plants (Deublein & Steinhauser, 2011). Currently in Germany about 5000 plants are operated (Hoelker, 2008). In European Union generally the boom on biogas power plants can also be observed, because in Austria over 300 plants are already running, in Czech Republic 40 new plants were commissioned in a few years time, and in Hungary in year 2005 2.5 MW plant was launched among other smaller (Deublein & Steinhauser, 2011). Moreover, due to Directive 2009/28/EC (Directive 2009/28/EC, 2009) it is expected that even more biogas power plants will be constructed and operated in European Union.

**Table 1 Specification of biogas power plants in Germany in year 2000 (Deublein & Steinhauser, 2011).**

	<b>No. Of biogas facilities</b>	<b>Installed electric power (MW)</b>	<b>Total electric power (MWh a<sup>-1</sup>)</b>
Sewage gas	217	85	61 000
Landfill gas	268	227	612 000
Agricultural biogas	1040	300	127 000
Total	1525	612	800 000

### 3.1.1.2. Anaerobic digestion process

In this part formation of the biogas is explained together with biochemistry behind the process.

#### 3.1.1.2.1. Bioreactions

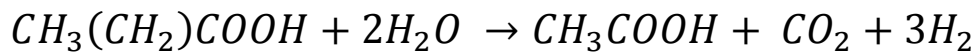
Organic material decomposition to biogas is a complex process, described by different authors in different number of stages. However, the generally accepted and commonly presented scheme of methane formation included 4 phases: hydrolysis, acidogenesis, acetogenesis, methanogenesis. Each of them is carried out by different groups of microorganisms, partially with different condition needs, simultaneously requiring very good correlation and timing between the phases. Furthermore, proportion of CO<sub>2</sub> and acid concentration may increase, resulting in pH drop below 7, if the hydrolysis and acidogenesis' phases are too rapid. Therefore, due to the close link between anaerobic digestion phases, hydrolysis and acidogenesis (1<sup>st</sup> stage), and between acetogenesis and methanation (2<sup>nd</sup> stage), process is also describe as 2 stages (Deublein & Steinhauser, 2011).

During the hydrolysis phase, long-chain water soluble compounds are decomposed to monomers by use of enzymes from facultative and obligatory anaerobic microorganisms. Hydrolases is rapidly (within a few hours) converting cellulose, hemicelluloses and starch to short-chain sugars. More time is necessary for proteases to break down proteins into amino acids, and for lipases to form fatty acids and glycerine from fats present in the substrate, because this might last a few days. Additionally, lignin and lignocelluloses are also converted, but gradually and incompletely (Batstone, et al., 2002; Deublein & Steinhauser, 2011).

In the acidogenic phase facultative and obligatory anaerobic microorganisms are further converting monomers from the hydrolysis phase to short-chain organic molecules, like butyric acid, propionic acid, acetic acid, valeric acid, or lactic acid, and also to alcohols, hydrogen and carbon dioxide. Short chain sugars are converted to pyruvate, which is further degraded into lactic acid (*Lactobacillales*) and into ethanol (yeast). Fatty acids are converted by *Acetobacter* by  $\beta$ -oxidation. On the other side, amino acids are following Stickland reaction accompanied by *Clostridium botulinum*, and it results in acetate, ammonia, and carbon dioxide. In addition to that, if cysteine is present, then hydrogen sulfide is formatted during splitting (Deublein & Steinhauser, 2011).

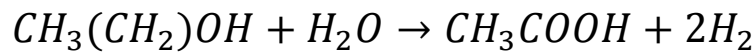
In the acetogenic phase endergonic degradation reactions of e.g. propionic acid or ethanol are occurring (Winter, 1985):

Equation 1



where  $\Delta G_f^o = 74 \text{ kJ mol}^{-1}$

Equation 2



where  $\Delta G_f^o = 9.6 \text{ kJ mol}^{-1}$

In addition to that homoacetogenic bacteria, despite low occurrence, reduces exergonically part of hydrogen and carbon dioxide to acetic acid (Deublein & Steinhauser, 2011):

Equation 3



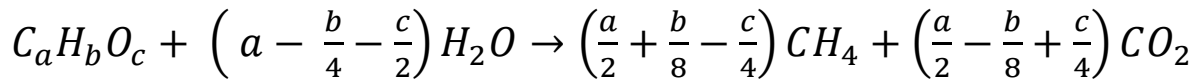
Simultaneously organic nitrogen and organic sulfur present are reduced to ammonia and hydrogen sulfide.

The final stage, methanogenic phase, where the methane is formed by methanogens, requires substrates like hydrogen, carbon dioxide and acetic acid. As a consequence, degradation of fatty acids and alcohols is energetically supported by bacteria from the 4<sup>th</sup> stage. However during this phase strict anaerobes are forming methane, and thanks to facultative microorganisms from participating in earlier phases the oxygen is used up, and the methanogenic phase is possible (Deublein & Steinhauser, 2011). Moreover, methanogens are slow growing group of bacteria (time of at least 100h), are very sensitive to pH (optimal 6,5-8,0), but carbon dioxide is crucial for the growth (Cheng, 2010). Consequently, if methanogenesis is disturbed, e.g hydrogen sulfide inhibition (Boehnke, et al., 1993), then acidification occurs and leads to further pH drop (Deublein & Steinhauser, 2011). Example of methanogens are *Methanosarcina* and *Methanothrix*, both converting acetic acid, and *Methanobacterium* converting hydrogen and carbon dioxide. Furthermore, despite reduction of carbon dioxide and hydrogen ( $\Delta G_f^o = -136 \text{ kJ mol}^{-1}$ ) is more exergonic, about 70% of methane is formed through acetic acid conversion( $\Delta G_f^o = -31 \text{ kJ mol}^{-1}$ ) (Cheng, 2010).

### 3.1.1.2.2. Biochemistry

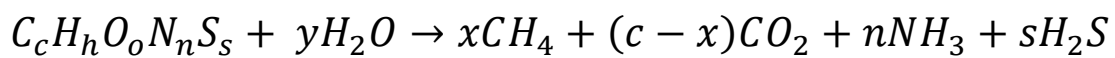
The build up of methane and carbon dioxide through anaerobic digestion was first described using stoichiometric approach by Buswell in 1936 (Buswell & Hatfield, 1936):

Equation 4



Then the equation was modified by Bolye in 1977 (Boyle, 1977) to represent also NH<sub>3</sub> and H<sub>2</sub>S formation (Deublein & Steinhauser, 2011):

Equation 5



where

Equation 6

$$x = \frac{1}{8} (4c + h - 2o - 3n - 2s)$$

Equation 7

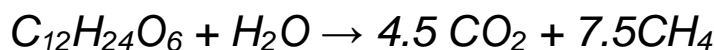
$$y = \frac{1}{4} (4c - h - 2o - 3n + 2s)$$

Applying this equation identifies correlation between biogas composition and substrates composition (Deublein & Steinhauser, 2011):

- Carbohydrates:



- Fats:



- Proteins:

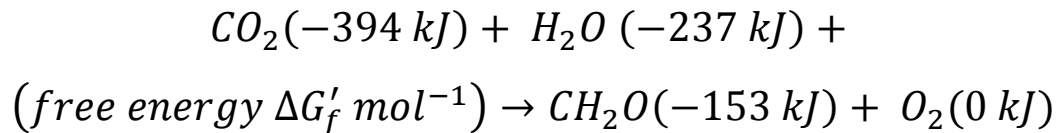


As a consequence, fats may be identified as an optimal source for biogas, and limiting the protein content would also reduce presence of contaminants like NH<sub>3</sub> or H<sub>2</sub>S. However, an excess of fats in anaerobic digestion may lead to acid overproduction, which is driving force for pH drop and destruction of the process stability (Deublein & Steinhauser, 2011).

Following Deublein and Steinhauser (Deublein & Steinhauser, 2011) the energy balance for creation of biomass, degradation of organic material to biogas, and combustion of methane can be calculated in this manner:

1. Build up of biomass through photosynthesis:

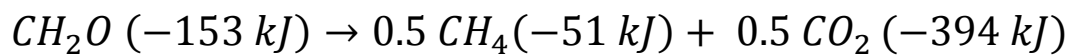
Equation 8



Therefore:  $\Delta G'_f = 478 \text{ kJ mol}^{-1}$  at pH = 7

2. Anaerobic digestion:

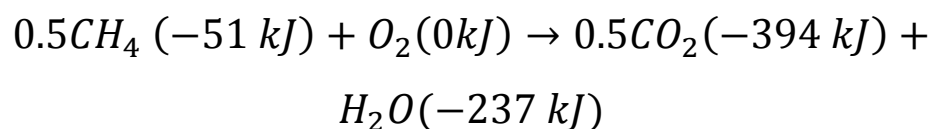
Equation 9



Therefore:  $\Delta G'_f = -70 \text{ kJ mol}^{-1}$

3. Combustion:

Equation 10



Therefore:  $\Delta G'_f = -408 \text{ kJ mol}^{-1}$

As a consequence, theoretically the energy needed for the photosynthesis is equal to energy gained during the combustion of methane and the energy set free during the anaerobic digestion process. However, in practise the degradation of organic material to biogas is not complete, and the heat is not entirely consumed, therefore the mass balance is not achieved and the whole energy is not utilized. Moreover, as indicated by the energy balance, there is a very little heat release during the conversion stage, hence insulation and heating is required for reactors (Deublein & Steinhauser, 2011).

### 3.1.1.3. Substrates

As a substrate all types of biomass, which as a main component contain carbohydrates, proteins or fats, are applicable for biogas power plants. From economical point of view,

substrates with high lignin content should be avoided, due to slow degradation rate of lignin. Nevertheless, substrate used should be free of harmful substances, which could reduce the efficiency of anaerobic digestion or could restrict applicability of the fermentation residues as a fertilizer. Moreover, biomass should not contain trash or e.g. sand, to avoid reduction of the effective volume of the reactor. In addition, organic content should also be in line with fermentation process chosen, and nutritional value should be as high as possible to ensure high generation of gas, and good quality fertilizer, however at the same time it needs to be considered that anaerobic digestion at biogas power plants is also a waste treatment technique. Furthermore, the substrates should not contain pathogens, other organisms or antibiotics, which could disturb the anaerobic digestion process (Deublein & Steinhauser, 2011). On the other side, substrates like animal wastes require hygienisation step before feeding to the fermenter, and later usage as a fertilizer (EWE Biogas GmbH & Co. KG., 2011). Common substrates used for biogas formation are often classified depending on origin into 5 groups (Deublein & Steinhauser, 2011):

1. Agricultural products: e.g. fresh substrates or silages (grass, maize, barley, sorghum) liquid manure (cow manure, pig manure), slaughterhouse waste
2. Residual waste and domestic waste: e.g. leftovers (kitchen waste),
3. Sewage sludge
4. Industrial wastewater
5. Algae

Potential of agricultural products like e.g. maize or other substrates with water content of 50-70%, are often increased by conservation method called ensiling. During this process substrates, often chopped, are wrapped with plastic material (figure 1) to ensure exclusion of air, which is followed by production of organic acids by lactic and acetic bacteria, leading to drop in pH to 4-4.5. As a consequence, this process has a conservative effect, an anaerobic degradation of complex organic material leads to predigestion of the substrate, therefore gas yield is increased and at the same time the volume (e.g. -17% of the dry maize) is reduced, so economical efficiency is improved. Therefore, most of the agricultural substrates used at biogas power plants, e.g. grass, maize, weeds, are prepared as silages (Cheng, 2010).



Figure 1. Ensiling conservation method (St-Pierre, 2013)

#### 3.1.1.4. Composition

The most valuable compound of biogas is methane, which is the main component of natural gas, therefore all other substances present are treated as contaminants. Characteristics of methane is listed as a table 2, and general properties of biogas are presented as a table 3.

Table 2. Pure component properties (Thermodynamics Research Center, 2014).

Component	Methane (CH <sub>4</sub> )	
Molecular weight	16.043	g mol <sup>-1</sup>
Normal boiling point	111.6539	K
Critical volume	0.09928	m <sup>3</sup> kmol <sup>-1</sup>
Critical pressure	4599949.2	N m <sup>-2</sup>
Critical temperature	190.5631	K

Table 3. General properties of biogas (Deublein & Steinhauser, 2011).

<b>Composition</b>	55-70% methane (CH <sub>4</sub> ) 30-45% carbon dioxide (CO <sub>2</sub> ) Traces of other gases
<b>Energy content</b>	6.0-6.5 kWh m <sup>-3</sup>
<b>Fuel equivalent</b>	0.60-0.651 oil m <sup>-3</sup> biogas
<b>Explosion limits</b>	6-12% biogas in air
<b>Ignition temperature</b>	650-750°C (with above mentioned methane content)
<b>Critical pressure</b>	75-89 bar
<b>Critical temperature</b>	-82.5°C
<b>Normal density</b>	1.2 kg m <sup>-3</sup>
<b>Smell</b>	Bad eggs (the smell of desulfurized biogas is hardly noticeable)

The common impurities of the biogas include carbon dioxide, hydrogen sulfide, ammonia, water vapour, oxygen, nitrogen and siloxanes. Effect of those components are summarized as a table 4, together with their typical content.

**Table 4. Content and effect of typical impurities (Deublein & Steinhauser, 2011).**

Component	Content	Effect
CO <sub>2</sub>	25-50 vol. %	<ul style="list-style-type: none"> <li>• <i>Lowers the calorific value</i></li> <li>• <i>Increases the methane number and the anti-knock properties of engines</i></li> <li>• <i>Causes corrosion (low concentrated carbon acid), if the gas is wet</i></li> <li>• <i>Damages alkali fuel cells</i></li> </ul>
H <sub>2</sub> S	0-0.5 vol. %	<ul style="list-style-type: none"> <li>• <i>Corrosive effect in equipment and piping systems (stress corrosion); many manufactures of engines therefore set an upper limit of 0.05 volume %</i></li> <li>• <i>SO<sub>2</sub> emissions after burners or H<sub>2</sub>S emissions with imperfect combustion – upper limit 0.1 volume %</i></li> <li>• <i>Spoils catalysts</i></li> </ul>
NH <sub>3</sub>	0-0.05 vol. %	<ul style="list-style-type: none"> <li>• <i>NO<sub>x</sub> emissions after burners damage fuel cells</i></li> <li>• <i>Increases the anti-knock properties of engines</i></li> </ul>
Water vapour	1-5 vol. %	<ul style="list-style-type: none"> <li>• <i>Causes corrosion of equipment and piping systems</i></li> <li>• <i>Condensates damage instruments and plants</i></li> <li>• <i>Risk of freezing of piping systems and nozzles</i></li> </ul>
Dust	> 5µm	<ul style="list-style-type: none"> <li>• <i>Blocks nozzles and fuel cells</i></li> </ul>
N <sub>2</sub>	0-5 vol. %	<ul style="list-style-type: none"> <li>• <i>Lowers the calorific value</i></li> <li>• <i>Increases the anti-knock properties of engines</i></li> </ul>
Siloxanes	0-50 mg m <sub>n</sub> <sup>-3</sup>	<ul style="list-style-type: none"> <li>• <i>Act like an abrasive and damages engines</i></li> </ul>

Two main components in biogas are methane (55-70 volume %) and carbon dioxide (25-50 volume %). The exact composition strongly depends on the substrates, therefore it may be influenced in such a way, that a higher methane content is achieved (Deublein & Steinhauser, 2011):

- As indicated in the biochemistry part (3.1.1.2.2.), addition of fats will result in increase of the methane content. However, excess of fats may lead to acids overproduction, hence to pH drop (Deublein & Steinhauser, 2011). As confirmed by Kaltschmitt and Hartmann (Kaltschmitt & Hartmann, 2001), the substrate with higher number of C-atoms enhance methane quantity.

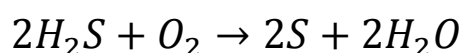
- Longer residence time allow better decomposition of the substrate, and enough time for methanogens to grow (Deublein & Steinhauser, 2011).
- Activation and preparation of the substrate, especially if lignin content is noticeable, with use of e.g. pre-treatment methods like steam explosion increase methane yield (Estevez, et al., 2012).
- Higher amount of carbon dioxide dissolved can be achieved by higher content of liquid in the. At the same time the lower temperature and higher pressure is also increasing CO<sub>2</sub> solubility (Deublein & Steinhauser, 2011).

Concerning nitrogen and oxygen content, it is increased during the desulfurization stage, when the air is introduced to enhance bacteria growth and sulfur removal. On the other side, content of the ammonia depends on the protein content of the substrates, and it is higher when e.g. rich in proteins liquid chicken manure is used as a substrate. Moreover, content of ammonia is directly correlated with pH, where increased pH enhanced ammonia content in the gas phase. Hydrogen Sulfide's presence is also depended on substrates feed. Without desulfurization step it may reach 0.2 volume %, and due to its corrosive character it is necessary to reduce its' content prior to combustion in CHP unit. Siloxanes, found in cosmetics, detergents, printing inks, and building materials are also necessary to be removed before combustion because at high temperatures SiO<sub>2</sub> is formed and covers machines with glass-like layer (Deublein & Steinhauser, 2011).

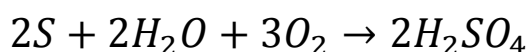
#### 3.1.1.5. Gas upgrading

As presented in earlier chapter, gas formed is containing several impurities, and depending on the further utilization they might need to be removed. The most significant contamination is hydrogen sulfide, which in contact with water became corrosive to the CHP unit, and consequently many manufactures of heat and power generators set limits of 0.05 volume % (100-500 mg Nm<sup>-3</sup>), and require continuous monitoring of the concentration. Therefore desulfurization and dehumidification units are installed at almost all biogas power plants. Hence different chemical, physical or biological techniques were developed to remove H<sub>2</sub>S, with different investment and operational costs, efficiencies and limitations, as presented in table 5. The most popular method is biological treatment, where *Thiobacillus* and *Sulfolobus* microorganisms are degrading hydrogen sulfide to elementar sulfur (usually 75 volume % of introduced H<sub>2</sub>S) and sulphate (Deublein & Steinhauser, 2011):

Equation 11



Equation 12

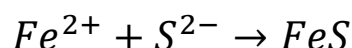


Equation 13

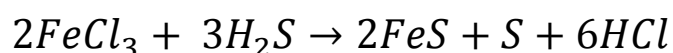


Bacterias require carbon and inorganic salts (N,P,K) as nutrients, along with trace elements (Fe, CO, Ni), which most of the time are present in the substrates. Since *Thiobacillus* and *Sulfolobus* are aerobes, sufficient amount of air (rate of 4-6 volume % of the biogas) is required by them, however air concentration cannot exceed 12 volume % due to explosion risk. Biological desulfurization can be performed *in situ*, in the reactor at smaller agricultural plants, where immobilization place above substrate level is secured. However, this may lead to reduction in methane yield, therefore at the industrial plants (> 200kW<sub>el</sub>) trickling filter or bioscrubber are economically efficient (Deublein & Steinhauser, 2011). Biological desulfurization is efficient up to 3000 mg m<sub>N</sub><sup>-3</sup> concentrations (Department for Environment, Food and Rural Affairs, 2010; Hoehener & Spirig, 2004), and may achieve desulfurization level for burning in gas engines. Another method, with higher efficiency is sulphide precipitation, where iron ions (Fe<sup>2+</sup> or Fe<sup>3+</sup>) are added to achieve sulfur precipitation (Deublein & Steinhauser, 2011):

Equation 14

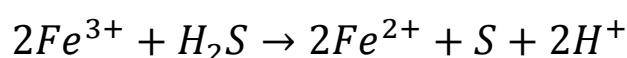


Equation 15

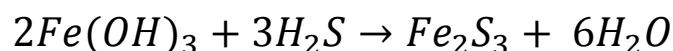


However, the running costs are significant in this method (US\$ 100 Mg<sup>-1</sup>), because continuous feed of fresh iron salt must be ensured. Therefore, absorption in a ferric chelate solution, which requires lower operational costs, where iron (III) ions is reduced to iron (II) ions, and elemental sulfur is obtained, and iron (II) ions are regenerated by introduction of oxygen (Deublein & Steinhauser, 2011):

Equation 16



Even higher removal efficiency is possible with adsorption on bog iron ore (Fe(OH)<sub>3</sub>) (Deublein & Steinhauser, 2011):



In desulfurization tower iron(III) hydroxide masses are stacked as layers of impregnated steel wool or as impregnated wooden chips or pallets. Another fine and interesting removal method is combination of carbon dioxide absorption with ethanolamines and simultaneous hydrogen sulfide removal, explained later in this chapter (Deublein & Steinhauser, 2011).

**Table 5. Desulfurization techniques (Deublein & Steinhauser, 2011).**

Technology	Investment costs	Operational costs	Air intake to the biogas required	Rough/fine decontamination	Remarks
Internal biological desulfurization	-	-	Yes	Very rough	Low dynamic in the change of load, corrosion hazard in the bioreactor 3-8% lower biogas yield
Percolating filter plant	+	-	Yes	Rough	Blocking hazard at low air intake
Bioscrubber plant	++	-	No	Rough	
Sulfide precipitation	+	++	No	Rough	
Ferric chelate	(+)++	-	Yes	Rough	
Bog iron ore	(+)++	+	(Yes)No	Fine	Fire hazard
Activated carbon; KI, K <sub>2</sub> CO <sub>3</sub> , KMnO <sub>4</sub>	-	++	No	Fine	Conversion of H <sub>2</sub> S into elemental sulphide – removal as hazardous waste
Absorption with ethanolamines	++	++	No	Fine	May be combined with fine CO <sub>2</sub> removal

Ammonia impurity coming from e.g. liquid manure is possible to be removed by air stripping or chemical precipitation with magnesium or phosphate (Abatzoglou & Boivin, 2009; Cheng, 2010). However, to satisfy economical efficiency it is recommended in the literature (Deublein & Steinhauser, 2011) to combine ammonium removal with other cleaning steps (e.g. desulfurization), or since ammonia is formed at high pH values, suitable process control are recommended to reduce ammonium conversion to ammonia.

Siloxanes removal is based on adsorption on activated charcoal, activated alumina, or silica gel, however to achieve possible high efficiency, other contaminants, e.g. water vapour, should be removed earlier (Abatzoglou & Boivin, 2009; Cheng, 2010; Deublein & Steinhauser, 2011).

Fine drying process is necessary to remove water prior to supplying biogas to natural gas network, as presented in table 6. Other techniques like cooling, or adsorption on activated charcoal or silica gel, or by absorption e.g. in glycol solutions are also possible (Deublein & Steinhauser, 2011; Kohl & Nielsen, 1997).

Solid particles together with oil-like components are removed with use of dust collectors or filters achieving 99,99% efficiency, if necessary (Deublein & Steinhauser, 2011).

#### 3.1.1.5.1. Carbon dioxide removal

Biogas upgrading to achieve level of “green gas” for vehicles in accordance to ISO/DIS 15403 or sending it to the natural gas network following DVGW G260 standard (table 6), requires carbon dioxide removal.

As a consequence there are different techniques available for biogas upgrading to biomethane standard, which require (Deublein & Steinhauser, 2011):

- Maximum methane slippage, and maximum carbon dioxide removal
- Low consumption and degradation of the material or reagent used, and possible regeneration
- “*Low flow resistance (low viscosity, large pores)*” (Deublein & Steinhauser, 2011)
- Minimum or no environmental impact of the material or reagent used
- Availability, low investment and operational cost.

Accordingly methods for upgrading the gas include absorption, adsorption, diaphragm separation, membrane separation and mineralization as presented in table 7. For the last mentioned method necessary is addition of quicklime (CaO), which reacts with carbon dioxide and forms calcium carbonate, a material used for construction of houses. However, taking into account quicklime preparation, where lime is “burning” and emitting one mole

carbon dioxide per one more of quicklime, this method has a questionable application during carbon dioxide removal (Deublein & Steinhauser, 2011).

**Table 6. Biogas qualities required for different applications in Europe (Deublein & Steinhauser, 2011; Franke, 2007; Keicher, et al., 2004; Keicher, et al., 2006; Reher, 2003; Schmack & Nusko, 2006)**

<b>Gross calorific value and gas components</b>	<b>“Green gas”for vehicles according to ISO/DIS 15403</b>	<b>Addition to natural gas according to DVGW G260</b>
Gross calorific value	No minimum value	8.4-13.1 kWh m <sup>-3</sup>
CH <sub>4</sub>	>96%	No minimum value
H <sub>2</sub> S	≤5 mg m <sub>n</sub> <sup>-3</sup>	<5 mg m <sub>n</sub> <sup>-3</sup>
Total sulfur without odorizing agents	<120 mg m <sub>n</sub> <sup>-3</sup>	<30 mg m <sub>n</sub> <sup>-3</sup>
Thiol (mercaptan) sulfur	<15 mg m <sub>n</sub> <sup>-3</sup>	<6 mg m <sub>n</sub> <sup>-3</sup>
CO <sub>2</sub>	<3%	<6 volume %
O <sub>2</sub>	<3%	<3 dry net % <5 humid net %
Hydrocarbons	<1%	< Dew point (at the relevant pressure/temperature)
Water	<30mg m <sub>n</sub> <sup>-3</sup>	<50 mg m <sub>n</sub> <sup>-3</sup>
Oil vapours (<C <sub>10</sub> )	<70-200mg m <sub>n</sub> <sup>-3</sup>	n.s.
Oil vapours (>C <sub>10</sub> )	<70-200mg m <sub>n</sub> <sup>-3</sup>	n.s.
Glycol/methanol	Technically free	n.s.
Dust	Technically free; <1µm	Technically free
Other like: particle size, NH <sub>3</sub> , CO, HG, Polysiloxanes, Chlorine, Fluorine, Heavy metals, Halogens	n.s.*	n.s.*

\*n.s. – not specified

Pressure swing adsorption is another very efficient technique, where only 0.1 mg m<sub>N</sub><sup>-3</sup> of impurities stays. Activated charcoal, zeolite or carbon molecular sieves are examples of possible adsorbers applicable for this method. However, this technique requires gas under pressure of 10-12 bar, which then needs to be cooled below 40°C before feeding to the first adsorber. Moreover, to reach methane concentration of 95% normally 4 adsorbers needs to be installed, and for lower impurities content, intermediate flashing and plant with 6 adsorbers is required. Therefore investment costs are significantly high. Moreover, the operational costs presented in table 7, from the literature (Deublein & Steinhauser, 2011),

are not explained in details. Therefore there is no information, if they include operational costs of compressor and cooler necessary to prepare the gas.

**Table 7. Biogas upgrading methods (Deublein & Steinhauser, 2011).**

Technology	Cots		Temperature	Pressure
	Investment	Operational		
Unit			[°C]	[bar]
<i>Physical absorption</i>				
In water	+	+	3-30	<7
N-Methylpyrrolidone	+	+	<40	>20
Methanol	+	+	<40	>20
Polyethylene glycol dimethyl ether	+	+	<40	20-30
Tetrahydrothiophenedioxide	+	+	<40	10-20
Methyl isopropyl ether	+	+	<40	10-20
Tetraethylene glycol dimethyl ether	+	+	<40	<7
<i>Chemical absorption</i>				
K <sub>2</sub> CO <sub>3</sub> (10% in water)	+	++	<40	20-30
K <sub>2</sub> CO <sub>3</sub> (15-30% in water)	+	++	<40	20-30
NaOH (8% in water)	+	++	<40	20-30
NH <sub>3</sub> (5% in water)	+	++	<40	20-30
Alcazid M in water	+	++	<40	20-30
Methanolamine	+	++	<40	20-30
Monoethanolamine (10-20% in water) + oxidation inhibitor	+	+	~40	20-30
Diethanolamine	+	+	20-55	8-70
Methyldiethanolamine (10-25% in water)	+	+	50-70	20-30
<i>Adsorption with pressure or vacuum changes</i>				
Zeolite	++	-	<40	10-12 or 1
Carbon	++	-	<40	10-12 or 1
<i>Other</i>				
Gas permeation	++	++	<40	30
Membrane-adsorption	++	++	<40	30
Cryogenic processes	++	++	<-80	200

Another common method is physical absorption, where the feature that acidic components are more easily dissolved in water, or other polar organic solvents which do not react with contaminants, than nonpolar hydrocarbons (e.g. methane), as presented in table 8. Thermodynamic of physical solubility is further explained in chapter 3.3.2. In this method to the absorption column, with packed material, compressed biogas (10-12 bar) is introduced at the bottom stage. In order to ensure counter current contact with warm water (5-25°C), it is feed at the top stage. As a consequence carbon dioxide is dissolved in water, discharged at the bottom, and recycled in a scrubber, which is operated at atmospheric pressure, hence allowing dissolved carbon dioxide release. Biomethane of over 95 volume % can be obtained, and most of the water or polar organic solvent is regenerated. The regeneration rate may be improved by vacuum application or elevated temperature of stripper, and the absorption rate is possible for optimisation, if higher pressure is applied, or water's temperature is in the lower range because the plant's capacity can be doubled if the temperature is 5°C, despite 25°C is applied (Austgen, 1989; Deublein & Steinhauser, 2011).

**Table 8. Solubility of different gases in water in different temperatures (Deublein & Steinhauser, 2011).**

Biogas component	Solubility in water at 1 bar partial pressure of diluted gas	
	0°C	25°C
Unit	[mmol kg <sup>-1</sup> bar <sup>-1</sup> ]	
Ammonia	53 000	28 000
Hydrogen sulfide	205	102
Carbon dioxide	75	34
Methane	2.45	1.32

Amine scrubbing is the most technically and commercially mature method, which can be easily retrofitted to an existing plant (Kohl & Nielsen, 1997), and according to Rochelle (Rochelle, 2009) in 2030 it probably will be the dominant method applied for coal-fired power plants. Moreover, according to Deublein and Steinhauser (Deublein & Steinhauser, 2011) even higher loads and selectivity are achieved with this method.

This method is characterized as a mass transfer from gas phase to liquid phase enhanced by chemical reaction, because following physical absorption, non-volatile ionic species are formed through acid-base buffer mechanism or directly with chemical solvents (Austgen, 1989). The mechanisms is explained by (Astarita, et al., 1983; Austgen, 1989) in a following manner:

- a) *“Diffusion of one or more acidic gas components from the bulk gas phase to the gas-liquid interface followed by absorption (dissolution) into the liquid. Physical equilibria is normally assumed for molecular species at the gas – liquid interface”.*
- b) *“Diffusion and convection of the reactants from the gas – liquid interface to the bulk liquid phase”.*
- c) *“Occurring simultaneously with mass transfer, reaction between the dissolved gas and the liquid reactant in the liquid phase”.*
- d) *“Diffusion of the reaction products into the bulk liquid phase due to concentration gradients created by the chemical reactions” (Austgen, 1989).*

Moreover, according to Austgen (Austgen, 1989) there are two main advantages of this method over physical absorption. Because the mass transfer is dependent on the difference between concentration of the acid gas in the gas phase, and concentration of the gas dissolved in the liquid phase, chemical absorption with alkanolamines is increasing the difference between concentrations, hence allowing more gas to be absorbed. In addition to that, since the physical solubility is governed by the partial pressure of the gas phase, where un-reacted acid gases in the vapour and liquid phase are in equilibrium, the non-volatile ionic species formed with alkanolamines, enhance significantly the acid gas removal.

Alkanolamines used in this method consists of hydroxyl groups, which decrease the vapour pressure and enhanced solubility in aqueous solution, and also consists of amino groups, which ensures alkaline condition necessary to react with acid gases. In this technique the most commonly used chemicals are monoethanolamine (MEA) and diethanolamine (DEA) (Kohl & Riesenfeld, 1985), diglycolamine (DGA), and methyldiethanolamine (MDEA) (Austgen, 1989). Depending on the amount of organic substituent present, despite hydrogen atoms bound in the ammonia, primary (one substituent), secondary (two substituents), tertiary (three substituents) amines may be recognized. In aqueous phase MEA (primary amine), DEA, and DGA (both secondary amines) react with H<sub>2</sub>S, since hydrogen sulfide is a Brönsted acid, and those chemical solvents are Brönsted bases (Astarita, et al., 1983; Austgen, 1989). Additionally, primary and secondary amines form carbamates (e.g. R<sub>2</sub>NCOO<sup>-</sup>) during the rapid reaction with CO<sub>2</sub> (Austgen, 1989). Depending on the carbamate stability, carbamate revision to bicarbonate may occur. As a consequence, if alkanolamines formed moderate stability carbamate, it reacts to bicarbonate and free amine, which is again available for carbon dioxide capture (Suda, et al., 1996). On the other side, reactions between those amines and acid gases are exothermic, therefore significant amount of energy is required for desorption step to reverse absorption reaction (Austgen, 1989).

Therefore, alkanolamines with moderate stability carbamates, requires less energy for regeneration (Mimura, et al., 1995; Mimura, et al., 1997; Mimura, et al., 1998; Suda, et al., 1996). Hydrogen sulfide is rapidly removed from the gas through the before mentioned proton donor mechanism, when methyldiethanolamine (MDEA) is used. However, MDEA as a tertiary amine cannot create carbamate, therefore reacts slower with carbon dioxide, creating bicarbonate, hence greater number of trays is required for absorption, but at the same time, energy necessary for desorption is lower. Consequently, blends of small amount of primary or secondary amines with MDEA are proved to improve carbon dioxide capture (Chakravarty, et al., 1985; Critchfield & Rochelle, 1987; Critchfield & Rochelle, 1988; Katti & Wolcott, 1987).

Typical absorption plant is presented as a figure 2, which usually operates under medium or low partial pressure. Alkanolamine heated up to 40°C is feed at the top stage of the absorber, and in order to allow counter current contact between both phases, biogas is introduced at the bottom of the column. Rich in carbon dioxide solution is leaving the column at the bottom, and is prepared for desorption by heating it to 110-130°C. At this temperature carbon dioxide is released in gas form from the stripper, and the alkanolamines after cooling in heat exchanger, is again feed to the absorber. Due to losses of alkanolamines and water, make up flow is commonly applied (Austgen, 1989; Luyben, 2013; Desideri & Paolucci, 1999). However, before feeding the gas to the absorption column, removal of solid particles, SO<sub>2</sub>, NO<sub>x</sub>, and oxygen is recommended, in order to avoid reduction in efficiency (Deublein & Steinhauser, 2011). Principles of physical and chemical absorption are explained in section 3.3.2. and 3.3.3.

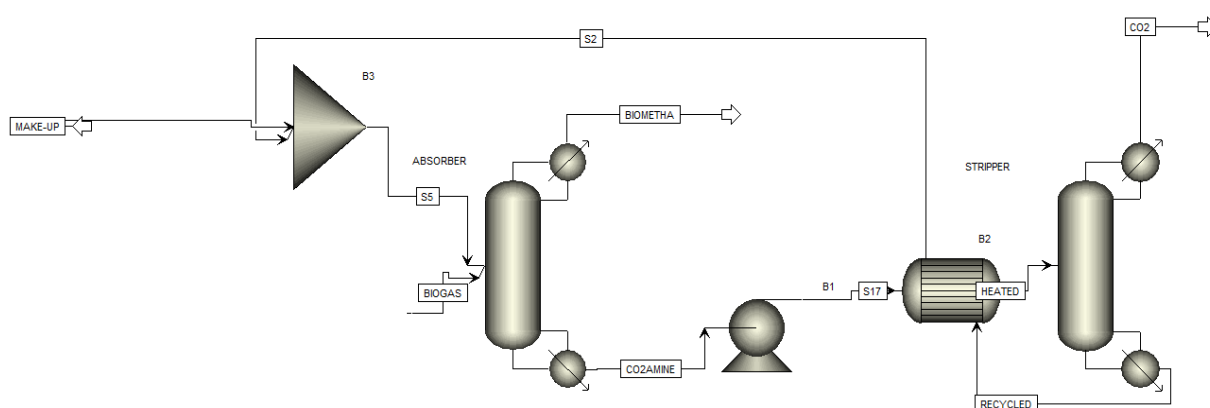


Figure 2. Typical chemical absorption plant.

### 3.1.1.5.2. 2-(Ethylamino)ethanol

2-(Ethylamino)ethanol (EAE) is a linear secondary amine which is linked to an ethyl group, and was chosen to be evaluated in this research. Unlike monoethanolamine (MEA), EAE has a small corrosion rate, even at higher concentrations. In addition, it requires less energy for

regeneration, and the absorption rate is higher due to creation of moderate stability carbamate (Suda, et al., 1996; Mimura, et al., 1995; Mimura, et al., 1997; Mimura, et al., 1998). An additional advantage is that, produced from agriculture products or residues ethanol is used to produce ethylamine and ethylene oxide. Both those chemicals react to form EAE (Sutar, et al., 2012). Moreover, methyldiethanolamine (MDEA) is often applied during amine washing to ensure H<sub>2</sub>S removal (Abatzoglou & Boivin, 2009), however its rate constant of second-order reaction is lower than for EAE (Mimura, et al., 1998), and existing biogas power plants already removed H<sub>2</sub>S prior to combustion at CHP unit (Abatzoglou & Boivin, 2009; Weiland, 2006). 2-(Ethylamino)ethanol has been already proved as an absorbent for CO<sub>2</sub> capture (Sutar, et al., 2012), and also as an activator in aqueous N,N-diethylethanolamine (DEEA) solutions (Vaidya & Kenig, 2007). However, there is still little experimental data on CO<sub>2</sub> capture with EAE at high loading rates, and while the focus was rather on kinetics of reaction (Mimura, et al., 1998; Sutar, et al., 2012; Vaidya & Kenig, 2007; Bavbek & Alper, 1999; Li, et al., 2007) , no publication on thermodynamic modelling representing vapour-liquid equilibrium in the CO<sub>2</sub> – EAE – H<sub>2</sub>O system was found.

#### 3.1.1.6. Potential

Biomethane, coming from purified biogas, is predicted to have more significant part as an energy source worldwide in the future, due to its constant supply of energy, possibility of storing energy, e.g. in form of methane, which is easier to store than hydrogen, local availability of different organic wastes (industrial wastewater, organic chemical waste, organic waste from households, or agricultural wastes like liquid manure), where biogas produced through anaerobic digestion is also a waste treatment technology. Moreover, sustainable development will also promote concept from 1930s began in Algeria, where farmhouses were supplied with energy and heat from small biogas plants (< 100 kW), and this could also be extended to biomethane production, which could be used as a fuel for tractors or agricultural machinery. Another aspect of biomethane plants, is a very good quality fertilizer gained from the residues, which could partially substitute fertilizers produced industrially in energy intensive manner, to again fulfil sustainable development requirements, hence also reduce pollution coming from the production and transportation. The final idea of biomethane plants additional advantage, is combination with *Power2Gas* concept (EUTEC, 2012). As indicated in the purification section (3.1.1.5.), from the stripper carbon dioxide of high purity is released, which could be combined with hydrogen, coming from an excess of wind (e.g. during night, when the energy demand is lower), in methanization process to form methane, which can be stored and used to cover energy peaks. The final aspect limiting biogas or biomethane potential is the cost. Plants are becoming more efficient, safer and easier to operate, however this leads investment costs to increase, and as indicated by the

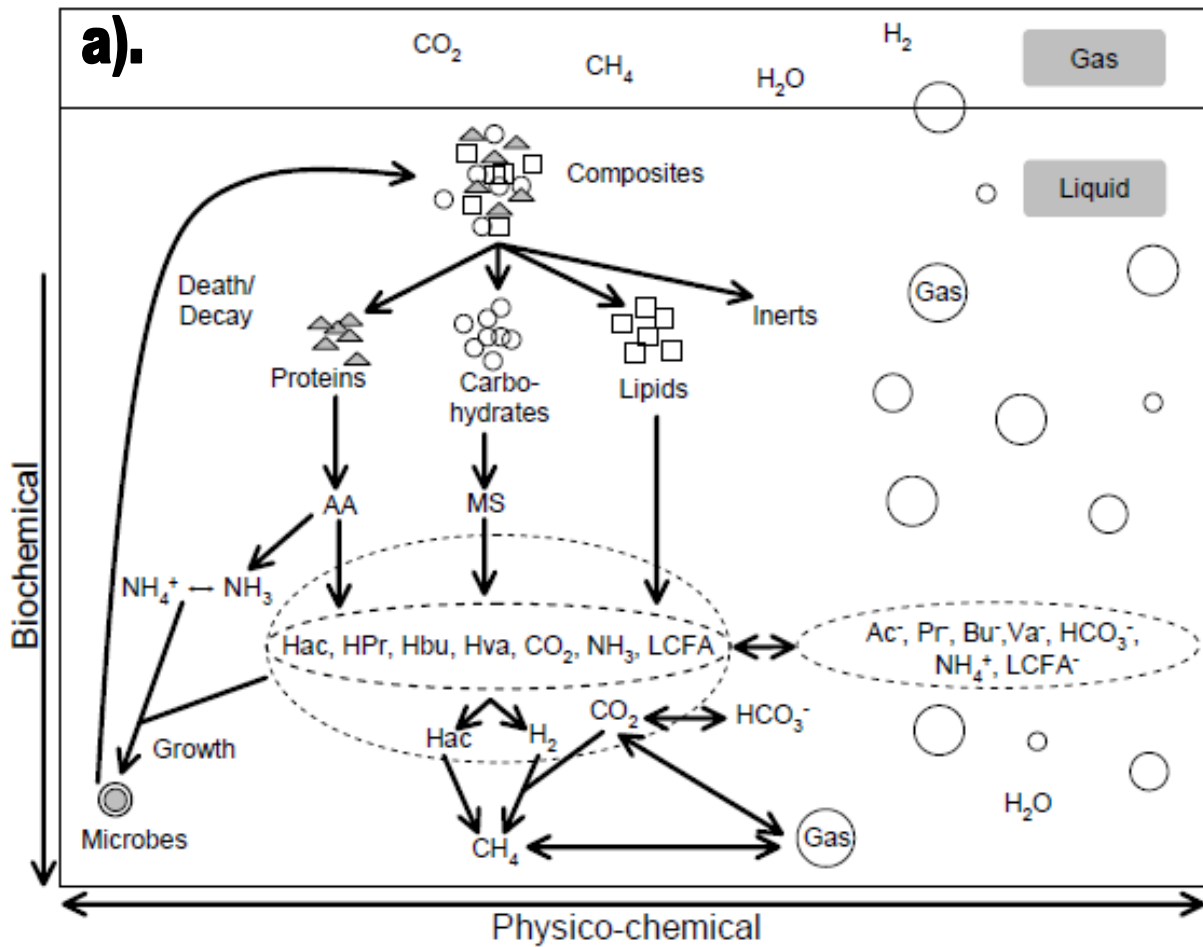
past situation in Germany, where biogas boom was caused by governmental subsidises. As a consequence, the biogas and biomethane plants should become cheaper, therefore available for other countries, or the growth will be dependent from governmental subsidises (Cheng, 2010; Deublein & Steinhauser, 2011; Weiland, 2006).

### 3.2. **Biochemical modelling of the anaerobic digestion**

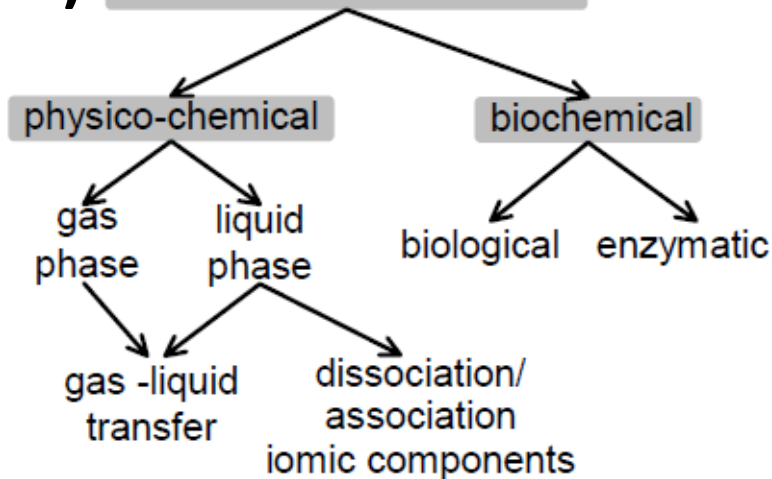
#### 3.2.1. **Anaerobic Digestion Model No. 1 (ADM1)**

The Anaerobic Digestion Model No. 1 (ADM1) was developed by the International Water Association's (IWA) Task Group (Batstone et al., 2002), and it was used in this research as a basic model for calculating biogas production. The strength of this model is in its consideration of seven separate biomass fractions and their decay, apart from incorporating four main stages of anaerobic degradation, and dividing them into 31 processes, where 19 of them are differential and 12 are algebraic equations, and 33 groups of fractions, where 24 of them are the dynamic states variables, coupled to 105 kinetic and stoichiometric parameters (Batstone, et al., 2002; ifak system GmbH, 2005; Kleerebezem & van Loosdrecht, 2006; Schoen, 2009). The ADM1's structure is presented as a figure 3a. Conversion processes occurring during the anaerobic digestion may be generally characterized as two types of conversions: biochemical and physico-chemical [figure 3b].

Intracellular or extracellular enzymes generated by microorganisms are applied during the biochemical conversion. Those enzymes enhance bioavailability of substrates for digestion by microorganisms. The extracellular step include disintegration and hydrolysis, hence acidogenesis, acetogenesis, and methanogenesis belong to intracellular step. On the other side, non biological processes like liquid – liquid phase and also gas – liquid phase reactions are as physico-chemical conversions. Furthermore, with use of algebraic equations dissociation and association processes, which express concentration of hydrogen ions, free ammonia, VFA and carbon dioxide, are calculated. Consequently, with physico-chemical reactions all gaseous compounds ( $\text{CO}_2$ ,  $\text{CH}_4$ ,  $\text{H}_2$ , and water vapour) are evaluated (Batstone, et al., 2002; Schoen, 2009).



**b). conversion processes**



MS: monosaccharides  
 AA: amino acids  
 LCFA: long chain fatty acids  
 LCFA: LCFA base equivalent  
 Hva: valeric acid  
 Va: valerate

Hbu: butyric acid  
 Bu: butyrate  
 HPr: propionic acid  
 Pr: propionate  
 Hac: acetic acid  
 Ac: acetate

Figure 3. Conversion processes occurring during the anaerobic digestion (Schoen, 2009).

In ADM1 as a basis for all intracellular biochemical reactions Monod-type kinetics is used, which describes substrate uptake [ $\text{kg}_{\text{COD}_{\text{SC}}}\text{ m}^{-3}\text{d}^{-1}$ ]:

Equation 18

$$\rho = k_m \cdot \frac{S_C}{K_S + S_C} \cdot X \cdot I_1 \cdot I_2 \cdot \dots \cdot I_n$$

where

$k_m$  – maximum specific uptake rate [ $\text{kg}_{\text{COD}_{\text{SC}}}\text{ kg}_{\text{COD}_{\text{X}}}^{-1}\text{d}^{-1}$ ]

$S_C$  – substrate concentration [ $\text{kg}_{\text{COD}_{\text{SC}}}\text{ m}^{-3}$ ]

$K_S$  – half saturation coefficient [ $\text{kg}_{\text{COD}}\text{ m}^{-3}$ ]

$X$  – substrate specific biomass concentration [ $\text{kg}_{\text{COD}_{\text{X}}}\text{ m}^{-3}$ ]

$I_n$  – inhibition, e.g. hydrogen inhibition on acetogenic groups, free ammonia inhibition on aceticlastic methanogens, or pH on all groups.

The biochemical processes incorporated in ADM1 are prepared in accordance to Peterson matrix format. Rows of the matrix include processes, and as columns model components are stated. Production of each substance is identified via stoichiometric coefficients, and consumption is indicated by negative sign of stoichiometric coefficients, resulting in indication of the change with time. Consequently, the accumulation of a substance  $i$  is expressed as an addition of production, to consumption, and to reaction, resulting in following mass balance (Schoen, 2009):

Equation 19

$$\frac{dS_{liq,i}}{dt} = \frac{Q_{in} \cdot S_{in,i}}{V_{liq}} - \frac{Q_{out} \cdot S_{liq,i}}{V_{liq}} + \sum_{j=1-19} \rho_j \cdot v_{i,j}$$

where

$\rho_j$  – kinetic rate for process  $j$  [ $\text{kg}_{\text{COD}}\text{ m}^{-3}\text{d}^{-1}$ ]

$v_{i,j}$  – stoichiometric coefficient [-]

$S_i$  – component concentration [ $\text{kg}_{\text{COD}}\text{ m}^{-3}$ ]

$Q$ - flow [ $\text{m}^3\text{d}^{-1}$ ]

$V_{liq}$ - volume of the reactor [ $\text{m}^3$ ]

The gas phase rate equations, after assuming a constant gas volume, may be expressed via (Schoen, 2009):

Equation 20

$$\frac{dS_{gas,i}}{dt} = -\frac{Q_{gas} \cdot S_{gas,i}}{V_{gas}} + \rho_{T,i} \cdot \frac{V_{liq}}{V_{gas}}$$

where

$S_{gas,i}$ – gas concentration [ $\text{kmole m}^{-3}$ ]

$Q_{gas}$  – is the gas flow [ $\text{m}^3 \text{d}^{-1}$ ]

$V_{liq}$  – volume of the reactor [ $\text{m}^3$ ]

$V_{gas}$  – volume of the headspace [ $\text{m}^3$ ]

In addition to that, the kinetic transfer rate  $\rho_{T,i}$  to the gas headspace [ $\text{kmole m}^{-3} \text{d}^{-1}$ ] may be determined e.g. for carbon dioxide using this equation (Schoen, 2009):

Equation 21

$$\rho_{T,CO_2} = k_L a_{CO_2} \cdot (S_{liq,CO_2} - K_{H,CO_2} \cdot p_{gas,CO_2})$$

where

$k_L$  – dynamic gas-liquid transfer coefficient [ $\text{d}^{-1}$ ]

$K_{H,CO_2}$  – Henry's law equilibrium constant [ $\text{kmol m}^{-3} \text{bar}^{-1}$ ]

$p_{gas,CO_2}$  – partial pressure of the carbon dioxide gas phase [bar]

$S_{liq,CO_2}$  – concentration of the liquid carbon dioxide [ $\text{kmole m}^{-3}$ ].

The model includes a composite fraction ( $X_C$ ), which represents a complex substrate, which is degraded into carbohydrates ( $X_{Ch}$ ), proteins ( $X_{Pr}$ ), lipids ( $X_{Li}$ ) and inerts ( $X_i$ ) fractions during the disintegration step, in accordance to stoichiometric factors (Batstone, et al., 2002; ifak

system GmbH, 2005). The base chemical component unit in ADM1 is chemical oxygen demand (COD) [ $\text{kg}_{\text{COD}} \text{m}^{-3}$ ], inorganic carbon is represented in [ $\text{kmoleC m}^{-3}$ ], and nitrogen is represented in [ $\text{kmoleN m}^{-3}$ ] (Batstone, et al., 2002; Schoen, 2009). The Peterson matrix form of ADM1, along with variables, coefficients, and abbreviations are included in Appendix A.

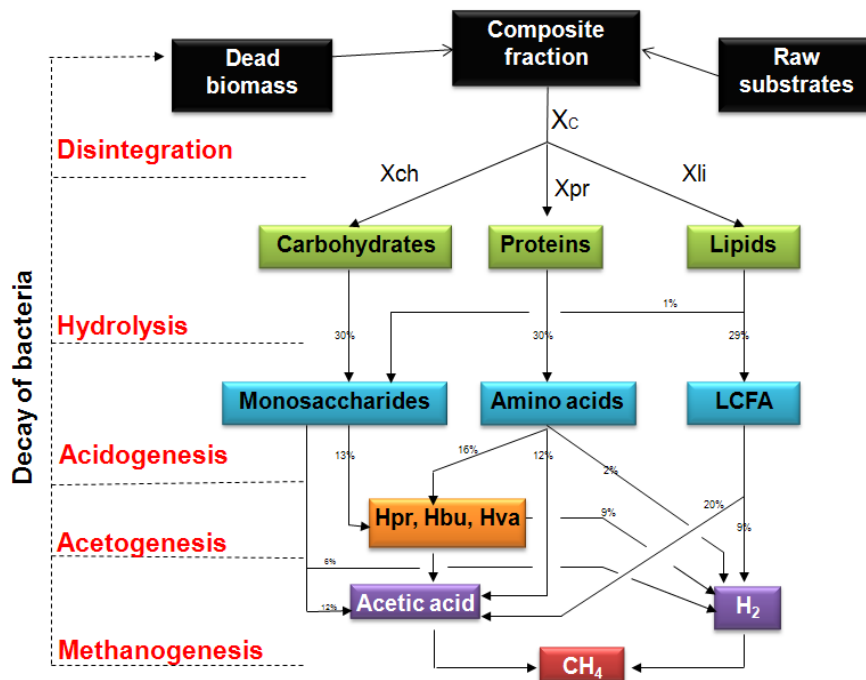


Figure 4. Biochemical processes included in Anaerobic Digestion Model No. 1 (Batstone, et al., 2002).

### 3.2.1.1. Modifications to the model (ADM1xp)

The ADM1 was updated by Wett et al. (Wett, et al., 2006) who added a new inert decay products fraction ( $X_P$ ) whose formation is described by a decayed biomass factor ( $f_P$ ). As a consequence, decayed biomass is not a feed to the composite fraction ( $X_C$ ), as prepared in the original ADM1, but part is accumulating as an inactive fraction ( $X_P$ ), and part is split among carbohydrates ( $X_{Ch}$ ), proteins ( $X_{Pr}$ ) and lipids ( $X_{Li}$ ) fractions, as stoichiometrically describe by Wett et al. (Wett, et al., 2006). According to Koch et al. (Koch, et al., 2010), this update ensures that nutrient mineralization is incorporated into the model. Accordingly, this update was incorporated by IFAK (ifak system GmbH, 2005) to the original ADM1, and it is indicated with a new name ADM1xp. The modified ADM1xp was used in this research.

### 3.2.1.2. Kinetic constants' describing disintegration and hydrolysis's phase

ADM1 was originally developed to describe anaerobic digestion of sludge from waste water treatment plants. The degradation of complex organic material is assumed to pass four stages starting from complex organic materials to monomers, to gaseous compounds.

The extracellular biological and non-biological breakdown of complex organic substrates to soluble substrates is expressed as disintegration and hydrolysis phase. The disintegration phase represents degradation of composite fraction ( $X_C$ ) into carbohydrates ( $X_{Ch}$ ), proteins ( $X_{Pr}$ ), lipids ( $X_{Li}$ ) and inerts ( $X_i$ ) fractions. Further enzymatic degradation of the non-inert fractions into monosaccharides ( $S_{SU}$ ), amino acids ( $S_{AA}$ ) and long chain fatty acids ( $S_{FA}$ ) represents the hydrolysis stage (Batstone, et al., 2002). This approach has been widely applied (Gali, et al., 2009; Schoen, et al., 2009; Wett, et al., 2006).

Disintegration and hydrolysis are described in ADM1 using first order kinetics. The disintegration kinetic constant for composite degradation is described as  $k_{Dis}$ , the hydrolysis constant for the hydrolysis of carbohydrates, lipids and proteins are  $k_{Hyd\_Ch}$ ,  $k_{Hyd\_Li}$  and  $k_{Hyd\_Pr}$ , respectively (Batstone, et al., 2002). The values for hydrolysis and disintegration phase kinetic constants as proposed by Batstone et al. (Batstone, et al., 2002) are listed in Table 9. The hydrolysis was reported to be the rate limiting step of the anaerobic degradation (Garcia-Heras, 2003; Flotats, et al., 2006), and as noted by Feng et al. (Feng, et al., 2006), ADM1's default values for solids are leading to the elimination of the influence of the hydrolysis step on the simulation. Consequently, as proposed by Garcia-Heras (Garcia-Heras, 2003), there is a need for further experimental validation of disintegration and hydrolysis kinetic constants. Since the kinetic constants summarized by Vavilin et al. (Vavilin, et al., 2008) are much lower than the ADM1's default values, indicating the possible range of this parameters (Table 9). Christ et al. (Christ, et al., 2000) also proposed much lower values for disintegration and hydrolysis constants. Furthermore, Wichern et al. (Wichern, et al., 2008) performed a calibration of ADM1 values during their investigation of cattle manure and lowered the disintegration constant from a default value of  $0.4 \text{ d}^{-1}$  to  $0.05 \text{ d}^{-1}$ , however, for monofermentation of grass silage, Wichern et al. (Wichern, et al., 2009), increased the disintegration constant to  $1.0 \text{ d}^{-1}$ . Therefore, there is a need for direct determination of the kinetic constants for substrates commonly used for biogas production. Table 9 presents hydrolysis and disintegration kinetic coefficients of the first-order rate for different substrates found in the literature.

**Table 9. Kinetic constant values found in the literature for mesophilic digestion of different substrates.**

<b>Description</b>	<b>References</b>	<b>k<sub>Dis</sub></b>	<b>k<sub>Hyd_Ch</sub></b>	<b>k<sub>Hyd_Pr</sub></b>	<b>k<sub>Hyd_Li</sub></b>
Unit	-	[d <sup>-1</sup> ]	[d <sup>-1</sup> ]	[d <sup>-1</sup> ]	[d <sup>-1</sup> ]
ADM1 values for solids	(Batstone, et al., 2002)	0.5	10	10	10
ADM1 values for high rate	(Batstone, et al., 2002)	0.4	0.25	0.2	0.1
ADM1 values for cattle manure	(Vavilin, et al., 1997)	0.13	-	-	-
ADM1 values for pig manure	(Vavilin, et al., 1997)	0.096	-	-	-
ADM1 values for food waste	(Vavilin, et al., 1998)	0.41	-	-	-
The most common values	(Garcia-Heras, 2003)	-	0.5 – 2.0	0.25 – 0.8	0.1 – 0.7
Different particular substances	(Christ, et al., 2000)	-	0.025 – 0.200	0.015 – 0.075	0.005 – 0.010
Grass silage	(Wichern, et al., 2008)	1	-	-	-
Grass silage	(Wichern, et al., 2009)	0.26	-	-	-
Grass silage	(Koch, et al., 2009)	-	0.6	0.6	0.6
Grass silage	(Koch, et al., 2010)	-	0.14/0.5	0.8	0.14/0.5
Agro-residues	(Gali, et al., 2009)	0.15	10	10	10
Mais silage	(Luebken, et al., 2010)	-	0.7/0.18	0.3	-
Corn stover	(Hu & Yu, 2005)	-	0.94	0.94	0.94
Crops and crops residues	(Lehtomaki, et al., 2005)	-	0.009-0.094	0.009-0.094	0.009-0.094

### 3.2.2. Literature review on the ADM1's usage

Due to its capability to describe the biogas production rate and composition, since 2002 the ADM1 was commonly used as an anaerobic degradation model for different substances and process flows. Parker (Parker, 2005) summarized earlier modifications and applications of ADM1, and he indicated that the precise characterization of the sludge is crucial for correct modelling. In addition to that, he indicated that in almost all cases the calculated results were in line with experimental results, apart from VFAs concentration for digesters with short SRTs, and also impact of pH on biokinetic rates for the acid-consuming bacteria was over-predicted. Furthermore, Luebken et al. (Luebken, et al., 2007) recommended Weender analysis with van Soest (Naumann & Bassler, 1993; van Soest & Wine, 1967) extension for analysing substrates composition, while testing inhomogeneous substrates, despite depending on COD measurements. He also applied ADM1 for calculating methane formation from cattle manure and renewable energy crops. The transferability of the substrates analysis, directly to the ADM1 was further presented by Koch et al. (Koch, et al., 2010). Methodology of splitting substrate's total COD to obtain required parameters for mathematical modelling was proposed by Girault et al. (Girault, et al., 2012), followed by Jimenez et al. (Jimenez, et al., 2014) technique of municipal sludge characterization, required to satisfy ADM1's requirements.

ADM1 was successfully used for calculating anaerobic degradation of sludge. Yasui et al. (Yasui, et al., 2008) modified structure of ADM1 to better represent degradation of primary sludge solid, followed by Derbal et al. (Derbal, et al., 2009) who used ADM1 for modelling co-digestion of municipal solid waste with activated sludge. Astals et al. (Astals, et al., 2013) evaluated seven different types of sludge from different wastewater treatment plants, to explain sludge characterisation and biodegradability, and he also proposed a methodology for ADM1's preparation, before calculating sludge's anaerobic degradation. Furthermore, Zaher et al. (Zaher, et al., 2007) presented a method of coupling model describing waste water treatment (ASM1) with ADM1, followed by Nopens et al. (Nopens, et al., 2009) further proposal of methodology for connecting both models.

On the other hand, the model was also implemented for investigation of pre-treatment methods. Ramirez et al. (Ramirez, et al., 2009a) proposed modification of ADM1's disintegration/hydrolysis phase, helpful for correct calculation of thermally pre-treated waste activated sludge during the thermophilic fermentation. Later Wett et al. (Wett, et al., 2010) evaluated with help of ADM1 two pre-treatment techniques, Thermo-Pressure-Hydrolysis and ball milling, of waste activated sludge. Concept of application of biochemical methane potential (BMP) for ADM1's parameters calibration was evaluated by Souza et al. (Souza, et

al., 2013a), and afterwards Souza et al. (Souza, et al., 2013b) investigated impact of pre-treatment and hydraulic retention time (HRT) on the effectiveness. In addition to that, Ramirez et al. (Ramirez, et al., 2009b) extended ADM1 to describe microbial diversity. Furthermore, acidification of the reactor caused by interactions between microorganisms were examined by Rivas-Garcia et al. (Rivas-Garcia, et al., 2013). On the other side, model was used for assessment of long chain fatty acids inhibition (Zonta, et al., 2013) and for evaluation of thermophilic fermentation (Palatsi, et al., 2010). Furthermore, ADM1 was applied for evaluation the inhibition of three pharmaceuticals (Fountoulakis, et al., 2008) and chlorophenols (Puyol, et al., 2012). Impact of the particle size of municipal solid waste in co-digestion with sewage sludge was assessed by Esposito et al. (Esposito, et al., 2011).

Modification of ADM1 were concentrated on enhancement of bioaccessibility of particulate organic matter representation (Mottet, et al., 2013), incorporating fermentable soluble substrates (Garcia-Gen, et al., 2013) including degradation of phenol compounds and homologues from olive mill wastewater and solid waste (Boubaker & Ridha, 2008; Fezzani & Cheikh, 2009), suspension and settling of organic matter (Yu, et al., 2013). Integrating of solids in modelling the anaerobic digestion was also accomplished (Zaher, et al., 2009), and the role of total solids was investigated by Abbassi-Guendouy et al. (Abbassi-Guendouz, et al., 2012). In order to calculate dry anaerobic of municipal solid waste, Bollon et al. (Bollon, et al., 2011) also modified the model. Methane potential from acidified sorghum extract coming from hydrogen generating reactor was also evaluated with use of ADM1 by Antonopolou et al. (Antonopoulou, et al., 2012a), and also investigated application of ADM1 framework to calculate hydrogen production from sweet sorghum biomass (Antonopoulou, et al., 2012b). In addition to that, earlier hydrogen fermentation was presented with use of modified ADM1 (Gadhamshetty, et al., 2010) and Ntaikou et al. (Ntaikou, et al., 2010) evaluated presentation of hydrogen generation by *Ruminococcus albus* from sweet sorghum extract by ADM1.

This biochemical model was also successfully applied to different anaerobic processes, like temperature-phased anaerobic digestion (TPAD) (Lee, et al., 2009), two-stage high solid system (Yu, et al., 2012), or anaerobic sequencing batch reactor with microbial storage (Schimada, et al., 2007), and also high rate UASB reactors (Mu, et al., 2008). Model was also modified by Xiao et al. (Xiao, et al., 2013) to represent and addition of zero-valent iron (ZVI), which enhance anaerobic digestion's performance of the less biodegradable pollutants. Modified ADM1 was also presented as a tool for supporting decision-making and planning of biogas power plants (Zhou, et al., 2011). Garcia-Dieiguez et al. (Garcia-Dieiguez, et al., 2011) used the mathematical model for evaluating performance of the process controller applied at biogas power plants. Bensmann et al. (Bensmann, et al., 2013) prepared

an assessment of biogas plants' configurations, and in order to receive unified results he used ADM1. This model was further applied for failure diagnosis of anaerobic reactor by Martinez-Sibaja et al. (Martinez-Sibaja, et al., 2013), steady state operations and recovery from disturbances (Bornhoeft, et al., 2012). Anaerobic Digestion Model No. 1 was applied for substrates like:

- mono-fermentation of grass silage (Thamsirioj & Murphy, 2011),
- condensate effluent generated in a sulphite pulp mill (Silva, et al., 2009),
- microalgae (Mairet, et al., 2011) and blue algae (Yuan, et al., 2014) ,
- opium alkaloid effluents (Dereli, et al., 2010)
- dairy manure and spent mushroom substrate (Shi, et al., 2014),
- winery effluent wastewater (Garcia-Dieguez, et al., 2013),
- co-digestion of pig manure and glycerine (Astals, et al., 2011),
- traditional Chinese medicine wastewater (Chen, et al., 2009),
- effluent from hydrogen production from olive pulp (Koutrouli, et al., 2009),
- grass silage (Koch, et al., 2009; Koch, et al., 2010; Wichern, et al., 2009),
- agro-waste (Gali, et al., 2009),
- agricultural substrates (Luebken, et al., 2010),
- cattle manure (Myint, et al., 2007; Schoen, et al., 2009; Wichern, et al., 2008),
- cattle manure and maize (Amon, et al., 2007)
- cattle manure and co-substrates (Luebken, et al., 2007).

### 3.3. Thermodynamic modelling of gas solubility

#### 3.3.1. Vapour-liquid phase equilibrium

On the  $PT$ -diagram (figure 5) melting, vapour pressure and sublimation pressure curves are presented, indicating the phase transition's border lines, where two or three phases can coexist. This phenomena has an crucial significance for thermal separations methods applied in technical processes. Therefore for following this research, it is crucial to understand the condition, where vapour-liquid phases are in equilibrium, and the explanation is based on (Gmehling, et al., 2012).

At vapour-liquid equilibrium, both phases have the same pressure (mechanical equilibrium) and temperature (thermal equilibrium), and then are called saturated vapour and saturated liquid. As an effect of this phenomena, when a saturated pure liquid is heated up at constant pressure, no increase in the temperature can be observed ( $T = \text{constant}$ ), but vapour is generated, to the moment when the whole liquid is vaporized. The opposite occurs, when

saturated vapour is cooled down. As a consequence, vapour-liquid equilibrium conditions may be described as (Gmehling, et al., 2012):

Equation 22

$$g^L = g^V, \text{ where}$$

$g^L$  – the specific Gibbs energy of boiling liquid [ $\text{J mol}^{-1}$ ],

$g^V$  – the specific Gibbs energy of saturated vapour [ $\text{J mol}^{-1}$ ].

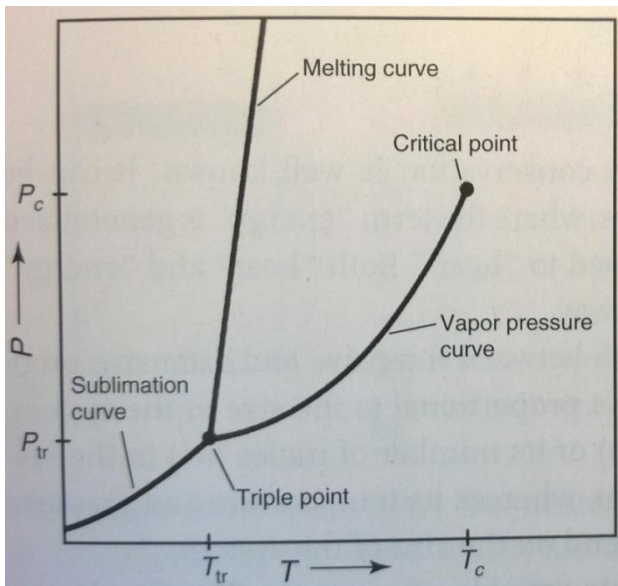


Figure 5. *PT*-diagram, representing triple point, and change phase curves (Gmehling, et al., 2012).

During the evaporation, when both phases coexist, temperature ( $T$ ) and pressure ( $P$ ) are constant, therefore characterization of the state of a pure substance via  $P$  and  $T$  is not sufficient. Consequently vapour fraction  $q$  was introduced (Gmehling, et al., 2012):

Equation 23

$$q = \frac{n^V}{n^L + n^V}, \text{ where}$$

$n^V$  – number of moles in vapour phase

$n^L$  – number of moles in liquid phase

Applying this equation will result in  $q = 0$  for boiling liquid, and  $q = 1$  for saturated vapour .

Vapour-liquid equilibrium for mixtures is obtained if temperature ( $T$ ), pressure ( $P$ ), and chemical potential ( $\mu_i$ ) of each component in the mixture is equal in both phases (Gmehling, et al., 2012):

Equation 24

$$T^\alpha = T^\beta = \dots = T^\varphi$$

Equation 25

$$P^\alpha = P^\beta = \dots = P^\varphi$$

Equation 26

$$\mu_i^\alpha = \mu_i^\beta = \dots = \mu_i^\varphi$$

Taking under consideration that chemical potential of a component is equal to partial molar Gibbs energy  $\bar{g}_i$ , the condition for phase equilibrium can also be expressed via (Gmehling, et al., 2012):

Equation 27

$$\bar{g}_i^\alpha = \bar{g}_i^\beta = \dots = \bar{g}_i^\varphi$$

In addition, because the fugacity  $f_i$  of a component is directly related to  $\bar{g}_i$  via the equation (Gmehling, et al., 2012):

Equation 28

$$\bar{g}_i = RT \ln \frac{f_i}{f^0}$$

It was shown by Lewis, that the following equation can be used instead of equation 27 (Gmehling, et al., 2012):

Equation 29

$$f_i^\alpha = f_i^\beta = \dots = f_i^\varphi$$

For practical applications auxiliary quantities were developed, which include activity coefficients  $\gamma_i$  and fugacity coefficients  $\varphi_i$ . The fugacity coefficient of component  $i$  is the ratio of fugacity of this component in the respective phase to the system pressure and

product of its mole fraction of this phase, whereas partial pressure  $p_i$  may substitute the denominator for the vapour phase (Gmehling, et al., 2012):

Equation 30

$$\varphi_i^L \equiv \frac{f_i^L}{x_i^P}$$

Equation 31

$$\varphi_i^V \equiv \frac{f_i^V}{y_i^P} \equiv \frac{f_i^V}{p_i}$$

On the other side, in the activity coefficient's expression the observed fugacity is divided by the fugacity calculated as applied by Raoult's law (Gmehling, et al., 2012):

Equation 32

$$\gamma_i \equiv \frac{f_i}{x_i f_i^0}$$

### 3.3.2. Physical solubility

Following (Gmehling, et al., 2012), there are two possible ways of describing the physical solubility. In the first one, phase equilibria is described with use of fugacity coefficient in the following relations of vapour-liquid equilibrium:

Equation 33

$$x_i \varphi_i^L = y_i \varphi_i^V$$

$y_i$  – mole fraction in vapour phase

$x_i$  – mole fraction in liquid phase

In this equation fugacity coefficients, which are describing deviation from ideal gas behaviour, are applied instead of pure liquid standard fugacity and activity coefficients. Moreover, fugacity coefficients can be calculated with use of equations of state that typically require mixing rules for the model parameters (Gmehling, et al., 2012).

However, because weak electrolytes are considered in this research, the second approach, where Henry constant as standard fugacity is applied, was used instead (Gmehling, et al., 2012):

$$P \cdot y_i \cdot \varphi_i = H_{ij} \cdot x_i \cdot \gamma_i^*, \text{ where}$$

$\varphi_i$  – fugacity coefficient in vapour phase

$H_{ij}$  - Henry's law constant of solute (*i*) in solvent (*j*) [Pa]

$\gamma_i^*$  - activity coefficient of solute in the solvent

In this equation, the infinite diluted behaviour extrapolated to the hypothetical pure dissolved gas was chosen as reference and the activity coefficient is unity at  $X_i = 0$ . It holds:

$$\gamma_i^* = \frac{\gamma_i}{\gamma_i^\infty}$$

And

$$H_{ij} \approx P_i^S \cdot \gamma_i^\infty, \text{ where}$$

$P_i^S$  - vapour pressure of component *i* [Pa]

### 3.3.3. Chemical solubility

The chemical solubility, which is the chemical equilibrium for the aqueous phase chemical reactions between water, amines, acid gases (e.g. CO<sub>2</sub>), together with physical solubility are representing the overall acid gases solubility in aqueous amines solutions. For representing chemical absorption, all chemical equilibria together with reaction kinetics and mass transfer are required (Gmehling, et al., 2012). As further presented on figure 6 (DDBST GmbH, 2014; Gmehling, et al., 2012) at lower partial pressure of the absorbed gas, chemical solubility is much more efficient, than physical solubility, and consequently it is important to consider both of them during the design process.

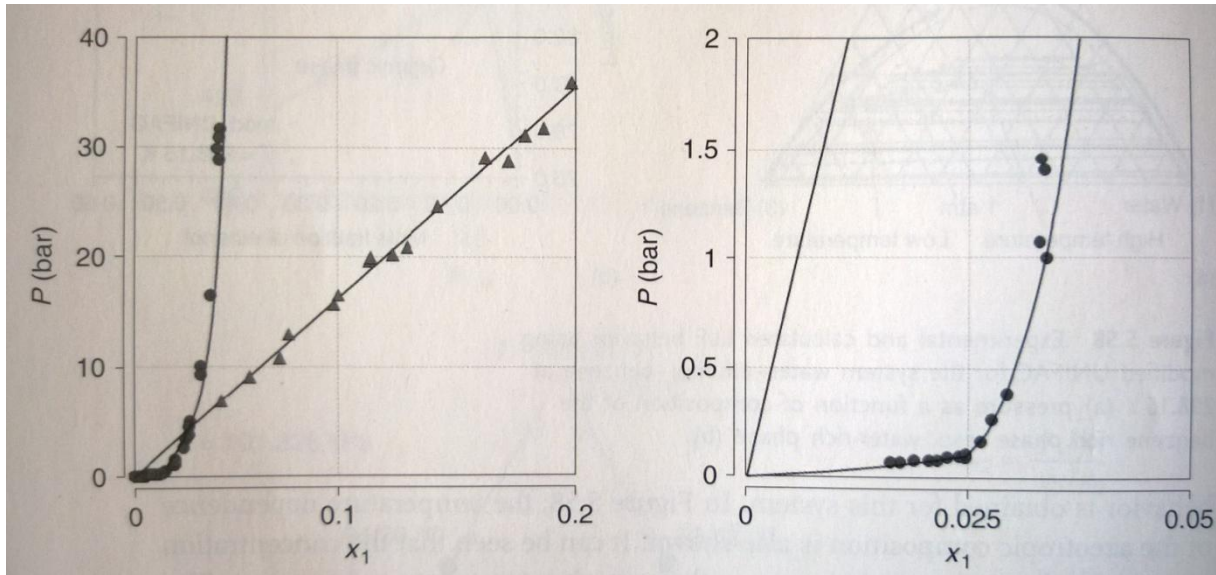


Figure 6. Carbon dioxide solubility in methanol (▲ - physical absorption) and 30 mass %aqueous monoethanolamine solution (● - chemical absorption) at  $T = 313.15\text{K}$  (DDBST GmbH, 2014; Gmehling, et al., 2012)

As soon as the Gibbs energy is at lowest value, the chemical equilibrium is reached, at constant pressure and constant temperature. The Gibbs energy change is describe via (Gmehling, et al., 2012):

Equation 37

$$dG = -SdT + VdP + \sum \mu_i dn_i$$

where

$S$  – entropy

$V$  – volume [ $\text{m}^3$ ]

$\mu_i$  - chemical potential of component  $i$  [ $\text{J mol}^{-1}$ ]

$n_i$  - number of moles of component  $i$  [mol]

Furthermore, this equation may be simplified at  $P = \text{const.}$  and  $T = \text{const.}$  to :

Equation 38

$$dG = \sum \mu_i dn_i$$

The general form of chemical equilibrium, as derived by (Gmehling, et al., 2012):

$$\sum_i v_i \mu_i = 0$$

where

$v_i$  - stoichiometric coefficient of component  $i$

The chemical potential of component  $i$  may be expressed via (Gmehling, et al., 2012):

$$\mu_i = \mu_i^0 + RT \ln \left( \frac{f_i}{f_i^0} \right)$$

where:

$\mu_i^0$  - chemical potential in the standard state [J mol<sup>-1</sup>],

$f_i$  - fugacity in the real state [Pa],

$f_i^0$  - fugacity in the standard state [Pa].

Additionally, the equation can be simplified, by introduction of chemical equilibrium constant  $K$  (Gmehling, et al., 2012):

$$K = \prod \left( \frac{f_i}{f_i^0} \right)^{v_i}$$

Combining equations 39, 40 and 41 we finally obtain formula to calculate the chemical equilibrium constant (Gmehling, et al., 2012):

$$\Delta g_R^0 = \sum_i v_i \Delta g_{f,i}^0 = \sum_i v_i \mu_i^0 = -RT \sum_i \ln \left( \frac{f_i}{f_i^0} \right)^{v_i} = -RT \ln(K)$$

where:

$\Delta g_R^0$  - standard Gibbs energy of reaction,

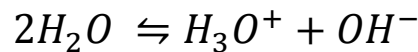
$\Delta g_{f,i}^0$  - molar Gibbs energy of formation.

Two different types of electrolyte can be distinguished (Austgen, 1989; Gmehling, et al., 2012):

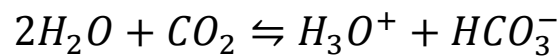
- Strong electrolytes, which dissociate completely in water
- Weak electrolytes, which dissociate only partially in water

This research is concentrated on carbon dioxide and alkanolamines, which both are weak electrolytes. Therefore, chemical reactions occurring for the system acid gas ( $CO_2$ ) – alkanolamines –  $H_2O$  can be summarized as follows, where here a secondary alkanolamines are represented with general formula ( $R_2NH$ ) (Austgen, 1989; Aspen Technology Inc., 2008):

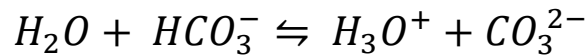
Equation 43



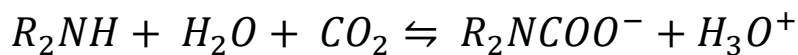
Equation 44



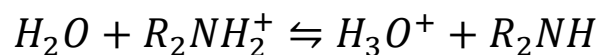
Equation 45



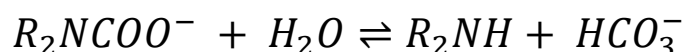
Equation 46



Equation 47



Reactions describe ionization of water (equation 43), dissociation of carbon dioxide (equation 44) dissociation of bicarbonate (equation 45), and amine deprotonation (equation 47). In addition to that, equation 46 represent carbamate formation, which is possible only for primary and secondary amines (Caplow, 1968). In addition to that, carbamate may convert back to bicarbonate, depending on the carbamate stability. This reaction is crucial for correct evaluation of amine's efficiency, and desorption sage, since less energy is required for removal of carbon dioxide in form of bicarbonate, than carbamate. As a consequence, this reaction is expressed via (Austgen, 1989; Suda, et al., 1996):



### 3.3.4. The Peng-Robinson Equation of State

Cubic equations of states as proposed by van der Waals (van der Waals, 1873) are important currently used type of equations of state (EOS), including the Redlich-Kwong EOS (Redlich & Kwong, 1949), the Soave-Redlich-Kwong EOS (Soave, 1972) the Peng Robinson EOS (Peng & Robinson, 1976), which are commonly used for calculating behaviour of real gases, due to their robustness and uncomplicated application to mixtures. The van der Waals EOS and all modifications follow the theory of an additive separate contributions (Gmehling, et al., 2012) :

$$z = z^{rep} + z^{att}, \text{ where}$$

$Z$  – compressibility factor, reflecting real gas variation from the ideal behaviour

$Z^{rep}$  – the intrinsic volume of the molecule; repulsion contribution

$Z^{att}$  – attractive intermolecular forces

Explanation of the condensation, vaporization and the two-phase region was achieved by van der Waals EOS, which has the form of (Gmehling, et al., 2012):

$$z \equiv \frac{Pv}{RT}$$

or

$$P = \frac{RT}{v - b} - \frac{a}{v^2}$$

where

$a$  – attractive parameter [ J m<sup>3</sup> mol<sup>-2</sup>]

$b$  – repulsive parameter [ $\text{m}^3 \text{mol}^{-1}$ ]

$P$  – total pressure [Pa]

$R = 8.314471$  [ $\text{J mol}^{-1} \text{K}^{-1}$ ] - universal gas constant

$T$  – absolute temperature [K]

$v$  – specific volume [ $\text{m}^3 \text{mol}^{-1}$ ]

Parameters  $a$  and  $b$  are typically determined for each substance from critical parameters  $T_C$  and  $P_C$ , as presented for Peng-Robinson EOS (PREOS) (Gmehling, et al., 2012), which is one of the modifications of the van der Waals EOS is the PREOS (Gmehling, et al., 2012; Peng & Robinson, 1976):

Equation 52

$$z = \frac{v}{v - b} - \frac{a(T) v}{RT[v(v + b) + b(v - b)]}$$

Equation 53

$$P = \frac{RT}{v - b} - \frac{a(T)}{v(v + b) + b(v - b)}$$

Equation 54

$$a(T) = 0.45724 \frac{R^2 T_c^2}{P_c} \alpha(T)$$

with

Equation 55

$$\alpha(T) = [1 + (0.37464 + 1.54226\omega - 0.26992\omega^2)(1 - T_r^{0.5})]^2$$

Equation 56

$$b = 0.0778 \frac{RT_c}{P_c}$$

$$T_r \equiv \frac{T}{T_c}$$

where

$T_r$  – reduced form of the temperature [K]

$T_c$  – critical temperature [K]

$P_c$  – critical pressure [Pa]

$\omega$  - acentric factor [-]

### 3.3.5. The electrolyte Non Random Two Liquid (eNRTL) model

When using the activity coefficient approach for physical solubility calculation, excess Gibbs energy models are required (Gmehling, et al., 2012). The Electrolyte-NRTL (eNRTL), an excess Gibbs energy expression, presented by Chen and Evans (Chen & Evans, 1986), extended by Mock et al. (Mock, et al., 1986) to mixed solvent electrolyte systems, is implemented in ASPEN Plus® V8.0 engineering software as ELECNRTL (Aspen Technology Inc., 2012) and used in this research. The proposed eNRTL model is based on two contributions. The first one describes long and middle range interactions, describing ion-ion interactions' outside the immediate neighbourhood of central ionic species. For this contribution Chen and Evans (Chen & Evans, 1986) implemented Pitzer's reformulation of the Debye-Hueckel formula (Pitzer, 1980). The Debye-Hueckel formula is based on Debye-Hueckel Limiting Law, obtained according to those assumption (Gmehling, et al., 2012; Polka, 1993):

- i. *“Only the electrostatic forces between the ions are regarded. All the other forces are negligible”.*
- ii. *“The electrostatic interaction energies are small in comparison to the thermal energies”.*
- iii. *“The ions are regarded as punctual charges with a spherical field”.*
- iv. *“The dielectric constants of the solution is equal to the one of the solvent”.*
- v. *“The electrolyte is completely dissociated”.*
- vi. *“The distribution of the ions around a center ion is governed by Boltzmann's law due to the electric potential:”*

$$\frac{c_i(r)}{c_i^{(0)}} = \exp\left(\frac{-z_i e \varphi^{el}(r)}{kT}\right), \text{ where}$$

$c_i(r)$  - volume concentration of ionic species in a volume element at distance  $r$  from the centre

$c_i^{(0)}$  - volume concentration of ionic species

$\varphi^{el}(r)$  - the electric potential at distance  $r$  from the centre

$Z_i$  – charge of ion  $i$

$e$ - elementary charge;  $e = 1.602189 \cdot 10^{-19}$  [C]

$k$  - Boltzmann's constant;  $k = 1.38048 \cdot 10^{-23}$  [J K<sup>-1</sup>]

Derivation presented in literature (Maurer, 2004; Moore & Hummel, 1986), which follows those assumptions, of an expression for mean activity coefficient equals to (Gmehling, et al., 2012):

$$\log \gamma_i^m = A_m z_i^2 I^{\frac{1}{2}}, \text{ where}$$

$I$  - ionic strength [mol kg<sup>-1</sup>], defined as:

$$I = \frac{1}{2} \sum_i m_i z_i^2$$

or based on the mole fractions:

$$I = \frac{1}{2} \sum_i x_i z_i^2$$

$A_m$  - characteristic of the solvent [ $\text{kg}^{0.5} \text{mol}^{-0.5}$ ], defined as

Equation 62

$$A_m(T) = 1.8248 \cdot 10^6 \frac{\sqrt{\frac{\rho_{solv}}{\left(\frac{g}{cm^3}\right)}}}{\left(\frac{T}{K} \varepsilon_r\right)^{1.5}}$$

where

$\varepsilon_r$  – reduced property of dielectric constant [ $\text{A}^2 \text{s}^4 \text{kg}^{-1} \text{m}^{-3}$ ]

In the electrolyte-NRTL model, a modification of Debye-Hueckel term (Pitzer, 1980) is applied (Gmehling, et al., 2012), that includes so called middle range interactions in electrolyte solutions of non-infinite dilution.

Equation 63

$$\ln \gamma_{i,DH}^* \frac{-A_\emptyset}{\sqrt{\frac{M_{solv}}{\left(\frac{kg}{mol}\right)}}} \left[ \left( \frac{2z_i^2}{14.9} \right) \ln(1 + 14.9\sqrt{I_x}) + \frac{z_i^2 \sqrt{I_x} - 2I_x^{1.5}}{1 + 14.9\sqrt{I_x}} \right]$$

where parameter  $A_\emptyset$  is obtained from formula:

$$\begin{aligned}
A_{\phi} = & -61.44534 \exp\left(\frac{\left(\frac{T}{K}\right) - 273.15}{273.15}\right) \\
& + 2.864468 \left[ \exp\left(\frac{\left(\frac{T}{K}\right) - 273.15}{273.15}\right) \right]^2 \\
& + 183.5379 \ln\left(\frac{\left(\frac{T}{K}\right)}{273.15}\right) - 0.6820223 \left(\frac{T}{K} - 273.15\right) \\
& + 0.0007875695 \left[\left(\frac{T}{K}\right)^2 - 273.15\right]^2 + 58.95788 \frac{273.15}{\left(\frac{T}{K}\right)}
\end{aligned}$$

“As the reference state of the electrolyte components refers to the infinitely diluted solution in pure water” (Gmehling, et al., 2012), the Born expression (Robinson & Stokes, 1970), which includes the difference between the dielectric constants of solvent mixture and water is used for correlating Pitzer’s reformulation of Debye-Hueckel via (Gmehling, et al., 2012):

$$\Delta_{Born} g^E = \frac{e^2 N_A}{8\pi \epsilon_0} \left( \frac{1}{\epsilon_{solv}} - \frac{1}{\epsilon_{H2O}} \right) \sum_i x_i \frac{z_i^2}{r_i}$$

where

$N_A = 6.023 \cdot 10^{23}$  - Avogadro’s number

$\epsilon$  –dielectric constant [ $A^2 s^4 kg^{-1} m^{-3}$ ]

$e = 1.602189 \cdot 10^{-19}$  [C] – elementary charge

$r_i = 3 \cdot 10^{-10}$  [m] (default value) - ionic radius

and the dielectric constants’ mixing rule is obtained from:

$$\varepsilon_{solv} = \sum_i w_i \varepsilon_i$$

where

$w_i$  - weight fraction of component  $i$ ,

and the pure solvent dielectric constants are obtained as a temperature dependent:

$$\varepsilon_i(T) = A_i + B_i \left( \frac{1}{T} - \frac{1}{298.15K} \right)$$

On the other side, the Non-Random Two Liquid (NRTL) theory developed by Renon and Prausnitz (Renon & Prausnitz, 1968) represents the short range interactions also present in non-electrolyte mixtures. It is based on the theory of like-ion repulsion and electroneutrality. According to this assumption, in a liquid phase where electrolytes are present three types of cells are to be recognized as presented on the Figure 7. Depending on the ion in the centre (Gmehling, et al., 2012):

- If a neutral molecule is centrally located, the surrounding can consist of anions, cations, and other molecules
- If an anion is centrally located, the surrounding can consist only of cations or other molecules, due to strong repulsive forces
- If a cation is centrally located, the surrounding can consist of only anions or other molecules, due to strong repulsive forces

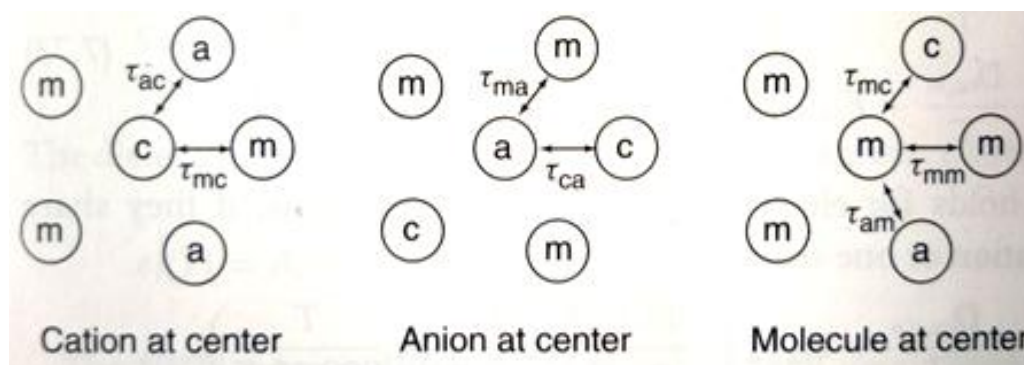


Figure 7. Like-ion repulsion and electroneutrality assumption (Gmehling, et al., 2012).

As a consequence, for the local concentrations it can be determined that (Gmehling, et al., 2012):

- Cation in the centre:

Equation 68

$$\Theta_{mc} + \Theta_{ac} = 1$$

- Anion in the centre:

Equation 69

$$\Theta_{ma} + \Theta_{ca} = 1$$

- Molecule in the centre:

Equation 70

$$\Theta_{cm} + \Theta_{am} + \Theta_{mm} = 1$$

- Electroneutrality of cell, with a molecule in the centre (Chen & Evans, 1986; Gmehling, et al., 2012):

Equation 71

$$\Theta_{am}|z_a| = \Theta_{cm}z_c$$

where

Z – charges of anions or cations

$\Theta_{ij}$  – local concentration of species *i* around species *j*

The correlation of overall mole fractions to local concentration is defined via (Gmehling, et al., 2012; Renon & Prausnitz, 1968):

Equation 72

$$\frac{\Theta_{ji}}{\Theta_{ii}} = \frac{x_j C_j}{x_i C_i} G_{ji}$$

where

$C_i = |z_i|$  - charge of ion *i* for ions

$C_i = 1$  – for molecules,

and

Equation 73

$$G_{ij} = \exp(-\alpha_{ij}\tau_{ij})$$

where, the nonrandomness factors  $\alpha_{ij}$  is usually set to 0.2 (Austgen, et al., 1989; Chen & Evans, 1986; Gmehling, et al., 2012), the interaction parameters  $\tau_{ij}$  are obtained as a temperature dependent(Austgen, et al., 1989; Gmehling, et al., 2012; Renon & Prausnitz, 1968):

Equation 74

$$\tau_{ij} = a_{ij} + \frac{b_{ij}}{T} + c_{ij} \ln\left(\frac{T}{K}\right) + d_{ij}T$$

where,

$a_{ij}, b_{ij}, c_{ij}, d_{ij}$  - binary interaction energy parameters.

In addition to binary interaction energy parameters, pair parameters are describing the interaction between molecules and electrolytes via (Gmehling, et al., 2012):

Equation 75

$$\tau_{m,ca} = C_{m,ca} + \frac{D_{m,ca}}{T} + E_{m,ca} \left( \left( \frac{298.15 K - T}{T} \right) + \ln \left( \frac{T}{298.15K} \right) \right)$$

Equation 76

$$\tau_{ca,m} = C_{ca,m} + \frac{D_{ca,m}}{T} + E_{ca,m} \left( \left( \frac{298.15 K - T}{T} \right) + \ln \left( \frac{T}{298.15K} \right) \right)$$

Equation 77

$$\begin{aligned} \tau_{ca,c'a} = & C_{ca,c'a} + \frac{D_{ca,c'a}}{T} + E_{ca,c'a} \left( \left( \frac{298.15 K - T}{T} \right) \right. \\ & \left. + \ln \left( \frac{T}{298.15K} \right) \right) \end{aligned}$$

Equation 78

$$\tau_{ca,ca'} = C_{ca,ca'} + \frac{D_{ca,ca'}}{T} + E_{ca,ca'} \left( \frac{298.15 K - T}{T} \right) + \ln \left( \frac{T}{298.15 K} \right)$$

Finally combination of both interactions, short-range and long-rang, results in (Aspen Technology Inc., 2012; Austgen, et al., 1989; Chen & Evans, 1986; Gmehling, et al., 2012):

Equation 79

$$g^E = g_{Debye-Huckel}^E + \Delta_{Born} g^E + g_{NRTL}^E$$

### 3.3.6. Literature review on the eNRTL's usage

The eNRTL's has been widely applied for calculating activity coefficients, necessary for modelling carbon dioxide solubility in:

- aqueous MEA (Zhang, et al., 2011),
- aqueous MEA and DEA (Austgen, et al., 1989),
- aqueous DGA (Aspen Technology Inc., 2008),
- aqueous MDEA (Zhang & Chen, 2011),
- aqueous DGA and MDEA (Pacheco, et al., 2000),
- aqueous blend od piperazine (PZ), potassium carbonate and MEA (Hilliard, 2008),
- aqueous potassium carbonate and PZ (Cullinane & Rochelle, 2005),
- aqueous MDEA and PZ (Pinto, et al., 2013)
- aqueous 2-amino-2-methyl-1-propanol (AMP) (Dash, et al., 2011),
- aqueous PZ-activated AMP (Dash, et al., 2012)
- aqueous solution of N,N-diethylethanolamine (DEEA) (Monteiro, et al., 2013),
- aqueous ammonia and aqueous blends of ammonia and (PZ) (Liu, et al., 2011),
- aqueous mixtures of diisopropanolamine (DIPA) +AMP +PZ (Haghtalab, et al., 2014a)

- aqueous NaCl solution (Ji, et al., 2007)
- aqueous solutions of MEA or AMP (Chen, et al., 2012)
- aqueous solutions of NaCl and Na<sub>2</sub>SO<sub>4</sub> (Yan & Chen, 2010; Yan & Chen, 2011)
- aqueous MEA or aqueous MDEA (Kim, et al., 2009)

In addition to application for carbon dioxide removal, eNRTL was also used for describing systems like:

- water+2-propanol+1-butyl-3-methylimidazolium chloride (Deng, et al., 2014),
- water + ethanol + 1-butyl-3-methylimidazolium acetate (Deng, et al., 2011),
- liquid - liquid equilibrium (Simoni, et al., 2007), and ternary liquid – liquid equilibrium (Simoni, et al., 2008; Simoni, et al., 2009; Simoni, et al., 2010),
- H<sub>2</sub>SO<sub>4</sub>–MgSO<sub>4</sub>–H<sub>2</sub>O, H<sub>2</sub>SO<sub>4</sub>–Al<sub>2</sub>(SO<sub>4</sub>)<sub>3</sub>–H<sub>2</sub>O and H<sub>2</sub>SO<sub>4</sub>–Fe<sub>2</sub>(SO<sub>4</sub>)<sub>3</sub>–H<sub>2</sub>O (Haghtalab, et al., 2004),
- H<sub>2</sub>S solubility in activated MDEA-AMP systems (Haghtalab, et al., 2014b),
- Sorbitol and xylitol in ionic liquids (Carneiro, et al., 2012),
- gas Clathrate Hydrate Equilibria (Kwaterski & Herri, 2014),
- water + 1-propanol + 1-butyl-3-methylimidazolium chloride (Zhang, et al., 2013),
- solubility of aniline hydrochloride in H-Mg-Na-Ca-Al-Cl-H<sub>2</sub>O System (Sun, et al., 2012),
- solubility of gypsum in ammonium solutions (Tian, et al., 2012).

Furthermore, eNRTL was also used for evaluation of seven stochastic global optimization methods (Bonilla-Petriciolet, et al., 2013) served as a basis for modelling solid-liquid equilibrium (Wang, et al., 2011) and for prediction of the octanol/water partition coefficients of 10 ionic liquids (Chapeaux, et al., 2007).

## **4. Materials and methods**

### **4.1. Optimisation of biogas power plants through process simulation**

#### **4.1.1. Experimental set-up**

##### **4.1.1.1. Characterization of complex substrates**

In order to enhance ADM1's capability of biogas plant optimization, commonly used substrates for biogas production were analysed and the kinetic constants for disintegration and hydrolysis phase were determined. The substrates were tested using the well-established Weender analysis and van Soest method (Koch, et al., 2010; Wichern, et al., 2008; Wichern, et al., 2009; van Soest & Wine, 1967) described in Naumann and Bassler (Naumann & Bassler, 1993). The outcome of the analysis indicates a fractionation of the organic matter between raw lipids (RL), raw protein (RP), raw fibre (RF) and N-free Extract (NfE). The sum of raw fibre (RF) and N-free Extract (NfE) represents the carbohydrate content of the substrate. The further split into starch, cellulose, hemicellulose and lignin can be reached with the use of the van Soest extension, where three other fractions are introduced: Neutral Detergent Fibre (NDF), Acid Detergent Fibre (ADF) and Acid Detergent Lignin (ADL). This approach was also recommended by Luebken et al. (Luebken, et al., 2007) while testing inhomogeneous substrates, despite depending on COD measurements.

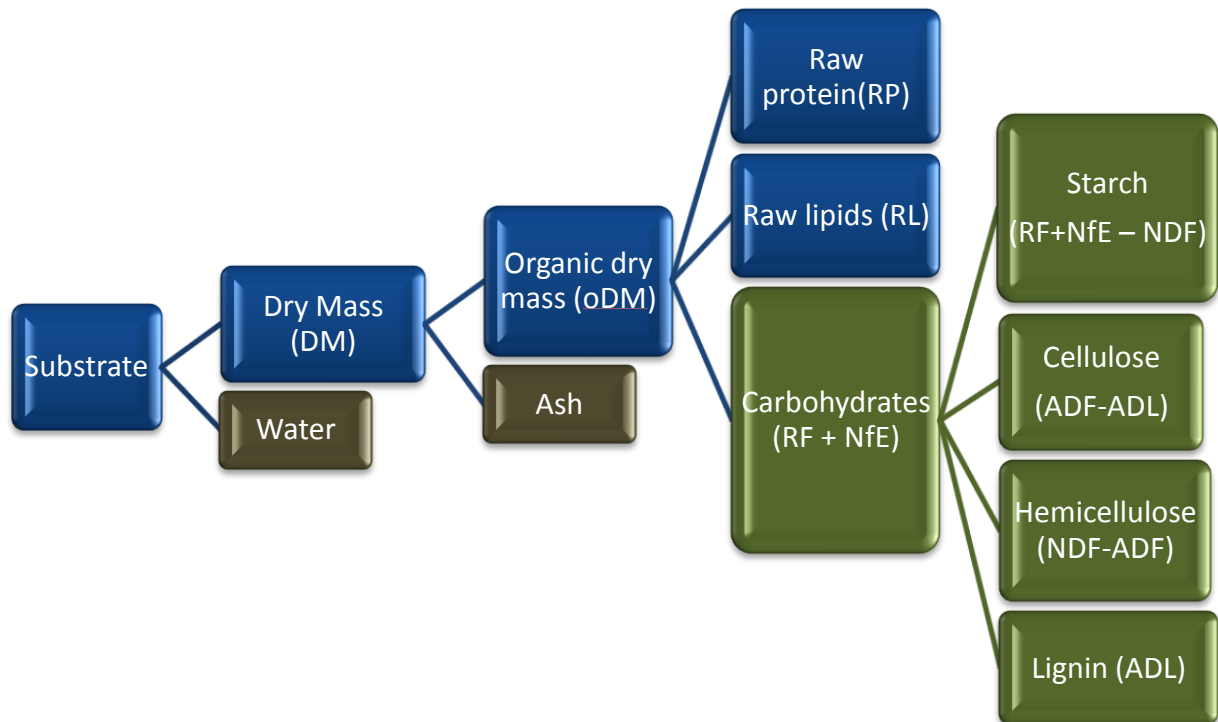


Figure 8. Weender analysis with van Soest extension (Koch, et al., 2010).

#### 4.1.1.2. Biogas potential measurement

Batch experiments were prepared in accordance with VDI 4630 (Verein Deutscher Ingenieure (VDI), 2006) however, because determination of the kinetic constants was of the main focus rather than the overall biogas produced from a substrate, experiments were carried out for 15 days to describe the beginning of biogas production as necessary for the determination of the kinetic constants. Since the duration of the batch tests depends on the inoculum concentration and activity of the inoculum (Angelidaki, et al., 2007) the evaluated substrates accounted for only 1 mass% of the reactor's overall mass to ensure an authentic biogas power plant feeding scenario, the reduction in the duration of the experiments was considered reasonable.

As reactors, bottles of 1100 ml volume were used. The contents were manually stirred and incubated in a waterbath at 38 °C. Biogas production was measured hourly with an ANKOM's (N1v0,4RF2; RFS#194) (Ankom Technology, 2011) gas production system and readings were transmitted electronically to a computer. The principle behind ANKOM's equipment is manometric, which means that a module measures the pressure increase in a bottle-reactor, simultaneously compares it with a "0" module, which measures the atmospheric pressure in the laboratory, and as an outcome delivers the pressure difference. This pressure is stored on a computer as a cumulative pressure. Following ANKOM's manual, it is used for calculating the biogas production, in [ml], with use of the ideal gas law:

$$n = P \left( \frac{V}{RT} \right),$$

and Avogadro's law (at 39°C):

$$\text{gas produced [ml]} = n \cdot 25.6 \cdot 1000$$

More information about ANKOM's system, together with example of calculation are included in appendix B.



**Figure 9. ANKOM wireless gas production system.**

Fresh inoculum was obtained from the EWE Wittmund biogas power plant (Wittmund, Lower Saxony, Germany) (EWE Biogas GmbH & Co. KG., 2011) prior to each experiment. Each inoculum was characterized, and in addition to basic characteristic (DM, oDM, pH), also total volatile fatty acids/alkalinity ratio (FOS/TAC ratio) analysis was performed with the Biogas Titration Manager from HACH LANGE. Moreover ammonium content was measured by use of the HACH LANGE cuvette test (LCK 303 and LCK 305). The main substrates used at the EWE Wittmund biogas power plant are cattle manure and organic waste, which is a mixture of food residues from kitchens, restaurants, slaughter house, and hospital. Grass, maize, and green weed silages were collected from local farmers. Industrial glycerine waste was provided by the EWE Wittmund biogas power plant.

The batch reactors (bottles) were filled with 495 g of inoculum before adding substrates to a level of 500 g, therefore ensuring 1 mass% of fresh substrate. First of all pre-incubation occurred, where bottle-reactors were placed in a water bath for 1 hour at 38°C. After pre-incubation the bottles were closed with ANKOM modules. Three batch reactors were prepared in parallel for each substrate and the whole experiment was repeated. Finally, in order to avoid variations of substrates activity between experiments coming from e.g. inoculum, the final experiment of all four substances analysed, prepared as triplicates, was conducted simultaneously in July 2011, consequently applying 16 bottle-reactors equipped each with ANKOM module.



Figure 10. Water baths used for conducting anaerobic digestion experiments.

#### 4.1.2. Continuous fermentation

##### 4.1.2.1. Characterization of the inoculum and substrate

Rape plants (cultivar Sherlock and Digger) were cultured on a farm in Glubczyce, Poland. Seeds were harvested in July 2011. Rape oilcake was obtained by cold pressing in NAPUS-OIL S.C., Kietrz, Poland. The oil cake was stored in room temperature before the use. The cow manure was obtained from a farm near Emden, Germany, in April 2012. In both substrates the following parameters were analyzed: dry mass (DM), volatile solids (VS), raw protein (RP), raw lipids (RL), raw fiber (RF), acid detergent fiber (ADF), neutral detergent fiber (NDF), acid detergent lignin (ADL) (Koch, et al., 2010; Wichern, et al., 2008; Naumann & Bassler, 1993; van Soest & Wine, 1967). Before fermentation experiments solid particles were removed from the manure with a 3.6 mm sieve, to prevent the clogging of pumps and pipes connected to the reactor. Then the manure was mixed with an appropriate amount of water and ground oilcake, then stored at 4 °C until use. Inoculum was obtained from the

agricultural biogas plant in Wittmund, (EWE Biogas GmbH, Wittmund, Lower Saxony, Germany) (EWE Biogas GmbH & Co. KG., 2011).

#### 4.1.2.2. **Batch experiments**

The biogas experiments were prepared in accordance to VDI 4630 norm (Verein Deutscher Ingenieure (VDI), 2006), and as it is described in chapter 4.1.1.2. The following substrates were tested: rapeseed oilcake and sieved cow manure. To 250 g of inoculum 2.5 g of substrate was added. All fermentation tests were prepared as triplicates. These experiments lasted for 21 days.

#### 4.1.2.3. **Continuous fermentation**

For continuous fermentation a 25 L glass reactor with a water jacket was used. The temperature in the system was set to 37 °C and was maintained by water bath with external circulation (model E306, Lauda Dr. R. Wobser GmbH & CO KG). The prepared substrate was stored at 4 °C and pumped into the reactor with a cavity pump model I-ID Type 0,03;10 (from Delasco PCM GmbH). A similar pump was used to remove the digested medium from the reactor. The fluid inside the reactor was continuously mixed at 0.833 Hz with laboratory stirrer Eurostar power-B (from IKA – Werke GmbH & Co. KG). The production of biogas was measured with a gas counter model GT05/5 (from Dr.-Ing. Ritter Apparatebau GmbH & Co. KG) connected to a PC. The methane concentration (defined as volume fraction) was measured with UNOR 6N infrared methane detector (SICK MAIHAK GmbH). Dosing pumps were turned on every 72 minutes. The volume of dosed substrate per day was about 0.66 L, which corresponded to a hydraulic retention time (HRT) of 30 days. Initially the reactor was loaded with 15 L of inoculum and filled up to 20 L with manure. After 2 days continuous feeding with manure was started, and it was continued for 21 days. After this period rapeseed oilcake was added to the feeding substrate. The concentration of rapeseed oilcake in substrate suspension (measured as a fresh weight) was increased from 20 g L<sup>-1</sup> up to 80 g L<sup>-1</sup> over a period of 35 days.

Every day samples were taken for the following analysis: pH, alkalinity, total volatile fatty acids. Additionally every three days the concentration of ammonium ions and content of volatile solids were measured.



Figure 11, Continuous fermentation lab-scale plant.

#### 4.1.3. Industrial size biogas power plant

As an existing biogas power plant, our partner EWE Wittmund Biogas Power Plant (Wittmund, Lower Saxony, Germany) was chosen. The plant was built in 1996 and it consists of 2 parallel fermenters, each 3500 m<sup>3</sup>, with an average hydraulic retention time of 20 days. The average, summarised for both reactors, input of 180 m<sup>3</sup> d<sup>-1</sup> of manure and 100 m<sup>3</sup> d<sup>-1</sup> of organic waste results in ca. 4570 m<sup>3</sup> d<sup>-1</sup> averaged cumulative biogas production, during the assessment period. The produced gas is measured from the cumulative gas flow, together with its composition using an infrared sensor. This biogas is converted in combined heat and power (CHP) units to electricity and heat. Before, the delivered industrial organic waste is collected in an underground tank (1900 m<sup>3</sup>), and the manure is fed directly to the mixing tank (620 m<sup>3</sup>), where both substrates are mixed to obtain a consistent mixture. This mixture is then kept for minimum 1 hour at minimum 70 °C in one of the 3 hygienisation tanks (30 m<sup>3</sup>), before feeding into the fermenters (EWE Biogas GmbH & Co. KG., 2011).



**Figure 12. EWE Wittmund Biogas Power Plant (EWE Biogas GmbH & Co. KG., 2011).**

The data were collected from the 19.03.2012 until 15.04.2012 (28 days). On each day samples were collected three times per day (morning, midday, afternoon), and then mixed together, as it is described in the German Industry Norm (DIN) 38402 (German Institute for Standardization (DIN), 1985), attachment 11: “sampling of waste water”. In addition, operator of the plant each day recorded basic data about the plant: pH in each reactor, temperature in each reactor, biogas production, biogas composition, and operational failure/disorder. During the assessment period no disorders or failures were recognized. However, in this simulation only the raw substrates were analysed and used for the final modelling, in order to follow the pragmatic approach of simulating existing biogas power plant, based only on the raw substrates.

Collected substrates were tested in a batch scale, in order to determine the kinetic constants and evaluate its activity. Because the substrates were collected over a longer period of time, the batch experiments were also employed for verification of substrates activity fluctuation. In addition to the both substrates used at the EWE Wittmund biogas power plant, chicken manure collected from local farmer was also analysed. The experimental procedure is in

accordance to VDI 4630 (Verein Deutscher Ingenieure (VDI), 2006), as described in chapter 4.1.1.2.

#### 4.1.4. Mathematical modelling and simulation

##### 4.1.4.1. Simulation's software

Among commercially available software with already included ADM1, SIMBA<sup>®</sup> simulation programme, developed by ifak system GmbH, was chosen. For simulating batch experiments, SIMBA<sup>®</sup> 5.1 was used, and for simulating EWE Wittmund, newer version SIMBA<sup>®</sup> 6 was already employed. However, for optimization of the disintegration and hydrolysis constants, ADM1 was created in MATLAB R2006b by author, together with accompanying optimization software, which is included in appendix C.

##### 4.1.4.2. Transferability of the experimental results to the ADM1

Koch et al. (Koch, et al., 2010) proposed a method to incorporate fodder analysis into ADM1 by calculating theoretical oxygen demand (*ThOD*) for each fraction of the substance (proteins, lipids, carbohydrates, lignin) as presented in table 10, and then calculating the composite material  $X_C$  using the following equation:

Equation 82

$$X_C = \rho_{substrate} \cdot DM \cdot \left( (RP \cdot ThOD_{Pr}) + (RL \cdot ThOD_{Li}) + (ADL \cdot ThOD_{Li}) + (RF + NfE - ADL) \cdot ThOD_{Ch} \right)$$

$X_C$  – Composite fraction, parameter used in Anaerobic Digestion Model No. 1  
 $[kg_{COD} \cdot m^{-3}]$

Table 10. Theoretical oxygen demand (ThOD) of different fractions [45].

Fraction	Elemental formula	Molar mass [g mol <sup>-1</sup> ]	ThOD [kg <sub>O2</sub> kg <sub>DM</sub> <sup>-1</sup> ]
Protein (Pr)	C <sub>5</sub> H <sub>7</sub> O <sub>2</sub> N	113	1.42
Lipid (Li)	C <sub>57</sub> H <sub>104</sub> O <sub>6</sub>	884	2.90
Starch, cellulose, hemicelluloses (Ch)	(C <sub>6</sub> H <sub>10</sub> O <sub>5</sub> ) <sub>n</sub>	162n	1.19
Lignin (l)	C <sub>10.92</sub> H <sub>14.24</sub> O <sub>5.76</sub>	237.44	1.56

In the ADM1,  $X_C$  is divided during the disintegration phase into carbohydrates ( $X_{CH}$ ), proteins ( $X_{PR}$ ), lipids ( $X_{LI}$ ) and inert fractions ( $X_I$ ) (Batstone, et al., 2002). The disintegration is described by the stoichiometric f-factors (e.g.  $f_{Pr\_Xc}$  – protein content), which Koch et al. (Koch, et al., 2010) determined by the equations:

Equation 83

$$f_{Pr\_Xc} = \frac{RP}{oDM} \left[ \frac{kg_{COD}}{kg_{COD}} \right]$$

Equation 84

$$f_{Li\_Xc} = \frac{RL}{oDM} \left[ \frac{kg_{COD}}{kg_{COD}} \right]$$

Equation 85

$$f_{Ch\_Xc} = \frac{(RF + NfE - NDF) + (NDF - ADL) \cdot d}{oDM} \left[ \frac{kg_{COD}}{kg_{COD}} \right]$$

Equation 86

$$f_{Xi\_Xc} = \frac{ADL + (NDF - ADL) \cdot (1 - d)}{oDM} \left[ \frac{kg_{COD}}{kg_{COD}} \right]$$

However, Koch et al. (Koch, et al., 2010) included also the  $d$  factor, which identifies the degradable part of cellulose and hemicellulose, obtained from the degradation level ( $D_{oDM}$ ). Since the kinetics of biogas production of each substrate were determined by using inoculums as an initial reactor state, determination of the  $D_{oDM}$  parameter by comparing the substances' organic dry mass before and after the anaerobic digestion was not applicable. Consequently, the degradability rate was taken from Association for Technology and Structures in Agriculture e. V. (Kuratorium fuer Technik und Bauwesen in der Landwirtschaft, 2014) (Table 11), and incorporated into calculations, obtaining values for  $f$ -factors.

**Table 11. Degradability rate and methane content of analysed substrates [160].**

<b>Substrate</b>	<b>Degradability rate of organic mass</b>	<b>Methane content</b>
Unit	[mass %]	[volume %]
Industrial glycerine	90.00	50.00
Grass silage	79.00	53.00
Maize silage	86.40	52.00
Green weed silage	79.00	53.00

#### 4.1.4.3. Parameters used in the modelling

The ADM1's stoichiometric parameters and dynamic state variable values remained mainly original, in order to follow the pragmatic approach, and are listed in appendix C. In addition to that, ADM1xp was used despite original ADM1 model, as explained in chapter 3.2.1.1. Also following the idea of Wett et al. (Wett, et al., 2007) and Schoen et al. (Schoen, et al., 2009), parameter ( $C_{X_C}$ ), representing the carbon mass fraction of the composite fraction was reduced to 28 mole  $kg^{-1}$  of COD.

#### 4.1.4.4. Determination of the kinetic constants

For each substrate, a set of four parameters, kinetic constants describing the phases of disintegration ( $k_{dis}$ ), hydrolysis of carbohydrates ( $k_{hyd\_ch}$ ), hydrolysis of lipids ( $k_{hyd\_li}$ ), and hydrolysis of proteins ( $k_{hyd\_pr}$ ), was calibrated with use of the optimization tool from experimental data, described in section 4.1.4.5.

#### 4.1.4.5. Optimization tool

In order to ensure precise determination of the optimal set of the kinetic constants, a numerical optimisation algorithm was used to simultaneously fit the four constants, describing the phases of disintegration ( $k_{dis}$ ), hydrolysis of carbohydrates ( $k_{hyd\_ch}$ ), hydrolysis of lipids ( $k_{hyd\_li}$ ), and hydrolysis of proteins ( $k_{hyd\_pr}$ ), for each substrate to gas generation data determined from experiments.

As objective function which needs to minimize the absolute difference between experimental and calculated data, the downhill simplex methods algorithm from Nelder and Mead (Nelder & Mead, 1965) was chosen. This algorithm was already used and appreciated by Batstone et al. (Batstone, et al., 2002) in the ADM1's parameters optimisation. This algorithm is implemented as function *fminsearch* in MATLAB (The MathWorks, Inc., 2011).

For each substrate, the four adjustable parameters ( $k_{dis}$ ,  $k_{hyd\_ch}$ ,  $k_{hyd\_li}$ ,  $k_{hyd\_pr}$ ) were simultaneously fitted. Data from table 9 were used as starting values for the optimization run. In order to ensure that the total biogas yield was adequately represented by the resulting model parameter set, data from the Association for Technology and Structures in Agriculture e. V. (Kuratorium fuer Technik und Bauwesen in der Landwirtschaft, 2014) were included in the optimization run by calculating the data given by the KTBL and introducing them as additional experimental data points with a time step of 100 days. The data points were not included in the graphs for scaling reasons.

#### 4.1.4.6. Optimization procedure

Batch experimental results obtained for substrates were used for finding disintegration and hydrolysis kinetic constants. Initially, from the substrates' experimental results, the experimental result for blanks has been subtracted, this way allowing the determination of the kinetic constants for substrates only. Subsequently, composite fraction ( $X_c$ ) and f-factors calculated were used for modelling, together with the ammonium content of inoculum. Afterwards, the ADM1 default values for disintegration and hydrolysis kinetic constants were tested, where the ADM1 values for high rate (table 9) identified as "default 1" and ADM1 values for solids (table 9) identified as "default 2" were used. Afterwards the optimization tool was used for determining optimal sets.

#### 4.1.4.7. Determination of the common constants

Since a pragmatic approach was adopted, it was intended to reduce the amount of parameters necessary for determination, prior to modelling with ADM1. According to the table 9, values of parameters describing hydrolysis' phase are also reported in the literature to be the same value for all three kinetic constants (Gali, et al., 2009; Koch, et al., 2009; Hu & Yu, 2005; Lehtomaki, et al., 2005). Furthermore, Schoen et al. (Schoen, et al., 2009) also determined  $k_{dis}$  during calibration of the model, leaving out hydrolysis constants. In addition to that, Wichern et al. (Wichern, et al., 2008) observed that kinetic constants of hydrolysis are less sensitive parameters for agricultural substrate, in contrast to  $k_{dis}$ , therefore he reduced  $k_{dis}$  to  $0.05 \text{ d}^{-1}$  for a mixture of cattle manure and fodder for cows. Besides, Wichern et al. (Wichern, et al., 2009) continued with this approach for grass silage, where he increased the  $k_{dis}$  to  $1 \text{ d}^{-1}$ , again confirming the individual character of  $k_{dis}$ . On the other hand, one value for all 3 hydrolysis kinetic constants, equalled to  $0.31 \text{ d}^{-1}$ , for cattle manure and energy crops, was successfully used by Luebken et al. (Luebken, et al., 2007), where he stated that different hydrolysis constants did not improve simulation results. Consequently, it was decided to evaluate a new concept, where the number of kinetic constants to be determined

for each new substance will be reduced from 4 parameters (kinetic constant for disintegration, hydrolysis of proteins, hydrolysis of carbohydrates, and hydrolysis of lipids) to 1 kinetic constant describing disintegration phase ( $k_{dis}$ ). Therefore, the common kinetic constants (CHC) describing the hydrolysis phase ( $k_{hyd\_ch}$ ,  $k_{hyd\_li}$ ,  $k_{hyd\_pr}$ ) were determined simultaneously for six substrates commonly used at biogas power plants (grass, maize, and green weed silages, industrial glycerine, cattle manure and food waste), ensuring applicability of those constants for a wide variety of substrates. The optimization tool describe in earlier section was modified in such a way, that the algorithm simultaneously adjusts the hydrolysis constants for all six substrates, and then determines the  $k_{dis}$ , individually for each of the six substrates. Afterwards, after receiving the first set of  $k_{dis}$ , a second loop is automatically started, where just determined  $k_{dis}$  are used, and CHC's are again determined. Consequently, the tool is designed in such a way, that it doesn't stop after the first iteration, but it continues until the cumulative errors of each substrate included, which describes the difference between experimental and simulation results on biogas production, is the smallest, and is not anymore improved by the change of the parameters. The modified optimization tool described here is included in appendix C.

## 4.2. Experimental study and thermodynamic modelling of carbon dioxide absorption capturing method

### 4.2.1. Experimental set-up

#### 4.2.1.1. Materials and solutions

All chemicals used during this research were of analytical reagent grade, and employed without further purification. CO<sub>2</sub> was acquired from Linde<sup>®</sup> AG (purity 99,5 volume%), and 2-(Ethylamino)ethanol (EAE; CAS: 110-73-6) was acquired from Sigma-Aldrich<sup>®</sup> Co. LLC. (purity of ≥98 volume%). In order to ensure excellent water quality necessary for HPLC pump, Milli-Q water was used, due to its high degree of de-ionizing and purity. It was prepared by use of Milli-Q Biocel unit (©EMD Millipore Corporation).

Before each experiment is was crucial to guarantee that water is not containing CO<sub>2</sub>, with the purpose of ensuring that solubility measurements are accurate. Therefore, prior to each experiment vacuum was applied to Duran<sup>®</sup> bottle, resistant to under- and over-pressure, filled with Milli-Q water. Afterwards aqueous alkanolamine solution was prepared gravimetrically. Subsequently prepared solution was purged with nitrogen, acquired from Linde<sup>®</sup> AG (purity 99,999%), before the final stage of placing it in ultrasonic bath (Branson 2210) for one hour.

#### 4.2.1.2. Development of a new experimental apparatus

In order to measure CO<sub>2</sub> solubility in aqueous alkanolamine solutions an experimental apparatus was developed, based on modified approach of Cadours et al. (Cadours, et al., 2007). The unit consists of two reactors acquired from Parr<sup>®</sup> Instrument Company (4560 Pressure Reaction Apparatus; volume of 0.45 dm<sup>3</sup>; maximum working pressure of 200 bar; operating temperature from -10°C to 350°C) directly connected to each other with high pressure stainless steel capillary with double-sided conical bolt connection (A506HC; Hose Assembly 6FT T316), as presented on figure 13. The second reactor is equipped with a stirrer (A1120HC6 Parr<sup>®</sup> Magnetic Drives; Turbine Type Impeller) controlled by Parr<sup>®</sup> 4875 Power Controller. Gas bottles located in gas safety cabinet (Asecos<sup>®</sup>, FWF 90) are connected to first reactor, also with use of Parr's<sup>®</sup> high pressure capillaries (A495HC, Hose Assembly 6FT Nylon). Both reactors were heated up with use of Lauda water bath (Ecoline Staredition 006), and the temperature inside each reactor was measured with use of Parr's<sup>®</sup> thermocouples ( A472E2; Thermocouple 9-1/2, T316 stainless steel, Type J ). Due to the measurement procedure reactors were equipped with PR-33X pressure sensors, both acquired from Keller<sup>®</sup> Druckmesstechnik, but with different pressure ranges: Keller PR-33X 0-10 bar (accuracy ±0.1% of full scale) and Keller PR-33X 0-30 bar (accuracy ±0.1% of full scale). Both sensors accuracy is documented in 5 points test report prepared by firma Keller<sup>®</sup> Druckmesstechnik. In order to create a vacuum at both reactors, ILMVAC<sup>®</sup> P4Z vacuum pump was used. For pumping water or aqueous alkanolamine solutions into reactor, a HPLC pump (KNAUER<sup>®</sup> Smartline pump 100, 50 ml min<sup>-1</sup>) was used. However, due to change in viscosity of the aqueous alkanolamine solutions, density of each solution was measured prior to pumping, with use of pycnometer corrected to three decimal places with thermometer (Assistant<sup>®</sup> 2572/325, volume of 25.003 cm<sup>3</sup> in 20°C), and the pumped amount was controlled gravimetrically (Sartorius<sup>®</sup> BL1500S). The data measured by sensors are collected in U12 LabJack<sup>®</sup> measurement and automation device, which is an interface between computers and the physical world. Afterwards collected data are sent via a Wi-Fi network at a PC workstation, where pressure and temperature of both reactors are recorded in a program, created in ProfiLab<sup>®</sup> environment. The recording interval can be determined in a range of 1 to 10000 seconds.

In addition to measuring the gas solubility, mixture's liquid heat capacity was measured with use of differential scanning calorimeter (Netzsch DSC 204 F1 Phoenix<sup>®</sup> ).

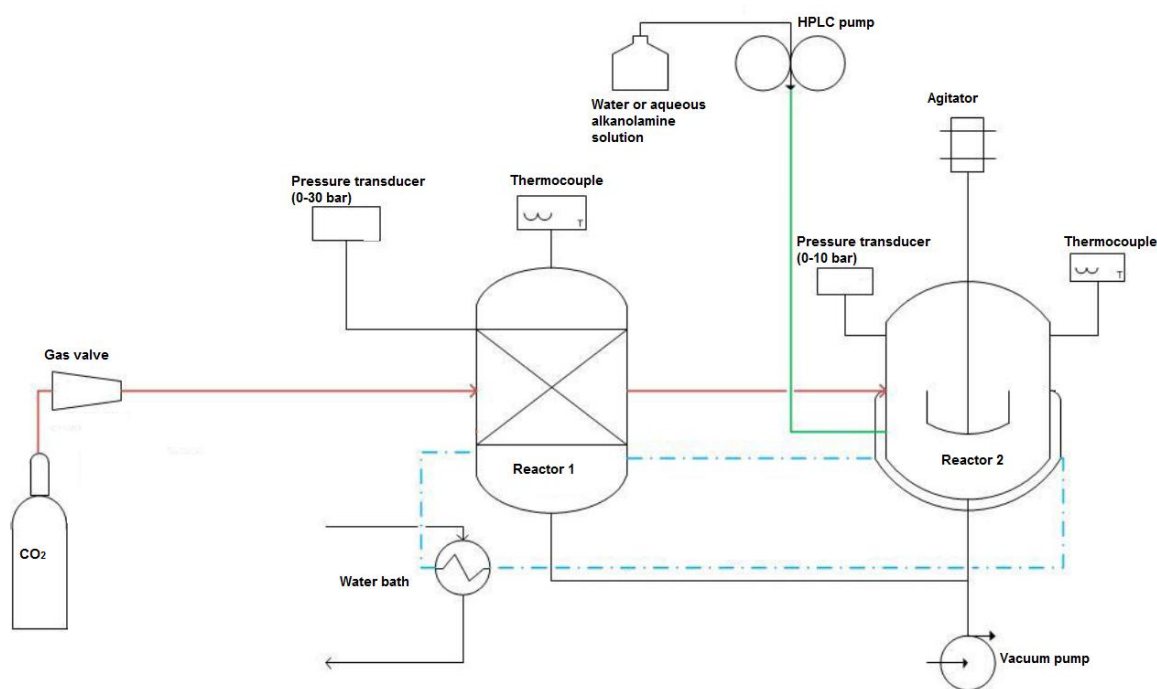


Figure 13. Apparatus for measuring gas solubility.

#### 4.2.1.3. Measuring procedure

Initially the apparatus' functionality and accuracy was verified. In order to do so, solubility of CO<sub>2</sub> in water was measured at temperature of 19.8°C, pressure range of 5 bar up to 12 bar, and compared to the literature. The results are presented in the results section.

The standard measuring procedure always starts with generating vacuum in both reactors, and simultaneously heating them up to a desired temperature. After reaching vacuum condition and constant temperature, reactors remained as such for 1 hour, to verify no pressure and temperature change, in order to confirm system's tightness. Afterwards CO<sub>2</sub> was introduced into the first reactor (figure 13), and the second reactor was filled with 0.225 dm<sup>3</sup> of water or amine solution. After obtaining desired temperature and steady pressure readings, CO<sub>2</sub> was introduced to the second reactor. Simultaneously the agitator was started. In the second reactor pressure increased (introducing CO<sub>2</sub>) was observed, followed by pressure decrease (absorption process). The end of absorption process is indicated by a constant pressure in the second reactor, and the reaction's duration depends on the solvent and loading (figure 14). However, to guarantee high accuracy of the results, each experiment lasted minimum one day, with agitator on during the whole measurement, despite equilibrium pressure was often obtained earlier. Each measurement was repeated, and also the correlation between points obtained was controlled.

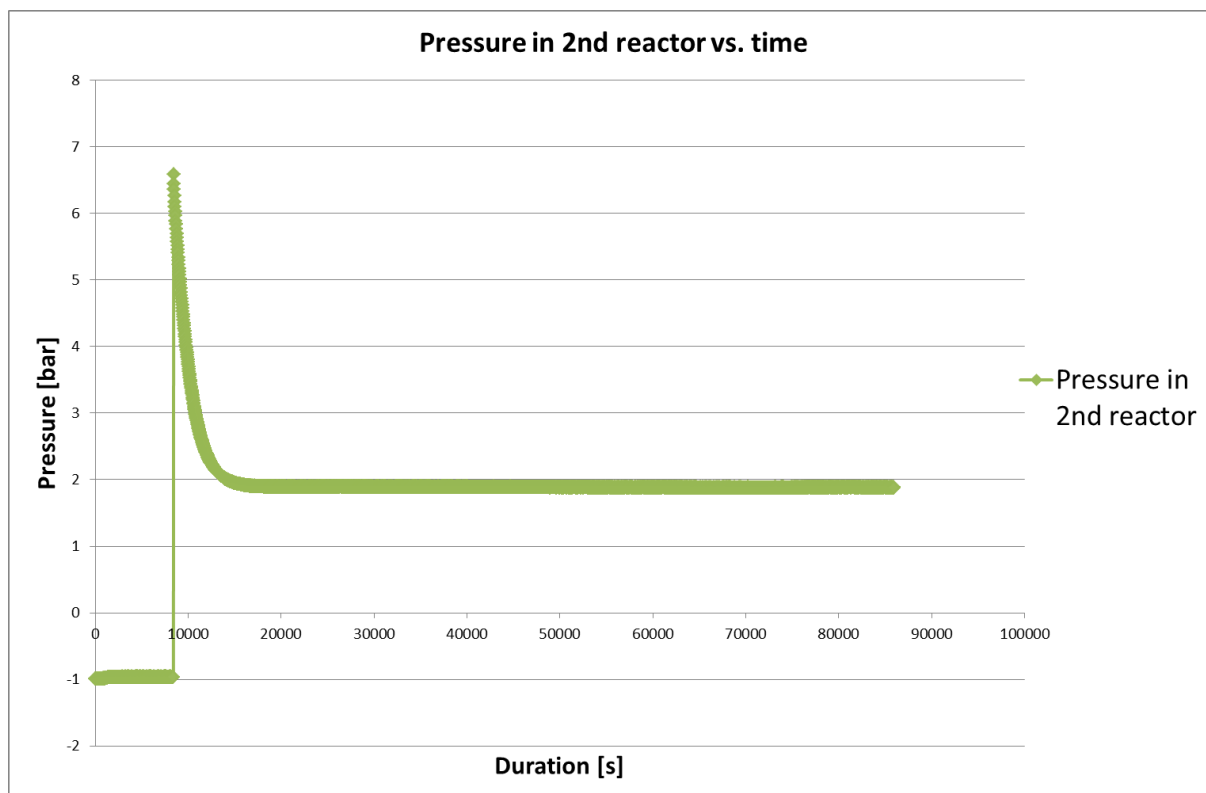


Figure 14. Measuring procedure presented base on pressure change in the 2nd reactor.

In order to measure heat capacity with use of differential scanning calorimeter, for each measurement baseline profile (empty sample pan), a standard sample profile (24.9 mg sapphire standard), and a sample profile (mass as close as possible to 24.9 mg), as further described in (Chiu, et al., 1999; NETZSCH GmbH & Co. Holding KG, 2007) were determined. Additionally, measuring method was prepared for this application, where starting temperature was 20°C, followed by heating (heating rate 5°C min<sup>-1</sup>) to 25°C, and then it is kept isothermally for 10 min, before the final heating to 82°C (heating rate 40 °C min<sup>-1</sup>), which is again followed by isothermal step for 10 min. Afterwards, cooling to 25°C was applied, allowing cp calculation during cooling step. Each measurement was prepared as triplicates. The method is in line with Netzsch (NETZSCH GmbH & Co. Holding KG, 2007) recommendation, and the results were analysed using the Proteus<sup>®</sup> Analysis (version 6.1) data analysis program from Netzsch company.

#### 4.2.1.4. Solubility calculation

The solubility determination is based on approach presented by Park and Sandall (Park & Sandall, 2001). However the calculation is modified, since Peng Robinson Equation of State (PREOS) (Peng & Robinson, 1976) is used, available in ASPEN Plus<sup>™</sup> V8.0 simulation software, rather than compressibility factors. As a consequence, number of CO<sub>2</sub> moles ( $n^1_{CO_2}$ ) in the first reactor (figure 13) just before feeding the gas to the second reactor (but

after obtaining constant pressure and temperature in the first reactor) is calculated with use of PREOS. After introducing the gas to the second reactor, and obtaining constant pressure and temperature in the first reactor,  $n_{CO_2}^2$  is calculated with PREOS. Finally number of CO<sub>2</sub> moles ( $n_{CO_2}^i$ ) introduced is calculated by subtracting  $n_{CO_2}^2$  from  $n_{CO_2}^1$ . The equilibrium pressure, obtained from the second reactor, is used for calculating the amount of remaining CO<sub>2</sub> ( $n_{CO_2}^e$ ). Finally, number of moles absorbed is calculated by subtracting remaining CO<sub>2</sub> moles ( $n_{CO_2}^e$ ) from introduced CO<sub>2</sub> moles ( $n_{CO_2}^i$ ):

Equation 87

$$n_{CO_2}^{abs} = (n_{CO_2}^1 - n_{CO_2}^2) - n_{CO_2}^e = n_{CO_2}^i - n_{CO_2}^e$$

#### 4.2.2. Thermodynamic modelling solubility

##### 4.2.2.1. Pure component parameters

Most of the pure component parameters' for 2-(Ethylamino)ethanol were acquired from NIST Databank (Thermodynamics Research Center, 2014). However, due to the limited number of data on EAE, it was decided to follow Austgen (Austgen, 1989) concept, where the dielectric constants for pure diglycolamine (DGA) was set equal to dielectric constants for diethanolamine (DEA), due to missing data. Therefore coefficients for Henry's constants (table 12) (Martin, et al., 1978), the dielectric constant (Austgen, 1989), equilibrium (Austgen, et al., 1989) and kinetic constants (Pacheco, et al., 2000) were based on DGA (Aspen Technology Inc., 2008). The dielectric constant  $D$  equalled to:

Table 12. Coefficients for Henry's constant (Aspen Technology Inc., 2008).

Component i	CO <sub>2</sub>
Component j	DGA
Temperature units	K
Property units	N m <sup>-2</sup>
AIJ	1037.6
BIJ	-35888.8
CIJ	-157.277
DIJ	0
T <sub>LOWER</sub>	0
T <sub>Upper</sub>	2000
EIJ	0

$$D = 28.01 + 9277.0 \cdot \left( \frac{1}{T} - \frac{1}{273.15} \right)$$

Parameters for CO<sub>2</sub> and H<sub>2</sub>O were acquired from ASPEN Plus<sup>®</sup> databanks (APV80.PURE27 and APV80.Binary).

#### 4.2.2.2. Binary interaction parameters

According to Austgen et al. (Austgen, et al., 1989) the adjustable parameters required by the eNRTL are only the NRTL' binary energy interaction parameters, where three types of interaction can be determined: molecule – molecule, molecule – ion pair (also ion pair – molecule), and ion pair – ion pair. However, as indicated by Chen and Evans (Chen & Evans, 1986) ion pair – ion pair parameters can be set to zero, because no significant impact on vapour-liquid equilibrium (VLE) is then caused. Moreover, because the experimental VLE data do not include in situ analysis of the VLE's composition, all water – ion pair, and ion pair-water binary parameters were kept at default values (8 and – 4) (Chen & Evans, 1986; Mock, et al., 1986; Austgen, et al., 1989). In addition, all other ion pair binary parameters (alkanolamine – ion pair; ion pair – alkanolamine; acid gas – ion pair; and ion pair – acid gas) were kept at values of 15 and -8. Besides that, binary interaction parameters for water and carbon dioxide (molecule – molecule interaction) are also already determined by Chen and Evans (Chen & Evans, 1986) and are presented in table 13.

Table 13. Binary interaction parameters for water and carbon dioxide (Chen & Evans, 1986).

Compounds	Parameter	
	a	b
H <sub>2</sub> O – CO <sub>2</sub>	10.064	-3268.14
CO <sub>2</sub> – H <sub>2</sub> O	10.064	-3268.14

The nonrandomness factor ( $\alpha$ ) for water – ion pair and for molecule – molecule interactions was fixed at 0.2, as recommended by Chen and Evans (Chen & Evans, 1986), and as proposed by Mock et al. (Mock, et al., 1986) it was kept at value of 0.1 for alkanolamine – ion pair and acid gas – ion pair.

#### 4.2.2.3. Determined parameters

The only binary interaction parameters left for determination, are the molecule-molecule binary interaction parameters, describing water – alkanolamines, and alkanolamines – water

systems. The binary energy interaction parameters included in ASPEN Plus<sup>®</sup> V8.0 are adopted as a temperature dependent as given by Austgen et al. (Austgen, et al., 1989):

Equation 89

$$\tau = a + \frac{b}{T}$$

Values of  $a$  and  $b$  for alkanolamine – water and water – alkanolamine interactions were determined with use of Data Regression System (DRS). Following path proposed by Austgen et al. (Austgen, et al., 1989), for determination of the interaction parameters the Deming algorithm was used, and as an objective function maximum likelihood was selected.

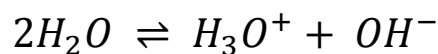
#### 4.2.2.4. Physical solubility

In this research fugacity coefficient, necessary for calculating the gas phase, was calculated with use of Redlich-Kwong EOS (Redlich & Kwong, 1949), and activity coefficient was determined with use of electrolyte Non Random Two Liquid model, and coefficients for Henry constant of 2-(Ethylamino)ethanol were based on diglycolamine (DGA) (Martin, et al., 1978).

#### 4.2.2.5. Chemical solubility

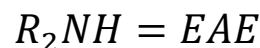
Subsequently are presented reaction describing chemical solubility, and those equilibrium reactions were developed for 2-(Ethylamino)ethanol following the reactions presented in chapter 3.3.3, because this amine is of main interest of this research. They are based on reactions presented by Zhang et al. (Zhang, et al., 2011), Austgen (Austgen, 1989), and also used in (Aspen Technology Inc., 2008), however EAE is substituting the general formula of secondary amines ( $EAE = R_2NH$ ):

Equation 90



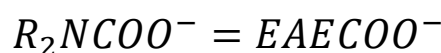
Since

Equation 91



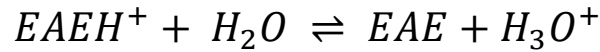
And

Equation 92

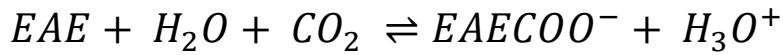


Then

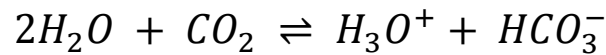
Equation 93



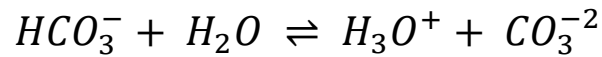
Equation 94



Equation 95

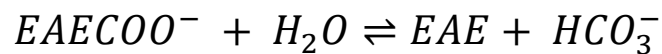


Equation 96



Reactions describe ionization of water (90), amine deprotonation (93), carbamate formation (94), dissociation of carbon dioxide (95) and bicarbonate (96). In addition to that, carbamate reversion to bicarbonate is also included in the chemical solubility, which is only possible for primary and secondary amines (Austgen, 1989; Aspen Technology Inc., 2008; Austgen, et al., 1989) however its implementation is crucial for correct evaluation of the amine's efficiency:

Equation 97



Equilibrium constants for reactions 90, and 93-96 (without 94) are presented as temperature dependent via:

Equation 98

$$\ln(K) = C_1 + \frac{C_2}{T} + C_3 \cdot \ln(T) + C_4 \cdot T$$

where the values for each reaction are presented in table 14. Equation 94 is presented as a kinetic reaction in chapter 4.2.2.6.

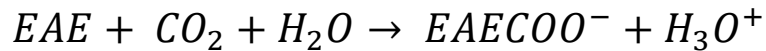
Table 14. Equilibrium constants for reactions 90, 93-97 (without 94).

Reaction	C <sub>1</sub>	C <sub>2</sub>	C <sub>3</sub>	C <sub>4</sub>	Source
90	132.899	-13445.9	-22.4773	0.0	(Maurer, 1980)
93	1.6957	-8431.64	0.0	0.005037	(Dingman, et al., 1983)
95	231.465	-12092.10	-36.7816	0.0	(Edwards, et al., 1978)
96	216.049	-12431.70	-35.4819	0.0	(Edwards, et al., 1978)
97	8.8334	-5274.40	0.0	0.0	(Austgen, 1989)

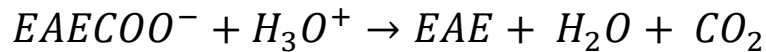
#### 4.2.2.6. Reaction kinetics

As already applied in ASPEN Plus™ V8.0 (Aspen Technology Inc., 2008) for DGA in the simulation phase, equation 94 and 95 were prepared as kinetic reactions:

Equation 99



Equation 100



Equation 101



Equation 102



For those rate controlled reactions (99-102) the reduced power law expressions were used, because reference temperature was not specified:

Equation 103

$$r = k_p T^n \exp\left(-\frac{E}{RT}\right) \prod_{i=1}^N C_i^{a_i},$$

Where rate of reaction ( $r$ ) is calculated from pre-exponential factor ( $k_p$ ), absolute temperature ( $T$ ), temperature exponent ( $n$ ), activation energy ( $E$ ), universal gas constant ( $R$ ), number of

components in the reaction ( $N$ ), concentration of component  $i$  ( $C_i$ ), and the stoichiometric coefficient of components  $i$  in the reaction equation ( $a_i$ ). Therefore, in this study the concentration basis is molarity and temperature exponent ( $n$ ) equalled to zero. The pre-exponential factor ( $k$ ) and the activation energy ( $E$ ) used in this study are presented in table 15.

**Table 15. The pre-exponential factor ( $k$ ) and activation energy ( $E$ ) parameters for reduced power law.**

Reaction	$k_p$	$E$	Source
Unit	$\left[ \frac{\left( \frac{kgmole \cdot K^{-n}}{sec \cdot m^3} \right)}{\left( \frac{kgmole}{m^3} \right)} \right]$	[cal mol <sup>-1</sup> ]	
99	1.94e +15	15813	(Pacheco, et al., 2000)
100	3e +26	25287	(Pacheco, et al., 2000)
101	4.32e +13	13249	(Pinsent, et al., 1956)
102	2.38e +17	29451	(Aspen Technology Inc., 2008)

### 4.3. Sustainability assessment of the biomethane production

Categories for sustainability assessments are based on the concept already introduced in the literature(Li, et al., 2011; Gangadharan, et al., 2012). However, because in this research we concentrate on evaluation of the carbon dioxide absorption by different aqueous solutions of alkanolamines, the sustainability assessment was modified as graphically presented (figure 15).

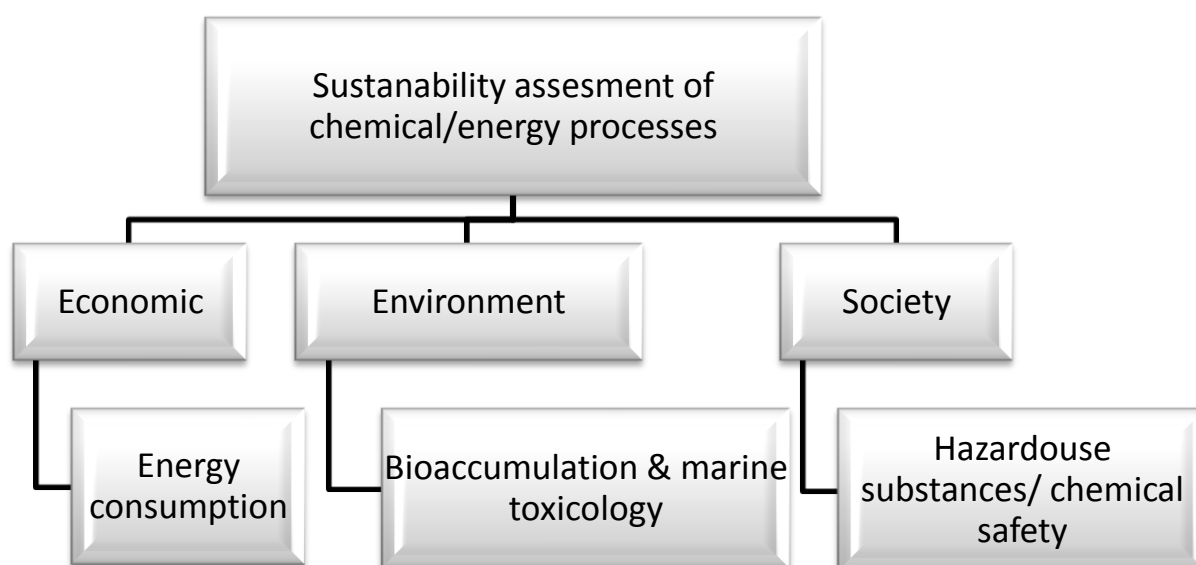


**Figure 15. Structure of the sustainability assessment applied in this research.**

Because the same plant design was used for each of the alkanolamines, the economical evaluation of the associated investment costs with use of the NPV or IRR methods was not applicable. Thus, it was decided to evaluate the running cost, which its' crucial part consists of the energy consumption during the desorption stage. Consequently, in the environmental impact assessment bioaccumulation and marine toxicity were only analyzed, since energy evaluation is already included in the economical part. On the other side, other authors (Li, et al., 2011; Gangadharan, et al., 2012) proposed to include chemical safety and plant safety as indicators of the social acceptance, which are obtained with use of the inherent safety index (Heikkila, 1999). However, in this research only the subindices for hazardous substances of the chemical inherent safety index (Heikkila, 1999) were recognized as applicable for this assessment.

#### 4.3.1. **Analysed system**

The chemical equilibrium for  $R_2NH - H_2O - CO_2$  system is already presented in chapter 3.3.3, and it is based on the literature (Austgen, 1989; Zhang, et al., 2011; Aspen Technology Inc., 2008), where  $R_2NH$  represents a secondary amine. In addition to that, carbon dioxide dissociation and carbamate formation are expressed as kinetic reactions with use of power law expression, as presented in chapter 4.2.2.6., in accordance to the literature (Austgen, 1989; Zhang, et al., 2011; Aspen Technology Inc., 2008).

#### 4.3.2. **Model used in this research**

In this research already published models were employed for describing the physical and chemical absorption of carbon dioxide in different aqueous alkanolamine solutions:

- Monoethanolamine (MEA, CAS: 141-43-5): prepared by Austgen (Austgen, 1989), implemented in ASPEN Plus® V 8.0 Simulation Software
- Diethanolamine (DEA, CAS: 111-42-2): prepared by Austgen (Austgen, 1989), implemented in ASPEN Plus® V 8.0 Simulation Software
- Diglycolamine (DGA, CAS: 929-06-6): prepared by Austgen (Austgen, 1989), implemented in ASPEN Plus® V 8.0 Simulation Software

In addition to that, the thermodynamic model developed in this research for 2-(Ethylamino)ethanol (EAE, CAS: 110-73-6) was also applied for the sustainability assessment.

#### 4.3.3. **Pure component properties**

Parameters for  $CO_2$ ,  $H_2O$ , DGA, DEA, and MEA were acquired from ASPEN Plus® databases (APV80.PURE27 and APV80.Binary), and for EAE from NIST database (Thermodynamics Research Center, 2014).

#### 4.3.4. Case study

The economical assessment of the biogas upgrading with use of alkanolamine solutions was decided to be prepared for a factual scenario. As a consequence, EWE Wittmund Biogas Power Plant (Wittmund, Lower Saxony, Germany) (EWE Biogas GmbH & Co. KG., 2011), in details described in chapter 4.1.3., was chosen as a source of biogas for upgrading in this assessment.

#### 4.3.5. Process design

The plant's design is based on the work of Desideri and Paolucci (Desideri & Paolucci, 1999), later applied by Luyben (Luyben, 2013). In this research for each of the analysed amines the plant's design is exactly the same, to allow comparison, as describe below. The plant consists of absorber, stripper, heat exchanger, and pumps. However, also additional heater was included, because in this research significantly lower mole flows were of interest, than in the literature (Luyben, 2013; Desideri & Paolucci, 1999), therefore the heat exchanger was not sufficient. The absorber, a *RadFrac* column, consists of 11 stages, operated at 101.325 kPa pressure with 1.38 kPa pressure drop. The feed biogas is compressed to 125.64 kPa at 336 K, as specified by Luyben (Luyben, 2013). The amines are feed at 100 kPa pressure and with temperature of 313 K. The rich solvent's temperature (amine + absorbed carbon dioxide) is with use of heat exchanger and an additional heater increased to 380 K prior to feeding it to the stripper. The stripper column, also the *RadFrac*, was specified to have 10 stages, and it operates at 202.65 kPa pressure, whereas 151.99 kPa operating pressure is set in reflux drum. The bottom of the stripper is estimated to reach 400 K, while in the condenser the temperature is set to 343 K, to remove most of the water. Both, absorber and stripper, are describe with use of equilibrium and kinetic reactions. For each amine stripper specification was set to:

- Distillate rate of 20 kmol hr<sup>-1</sup>
- Reflux ration of 0.75 (mole basis)
- Water was additionally removed from condenser, and mixed with recycled hot solvent, coming from the bottom

## 5. Results

### 5.1. ***“Application of Anaerobic Digestion Model No.1 for describing anaerobic digestion of grass, maize, green weed silage, and industrial glycerine”***

#### 5.1.1. **Characterization of the reactors initial state**

The inoculums from the EWE Wittmund biogas power plant contained 4.72 mass% dry matter (DM) of which 69.8 mass% was organic dry matter. The ammonium content was 3.069 g L<sup>-1</sup> and the pH was 7.8. The total volatile fatty acids/alkalinity ratio (FOS/TAC ratio) was 0.196 and therefore it was expected that inoculum from the EWE Wittmund biogas power plant would support efficient fermentation and stable operation since the FOS/TAC ratio was below 0.3 (Rieger & Weiland, 2006). Additionally, the ammonium content measured, was used as a value for the ammonium fraction ( $S_{NH4}$ ) in the ADM1xp model.

#### 5.1.2. **Characterization of the complex substrates**

Table 16 presents characteristics of the four substrates and their calculated values. Koch et al. (Koch, et al., 2010) also examined grass silage with fodder analysis, and their results are in good correlation with those from the current study. Following the biochemistry discussion held in this dissertation, the high raw lipids content of industrial glycerine (22.9 %DM), which is over four times higher than of other examined substrates, indicates that the highest total biogas production for batch experiments will be achieved from industrial glycerine. Moreover, grass silage and green weed silage has the highest value of inerts content stoichiometric factor, and high inerts content indicates that those substrates will deliver the lowest amount of biogas. Taking also under consideration much higher water content of green weed silage than of grass silage, the lowest total biogas production is most likely to be achieved by green weed silage.

**Table 16. Characteristics of the examined substrates.**

<b>Parameter</b>	<b>Unit</b>	<b>Grass silage</b>	<b>Maize silage</b>	<b>Industrial glycerine</b>	<b>Green weed silage</b>
Dry mass (DM)	[mass %]	41.9	31.1	64.3	26.1
Organic dry mass	[% DM]	87.9	93.2	47.8	88.9
Raw protein	[% DM]	18.5	10.3	0.5	12.0
Raw lipids	[% DM]	3.5	5.1	22.9	4.5
Raw fibre	[% DM]	26.3	15.5	1.1	30.8
Neutral Detergent Fibre (NDF)	[% DM]	57.2	71.0	2.2	65.0
Acid Detergent Fibre (ADF)	[% DM]	15.0	33.4	2.5	47.2
Acid Detergent Lignin (ADL)	[% DM]	4.5	11.6	0.7	3.2
Nitrogen free Extracts (NfE)*	[% DM]	39.6	62.4	23.4	41.6
Ash	[% DM]	12.1	6.8	52.2	11.1
Composite fraction (Xc)*	[kg <sub>COD</sub> m <sup>-3</sup> ]	488.59	393.27	619.25	306.30
Protein content stoichiometric factor ( $f_{Pr,Xc}$ )**	[-]	0.210	0.110	0.010	0.135
Lipids content stoichiometric factor ( $f_{Li,Xc}$ )**	[-]	0.040	0.055	0.478	0.051
Carbohydrates content stoichiometric factor ( $f_{Ch,Xc}$ )**	[-]	0.540	0.695	0.492	0.604
Inerts content stoichiometric factor ( $f_{Xi,Xc}$ )**	[-]	0.210	0.140	0.020	0.210

\* - calculated value

\*\* - calculated values, using equations from chapter 4.1.4.2.

### 5.1.3. Batch experiments and simulation

The new kinetic constants, describing the phases of disintegration ( $k_{dis}$ ), hydrolysis of carbohydrates ( $k_{hyd\_ch}$ ), hydrolysis of lipids ( $k_{hyd\_li}$ ), and hydrolysis of proteins ( $k_{hyd\_pr}$ ), were determined by using the optimization tool, and are presented in table 17.

**Table 17. Optimized disintegration and hydrolysis kinetic constants according to the downhill simplex methods algorithm from Nelder and Mead (Nelder & Mead, 1965).**

<b>Substrate</b>	<b><math>k_{dis}</math></b>	<b><math>k_{hyd\_ch}</math></b>	<b><math>k_{hyd\_pr}</math></b>	<b><math>k_{hyd\_li}</math></b>
Industrial glycerine	1.3236	1.2516	0.0018	0.0086
Grass silage	1.7433	0.7366	0.0104	0.0149
Maize silage	0.7705	0.6865	0.2446	0.1216
Green weed silage	0.8168	0.6659	0.0014	0.0513

Finding optimal sets of disintegration and hydrolysis kinetic constants for complex substances characterized by the Weender analysis/van Soest method (figure 16, 17, 18,19) illustrates that the goal of a more precise description of the anaerobic degradation kinetics was achieved. The ADM1 default values for disintegration and hydrolysis kinetic constants used for comparison, where the ADM1 values for high rate (table 9) identified as “default 1” and ADM1 values for solids (table 9) identified as “default 2”. The results show a very good correlation between experimental and simulation results, after optimization of the kinetic constants, and by keeping most of the parameters and fractions available in ADM1 unchanged. On the top of that, calculated anaerobic digestion is correctly illustrating the individual kinetics of each substrate decomposition. Moreover, as predicted in chapter 5.1.2, the industrial glycerine delivers the most gas, whereas the green weed silage bring the lowest amount.

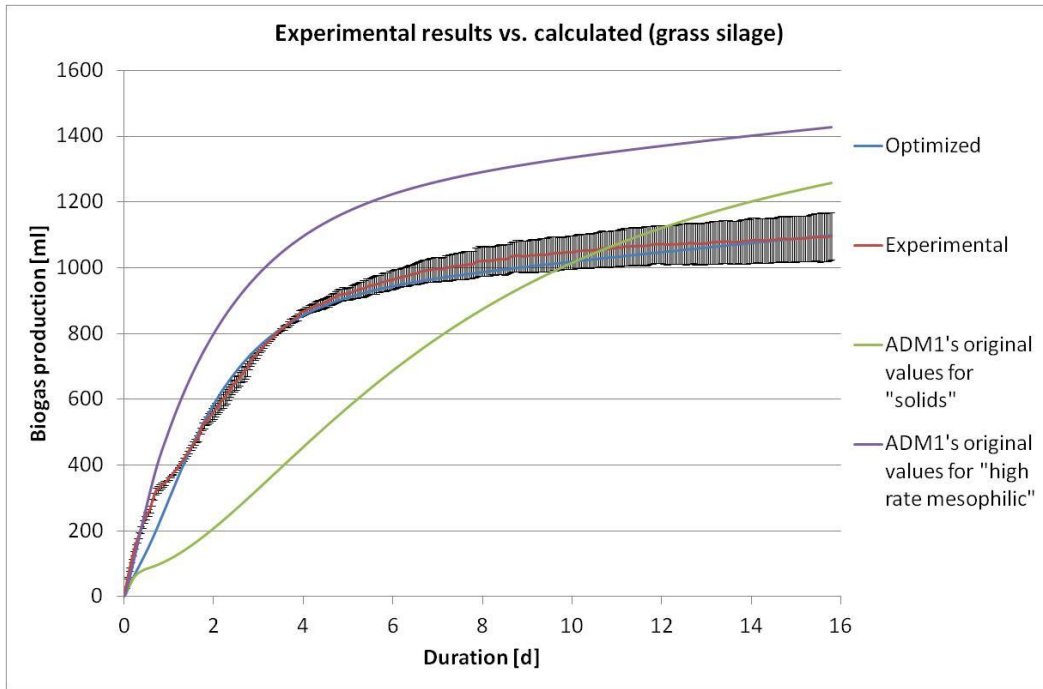


Figure 16. Comparison of the experimental cumulative biogas production from grass silage to simulation results, where the ADM1 default values for disintegration and hydrolysis kinetic constants were used.

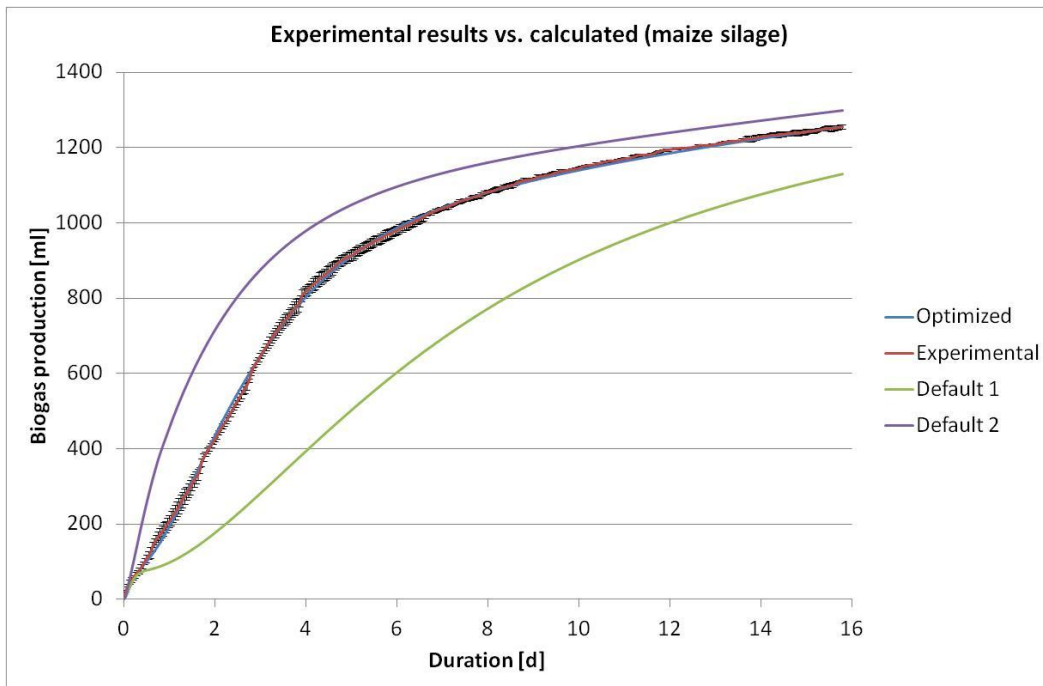


Figure 17. Comparison of the experimental cumulative biogas production from maize silage to simulation results, where the ADM1 default values for disintegration and hydrolysis kinetic constants were used.

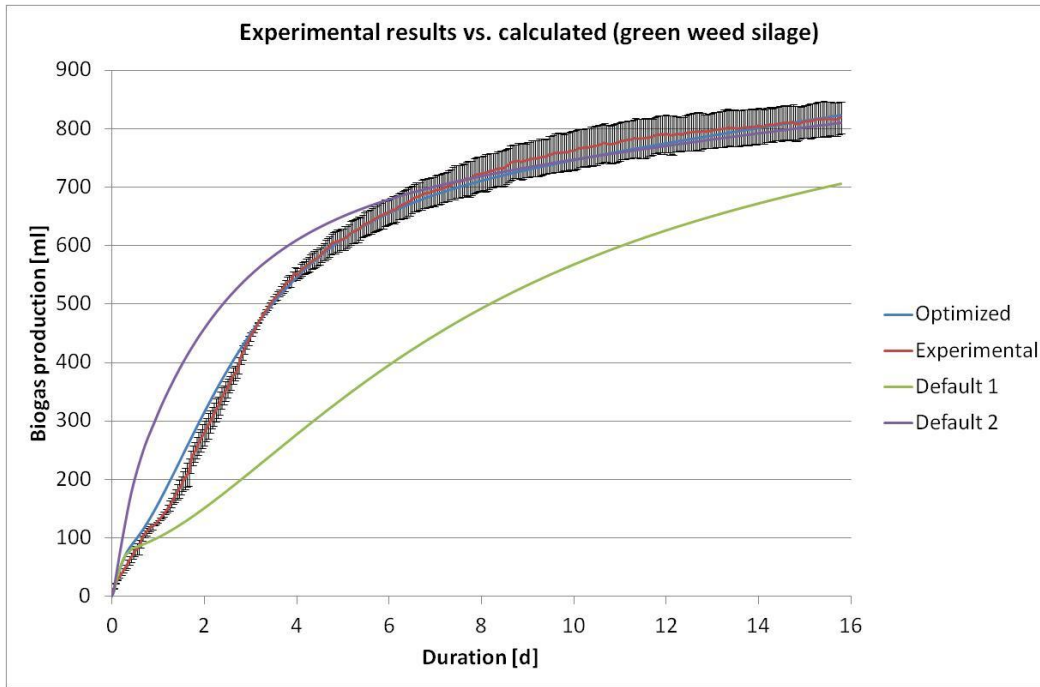


Figure 18. Comparison of the experimental cumulative biogas production from green weed silage to simulation results, where the ADM1 default values for disintegration and hydrolysis kinetic constants were used.

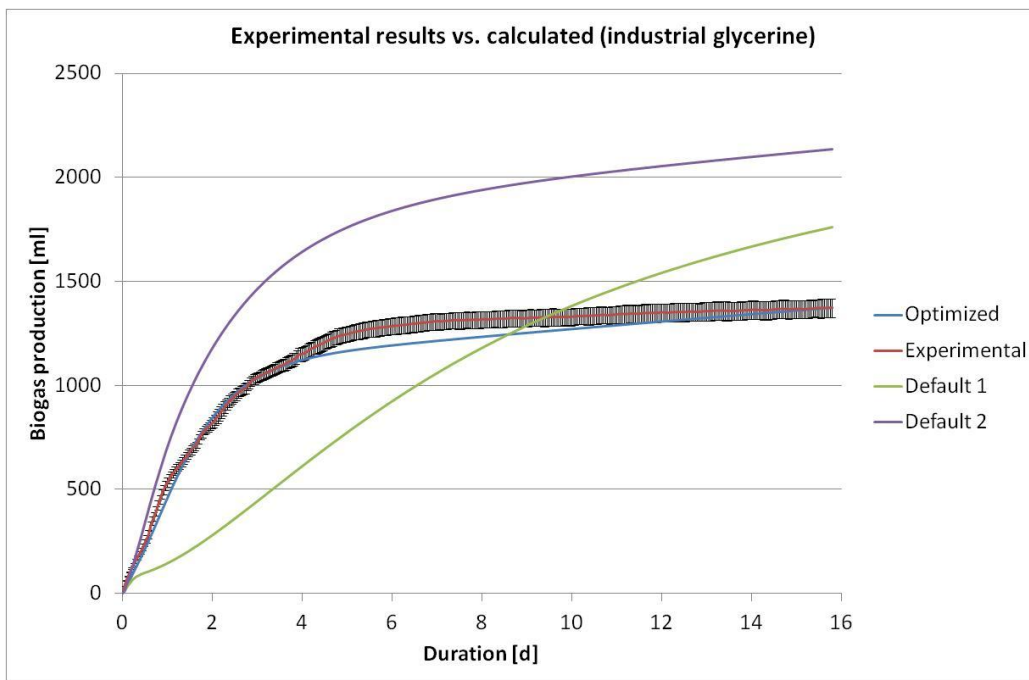


Figure 19. Comparison of the experimental cumulative biogas production from industrial glycerine to simulation results, where the ADM1 default values for disintegration and hydrolysis kinetic constants were used.

In addition, the methane content results also indicate a very good correlation between the simulation and expected results (table 18).

**Table 18. Correlation between literature and calculated values for methane content.**

Substrate	Methane content	
	(Kuratorium fuer Technik und Bauwesen in der Landwirtschaft, 2014)	Calculated
Source		
Unit	[volume %]	[volume %]
Industrial glycerine	50.00	49.33
Grass silage	53.00	52.36
Maize silage	52.00	52.04
Green weed silage	53.00	48.77

This applies especially for maize silage where the simulation fits the experimental results perfectly. However, the result for glycerine demonstrates that the model needs further improvement. Additionally, the optimized values of disintegration and hydrolysis kinetic constants are in accordance with those in the literature. Heukelekian (Heukelekian, 1958) has already stated that proteins are hydrolysed slower than carbohydrates, and those findings were confirmed by Gavala et al. (Gavala, et al., 2003). Moreover, Christ et al. (Christ, et al., 2000) also proposed a range of kinetic constants (Table 9), and values for proteins and lipids are also lower than those for carbohydrates. The faster hydrolysis of lipids than of proteins was also confirmed by Bischofsberger et al. (Bischofsberger, et al., 2005). Despite the fact that the value of  $k_{dis}$  is bigger than the values for hydrolysis for all analysed substrates, they cannot be neglected. Since the values of  $k_{dis}$  and  $k_{hyd\_ch}$  are of the same order of magnitude, the relation between both values is important for the gas generation rate. Only if  $k_{dis}$  is a lot faster than the value of  $k_{hyd}$ , does  $k_{hyd}$  not play a role, and this level has not been reached.

#### 5.1.4. Sensitivity analysis

Using a mathematical solver like the downhill simplex methods algorithm from Nelder and Mead (Nelder & Mead, 1965) does mean that the final values are a "random output", and so there could be indefinite pairs of kinetic constants giving a satisfying fitting. Therefore, a sensitivity analysis was performed, in order to verify correctness of the determined parameters. As a result, the accuracy of the optimization's output is confirmed by the three-dimensional graphs. In figure 20 the graph for maize silage is presented, and the other three graphs are included as supplemental data (appendix D). Additionally, two-point charts

representing the proceedings of the optimization tool, where the starting points were chosen to be a boundary values, are included as a figure 21.

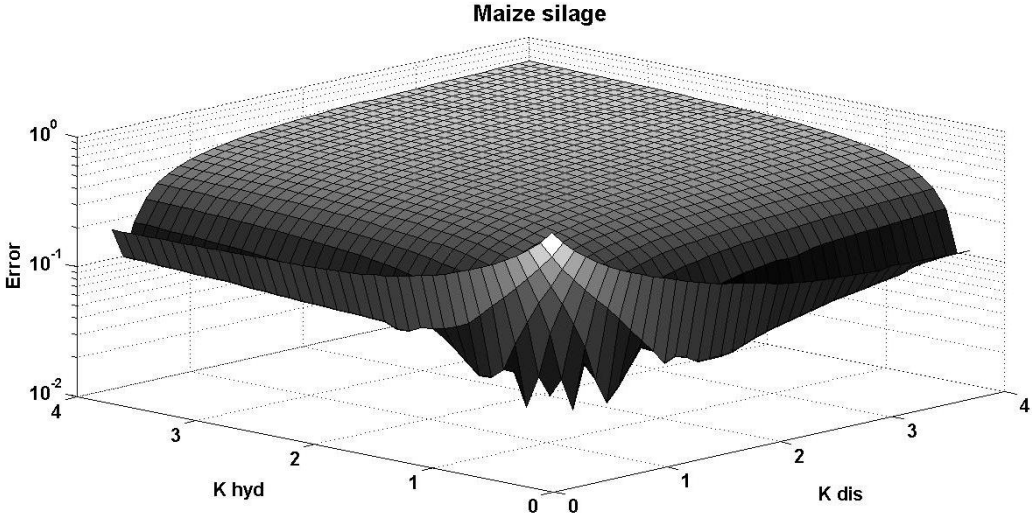


Figure 20. Disintegration ( $k_{dis}$ ) and hydrolysis ( $k_{hyd}$ ) kinetic constants sensitivity analysis for maize silage, where the lowest error represents the best correlation between simulated and experimental results.

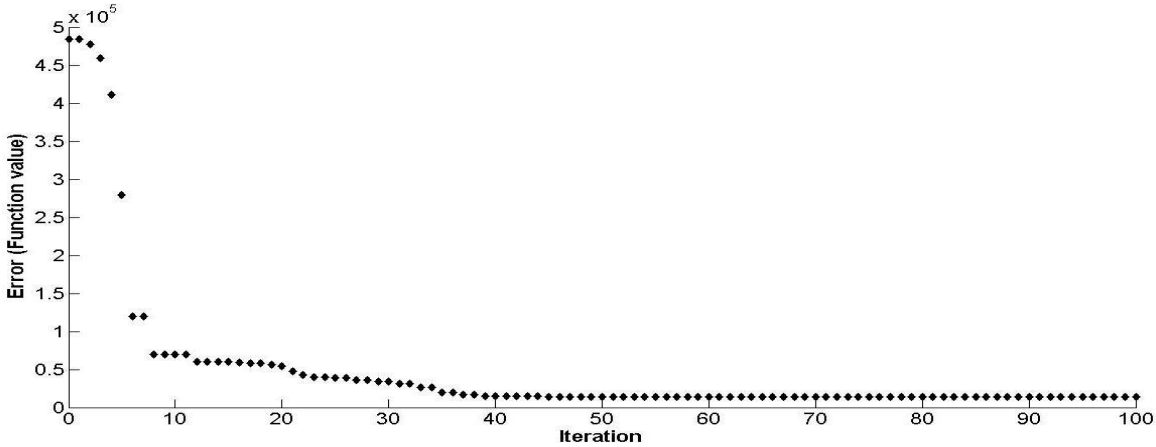
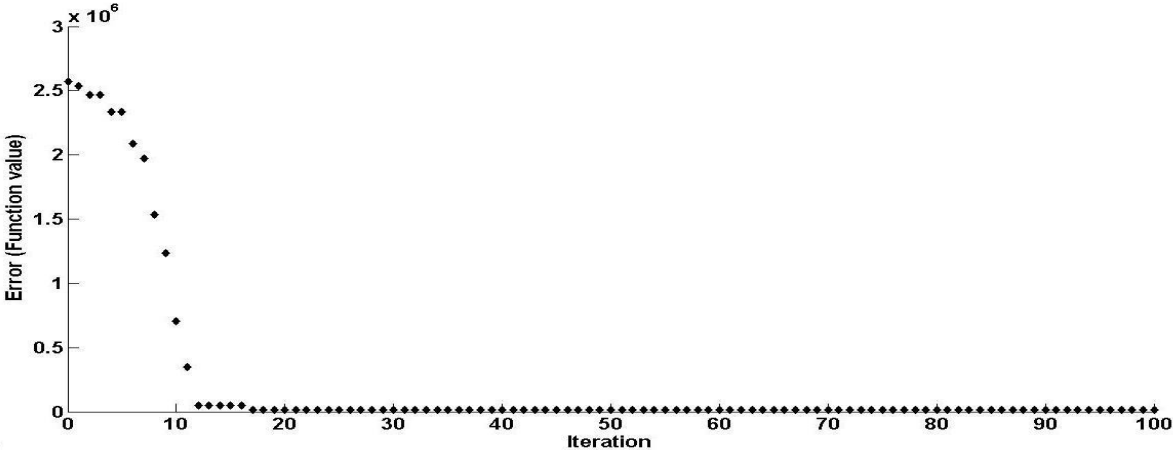


Figure 21. Two-point charts representing the proceedings of the optimization tool, where the starting points were chosen to be a boundary values.

## 5.2. **“Application of Anaerobic Digestion Model No. 1 for describing an existing biogas power plant”**

### 5.2.1. **Characterization of the reactors initial state and an existing biogas power plant**

The carrier substance for batch experiments, an inoculum, so an extract from the EWE Wittmund Biogas Power Plant's (EWE Biogas GmbH & Co. KG., 2011) operating reactor, responsible for the reactors initial state was characterized. The inoculum has a dry matter mass fraction of 4.83 %, the organic dry matter mass fraction of 3.39 %, and pH was 7.84. The HACH LANGE cuvette test (LCK 303 and LCK 305) was used for measuring the ammonium content, which equalled to  $3.1 \text{ kg m}^{-3}$ , and this value was used as a value for the ammonium fraction ( $S_{NH_4}$ ). The basic characteristic was extended by Total Volatile Fatty Acids/Alkalinity ratio (FOS/TAC ratio), and the result was 0.19, analysed with use of the Biogas Titration Manager from HACH LANGE. According to Rieger and Weiland (Rieger & Weiland, 2006) due to FOS/TAC ratio below 0.3, EWE Wittmund's inoculum used for the batch experiments was ensured to be fresh and it guaranteed efficient fermentation.

### 5.2.2. **Analysis of the substrates used**

Substrates used at EWE Wittmund Biogas Power Plant (EWE Biogas GmbH & Co. KG., 2011), cattle manure and organic waste, were analysed with use of Weender analysis van Soest extension (Koch, et al., 2010; Naumann & Bassler, 1993; van Soest & Wine, 1967), and following Koch et al. (Koch, et al., 2010) the parameter and fractions necessary for ADM1 were calculated. In addition to that, also chicken manure was characterised in this method. The results are presented as a table 19.

The pragmatic approach intended to reduce the amount of parameters necessary for determination, prior to modelling with ADM1, resulted in reduction of the simulation's precision. Consequently, simulation results received with IHC are more precisely describing kinetics of biogas formation, obtained from the experimental results, as can be seen from figures 21-26.

**Table 19. Characteristics of the examined substrates.**

Parameter	Unit	Cattle manure	Food waste	Chicken manure
Dry mass (DM)	[%]	5.23	30.55	9.8
Organic dry mass	[% DM]	4.01	27.83	7.54
Raw protein	[% DM]	0.74	7.47	1.66
Raw lipids	[% DM]	0.17	9.41	0.89
Raw fibre	[% DM]	1.15	1.17	2.60
Neutral Detergent Fibre (NDF)	[% DM]	2.24	9.53	4.34
Acid Detergent Fibre (ADF)	[% DM]	2.22	9.15	3.89
Acid Detergent Lignin (ADL)	[% DM]	0.74	3.66	1.09
Nitrogen free Extracts (NfE)*	[% DM]	1.96	9.78	2.39
Ash	[% DM]	1.22	2.72	2.26
Composite fraction ( $X_c$ )*	[kg <sub>COD</sub> m <sup>-3</sup> ]	55.07	522.88	120.17
Protein content stoichiometric factor ( $f_{Pr\_Xc}$ )*	[-]	0.185	0.268	0.219
Lipids content stoichiometric factor ( $f_{Li\_Xc}$ )*	[-]	0.042	0.338	0.119
Carbohydrates content stoichiometric factor ( $f_{Ch\_Xc}$ )*	[-]	0.264	0.183	0.306
Inerts content stoichiometric factor ( $f_{Xi\_Xc}$ )*	[-]	0.509	0.210	0.356

\*- calculated values

### 5.2.3. Bach results with the common hydrolysis constants

Kinetic constants describing disintegration and hydrolysis phase were individually determined ,with use of the optimization tool, for cattle manure and organic waste, and are presented in table 20. This approach is later referred as individual hydrolysis constants (IHC).

**Table 20. Optimized disintegration and hydrolysis kinetic constants according to the downhill simplex methods algorithm from Nelder and Mead (Nelder & Mead, 1965).**

<b>Substrate</b>	<b><math>k_{dis}</math></b>	<b><math>k_{hyd\_ch}</math></b>	<b><math>k_{hyd\_pr}</math></b>	<b><math>k_{hyd\_li}</math></b>
Units	[d <sup>-1</sup> ]	[d <sup>-1</sup> ]	[d <sup>-1</sup> ]	[d <sup>-1</sup> ]
Cattle manure	1.540	0.037	0.099	0.225
Food waste	1.043	1.044	0.233	0.980

Afterwards, following the approach described in chapter 4.1.4.7, three CHC describing the hydrolysis phase were regressed simultaneously for six substrates commonly feed to biogas power plants, and those values were obtained:  $k_{hyd\_ch} = 0.602 \text{ d}^{-1}$ ;  $k_{hyd\_li} = 0.0257 \text{ d}^{-1}$ ;  $k_{hyd\_pr} = 0.284 \text{ d}^{-1}$ . In addition to that, six individual kinetic constants describing disintegration phase, listed in table 21, were also determined. This approach is later referred as common hydrolysis constants (CHC).

**Table 21. Optimized disintegration kinetic constants, for CHC approach, according to the downhill simplex methods algorithm from Nelder and Mead (Nelder & Mead, 1965).**

<b>Substrate</b>	<b><math>k_{dis}</math></b>
Units	[d <sup>-1</sup> ]
Industrial glycerine	6.741
Grass silage	1.354
Maize silage	1.390
Green weed silage	0.451
Cattle manure	0.263
Food waste	1.725

Finally both approaches, IHC and CHC, were compared, and presented as a figures 22-27. The pragmatic approach intended to reduce the amount of parameters necessary for determination, prior to modelling with ADM1, resulted in reduction of the simulation's precision. Consequently, simulation results received with IHC are more precisely describing kinetics of biogas formation, obtained from the experimental results.

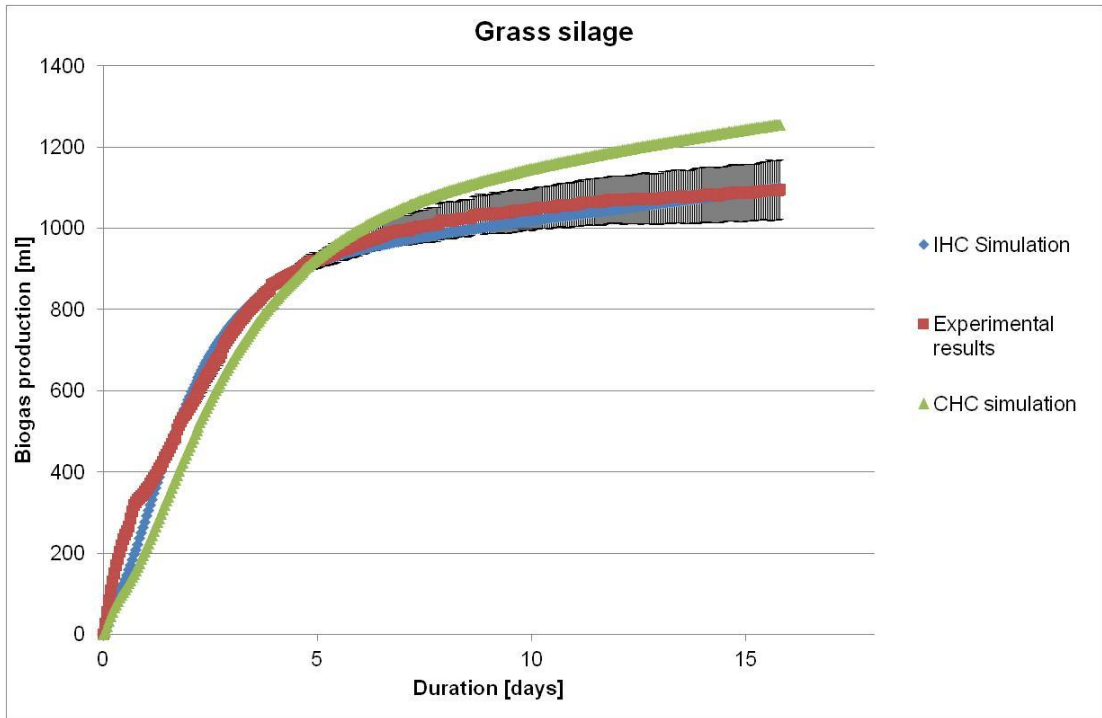


Figure 22. Comparison of the experimental cumulative biogas production from grass silage to simulation results, where the “IHC” indicates individually determined all kinetic constants, whereas the common hydrolysis phase constants and an individual determined kinetic constant for disintegration are used for “CHC”.

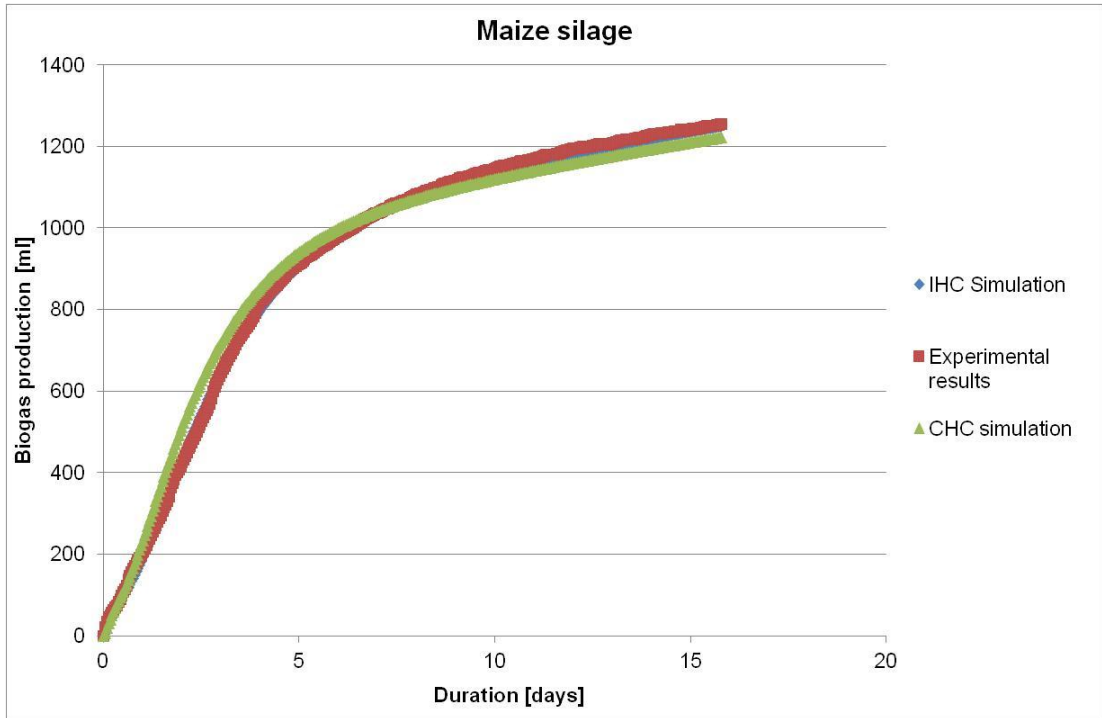


Figure 23. Comparison of the experimental cumulative biogas production from maize silage to simulation results, where the “IHC” indicates individually determined all kinetic constants, whereas the common hydrolysis phase constants and an individual determined kinetic constant for disintegration are used for “CHC”.

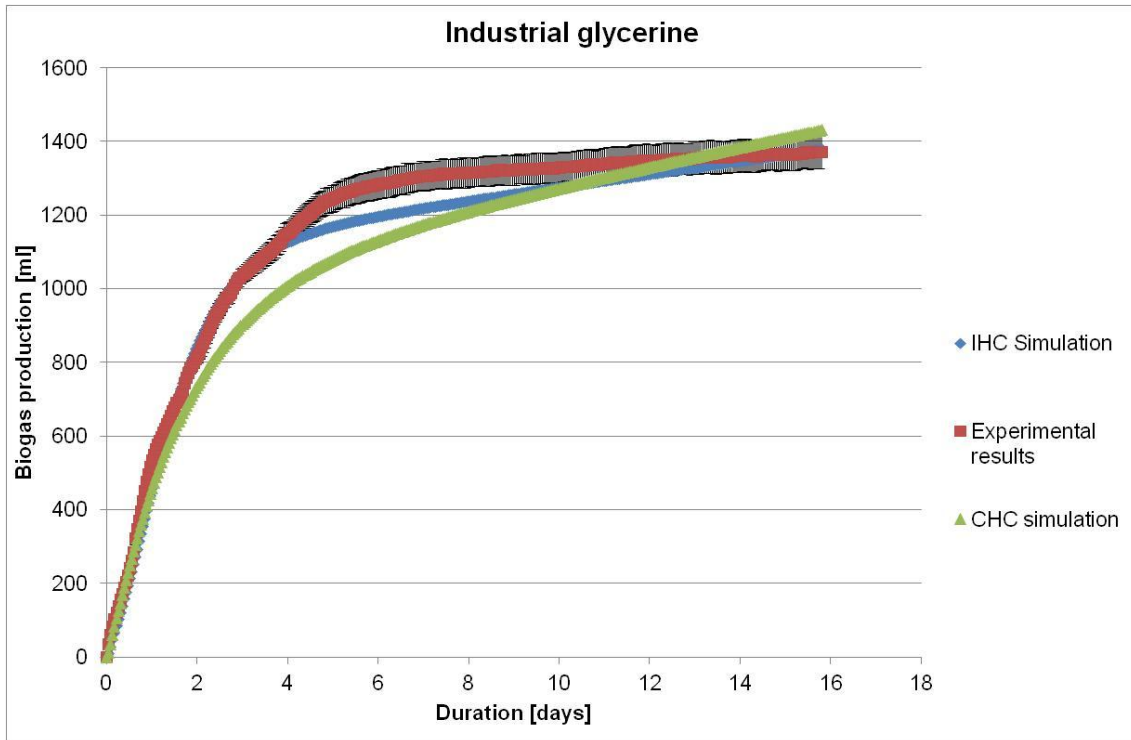


Figure 24. Comparison of the experimental cumulative biogas production from industrial glycerine to simulation results, where the “IHC” indicates individually determined all kinetic constants, whereas the common hydrolysis phase constants and an individual determined kinetic constant for disintegration are used for “CHC”.

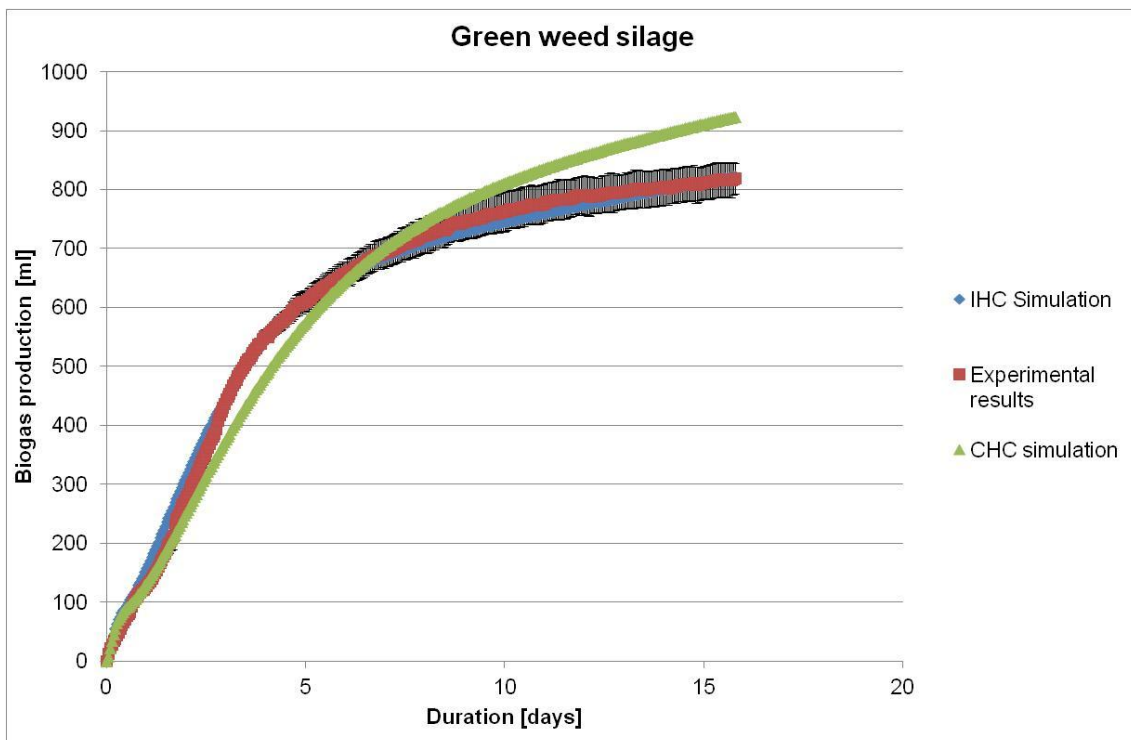


Figure 25. Comparison of the experimental cumulative biogas production from green weed silage to simulation results, where the “IHC” indicates individually determined all kinetic constants, whereas the common hydrolysis phase constants and an individual determined kinetic constant for disintegration are used for “CHC”.

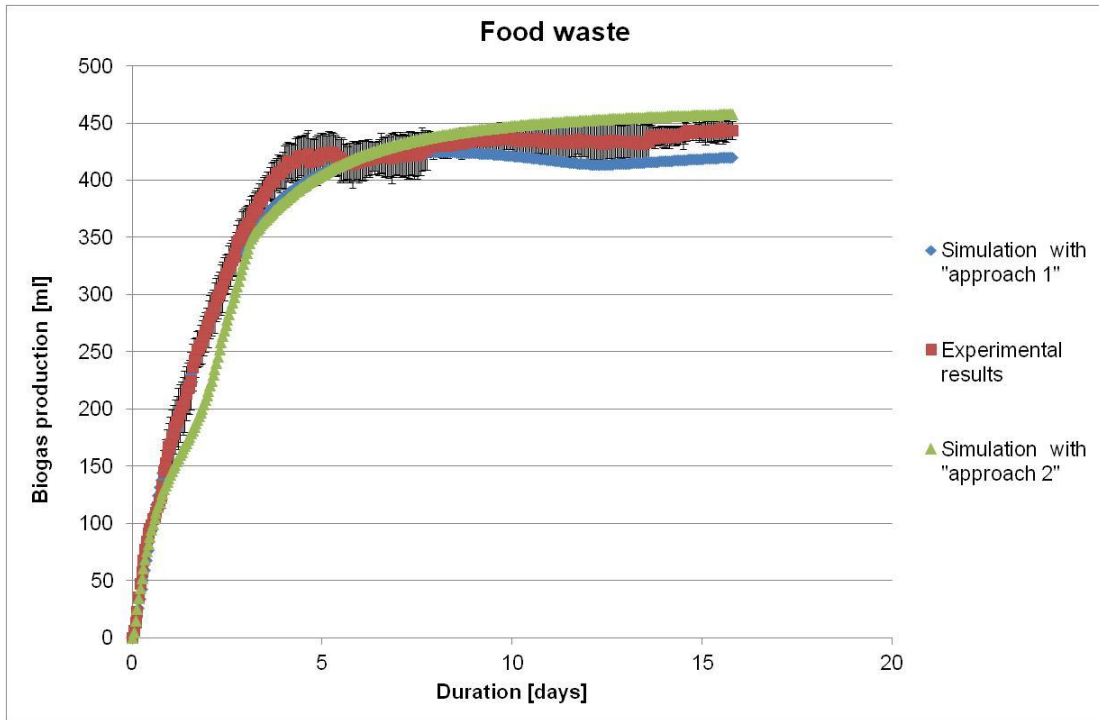


Figure 26. Comparison of the experimental cumulative biogas production from organic waste (food waste) to simulation results, where the “IHC” indicates individually determined all kinetic constants, whereas the common hydrolysis phase constants and an individual determined kinetic constant for disintegration are used for “CHC”.

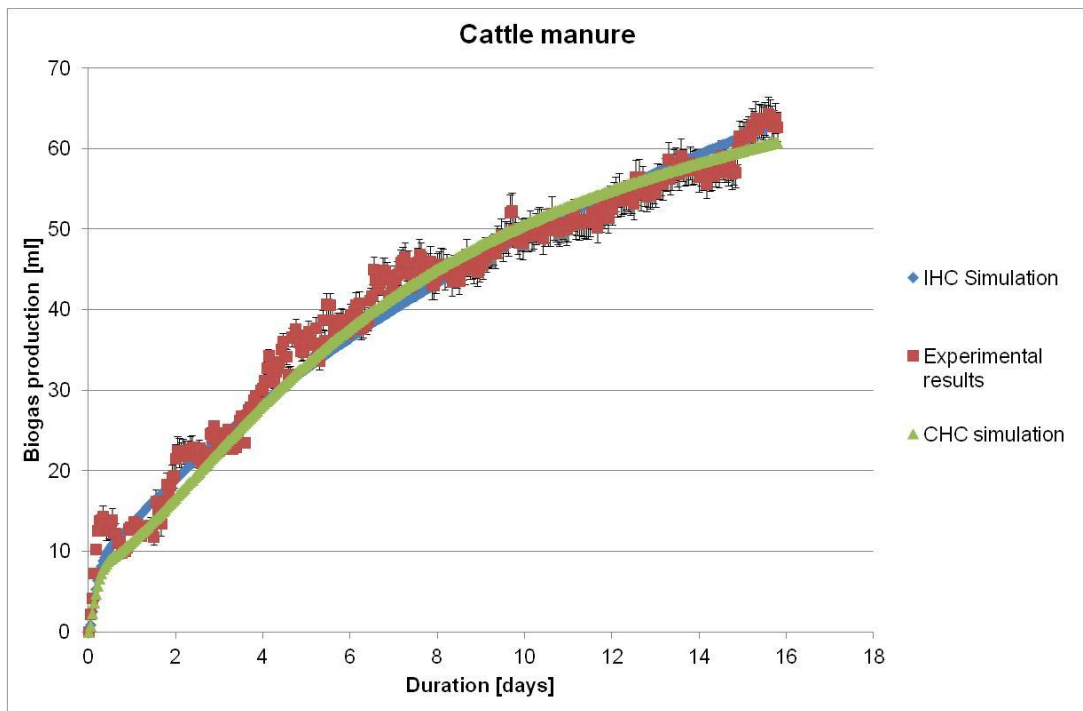


Figure 27. Comparison of the experimental cumulative biogas production from cattle manure to simulation results, where the “IHC” indicates individually determined all kinetic constants, whereas the common hydrolysis phase constants and an individual determined kinetic constant for disintegration are used for “CHC”.

#### 5.2.4. Application of the common hydrolysis constants

In order to test the CHC presented in chapter 5.2.3, a new substance was chosen, which was not included in the CHC determination phase. As a consequence, CHC are not adjusted to the test substance, allowing impartial verification of CHC application to a new substrate. As a test substance chicken manure (CM) was chosen. The substance analysis is included in table 19. The determined  $k_{dis}$  equalled to  $2.7 \text{ d}^{-1}$ , and on figure 28 is presented the comparison between the experimental and simulation results.

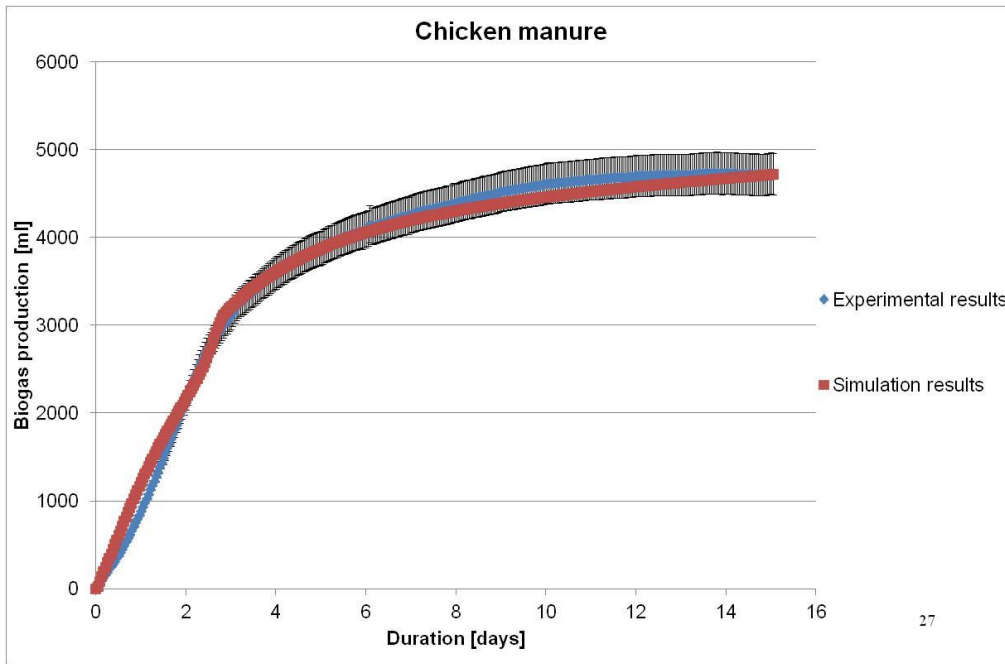


Figure 28. Validation of determined common hydrolysis constants for chicken manure.

Outcome of CHC application to describe substrate, which was not used during the determination phase of CHC, delivered very good fit between experimental and simulation results, since it precisely described kinetics of biogas production.

#### 5.2.5. Industrial size biogas power plant simulation

The necessary final stage for any modification of the model responsible for biogas production is an assessment against industrial size biogas power plant. Accordingly, for such a review EWE Biogas Power Plant (Wittmund, Lower Saxony, Germany) (EWE Biogas GmbH & Co. KG., 2011) was chosen, which is described in chapter 4.1.3. The analysed cattle manure and organic waste are the main substrates used at this biogas power plant. However, the composition of the organic waste can vary over the time, since it is a mixture of food residues from kitchens, restaurants, slaughterhouse, and a hospital. Consequently modelling the EWE Wittmund biogas power plant is an ambitious task. Hence, in this case a satisfactory fit between simulation and a real life situation proves a reliability of the model and its upgrade.

The model from Rojas et al. (Rojas, et al., 2010) of the EWE Wittmund Biogas Power Plant was modified, hence adjusted to an original ADM1xp, both substrates' characteristics determined earlier, along with the new parameters, were incorporated into the model. The model of EWE Wittmund Biogas Power Plant is presented as a figure 29, and figure 30 shows the acquired results. The total biogas produced at EWE Wittmund Biogas Power Plant from the 19.03.2012 until 15.04.2012 (28 days) equalled to 1.277 Mm<sup>3</sup>, whereas IHC simulation's outcome was 1.279 Mm<sup>3</sup> (1.84km<sup>3</sup> difference between an existing biogas power plant and simulation), and 1.191 Mm<sup>3</sup> (-86.2 km<sup>3</sup> difference between an existing biogas power plant and simulation) were obtained with CHC simulation.

The change of methane content over time is presented in figure 31. The averaged methane volume fraction over 28 days research was 66.85 volume % from EWE Wittmund, 65.11 volume % from simulation with IHC, and CHC simulation resulted in 64.44 volume %.

Taking under consideration very difficult to predict composition of the organic waste substrate, the obtained result from "IHC" is a satisfactory fit, and it proves the reliability of the model and it's new parameters, along with characteristics of the substrates. However, despite the fact that the results from "CHC" are underestimating the biogas production, and also biogas composition, the pragmatic approach of individually determining only one kinetic constant, despite four constants, could be considered as an option for the preliminary design stage, but with reflection on lower precision of the results.

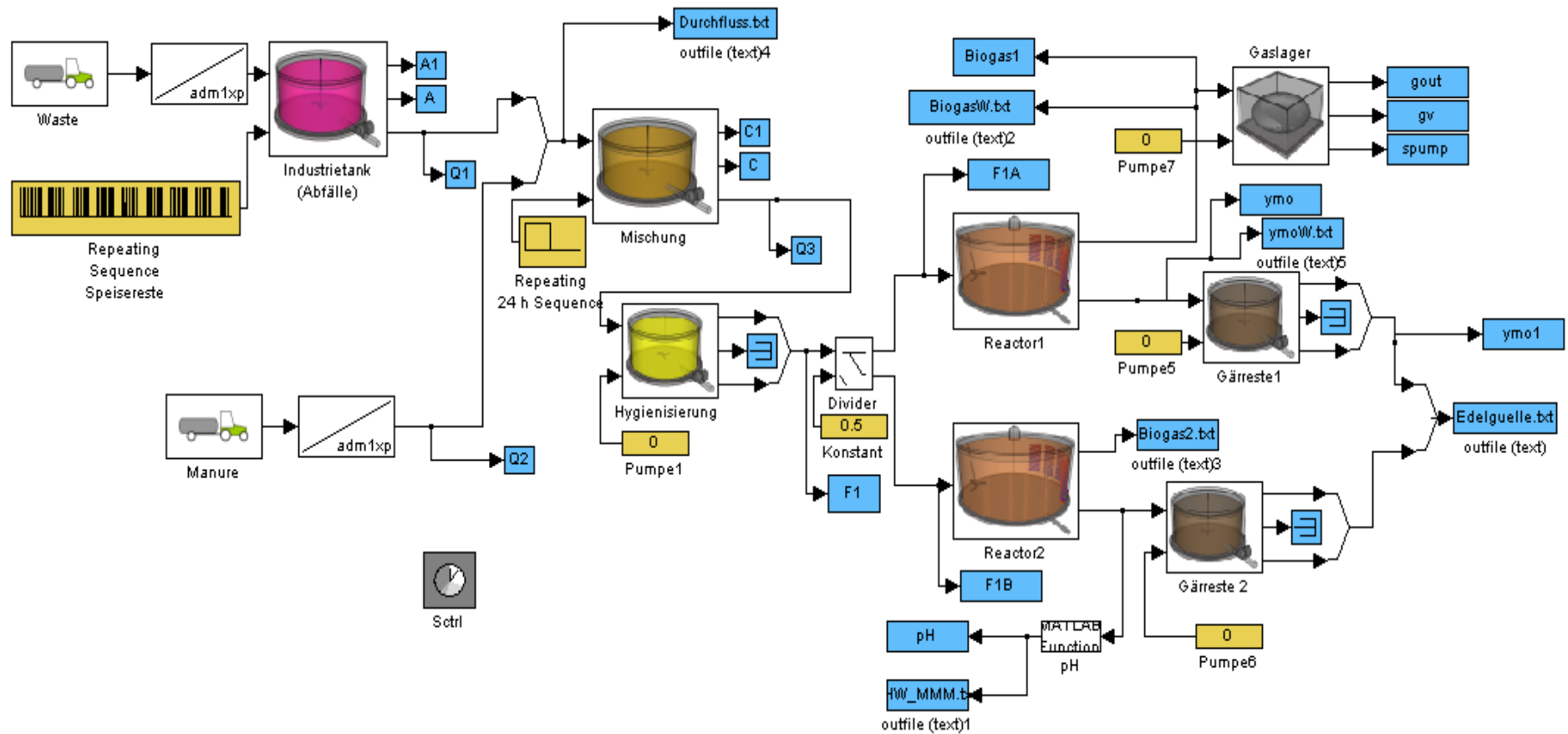


Figure 29. The model of EWE Wittmund Biogas Power Plant (EWE Biogas GmbH & Co. KG., 2011) prepared in SIMBA® simulation software (ifak system GmbH, 2005) by Rojas et al. (Rojas, et al., 2010) and modified for this research.

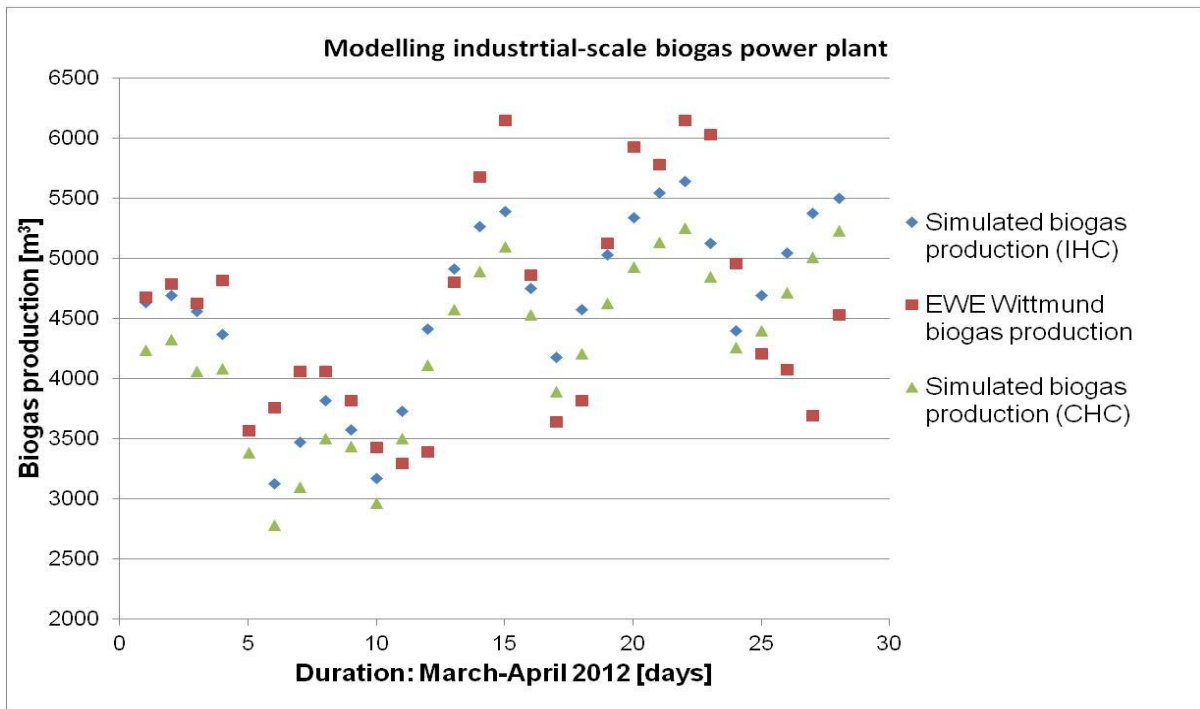


Figure 30. Assessment of the simulation results against the industrial size EWE Wittmund Biogas Power Plant (EWE Biogas GmbH & Co. KG., 2011), where the “IHC” indicates individually determined all kinetic constants, whereas the common hydrolysis phase constants and an individual determined kinetic constant for disintegration are used for “CHC”.

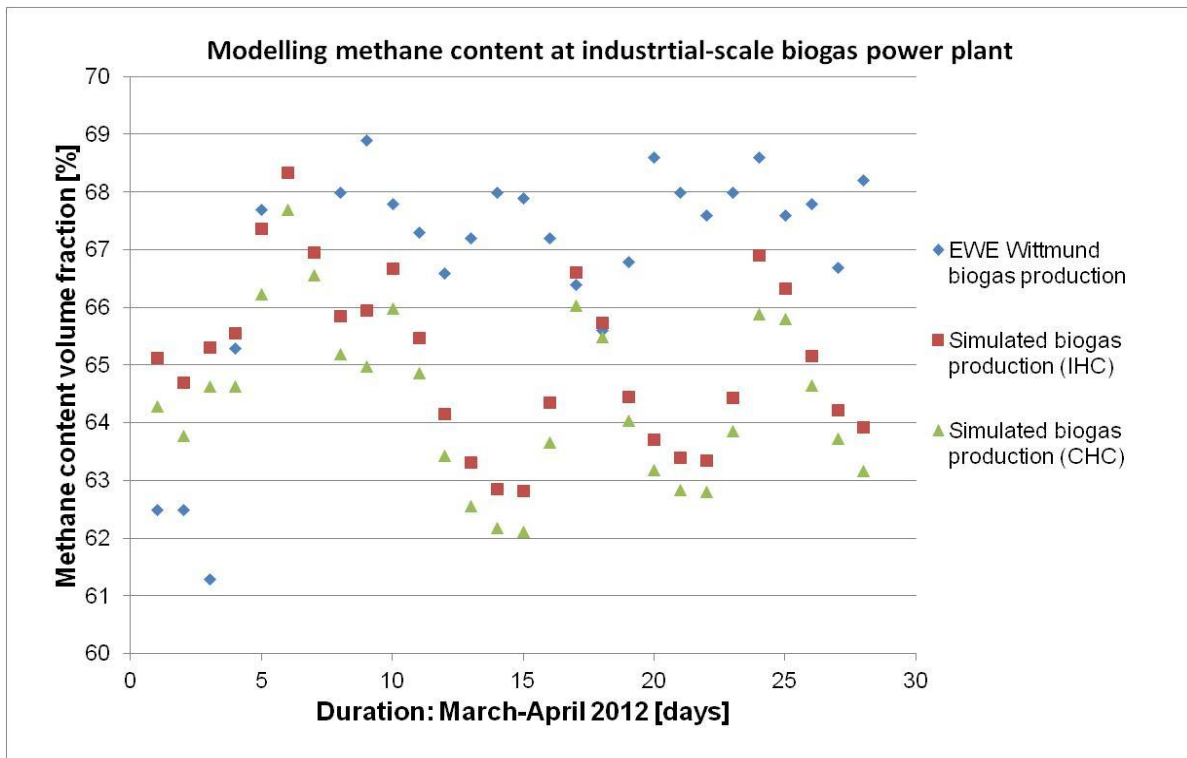


Figure 31. Assessment of the methane content in biogas from the industrial size EWE Wittmund Biogas Power Plant (EWE Biogas GmbH & Co. KG., 2011), and in two simulation methods, where the “IHC” indicates individually determined all kinetic constants, whereas the common hydrolysis phase constants and an individual determined kinetic constant for disintegration are used for “CHC”.

### 5.3. “Continuous mesophilic anaerobic digestion of manure and rape oilcake - modelling with ADM1”

#### 5.3.1. Substrate composition

Characteristics of inoculum obtained from EWE Wittmund Biogas Power Plant (EWE Biogas GmbH & Co. KG., 2011) and used for starting the continuous fermentation is presented as a table 22.

**Table 22. Characteristics of inoculum obtained from EWE Wittmund Biogas Power Plant (EWE Biogas GmbH & Co. KG., 2011) used for continuous fermentation.**

Parameter	Value	Unit
pH	8.2	[-]
FOS/TAC	0.243	[-]
Alkalinity (CaCO <sub>3</sub> )	9677	[mg·L <sup>-1</sup> ]
Org. acids (CH <sub>3</sub> COOH)	2352	[mg·L <sup>-1</sup> ]
Dry weigh	4.08	[mass %]
Ash	1.47	[mass %]
VS	26.0	[g·L <sup>-1</sup> ]
Ammonium - N	1440	[mg·L <sup>-1</sup> ]

All used substrates were investigated with Weender analysis and van Soest extension (Koch, et al., 2010; Naumann & Bassler, 1993; van Soest & Wine, 1967), and table 23 presents the results.

**Table 23. Characteristics of substrates used for continuous fermentation.**

Parameter	Unit	Rape seedcake oilcake	Sieved manure	Manure
Dry mass	[mass %]	90.48	8.60	10.79
Organic dry mass (oDM)	[DM %]	93.23	65.50	71.49
Raw lipids (RL)	[DM %]	11.17	3.99	3.72
Raw proteins (RP)	[DM %]	30.14	17.05	13.73
Raw fiber (RF)	[DM %]	15.46	14.61	21.78
ADF	[DM %]	25.11	43.02	40.89
ADL	[DM %]	9.10	25.87	18.43
NDF	[DM %]	39.67	37.04	44.80
NfE *	[DM %]	36.46	29.86	32.25

\*- calculated value

The rapeseed oilcake contained low mass fraction of water (dry mass 90.48 mass%). The majority of dry weight fraction were the organic compounds (volatile solids 93.23 dry

mass%). The two main components of organic fraction were proteins (30.14%) and fiber compounds (NDF 39.67 dry mass%). The lignin fraction in rapeseed oilcake is low (ADL 9.1 dry mass%) ensuring good gas production efficiency, since lignin is not digested in anaerobic conditions (Deublein & Steinhauser, 2011). The composition of analyzed rapeseed oilcakes was similar to the results obtained by other authors (Ramachandran, et al., 2007).

The dry mass fraction in manure was much lower than in the rapeseed oilcake (8.06 mass% in sieved and 10.79 mass% in raw manure respectively). Also the concentration of organic compounds in solid fraction was lower in comparison to rapeseed oilcake (65.5 DM% in sieved and 71.49 DM% in raw manure). The expected methane yields from cow manure are lower than those from oilcake due to the lower content of lipids and proteins, and the higher content of lignin.

The analysis of the manure revealed that the sieving process reduced the content of organic matter in the substrate (organic dry mass were reduced from 71.49 DM% to 65.50 DM%). One can also observe that the proportions between individual biopolymers present in the samples were changed. In sieved manure proteins and lignin made up higher part of volatile solids (proteins 17.05 DM%, lignin 25.9 DM%) when compared with raw manure (proteins 13.73 DM%, lignin 18.43 DM%). The observed changes may be explained by better availability of substrates in smaller particles which were passed through the sieve.

The model input data calculation are in accordance with chapter 4.1.4.2, hence the parameters used in the modelling are presented in table 24.

**Table 24. Parameters used in the modelling.**

Parameter	Unit	Rape seedcake	Sieved manure	Raw manure
$X_C$	[kg <sub>COD</sub> m <sup>-3</sup> ]	1269.84	84.45	109.47
$f_{pr}$	[-]	0.323	0.260	0.192
$f_{li}$	[-]	0.120	0.061	0.052
$f_{ch}$	[-]	0.425	0.198	0.312
$f_{xi}$	[-]	0.132	0.481	0.444
Degradability (Kuratorium fuer Technik und Bauwesen in der Landwirtschaft, 2014)	[DM %]	89.50	49.50	49.50

### 5.3.2. Batch fermentation

For an estimation of disintegration and hydrolysis kinetic constants batch fermentation experiments were prepared. Biogas production from individual substrates is illustrated on figures 32 and 33. The digestion of rapeseed oilcake was completed in 6 days (figure 32). The biogas volume reached 1218 ml, corresponding to a production efficiency of

$0.5706 \text{ m}^3 \text{ kg}^{-1}$ . Biogas production efficiency obtained during batch experiments was comparable to the results obtained by Bohdziewicz et al.(Bohdziewicz, et al., 2012).

The production of biogas from rape oil cake was higher when compared with *Jaropha curcas* oilcake and sunflower oilcake (Staubmann, et al., 1997; Monlau, et al., 2013) digested without any pretreatment.

The presented results suggest that the anaerobic digestion of rape oil cake could be done with low hydraulic retention times. The digestion process during batch experiment was completed in six days, what is four times faster when compared with retention times in agricultural biogas plants.

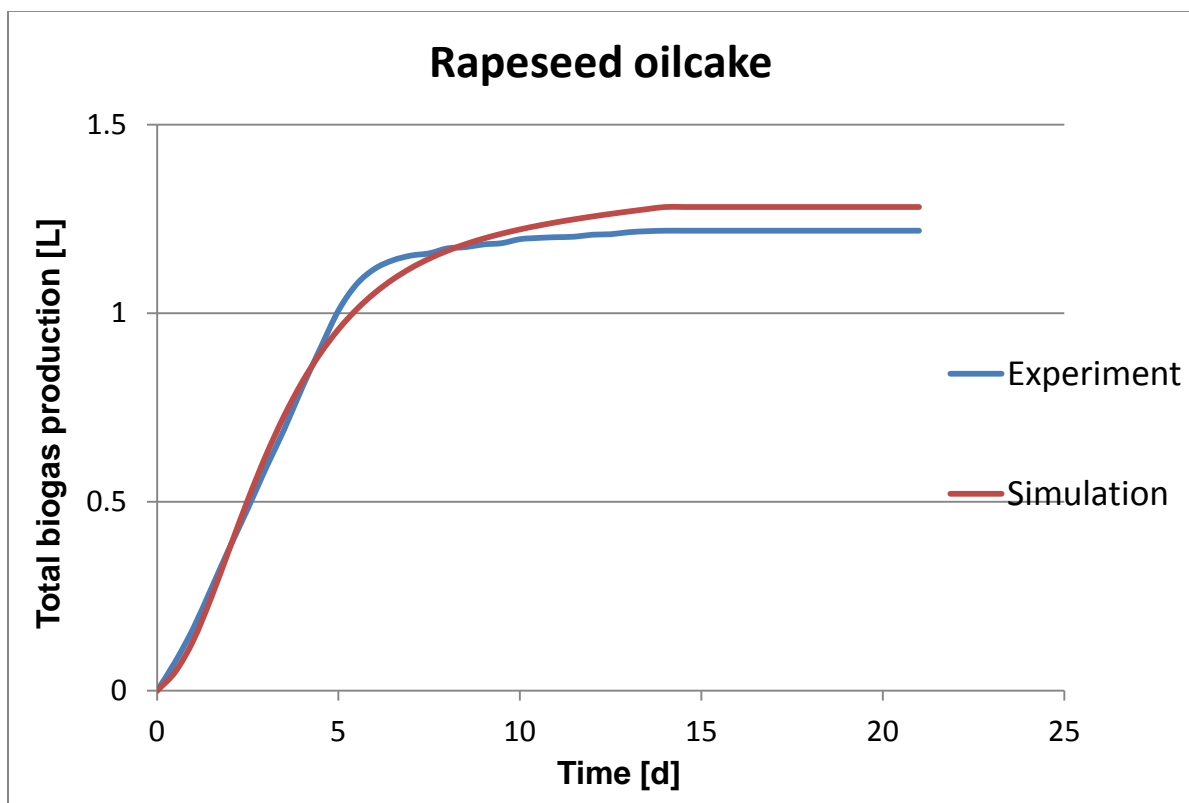


Figure 32. Experimental batch anaerobic digestion and simulation of rapeseed oilcake.

Total gas production from sieved manure was 395 cm<sup>3</sup> with an efficiency of 0.281 m<sup>3</sup> kg<sup>-1</sup>. Gas production rates reached the highest level between the second and fourth days of experiment and gradually decreased until the end of batch trials.

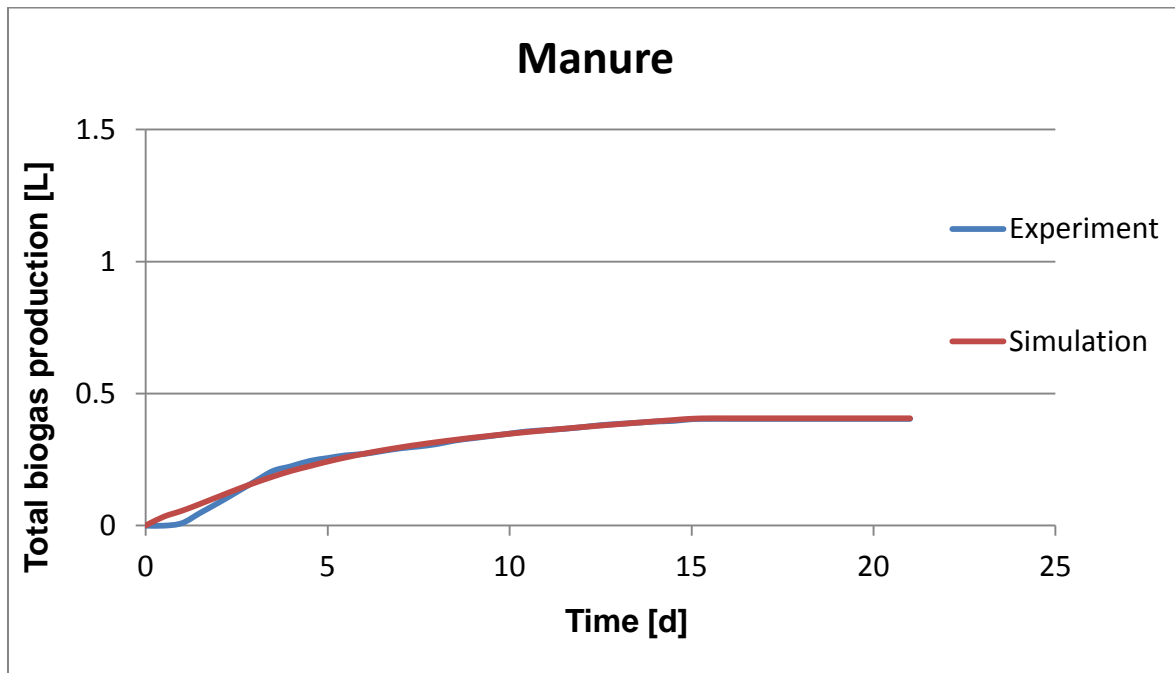


Figure 33. Experimental batch anaerobic digestion and simulation of rapeseed oilcake.

Optimized kinetic constants for hydrolysis and disintegration phases for rapeseed oilcake and sieved manure are presented in table 25.

Table 25. Optimized disintegration kinetic constants, according to the downhill simplex methods algorithm from Nelder and Mead (Nelder & Mead, 1965).

Substrate	Parameter			
	$k_{dis}$	$k_{hyd\_Ch}$	$k_{hyd\_Pr}$	$k_{hyd\_Li}$
Unit	[d <sup>-1</sup> ]	[d <sup>-1</sup> ]	[d <sup>-1</sup> ]	[d <sup>-1</sup> ]
Rapeseed cake	0.7716	0.5478	0.5695	0.3036
Sieved manure	0.4691	0.7498	0.0646	0.001

The decomposition rate ( $k_{dis}$ ) optimized for sieved cattle manure was similar to the results obtained by Wett et al. (Wett, et al., 2007) The parameters obtained by the authors of ADM1 were about two times lower, but these parameters were determined in other temperature conditions (55 °C) and the manure was not sieved (Batstone, et al., 2002). The decomposition constant obtained by Wichern et al. (Wichern, et al., 2008) is one order of magnitude lower in comparison to the presented results. In experiments presented by

Wichern et al. (Wichern, et al., 2008) the substrate was a mixture of manure and fodder, and the parameter was optimized for this blend. Lower constants could be caused by presence of unscrambled plant material.

Hydrolysis constants obtained for both examined substrates are in the range between 0.3 and 0.8 (only hydrolysis of proteins and lipids from sieved manure was lower ). Protein and carbohydrate hydrolysis constants optimized for rapeseed oilcake were around 0.5. These values are usually higher than obtained for other popular substrates (Batstone, et al., 2002). The carbohydrate hydrolysis constant optimized for sieved manure is 0.7698. This value is in the lower part of the range proposed by Garcia-Hares (Garcia-Heras, 2003), but it is higher than the values obtained for other substrates (Batstone, et al., 2002; Luebken, et al., 2007).

The digestion of rapeseed oilcake batch trials was faster than the digestion of sieved manure, and this is reflected by the decomposition and hydrolysis constants, which optimized for rapeseed oilcake were higher in comparison to the results obtained for cattle manure. Better bioavailability of organic matter probably arises from differences in the structure of plant elements present in the substrates used. The majority of biomass in case of rapeseed oilcake originates from cotyledons (Leubner, 2012). In case of *Brassica napus* the reserve materials for the embryo are stored in the cotyledons thus the easily biodegradable biopolymers (proteins and lipids) represent large mass fraction of biomass in oilcake. On the other hand biopolymers, present in stems and leaves (which represent the main position in the cattle diet) form a scaffold and protective structure in a plant. The mass fraction of hardly biodegradable polymers in those parts of a plant is higher in comparison to seeds. Furthermore the fast digestion of oilcake may arise from the breakdown of plant tissue during the pressing process.

### 5.3.3. Continuous fermentation and simulation

The data gathered during the continuous fermentation process of cow manure and rapeseed oilcake are presented in figure 34.

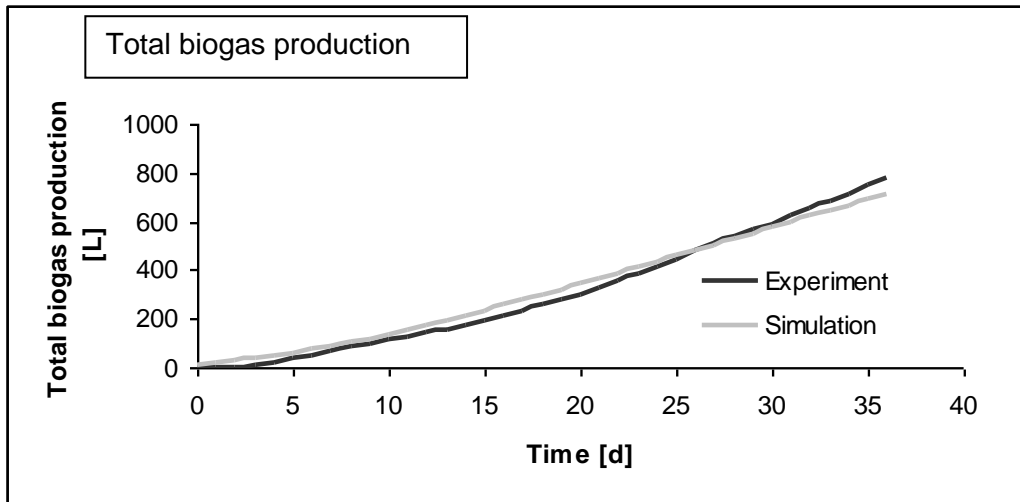


Figure 34. Total biogas production during the continuous fermentation.

During continuous fermentation the concentration of rapeseed oilcake (measured as a fresh weight) in substrate was increased from 20 to 80 g L<sup>-1</sup>, which corresponds to the increase in the organic loading rates (expressed as oDM) from 0.957 g L<sup>-1</sup>d<sup>-1</sup> to 3.18 g L<sup>-1</sup>d<sup>-1</sup> (figure 35).

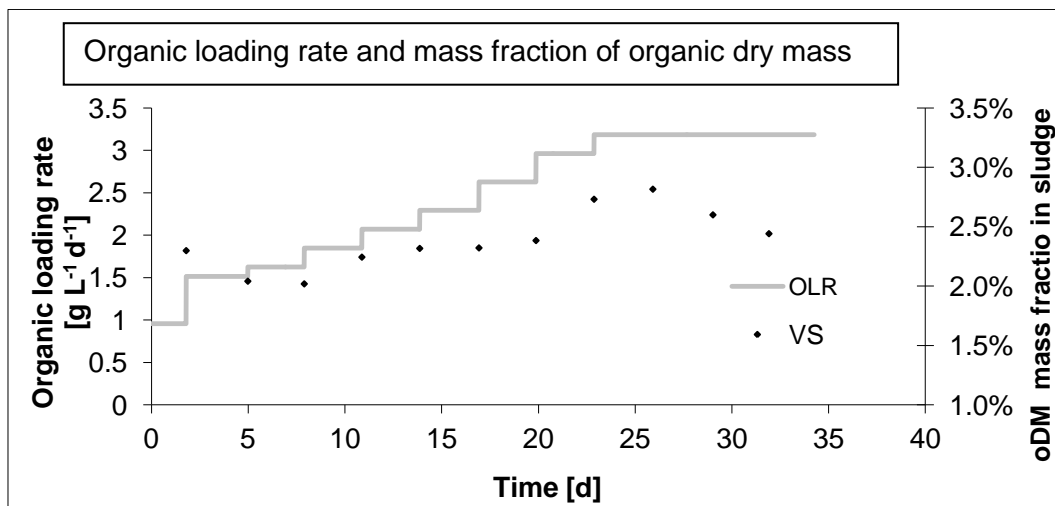


Figure 35. Organic loading rate and mass fraction of organic dry mass in the digested sludge.

Biogas production rate increased from 0,4 L L<sup>-1</sup>d<sup>-1</sup> up to 1,38 L L<sup>-1</sup>d<sup>-1</sup> at the end of experiment. This values corresponds to a production efficiency (referring to organic matter measured as oDM) of 0.42 L g<sup>-1</sup>. Methane concentration at the beginning of the experiment was 57 volume% and decreased with the increase of the organic loading rate to 50 volume% in the last part of experiment (figure 36).

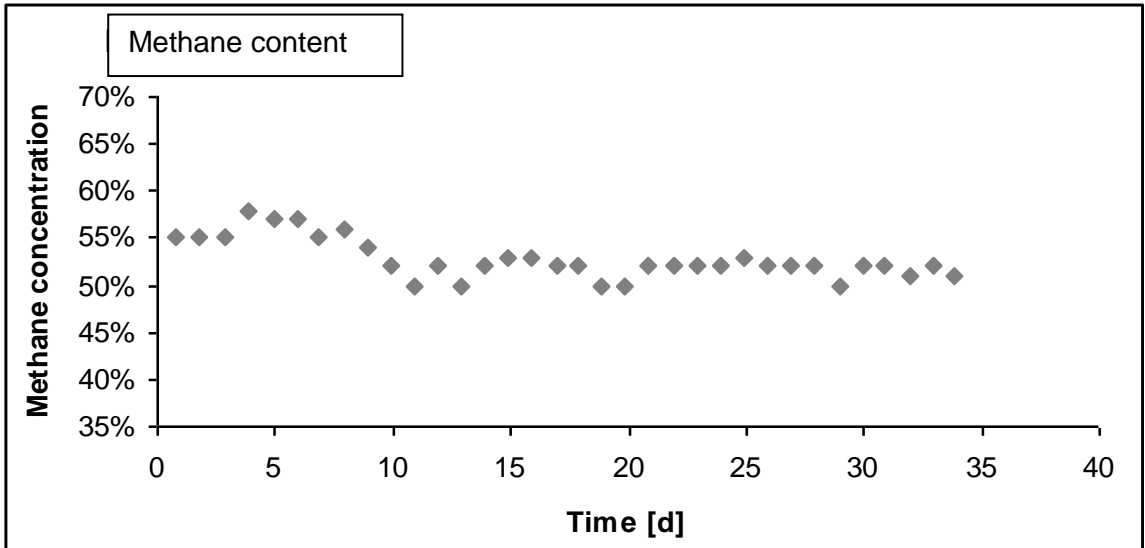


Figure 36. Methane content in the biogas formed.

During the whole experiment the pH value oscillated between 7.52 and 7.78 (figure 37). These values are only slightly above the optimal pH range for anaerobic digestion, which is assumed between 6.8 and 7.5.

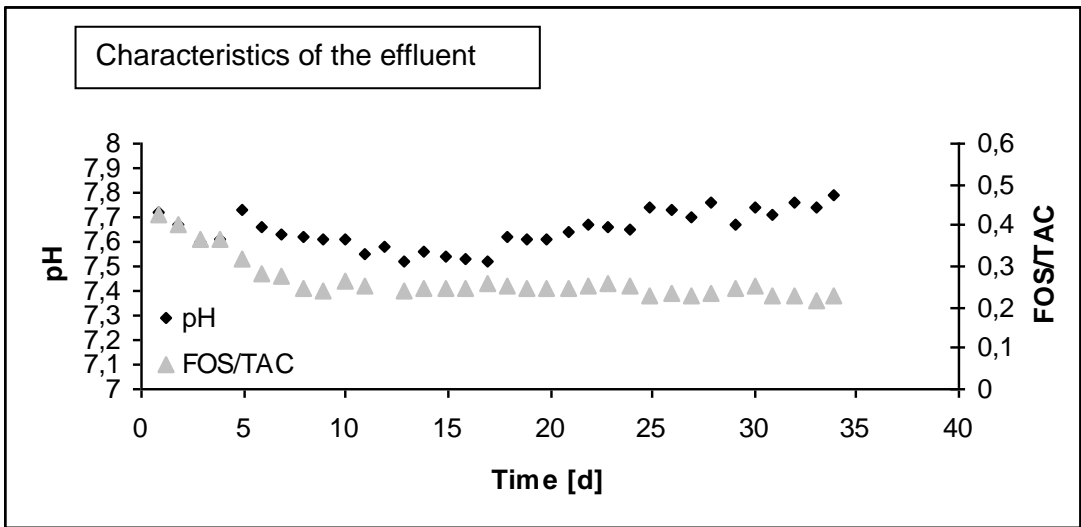


Figure 37. The pH and FOS/TAC ratio of the reactor's effluent.

The FOS/TAC ratio dropped from 0.427 to 0.273 during first six days of fermentation and remained below this value until the end of the experiment. Low values of the FOS/TAC ratio suggest that the digestion system was still below its optimal organic loading rate.

The concentration of ammonium ions during continuous fermentation remained between 1.5 g L<sup>-1</sup> and 2.5 g L<sup>-1</sup> (figure 38). These values are in the upper range of concentrations optimal for anaerobic digestion and a further increase in ammonium ions concentration could cause inhibition problems (Nielsen & Angelidaki, 2008).

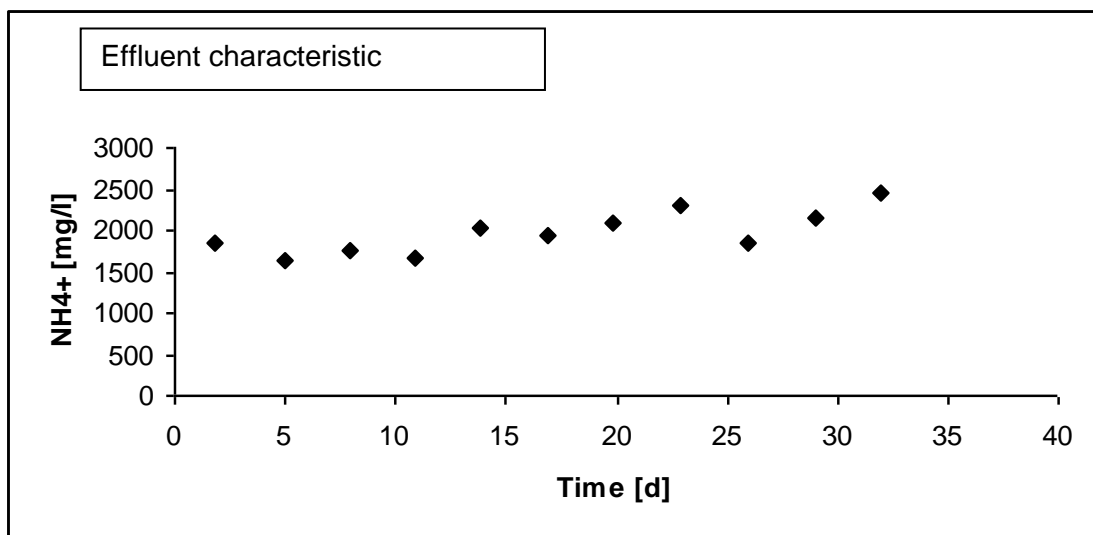


Figure 38. Concentration of the ammonium in the effluent.

The presented results show that the continuous fermentation process showed good stability. We have not encountered any problems with acidification of the reactor nor the accumulation of ammonium. Moreover, the results of modelling and fermentation showed a good correlation with methane concentration. The difference in total biogas production between experimental results and the computer simulation was only 7.8 volume% (figure 33). Predicted gas production was slightly underestimated when compared with observed gas readings. A good correlation between the simulation results and experimental data for continuous fermentation confirms the accuracy of kinetic parameters optimized for batch experiments. Further increase in accuracy might involve optimization of other model parameters.

#### 5.4. ***“Experimental Measurements and Thermodynamic Modelling of biogas upgrading process with use of 2-(Ethylamino)ethanol”***

##### 5.4.1. **Experimental results**

##### 5.4.1.1. **Assessment of the apparatus precision**

Aim of this part was to provide precise experimental results on CO<sub>2</sub> solubility in aqueous EAE solutions acquired with apparatus described in section 4.2.1.2.

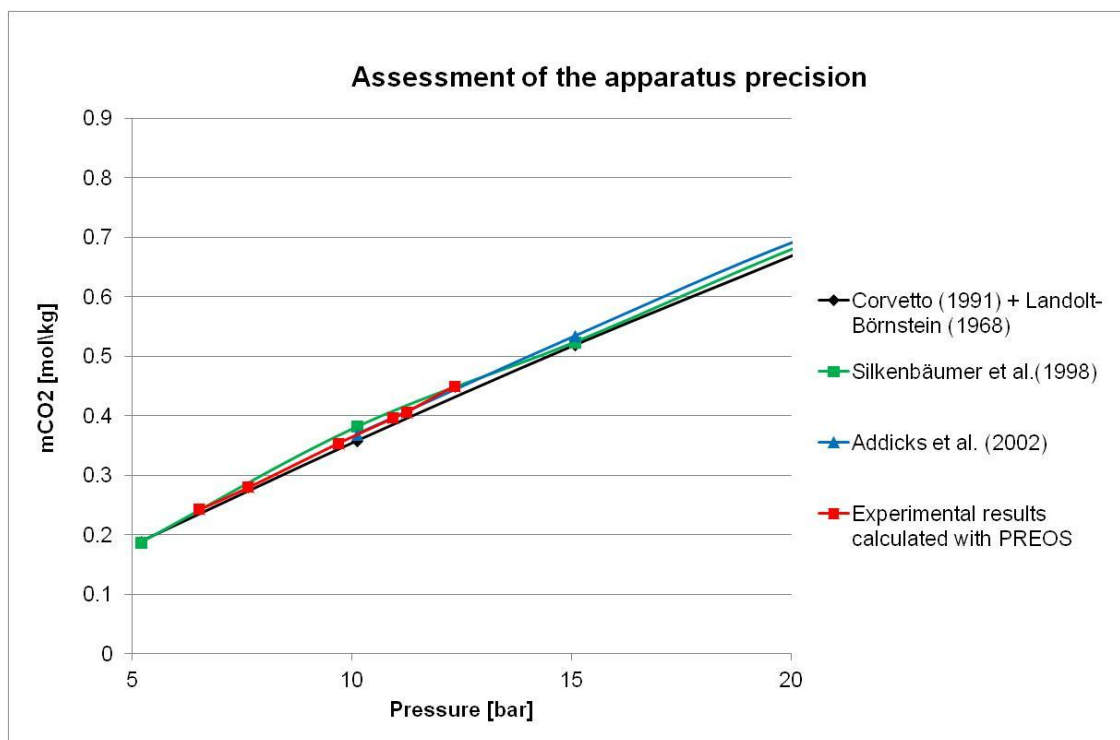


Figure 39. Comparison of the experimental results to the literature found at Dortmund Data Bank (DDBST GmbH, 2014) on solubility of CO<sub>2</sub> in water at a temperature of 19.8°C, pressure range of 5 up to 12 bar.

Therefore, in order to ensure correct functionality of the apparatus, and high accuracy of the experimental results, solubility of CO<sub>2</sub> in water was measured at temperature of 19.8°C, pressure range of 5 bar up to 12 bar, and compared to the literature found in Dortmund Data Bank® (DDBST GmbH, 2014): Silkenbaeumer et al. (Silkenbaeumer, et al., 1998), Crovetto (Crovetto, 1991), Landolt-Börnstein (Landolt-Boernstein, 1968), and Addicks et al. (Addicks, et al., 2002). The results are presented as a figure 39, indicating very good fit.

#### 5.4.1.2. Solvent characteristics

##### 5.4.1.2.1. Density

As explained in section 4.2.1.2., due to change in viscosity of the aqueous alkanolamine solutions, prior to each filling of the second reactor (figure 13) with the solution, its' density was measured. The averaged density of 2,5 mass % solution was measured to be 0.9969 ( $\pm$  0.1%), and the averaged density of 5 mass % solution was measured to be 0.9959 ( $\pm$  0.1%).

##### 5.4.1.2.2. Mixtures liquid heat capacity

The binary NRTL interaction energy parameters are necessary prior to eNRTL model's application for activity coefficient calculations, which are then used for aqueous phase chemical equilibrium, phase equilibrium, enthalpy of absorption, liquid enthalpy and liquid heat capacity determination (Austgen, et al., 1989). However, accurate prediction of mixture's liquid heat capacity is necessary for correct calculation of desorption step, necessary for complete assessment of industrial upgrading installations.

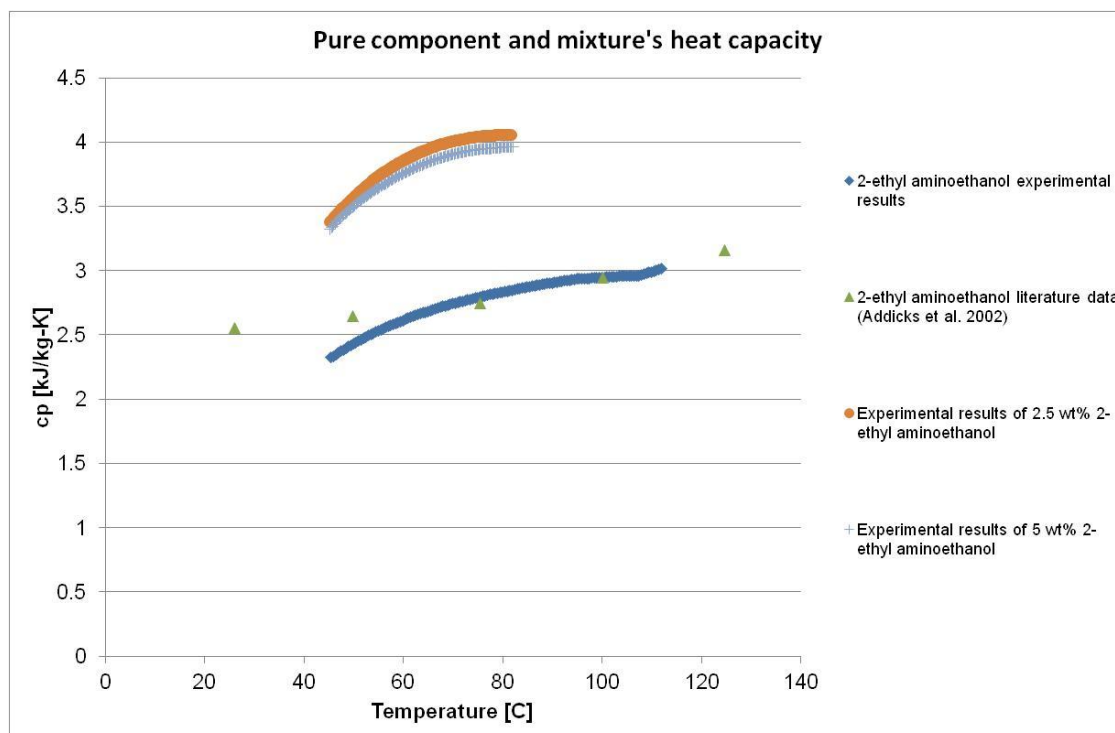


Figure 40. Experimental results of pure compound and mixture's liquid heat capacity, compared to the literature results.

Liquid heat capacity of pure EAE was measured and compared to the literature (Maham, et al., 1997). Together with aqueous solutions results are presented as a figure 40. In addition to that, experimental mixtures' liquid heat capacity is also compared to the simulation. However, because used calorimeter was cooled with air, therefore precise measurement in the lower temperature range was not possible, as can be seen on the graph.

#### 5.4.1.3. Results of the solubility measurements

Experimental range of interest was from 2,89 up to 10.11 bar, at 293.00 K, 313.15 K, and 333.15 K. The solvent consisted of in 2.5 mass % and 5 mass % aqueous alkanolamines. The measured results are presented as table 26. For each chosen temperature and concentration, presented data consists of five points, hence of five end pressures. Due to the measuring procedure, specifically filling of the first reactor with use of regular pressure regulator at the gas bottle, it was impossible to exactly repeat each measurement. Moreover, correction of the moles of carbon dioxide in the first reactor with use of the gas release valves, was also attempted but did not deliver accurate results. As a consequence, for each chosen temperature and concentration minimum 10 measurements were conducted, and the 5 presented points were chosen base on standard deviation from the results obtained.

Table 26. CO<sub>2</sub> solubility in 2-(Ethylamino)ethanol (EAE).

		2.5 mass % EAE			5 mass % EAE		
Parameter	<i>T</i>	<i>loading</i>	<i>p</i> <sub>CO2</sub>	<i>η</i>	<i>loading</i>	<i>p</i> <sub>CO2</sub>	<i>η</i>
Unit	[K]	[mol CO2 mol EAE <sup>-1</sup> ]	[bar]	[-]	[mol CO2 mol EAE <sup>-1</sup> ]	[bar]	[-]
	293.00	1.4105	3.14	1.42	1.1270	4.05	1.14
	293.00	1.7591	5.41	1.76	1.2222	5.14	1.23
	293.00	1.9493	6.53	1.95	1.2698	5.51	1.28
	293.00	2.1078	7.51	2.11	1.4841	7.21	1.49
	293.00	2.5832	10.11	2.58	1.5873	8.40	1.59
	313.15	1.1569	2.89	1.16	1.0238	4.10	1.03
	313.15	1.3154	4.16	1.32	1.1905	6.68	1.20
	313.15	1.4263	5.23	1.43	1.2619	7.50	1.27
	313.15	1.5214	5.61	1.53	1.3730	8.56	1.38
	313.15	1.5689	6.37	1.57	1.3968	9.46	1.40
	330.15	1.1569	4.44	1.16	1.1032	5.64	1.07
	330.15	1.2520	5.24	1.26	1.1270	7.23	1.14
	330.15	1.4263	6.53	1.43	1.1905	7.90	1.20
	330.15	1.6323	7.86	1.64	1.2540	8.90	1.26
	330.15	1.7116	8.52	1.71	1.3492	10.10	1.36

Despite the fact that more carbon dioxide is captured at lower temperatures and at higher concentration of EAE, the absorption efficiency was verified with use of this equation:

Equation 104

$$\eta = \left( \frac{n_{CO_2}^{abs}}{n_{EAE}} \right)$$

where

$n_{CO_2}^{abs}$  - amount of carbon dioxide moles absorbed, expressed in mole fraction

$n_{EAE}$  - amount of EAE moles in the solution, expressed in mole fraction

The intention of this efficiency is determination of amount of moles absorbed per 1 mole of EAE, and the results are included in table 26, and according to them the higher efficiency is correctly achieved at lower temperatures, as presented in table 8. Moreover, higher efficiency is correctly achieved at higher loading rate, hence when more carbon dioxide is absorbed. However, the efficiency of 5 mass% EAE aqueous solution is lower than 2,5 mass% EAE aqueous solution. This phenomena might be explained, following Suda et al. (Suda, et al., 1996) statement, that EAE has a moderate stability carbamate, hence part of the carbamate is converted back to free amine and bicarbonate, however for this reaction , per each mole of carbamate reacting one mole of water is required, therefore the efficiency might be reduced due to lower water content.

## 5.4.2. Thermodynamic modelling

### 5.4.2.1. Carbamate stability parameters

Suda et al. (Suda, et al., 1996) conducted NMR measurements for EAE, where he indicated that EAE is forming moderate stability carbamate. An assessment of equilibrium coefficients used for describing equation 97, taken from (Austgen, 1989), which were also used for DGA (Aspen Technology Inc., 2008) as presented in table 14, was conducted, indicating a very good correlation with Suda et al.'s (Suda, et al., 1996) research result. Therefore it was decided not to modify used equilibrium coefficients describing carbamate stability, hence reversion of carbamate to bicarbonate.

### 5.4.2.2. Heat capacity parameters

The heat capacity experimental results were used for regressing *CPIG* Parameters given in table 27, and used for calculating results on the figure 41, As can be noticed from table 27, only 6 coefficients were determined, because the others did not have an influence on the

results according to Data Regression System (DRS) build in ASPEN® V8.0. Consequently coefficients 7-11 were kept equal to the starting values, taken from DGA's model (Aspen Technology Inc., 2008)

**Table 27. Temperature dependent coefficients of ideal gas heat capacity equation (CPIG).**

<b>Component</b>	<b>2-(ethylamino)ethanol</b>	<b>Standard deviation</b>
Temperature Unit	[C]	[-]
Property Unit	[kJ kmol <sup>-1</sup> K <sup>-1</sup> ]	
Coefficient 1	-1,58E+02	1.79E+03
Coefficient 2	9,98E+00	5.15E+00
Coefficient 3	-1,42E-01	5.21E+00
Coefficient 4	1,14E-03	4.18E-02
Coefficient 5	-4,98E-06	1.27E-04
Coefficient 6	9,49E-08	1.39E-07
Coefficient 7	-2,73E+02	-
Coefficient 8	7,27E+02	-
Coefficient 9	0,00E+00	-
Coefficient 10	0,00E+00	-
Coefficient 11	0,00E+00	-

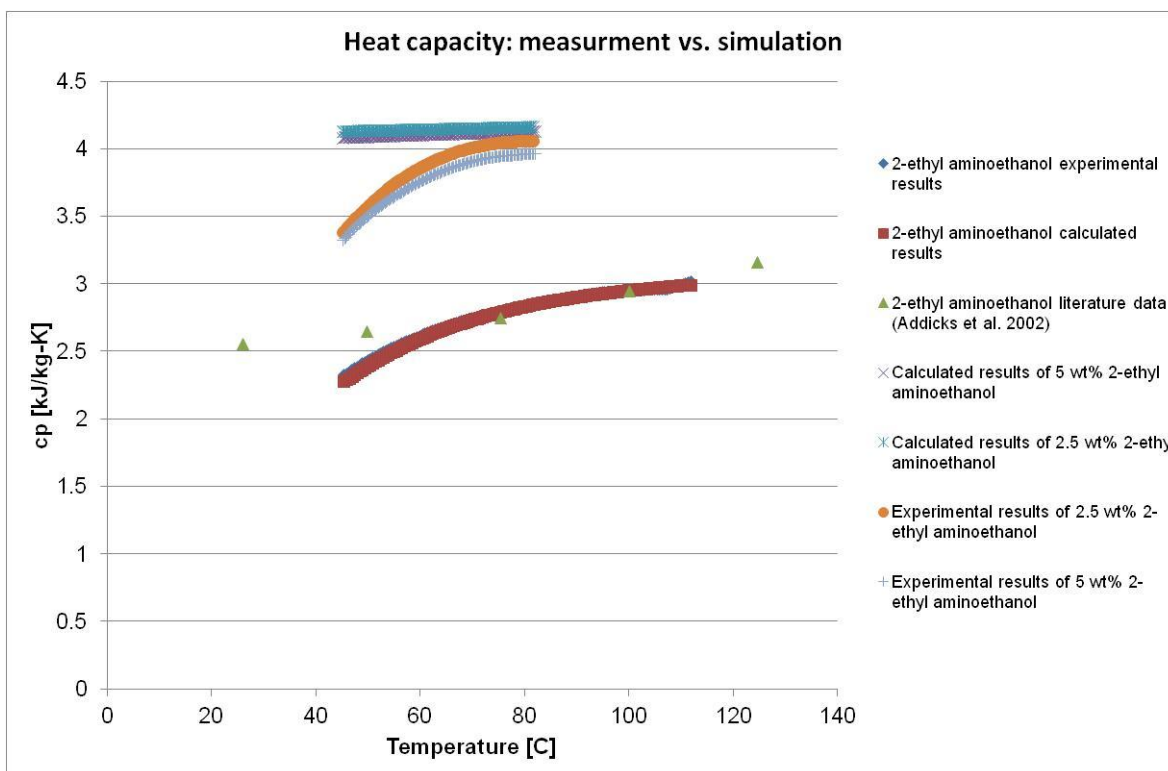


Figure 41. Modelling mixture's liquid heat capacity, and comparison to the experimental results.

#### 5.4.2.3. NRTL's interaction binary parameters

Regressed values of the NRTL binary interaction parameters used for local contribution in eNRTL model are included in table 28.

Table 28. NRTL's binary interaction parameters obtained with use of ASPEN Plus® V8.0 Data Regression System (DRS).

Parameter	Component i	Component j	Value	Standard deviation
a	H2O	EAE	16.514	0.128
a	EAE	H2O	-3.958	0.026
b	H2O	EAE	-16.141	40.443
b	EAE	H2O	-3.211	8.031

Evaluation of the new values' applicability in representing the experimental results from table 26 is reported as a figures 42-44. Summarizing, it can be stated that a good fit between model and experimental results was achieved, especially taking under consideration limited data, and pragmatic approach of fitting values from DGA for EAE.

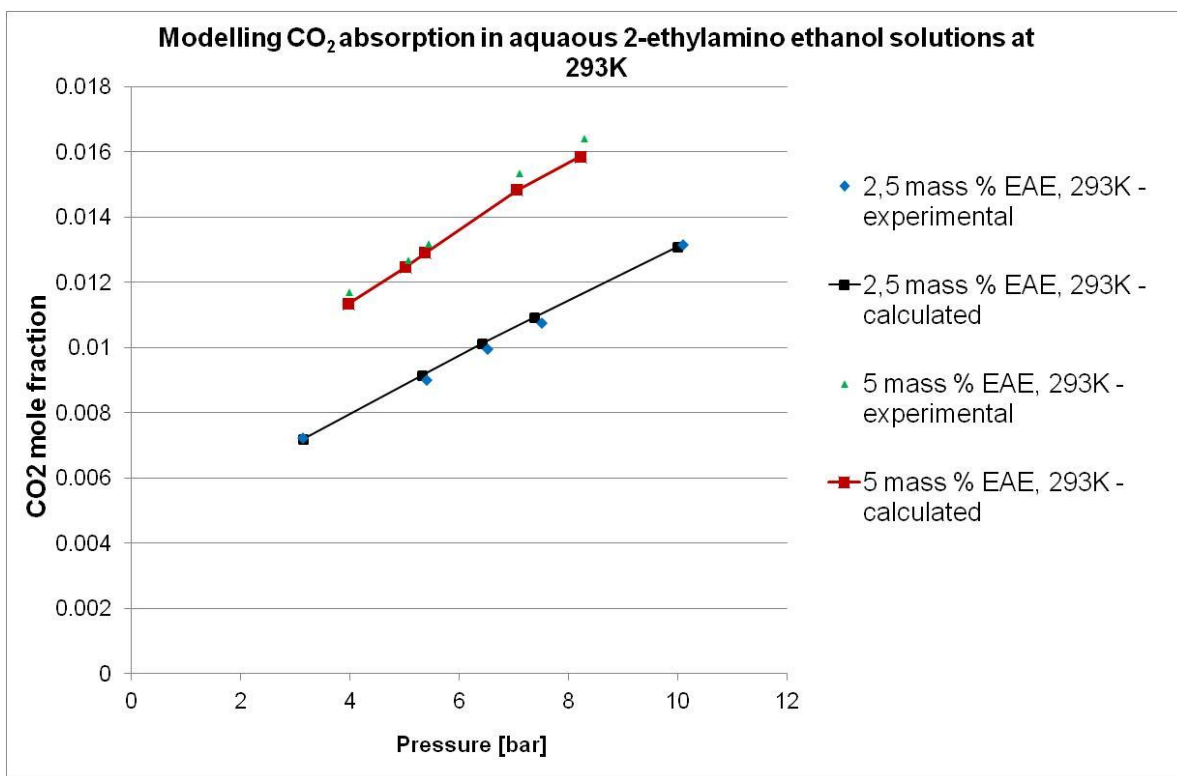


Figure 42. Modelling CO<sub>2</sub> absorption in aqueous 2-(Ethylamino)ethanol solutions at 293 K, and comparison to the experimental results.

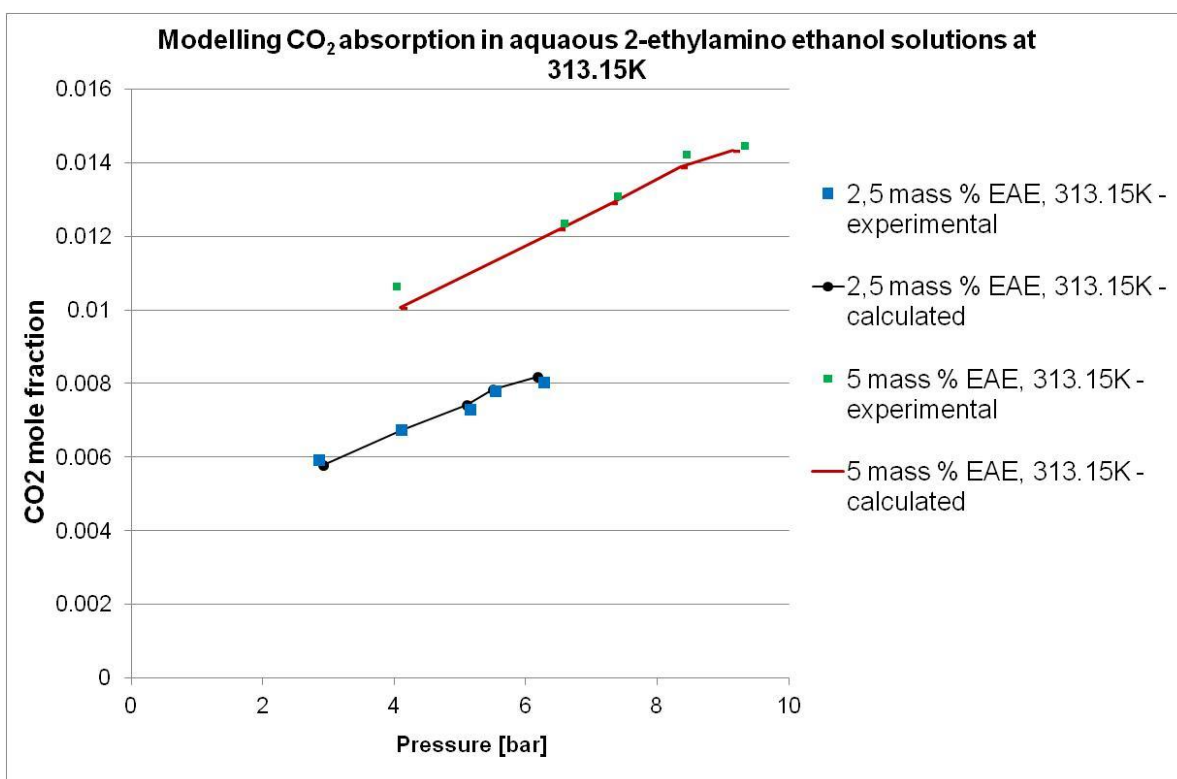


Figure 43. Modelling CO<sub>2</sub> absorption in aqueous 2-(Ethylamino)ethanol solutions at 313.15 K, and comparison to the experimental results.

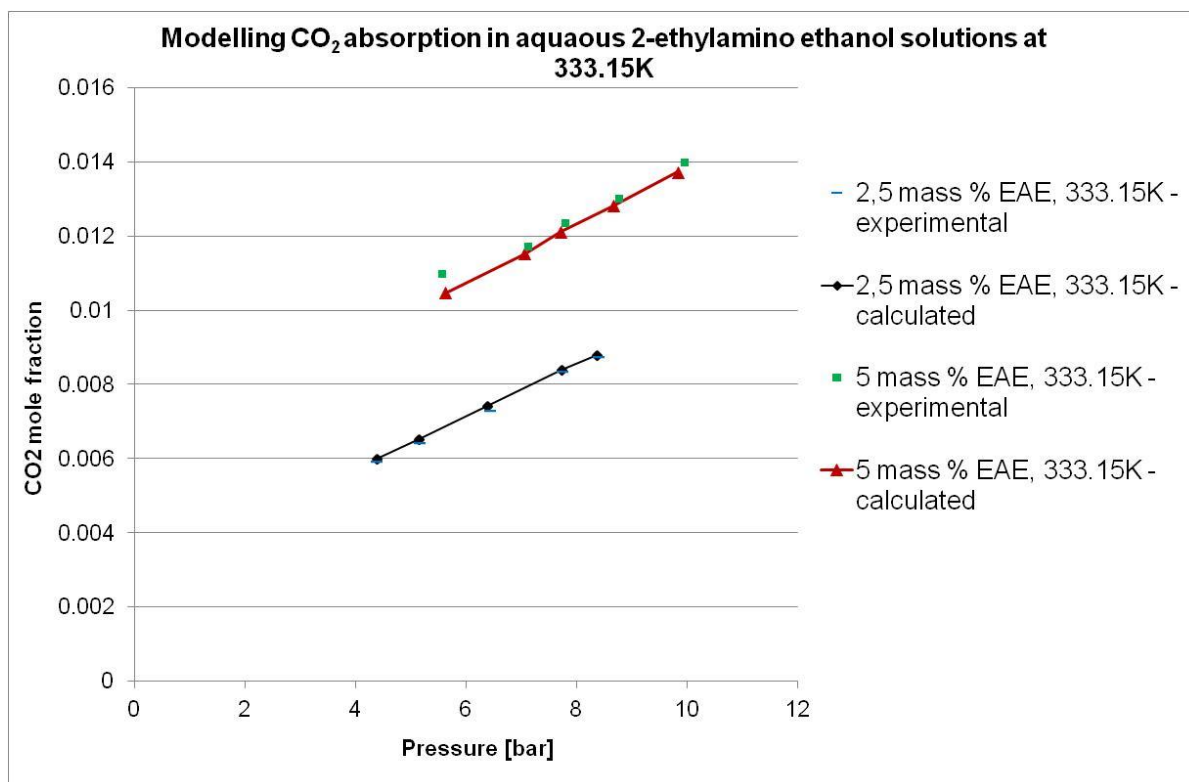


Figure 44. Modelling CO<sub>2</sub> absorption in aqueous 2-(Ethylamino)ethanol solutions at 333.15 K, and comparison to the experimental results.

## 5.5. “Sustainability assessment of the biomethane production”

### 5.5.1. Ecological assessment

Marine biodegradability and ecotoxicity of 43 different amines were measured and evaluated by Eide-Haugmo et al. (Eide-Haugmo, et al., 2012), and 10 interesting for this research amines are here summarized (table 29).

Following the Norwegian Activities Regulation (The Norwegian Activities Regulation (PSA), 2010) the minimum recommended value of ecotoxicity, represented by lethal concentration to 50% of the population (EC50/LC50), should be equal or higher than 10 mg L<sup>-1</sup>. The marine biodegradability, represented in percentage of the theoretical oxygen demand, should be higher than 20%, but preferably it should be above 60%. As a consequence amines like DIPA, MDEA, AMP or PZ do not fulfil marine biodegradability requirements, and also Piperidine do not meet minimal recommended value for ecotoxicity. Despite DGA also do not satisfy the marine biodegradability requirements, it was further evaluated and compared to EAE since some parameters used in modelling EAE, were set equal to parameters for DGA. Furthermore, amines like MEA, DEA, and EAE, where all three are natural substances, are above limit values. On the other side, DEA is recognized to have the lowest toxicity to the marine organisms, whereas EAE is classified as a substance with slight acute toxicity

(10 – 100 mg l<sup>-1</sup>), but it is still not found to be a problematic substance (Eide-Haugmo, et al., 2012). Concerning the marine biodegradability all 3 substances achieved level of high biodegradability (>60% ThOD), with leading EAE (70.4 %ThOD). As a consequence, DEA, EAE and MEA were found to have the best ecological profile, therefore they were used for the economical assessment.

**Table 29. Marine biodegradability and ecotoxicity of 10 amines(Eide-Haugmo, et al., 2012).**

Compound	Abbrev.	Biodegradability		Ecotoxicity		Natural
		ThOD <sub>NH3</sub>	BOD28	EC-50	(95% confidence interval)	
			[%ThOD]	[mg L <sup>-1</sup> ]	[mg L <sup>-1</sup> ]	
<u>Minimum values</u>	-	-	20/60	10	-	
Monoethanolamine	MEA	1.31	68	198	(189-208)	Yes
Diglycolamine	DGA	1.52	<1	493	(457-527)	No
Diethanolamine	DEA	1.52	62.8	357	(323-382)	Yes
Diisopropanolamine	DIPA	1.92	<1	240	(208-268)	No
2-(Ethylamino)ethanol	EAE	1.97	70.4	27	(26-29)	Yes
N-methyldiethanolamine	MDEA	1.75	<1	141	(140-143)	Yes
Diethylaminoethanol	DEEA	2.32	2.2	34	(28-37)	Yes
2-Amino-2-methylpropanol	AMP	1.97	<1	119	(111-125)	No
Piperazine	PZ	1.86	3.0	472	(460-486)	No
Piperidine	Piper	2.63	85.5	1.8	(1.8-1.9)	Yes

### 5.5.2. Social analysis

According to the subindices for hazardous substances in the inherent safety index, there are four parameters evaluated to ensure safety of the chemicals applied, which according to the

literature(Li, et al., 2011; Gangadharan, et al., 2012) satisfies the social analysis (Heikkila, 1999):

Flammability Subindex  $I_{FL}$ : 0-4

Explosiveness Subindex  $I_{EX}$ : 0-4

Toxic Exposure Subindex  $I_{TOX}$ : 0-6

Corrosiveness Subindex  $I_{COR}$ : 0-2

The scale described the severity of the parameter, thus the lower the value the lower the e.g. toxicity. The parameters, characteristic of the amines, along with the results are included in table 30.

**Table 30. Hazardous substances' safety.**

Parameter	Unit	Methanol	MEA	DEA	EAE	DGA
Flash Point	[°C]	<b>9.7</b> (Sigma-Aldrich Co. LLC, 2013b)	<b>86</b> (Sigma-Aldrich Co. LLC, 2014)	<b>138</b> (Sigma-Aldrich Co. LLC, 2012b)	<b>71</b> (Sigma-Aldrich Co. LLC, 2012a)	<b>&gt; 113</b> (Sigma-Aldrich Co. LLC, 2013a)
$I_{FL}$	[-]	<b>3</b> (Li, et al., 2011)	<b>1</b>	<b>1</b>	<b>1</b>	<b>1</b>
Lower explosive limit	[ vol %]	<b>6</b> (Sigma-Aldrich Co. LLC, 2013b)	<b>2.5</b> (Sigma-Aldrich Co. LLC, 2014)	<b>1.6</b> (Sigma-Aldrich Co. LLC, 2012b)	<b>1.1</b> (Sigma-Aldrich Co. LLC, 2012a)	<b>2.6</b> (Sigma-Aldrich Co. LLC, 2013a)
Higher explosive limit	[ vol %]	<b>36</b> (Sigma-Aldrich Co. LLC, 2013b)	<b>17</b> (Sigma-Aldrich Co. LLC, 2014)	<b>10.6</b> (Sigma-Aldrich Co. LLC, 2012b)	<b>11.7</b> (Sigma-Aldrich Co. LLC, 2012a)	<b>11.7</b> (Sigma-Aldrich Co. LLC, 2013a)
$I_{EX}$	[-]	<b>2</b> (Li, et al., 2011)	<b>1</b>	<b>1</b>	<b>1</b>	<b>1</b>
$I_{TOX}$	[-]	<b>2</b> (Li, et al., 2011)	<b>1</b>	<b>2</b>	<b>2</b>	<b>1</b>
$I_{COR}$	[-]	<b>1</b> (Li, et al., 2011)	<b>2</b>	<b>2</b>	<b>1</b>	<b>2</b>
$\Sigma$	[-]	<b>8</b>	<b>5</b>	<b>6</b>	<b>5</b>	<b>5</b>

The parameters  $I_{FL}$  and  $I_{EX}$  were determined with use of the flash point value, lower and higher explosive limit value respectively, as proposed by Heikkila (Heikkila, 1999). Unfortunately due to lack of information about the threshold limit values and clear information about required construction material the approach of Heikkila (Heikkila, 1999) was modified. As a consequence, an example of the subindices for hazardous substances in the inherent safety index for methanol was found in the literature (Li, et al., 2011), and determination of the  $I_{TOX}$  was based on it. Methanol is classified according to the Regulation (EC) No 1272/2008 as a category 3 acute toxic substance (acute toxicity: inhalation, dermal and oral) and also it is recognized as a category 1 toxic substance: specific target organ toxicity – single exposure (Sigma-Aldrich Co. LLC, 2013b). Therefore, it was decided to compare the toxicity of the evaluated amines to the toxic character of methanol, which's toxic exposure subindex was determined to be 2 (Li, et al., 2011). As a consequence, since MEA and DGA are classified as a category 4 acute toxic substances (Sigma-Aldrich Co. LLC, 2014; Sigma-Aldrich Co. LLC, 2013a), they were here recognized as a  $I_{TOX} = 1$ . On the other side, since EAE is classified as a category 3 acute toxic substance (Sigma-Aldrich Co. LLC, 2012a), and DEA is classified as category 1 acute toxic substance for specific target organ toxicity – single exposure (Sigma-Aldrich Co. LLC, 2012b), both were here recognized as  $I_{TOX} = 2$  just as methanol was by Li et al. (Li, et al., 2011). Furthermore, the corrosiveness subindex was also determined in an indirect way. According to the database of European Chemicals Agency (ECHA) EAE was not found to be corrosive to metals (European Chemicals Agency, 2013), therefore  $I_{COR} = 1$ . On the other side, according to the literature (Suda, et al., 1996; Sutar, et al., 2012) EAE is less corrosive than MEA, and according to Rawat et al. (Rawat, et al., 2011) DEA and MEA are significantly corrosive. Moreover, according to the Hazardous Substance Fact Sheet DGA is not allowed to be stored in metal containers (New Jersey Department of Health, 2008), therefore the  $I_{COR}$  for MEA, DEA, and DGA was decided to be 2.

Summing the four parameters, which are the subindices for hazardous substances in the inherent safety index, application of MEA, EAE or DGA during the carbon dioxide capture at a biomethane power plant would be safer than DEA. However, since the results are very close, and the simplified parameters' determination methodology was applied, before the final decision a full chemical safety analysis with use of inherent safety index is recommended.

### 5.5.3. Economical evaluation of the biomethane upgrading facility

The 10.156 kmol hr<sup>-1</sup> (6.789 kmol CH<sub>4</sub> hr<sup>-1</sup>) of biogas formed at EWE Wittmund biogas power plant was purified with 4 different alkanolamines. Because the main interest of this research, was a comparison of 2-(Ethylamino)ethanol to other commonly applied amines, the biogas was first upgraded with 3.2 mass % aqueous EAE solution, and then compared to DGA, DEA and MEA. The goal was to obtain high purity biomethane (>96 mass%), which can be, after drying, send to the natural gas grid. Additionally, the purity of the carbon dioxide and efficiency of the desorption step were also included in the economical assessment. Finally, the energy consumption of the condenser and reboiler were used for the final economical evaluation. The calculation results are presented as a table 31. Despite the lowest amine flow of 2-(Ethylamino)ethanol (4.593 kmol hr<sup>-1</sup>), biomethane of a very high purity (carbon dioxide content was identified as a “trace” by ASPEN® V8.0 Simulation Software), at the same time with one of the highest carbon dioxide recovery efficiency, was achieved. The similar efficiency of carbon dioxide removal could only be achieved by DGA. The satisfactory result was achieved with amine flow of 7.181 kmol hr<sup>-1</sup> (in 30 mass % aqueous solution) for MEA, as indicated by Luyben(Luyben, 2013). Higher concentration of EAE ( 30 mass % aqueous solution; 8.657 kmol hr<sup>-1</sup>) also delivers acceptable efficiency, however it is important to mention that this calculation is an extrapolation of the model, because the binary energy interaction parameters were determined based on experimental results with carbon dioxide solubility in 2,5 and 5 mass % aqueous solutions of EAE, as described in chapter 5.4. Unfortunately, the DEA result of 42.66 kmol hr<sup>-1</sup> amine flow is recognized to be unrealistic, and application of the 2,5 mol of DEA per mol of CO<sub>2</sub> (mole flow of 7.901 kmol hr<sup>-1</sup>) also did not deliver the expected results. Therefore it can be stated, that DEA model implemented in ASPEN® V8.0 is not applicable for biogas upgrading (content of carbon dioxide in incoming gas was equal to 30 mass %) and future research will focus on optimization of the model.

Concerning the energy consumption, which directly influenced the maintenance costs of an upgrading plant, is represented as a MW of energy consumed per each mol of carbon dioxide recovered. As a consequence, the highest efficiency was achieved with both concentrations of 2-(Ethylamino)ethanol and with DGA, leading to the lowest cost of each mole of carbon dioxide recovered.

Table 31. Calculation results of the EWE Wittmund biogas' upgrading.

Par.	Unit	Amines							
		EAE	EAE	DGA	DEA	DEA	DEA	MEA	MEA
Amine aqueous solution flow	[kmol hr <sup>-1</sup> ]	400.1	55.57	390	924.8	115.6	142.2	547.0	64
Amine aqueous solution flow	[l min <sup>-1</sup> ]	124.2	23.5	126.6	5458	2772	97.66	171.1	24.23
Amine flow	[kmol hr <sup>-1</sup> ]	4.593	8.657	6.616	8.276	7.901	42.66	8.361	7.181
Biomethane									
Methane	[kmol hr <sup>-1</sup> ]	6.785	6.789	6.785	6.777	6.789	6.788	6.783	6.789
Carbon Dioxide	[kmol hr <sup>-1</sup> ]	"trace"	0.195	"trace"	1.648	1.42	0.194	0.497	0.195
Water mol fraction	[-]	0.075	0.546	0.072	0.074	0.09	0.044	0.076	0.429
Carbon dioxide									
Carbon dioxide	[kmol hr <sup>-1</sup> ]	3.246	3.169	3.248	1.699	1.938	3.168	2.296	2.539
Water	[kmol hr <sup>-1</sup> ]	0.844	0.823	0.845	0.444	0.504	0.823	0.598	0.658
Energy consumption at desorption stage									
Temperature of condenser	[K]	343.0	343.0	343.0	343.0	343.0	343.0	343.0	343.0
Heat duty of the condenser	[MW]	-0.334	-0.338	-0.336	-0.358	-0.355	-0.340	-0.349	-0.346
Temperature of the reboiler	[K]	393.2	422.6	394.6	394.3	397.2	415.1	394.4	399.2
Heat duty of the reboiler	[MW]	0.517	0.339	0.476	0.656	0.426	0.607	0.570	0.433
Σ energy consumption	[MW]	0.851	0.677	0.810	1.01	0.781	0.946	0.918	0.780
η*	[MW mol <sup>-1</sup> ]	0.262	0.214	0.249	0.594	0.403	0.299	0.400	0.307

η\* - energy consumption per mol carbon dioxide recovered

## 6. Conclusion and Recommendations

Commonly used substrates at biogas power plants, like cattle manure, grass silage, maize silage, green weed silage, industrial glycerine and organic waste, were characterized and the results were transferred into the ADM1 (Batstone, et al., 2002) simulation environment. New kinetic constants for disintegration and hydrolysis phases were determined via the simplex algorithm from Nelder and Mead (Nelder & Mead, 1965). The obtained results indicate that the ADM1, with Wett et al. (Wett, et al., 2006) modification, is capable of simulating biogas production from agricultural and industrial substrates, after precise characterisation of the substrates and adjustment of the kinetic constants.

On the other hand, continuous fermentation results show that the anaerobic digestion of rapeseed oilcake with cattle manure is one of the possible ways of adding value to material which cannot be used as fodder. Batch fermentation experiments and composition analysis shows that anaerobic digestion of rapeseed oilcake is faster than digestion of other substrates often used in agricultural biogas plants. The fermentation process showed good stability indicated by low VFA concentration, pH values in the optimal range and good biogas production efficiency. Thus the hydraulic retention time in systems treating this substrate might be shorter than 20 days. Kinetic constants describing disintegration phases and hydrolysis of proteins, lipids, and carbohydrates were optimized on the basis of batch experiments proved to be suitable in the modelling of continuous fermentation. The model of continuous fermentation process based on the optimized hydrolysis constants and substrate composition analysis showed 7,8 volume% deviation from experimental results. Such an accuracy should be sufficient for the use of this optimization method in modelling of full scale process, at e.g. the designing stage.

Afterwards, pragmatic approach of the common hydrolysis constants, where the number of parameters to be determined per substrate was reduced from four to one kinetic constant describing disintegration, was tested against batch experiments and industrial size EWE Wittmund Biogas Power Plant (2 parallel fermenters, each 3 500 m<sup>3</sup>) (EWE Biogas GmbH & Co. KG., 2011). The outcome of the simulation proved that those constants, together with an individually identified kinetic constant for disintegration, could be considered as an option for the preliminary design stage, and initial screening of the biogas potential from different substrates, but with reflection on lower precision of the results. Concurrently, satisfactory fit between simulation and an existing biogas power plant, was achieved with the individually determined kinetic constants since methane content was underestimated by 1.74 volume% volume, and total production over 28 days was overestimated by 1.84 km<sup>3</sup> difference between an existing biogas power plant and simulation. Summarizing, IWA's Anaerobic

Digestion Model No. 1 was proved as an engineering tool for simulation of existing biogas power plants, therefore application of ADM1 as a tool for optimizing or designing biogas power plants is proposed.

The second milestone of the project was optimization of biogas upgrading, where among the methods applied for capturing carbon dioxide, chemical absorption with alkanolamines was identified as an interesting option, because this technique is already proven to be mature method, simple for retrofitting to an existing plant (Kohl & Nielsen, 1997), and it is predicted by Rochelle to be the dominant method in year 2030 (Rochelle, 2009). In addition to that, this method is allowing carbon dioxide recovery (Austgen, 1989; Deublein & Steinhauser, 2011), which later may be utilized for *Power2Gas* concept (EUTEC, 2012). Therefore, to support model based optimization of the biogas power plants to biomethane power plants, carbon dioxide solubility in 2-(Ethylamino)ethanol (EAE), a promising alternative to diethanolamine (DEA) or monoethanolamine (MEA), was analysed. Then the thermodynamic model representing chemical absorption of carbon dioxide in EAE was prepared, however due to insufficient data on EAE, pragmatic approach of using Diglycolamine's (DGA) parameters like Henry constants, equilibrium constants, dielectric constants or parameters for kinetic reactions for EAE was adopted. Obtained experimental data on carbon dioxide solubility in 2,5 mass % and 5 mass % aqueous EAE solutions, at 298.00K, 313.15K, and 333.15K, and in pressure range from 289 kPa to 1011 kPa were used to regress NRTL's binary interaction parameters, necessary for eNRTL model (Austgen, 1989). Those parameters are essential for the development of efficient industrial upgrading installations. Outcome of the simulation, despite lack of data, indicated a good fit between experimental and calculated results.

The final stage of the research project was a sustainability assessment of the biomethane preparation, where an economical, social and ecological assessment of the alkanolamines were prepared, where the main goal was purification of the biogas coming from an existing biogas power plant. The ecological assessment, where marine ecotoxicity and biodegradability were evaluated (Eide-Haugmo, et al., 2012), revealed that Diethanolamine (DEA), Monoethanolamine (MEA) and 2-(Ethylamino)ethanol (EAE) are fulfilling the requirements for a chemical to be used on an industrial scale. Furthermore, the subindices for hazardous substances in the inherent safety index used for evaluation of the chemical safety (Heikkila, 1999), which is directly linked to social acceptance, were also prepared. As a consequence, MEA, EAE, and DGA had better results than DEA, however due to the simplified methodology applied, and similar results, it is recommended to conduct the full chemical safety analysis with use of inherent safety index before the final decision. On the other side, in the economical analysis efficiency of the carbon dioxide removal, recovery of the CO<sub>2</sub>, and energy consumption were assessed. The final result, indicated that EAE and

Diglycolamine (DGA) are achieving low energy consumption per each mole of carbon dioxide removed, with slightly worst result of MEA, and unfortunately DEA was not possible to be fully evaluated. Summarizing, promising from the economical point of view DGA, due to its' slow biodegradability in marine environment is not recommended for further utilization. On the other side, MEA is proved to be reasonable amine, due to its efficiency, along with low environmental impact. Furthermore taking under consideration ecological and economical profile, it can be stated that EAE (2-(Ethylamino)ethanol) is an interesting substitution of the currently applied amines (also MEA), especially incorporating the fact, that the main substrate used for synthesis of EAE could be bio-ethanol (Sutar, et al., 2012).

Summarizing, the main intention of this dissertation was an sustainable biomethane production, where biogas formation together with its' upgrading are represented via mathematical modelling, allowing optimal configuration, at the same time taking under consideration economical, social and ecological aspects. As a consequence, a procedure to use numerical modelling tools in combination with each other is presented and evaluated. As a result model based designing of biomethane power plants or optimizing existing biogas power plant to produce sustainable biomethane is promoted.

## 7. Recommendations for future work

Due to the limited scope and time of this research, and due to fact, that “*as we acquire more knowledge, things do not become more comprehensible, but more mysterious*” (Albert Schweitzer (Wikimedia, 2011)) author would like to point out a few recommendations for future work:

- Despite ADM1 was proved to correctly represent anaerobic digestion at an existing biogas power plant, there is a lack of field tests of ADM1’s optimization potential
- Incorporating H<sub>2</sub>S vapour phase fraction to the ADM1 would enhance usefulness of the model
- Further improvement of the ADM1’s default values for biomass fractions, and methodology for transferring inoculum’s biomass activity into the ADM1 would be appreciated
- Experimental data on hydrogen sulfide solubility in aqueous solutions of 2-(Ethylamino)ethanol (EAE), along with determination of parameters (e.g. dielectric constant etc.) of EAE necessary for enhancement of the CO<sub>2</sub> – H<sub>2</sub>S – EAE – H<sub>2</sub>O system representation are essential for further improvement of the eco-efficient biomethane production
- Experimental data on carbon dioxide solubility in blend of e.g. EAE and MDEA would be an useful enhancement
- Repetition of the DEA’s economical analysis, due to unsolved issues during the modelling, and un realistic results.

## 8. References

- Abatzoglou, N. & Boivin, S., 2009. A review of biogas purification processes. *Biofuels, Bioproduction, Biorefinery*, Volume 3, pp. 42-47.
- Abbassi-Guendouz, A. et al., 2012. Total solids content drives high solid anaerobic digestion via mass transfer limitation. *Bioresource Technology*, Volume 111, pp. 55-61.
- Addicks, J., Owren, G. A., Fredheim, A. O. & Tangvik, K., 2002. Solubility of Carbon Dioxide and Methane in Aqueous Methyldiethanolamine Solutions. *Journal of Chemical and Engineering Data*, Volume 47, pp. 855-860.
- Amon, T. et al., 2007. Biogas production from maize and dairy manure - Influence of biomass composition on the methane yield.. *Agriculture, Ecosystems & Environment*, 118(1-4), pp. 173-182.
- Angelidaki, I. et al., 2007. *Anaerobic Biodegradation, Activity and Inhibition (ABAI)*. Task Group Meeting, 9th and 10th October 2006, Prague: Institute of Environmental & Resources, Technical University of Denmark. ISBN: 978-87-91855-44-3.
- Ankom Technology, 2011. *ANKOMRF Gas Production System - Operator's Manual*. s.l.:Ankom Technology.
- Antonopoulou, G., Gavala, H. N., Skiadas, I. V. & Lyberatos, G., 2012a. ADM1-based modeling of methane production from acidified sweet sorghum extract in a two stage process. *Bioresource Technology*, Volume 106, pp. 10-19.
- Antonopoulou, G., Gavala, H. N., Skiadas, I. V. & Lyberatos, G., 2012b. Modeling of fermentative hydrogen production from sweet sorghum extract based on modified ADM1. *International Journal of Hydrogen Energy*, 37(1), pp. 191-208.
- Aspen Technology Inc., 2008. *Aspen Plus: Rate-Based Model of the CO2 Capture Process by Diglycolamine using Aspen Plus*, s.l.: Aspen Technology Inc. Version Number: V8.0.
- Aspen Technology Inc., 2012. *Aspen Physical Property System: Physical Property Models*. s.l.:Aspen Technology Inc. Version Number: V8.0.
- Astals, S., Ariso, M., Gali, A. & Mata-Alvarez, J., 2011. Co-digestion of pig manure and glycerine: Experimental and modelling study. *Journal of Environmental Management*, 92(4), pp. 1091-1096.

- Astals, S. et al., 2013. Anaerobic digestion of seven different sewage sludges: A biodegradability and modelling study. *Water Research*, 47(16), pp. 6033-6043.
- Astarita, G., Savage, D. W. & Bisio, A., 1983. *Gas Treating with Chemical Solvents*. New York: John Wiley and Sons.
- Austgen, D. M., 1989. *A Model of Vapour - Liquid Equilibria for Acid Gas - Alkanolamine - Water Systems*. Austin: PhD Dissertation, University of Texas at Austin.
- Austgen, D. M., Rochelle, G. T., Peng, X. & Chen, C. -C., 1989. Model of Vapor-Liquid Equilibria for Aqueous Acid Gas-Alkanolamine System Using the Electrolyte-Nrtl Equation. *Industrial and Engineering Chemical Research*, Volume 28, pp. 1060-1073.
- Batstone, D. J. et al., 2002. *Anaerobic Digestion Model No. 1*, London: International Water Association.
- Bavbek, O. & Alper, E., 1999. Reaction Mechanism and Kinetics of Aqueous Solutions of Primary and Secondary Alkanolamines and Carbon Dioxide. *Turkish Journal of Chemistry*, Volume 23, pp. 293-300.
- Bensmann, A., Hanke-Rauschenbach, R. & Sundmacher, K., 2013. Reactor configurations for biogas plants - a model based analysis. *Chemical Engineering Science*, 104(18), pp. 413-426.
- Bischofsberger, W. et al., 2005. *Anaerobtechnik*. s.l.:Springer. ISBN: 3-540-06850-3.
- Boehnke, B., Bischofsberger, W. & Seyfried, C. F., 1993. *Anaerobtechnik*. Berlin: Springer Verlag.
- Bohdziewicz, J., Piotrowski, K. & Cebula, J., 2012. Kinetyka chemiczna fermentacji metanowej makuchu rzepakowego. In: A. Cenian, ed. *Ekoenergetyka - Biogaz*. Gdansk: Wydawnictwo Gdanskiej Szkoły Wyższej, p. 24.
- Bollon, J., Le-hyarc, R., Benbelkacem, H. & Buffiere, P., 2011. Development of a kinetic model for anaerobic dry digestion processes: Focus on acetate degradation and moisture content. *Biochemical Engineering Journal*, 56(3), pp. 212-218.
- Bonilla-Petriciolet, A., Fateen, S. E. & Rangaiah, G. P., 2013. Assessment of capabilities and limitations of stochastic global optimization methods for modeling mean activity coefficients of ionic liquids. *Fluid Phase Equilibria*, Volume 340, pp. 15-26.

- Bornhoeft, A., Hanke-Rauschenbach, R. & Sundmacher, K., 2012. Steady-state multiplicity of a biogas production system based on anaerobic digestion. *Computer Aided Chemical Engineering*, Volume 31, pp. 1377-1381.
- Boubaker, F. & Ridha, B. C., 2008. Modelling of the mesophilic anaerobic co-digestion of olive mill wastewater with olive mill solid waste using anaerobic digestion model No. 1 (ADM1). *Bioresource Technology*, 99(14), pp. 6565-6577.
- Boyle, W. C., 1977. Energy recovery from sanitary landfills. In: A. G. Schlegel & J. Barnea, eds. *Microbial Energy Conversion*. s.l.:Unitar, pp. 119-138.
- Buswell, A. M. & Hatfield, W. D., 1936. *Anaerobic fermentations*. Urbana, Illinois: State of Illinois Department of Registration & Education, Division of the State Water Survey.
- Cadours, R., Roquet, D. & Perdu, G., 2007. Competitive Absorption - Desorption of Acid Gas into Water - DEA Solutions. *Industrial and Engineering Chemical Research*, Volume 46, pp. 233-241.
- Caplow, M., 1968. Kinetics of Carbamate Formation and Breakdown. *Journal of American Chemical Society*, Volume 90, pp. 6795-6803.
- Carneiro, A. P., Rodriguez, O. & Macedo, E. A., 2012. Solubility of xylitol and sorbitol in ionic liquids - Experimental data and modelling. *The Journal of Chemical Thermodynamics*, Volume 55, pp. 184-192.
- Chakravarty, T., Phukan, U. K. & Weiland, R. H., 1985. Reaction of Acid Gases with Mixtures of Amines. *Chemical Engineering Progress*, 81(4), pp. 26-32.
- Chapeaux, A., Simoni, L. D., Stadtherr, M. A. & Brennecke, J. F., 2007. Liquid Phase Behavior of Ionic Liquids with Water and 1-Octanol and Modeling of 1-Octanol/Water Partition Coefficients. *Journal of Chemical Engineering Data*, 52(6), pp. 2462-2467.
- Chen, C. -C. & Evans, L. B., 1986. A Local Composition Model for the Excess Gibbs Energy of Aqueous Electrolyte Systems. *American Institute of Chemical Engineers*, Volume 32, pp. 444-454.
- Cheng, J., 2010. *Biomass to renewable energy processes*. s.l.:CRC Press. ISBN: 978-1-420-09517-3.
- Chen, Y. et al., 2012. Modeling and Simulation of CO<sub>2</sub> Absorption with Amine Component Solvent. *Computer Aided Chemical Engineering*, Volume 31, pp. 525-529.

Chen, Z. et al., 2009. Modelling of two-phase anaerobic process treating traditional Chinese medicine wastewater with the IWA Anaerobic Digestion Model No. 1. *Bioresource Technology*, 100(20), pp. 4631-4632.

Chiu, L. -F., Liu, H. -F. & Li, M. -H., 1999. Heat capacity of Alkanolamines by Differential Scanning Calorimetry. *Journal of Chemical Engineering Data*, Volume 44, pp. 631-636.

Christ, O., Wilderer, P. A., Angerhofer, R. & Faulstich, M., 2000. Mathematical modelling of the hydrolysis of anaerobic processes. *Water Science & Technology*, 41(3), pp. 61-65.

Critchfield, J. E. & Rochelle, G. T., 1987. *CO<sub>2</sub> Absorption into Aqueous MDEA and MDEA/MEA solutions*. Houston, AIChE National Meeting, Paper No. 43e.

Critchfield, J. E. & Rochelle, G. T., 1988. *CO<sub>2</sub> Desorption from DEA and DEA-Promoted MDEA solutions*. New Orleans, AIChE National Meeting, Paper No. 68b.

Crovetto, R., 1991. Evaluation of Solubility Data of the System CO<sub>2</sub>- H<sub>2</sub>O from 273 K to the Critical Point of Water. *Journal of Physical and Chemical Reference Data*, Volume 20, pp. 575-589.

Cullinane, J. T. & Rochelle, G. T., 2005. Thermodynamics of aqueous potassium carbonate, piperazine, and carbon dioxide. *Fluid Phase Equilibria*, 227(2), pp. 197-213.

Dash, S. K., Samanta, A. N. & Bandyopadhyay, S. S., 2011. (Vapour + liquid) equilibria of CO<sub>2</sub> in aqueous solutions of 2-amino-2-methyl-1-propanol: New data and modelling using eNRTL-equation. *The Journal of Chemical Thermodynamics*, 43(8), pp. 1278-1285.

Dash, S. K., Samanta, A. N. & Bandyopadhyay, S. S., 2012. Experimental and theoretical investigation of solubility of carbon dioxide in concentrated aqueous solution of 2-amino-2-methyl-1-propanol and piperazine. *The Journal of Chemical Thermodynamics*, Volume 51, pp. 120-125.

DDBST GmbH, 2014. *The Dortmund Data Bank*. [Online]  
Available at: <http://www.ddbst.com>  
[Accessed 15 03 2014].

de Neves, L. C., Converti, A. & Vessoni Penna, T. C., 2009. Biogas Production: New Trends for Alternative Energy Sources in Rural and Urban Zones. *Chemical Engineering Technology*, 32(8), pp. 1147-1153.

Deng, D. et al., 2014. Measurement and Modeling of Vapour-Liquid Equilibrium for Ternary System Water+ 2-Propanol+ 1-Butyl-3-Methylimidazolium Chloride. *Chinese Journal of Chemical Engineering*, 22(2), pp. 164-169.

Deng, D. et al., 2011. Vapor-Liquid Equilibrium Measurements and Modelling for Ternary System Water + Ethanol + 1-Butyl-3-methylimidazoliumAcetate. *Chinese Journal of Chemical Engineering*, 19(4), pp. 703-708.

Department for Environment, Food and Rural Affairs, 2010. *Saving mondey by reducing waste*. [Online]

Available at: <http://archive.defra.gov.uk/environment/waste/topics/farm/documents/waste-minimisation.pdf>

[Accessed 15 03 2014].

Derbal, K. et al., 2009. Application of the IWA ADM1 model to simulate anaerobic co-digestion of dairy manure and spent mushroom substrate. *Bioresource Technology*, 100(4), pp. 1539-1543.

Dereli, R. K. et al., 2010. Applicability of Anaerobic Digestion Model No. 1 (ADM1) for a specific industrial wastewater: Opium alkaloid effluents. *Chemical Engineering Journal*, 165(1), pp. 89-94.

Desideri, U. & Paolucci, A., 1999. Performance modeling of a carbon dioxide removal system for power plants. *Energy Conversion and Management*, Volume 40, pp. 1899-1915.

Deublein, D. & Steinhauser, A., 2011. *Biogas from Waste and Renewable Resources*. 2nd edition ed. Weinheim: Wiley-VCH Verlag GmbH & Co. KGaA. ISBN: 978-3-527-32798-0.

Dingman, J. C., Jackson, J. L., Moore, T. F. & Branson, J. A., 1983. *Equilibrium Data For The H<sub>2</sub>S-CO<sub>2</sub>-Diglycolamine Agent -Water System*. San Francisco, s.n.

Directive 2009/28/EC, 2009. *Directive of the European Parliament and of the Council of 23 April 2009 on the promotion of the use of energy from renewable sources and amending the subsequently repealing Directives 2001/77/EC and 2003/30/EC*. s.l.:Official Journal of The European Union.

Edwards, T. J., Newman, J. & Prausnitz, J. M., 1978. Thermodynamics of Aqueous Solutions Containing Volatile Weak Electrolytes. *American Institute of Chemical Engineers*, 24(6), pp. 966-976.

Eide-Haugmo, I. et al., 2012. Marine biodegradability and ecotoxicity of solvents for CO<sub>2</sub> - capture of natural gas. *International Journal of Greenhouse Gas Control*, Volume 9, pp. 184-192.

Eladawy, A., 2005. *Modelling of Anaerobic Sewage Sludge Digestion - Sludge Characterisation and Process Analysis*. Austria: PhD Thesis. University of Innsbruck.

Esposito, G., Frunzo, L., Panico, A. & Pirozzi, F., 2011. Modelling the effect of the ORL and OFMSW particle size on the performance of an anaerobic co-digestion reactor. *Process Biochemistry*, 42(2), pp. 557-565.

Estevez, M. M., Linjordet, R. & Morken, J., 2012. Effects of steam explosion and co-digestion in the methane production from *Salix* by mesophilic batch assays. *Bioresource Technology*, Volume 104, pp. 749-756.

European Chemicals Agency, 2013. *2-(Ethylamino)Ethanol - Substance characteristics*.

[Online]

Available at: [http://apps.echa.europa.eu/registered/data/dossiers/DISS-dcee03af-b431-5723-e044-00144f67d031/AGGR-6765098b-eb35-4ff8-a5c3-3f08fce063b9\\_DISS-dcee03af-b431-5723-e044-00144f67d031.html#GEN\\_RESULTS\\_HD](http://apps.echa.europa.eu/registered/data/dossiers/DISS-dcee03af-b431-5723-e044-00144f67d031/AGGR-6765098b-eb35-4ff8-a5c3-3f08fce063b9_DISS-dcee03af-b431-5723-e044-00144f67d031.html#GEN_RESULTS_HD)

[Accessed 16 05 2014].

EUTEC, 2012. *Hochschule Emden/Leer*. [Online]

Available at: <http://www.hs-emden-leer.de/forschung-transfer/institute/eutec/laufende-projekte/klaeranlagen-als-energiespeicher.html>

[Accessed 22 03 2014].

EWE Biogas GmbH & Co. KG., 2011. *Wittmund biogas power plant: Important data at a glance*. [Online]

Available at: [http://www.ewe-biogas.de/english/index\\_28.php](http://www.ewe-biogas.de/english/index_28.php)

[Accessed 06 08 2011].

Feng, Y., Behrendt, J., Wendland, C. & Otterpohl, R., 2006. Parameter analysis of the IWA Anaerobic Digestion Model No. 1 for the anaerobic digestion of blackwater with kitchen refuse. *Water Science & Technology*, 54(4), pp. 139-147.

Fezzani, B. & Cheikh, R. B., 2009. Extension of the anaerobic digestion model No. 1 (ADM1) to include phenolic compounds biodegradation processes for the simulation of anaerobic co-digestion of olive mill wastes at thermophilic temperature. *Journal of Hazardous Materials*, 162(2-3), pp. 1563-1570.

- Flotats, X., Palatsi, J., Ahring, B. K. & Angelidaki, I., 2006. Identifiability study of the proteins degradation model, based on ADM1, using simultaneous batch experiments. *Water Science & Technology*, 54(4), pp. 31-39.
- Fountoulakis, M. S., Stamatelatou, K. & Lyberatos, G., 2008. The effect of pharmaceuticals on the kinetics of methanogenesis and acetogenesis. *Bioresource Technology*, 99(15), pp. 7083-7090.
- Franke, S., 2007. *Biogasaufbereitungsverfahren*. Freiberg, DBI-Gastechnologisches Institut GmbH.
- Gadhamshetty, V., Arudchelvam, Y., Nirmalakhandan, N. & Johnson, D. C., 2010. Modeling dark fermentation for biohydrogen production: ADM1-based model vs. Gompertz model. *International Journal of Hydrogen Energy*, 35(2), pp. 479-490.
- Gali, A., Benabdallah, S., Astals, J. & Mata-Alvarez, J., 2009. Modified version of ADM1 model for agro-waste application. *Bioresource Technology*, Volume 100, pp. 2783-2790.
- Gangadharan, P. et al., 2012. Sustainability assesment of polygeneration processes based on syngas derived from coal and natural gas. *Computers and Chemical Engineering*, Volume 39, pp. 105-117.
- Garcia-Dieguez, C., Bernard, O. & Roca, E., 2013. Reducing the Anaerobic Digestion Model No. 1 for its application to an industrial wastewater treatment plant treating winery effluent wastewater. *Bioresource Technology*, Volume 132, pp. 244-253.
- Garcia-Dieguez, C., Mollina, F. & Roca, E., 2011. Multi-objective cascade controller for an anaerobic digester. *Process Biochemistry*, 46(4), pp. 900-909.
- Garcia-Gen, S., Lema, J. M. & Rodriguez, J., 2013. Generalised modelling approach for anaerobic co-digestion of fermentable substrates. *Bioresource Technology*, Volume 147, pp. 525-533.
- Garcia-Heras, J. L., 2003. Reactor sizing, process kinetics and modelling of anaerobic digestion of complex wastes. In: J. Mata-Alvarez, ed. *Biomethanization of the Organic Fraction of Municipal Solid Wastes*. London: International Water Association.
- Gavala, H. N., Angelidaki, I. & Ahring, B. K., 2003. Kinetics and modelling of anaerobic digestion process. In: T. Scheper & B. K. Ahring, eds. *Biomethanization 1..* Berlin: Springer-Verlag.

German Institute for Standardization (DIN), 1985. *DIN 38402-11: German standard methods for the examination of water, waste water and sludge - General information (group A) - Part 11: Sampling of waste water (A11)*, s.l.: s.n.

Girault, R. et al., 2012. A waste characterisation procedure for ADM1 implementation based on degradation kinetics. *Water Research*, 46(13), pp. 4099-4110.

Gmehling, J., Kolbe, B., Kleiber, M. & Rarey, J., 2012. *Chemical Thermodynamics for Process Simulation*. s.l.:Wiley-VCH Verlag & Co. KGaA. ISBN: 978-3-527-31277-1.

Haghtalab, A., Eghbali, H. & Shojaeian, A., 2014a. Experiment and modeling solubility of CO<sub>2</sub> in aqueous solutions of Diisopropanolamine + 2-amin-2-methyl-1-propanol + Piperazine at high pressures. *The Journal of Chemical Thermodynamics*, Volume 71, pp. 71-83.

Haghtalab, A., Izadi, A. & Shojaeian, A., 2014b. High pressure measurement and thermodynamic modeling the solubility of H<sub>2</sub>S in the aqueous N-methyldiethanolaminoe+2+amino-2-methyl-1-propanol+piperazine systems. *Fluid Phase Equilibria*, Volume 363, pp. 263-275.

Haghtalab, A., Papangelakis, V. G. & Zhu, X., 2004. The electrolyte NRTL model and speciation approach as applied to multicomponent aqueous solutions of H<sub>2</sub>SO<sub>4</sub>, Fe<sub>2</sub>(SO<sub>4</sub>)<sub>3</sub>, MgSO<sub>4</sub> and Al<sub>2</sub>(SO<sub>4</sub>)<sub>3</sub> at 230-270 C. *Fluid Phase Equilibria*, 220(2), pp. 199-209.

Heikkila, A. M., 1999. *Inherent Safety in Process Plant Design, An Index Based Approach*, Helsinki: Helsinki University of Technology.

Heukelekian, H., 1958. Basic principles of sludge digestion. In: J. McCabe & W. W. Eckenfelder, eds. *Biological treatment of sewage and industrial wastes*. New York: Reinhold.

Hilliard, M. D., 2008. *A Predictive Thermodynamic Model for an Aqueous Blend of Potassium Carbonate, Piperazine, and Monoethanolamine for Carbon Dioxide Capture from Flue Gas*, PhD Thesis. Austin: University of Texas at Austin.

Hoehener, K. & Spirig, M., 2004. *Abklaerung der Potenziale der Teil und Gesamtsysteme zur Verbesserung der Verstromung biogener Gase mit dem Gasmotor*. [Online]

Available at:

[http://www.bfe.admin.ch/php/includes/container/enet/flex\\_enet\\_anzeige.php?lang=de&publication=8060&height=400&width=600](http://www.bfe.admin.ch/php/includes/container/enet/flex_enet_anzeige.php?lang=de&publication=8060&height=400&width=600)

[Accessed 15 03 2014].

Hoelker, U., 2008. *Anlagendaten*. [Online]

Available at: <http://www.biogaswissen.de/index.php/anlagendaten>

[Accessed 19 02 2014].

Hu, Z. & Yu, H., 2005. Application of rumen microorganisms for enhanced anaerobic fermentation of corn stover. *Process Biochemistry*, 40(7), pp. 2371-2377.

ifak system GmbH, 2005. *SIMBA(R) 5.1 User's guide*, Magdeburg: ifak system GmbH.

Imhoff, K., 1980. Zum Wert der Schlammfäulung und Hinweise zum Faulverfahren. *Korrespondenz Abwasser*, 27(12), pp. 824-831.

Jimenez, J. et al., 2014. Prediction of anaerobic biodegradability and bioaccessibility of municipal sludge by coupling sequential extractions with fluorescence spectroscopy: Towards ADM1 variables characterization. *Water Research*, Volume 50, pp. 359-372.

Ji, Y. et al., 2007. Progress in the Study on the Phase Equilibria of the CO<sub>2</sub>-H<sub>2</sub>O and CO<sub>2</sub>-H<sub>2</sub>O-NaCl Systems. *Chinese Journal of Chemical Engineering*, 15(3), pp. 439-448.

Kaltschmitt, M. & Hartmann, H., 2001. *Energie aus Biomasse*. Berlin: Springer-Verlag.

Katti, S. S. & Wolcott, R. A., 1987. *Fundamental Aspects of Gas Treating with Formulated Amine Mixtures*. Minneapolis, AIChE National Meeting.

Keicher, K., Krampe, J. & Rott, U., 2004. *Systemintegration von Brennstoffzellen in Kläranlagen - Potenzialabschätzung fuer Baden-Wuerttemberg*, s.l.: BWI 22006.

Keicher, K. et al., 2006. *Systemintegration von Brennstoffzellen auf Kläranlagen - Potenzialabschätzung fuer Baden-Wuerttemberg*. [Online]

Available at: <http://elib.uni->

[stuttgart.de/opus/volltexte/2004/2149/pdf/Schlussbericht\\_BWI22006.pdf](http://elib.uni-stuttgart.de/opus/volltexte/2004/2149/pdf/Schlussbericht_BWI22006.pdf)

[Accessed 15 03 2014].

Kim, I., Hessen, E. T., Haug-Warberg, T. & Svendsen, H. F., 2009. Enthalpies of absorption of CO<sub>2</sub> in aqueous alkanolamine solutions from e-NRTL model. *Energy Procedia*, 1(1), pp. 829-835.

Kleerebezem, R. & van Loosdrecht, M. C., 2006. Critical analysis of some concepts proposed in ADM1. *Water Science and Technology*, 54(4), pp. 51-57.

Koch, K. et al., 2010. Biogas from grass silage - Measurements and modelling with ADM1. *Bioresource Technology*, Volume 101, pp. 8158-8165.

- Koch, K., Wichern, M., Luebken, M. & Horn, H., 2009. Mono fermentation of grass silage by means of loop reactors. *Bioresource Technology*, Volume 100, pp. 5934-5940.
- Kohl, A. L. & Nielsen, R. B., 1997. *Gas purification*. ISBN-10: 0884152200 ed. Houston: Gulf Professional Publishing.
- Kohl, A. L. & Riesenfeld, F. C., 1985. *Gas Purification*. 4th ed. Houston: Gulf Publishing Co..
- Koutrouli, E. C. et al., 2009. Hydrogen and methane production through two-stage mesophilic anaerobic digestion of olive pulp. *Bioresource technology*, 100(15), pp. 3718-3723.
- Kuratorium fuer Technik und Bauwesen in der Landwirtschaft, 2014. *Wirtschaftlichkeitsrechner Biogas*. [Online]  
Available at: <http://daten.ktbl.de/biogas/startseite.do>  
[Accessed 24 03 2014].
- Kwaterski, M. & Herri, J. M., 2014. Modelling of Gas Clathrate Hydrate Equilibria using Electrolyte Non-Random Two-Liquid (eNRTL) Model. *Fluid Phase Equilibria*, Volume <http://dx.doi.org/10.1016/j.fluid.2014.02.032>.
- Landolt-Boernstein, 1968. *Zahlenwerte und Funktionen aus Physik, Chemie, Astronomie, Geophysik und Technik, 6 Auflage, II Band, 2 Teil, Bandteil b*. Heidelberg: Springer - Verlag.
- Lee, M.-Y., Suh, C.-W., Ahn, Y.-T. & Shin, H.-S., 2009. Variaton of ADM1 by using temperature-phased anaerobic digestion (TPAD) operation. *Bioresource Technology*, 100(11), pp. 2816-2822.
- Lehtomaki, A., Vavilin, V. A. & Rintala, J. A., 2005. Kinetic analysis of methane production from energy crops. In: B. K. Ahring & H. Hartmann, eds. Copenhagen: Proceedings of the Fourht International Symposium on Anaerobic Digestion of Solid Waste, vol. 2, pp. 67-72.
- Leubner, G., 2012. *The seed biology place*. [Online]  
Available at: <http://www.seedbiology.de/structure.asp#pea1>  
[Accessed 2014 03 27].
- Li, J., Henni, A. & Tontiwachwuthikul, P., 2007. Reaction Kinetics of CO<sub>2</sub> in Aqueous Ethylenediamine, Ethyl Ethanolamine, and Diethyl Monoethanolamine Solutions in the Temperature Range of 298 - 313 K, Using Stopped - Flow Technique. *Industrial and Enginerring Chemistry Research*, Volume 46, pp. 4426-4434.
- Liu, J. et al., 2011. Vapor-liquid equilibria of NH<sub>3</sub> in (NH<sub>3</sub> + H<sub>2</sub>O) and (NH<sub>3</sub> + PZ + H<sub>2</sub>O) system. *Fluid Phase Equilibria*, Volume 311, pp. 30-35.

- Li, X. et al., 2011. Incorporating Exergy Analysis and Inherent Safety Analysis for Sustainability Assessment of Biofuels. *Industrial & Engineering Chemistry Research*, Volume 50, pp. 2981-2993.
- Luebken, M., Gehring, T. & Wichern, M., 2010. Microbiological fermentation of lignocellulosic biomass: current state and prospects of mathematical modelling. *Applied Microbiology and Biotechnology*, 85(6), pp. 1643-1652.
- Luebken, M., Wichern, M., Schlattmann, M. & Gronauer, A., 2007. Modelling the energy balance of an anaerobic digester fed with cattle manure and renewable energy crops. *Water Research*, Volume 41, pp. 4085-4096.
- Luyben, W. L., 2013. *Distillation Design and Control Using Aspen Simulation*. 2 ed. s.l.:John Wiley + Sons. ISBN: 1118411439.
- Maham, Y. et al., 1997. Molar heat capacities of alkanolamines from 299.1 to 397.8 K. *Journal of the Chemical Society, Faraday Transactions*, Volume 93, pp. 1747-1750.
- Mairet, F. et al., 2011. Modelling anaerobic digestion of microalgae using ADM1. *Bioresource Technology*, 102(13), pp. 6823-6829.
- Martinez-Sibaja, A. et al., 2013. Dedicated Observer Scheme for Fault Diagnosis and Isolation in Instruments of an Anaerobic Reactor. *Procedia Technology*, Volume 7, pp. 173-180.
- Martin, J. L., Otto, F. D. & Mather, A. E., 1978. Solubility of Hydrogen Sulfide and Carbon Dioxide in a Diglycolamine Solution. *Journal of Chemical Engineering Data*, Volume 23, pp. 163-164.
- Maurer, G., 1980. On the Solubility of Volatile Weak Electrolytes in Aqueous Solutions. In: S. A. Newman, ed. *Thermodynamics of Aqueous Systems with Industrial Applications*. ACS Symposium Series 133 ed. Washington DC: American Chemical Society, pp. 139-186.
- Maurer, G., 2004. Electrolyte solutions. In: P. Giericz & S. Malanowski, eds. *Thermodynamics for Environment*. Warszawa: Information Processing Centre.
- Mimura, T. et al., 1995. Research and development on energy saving technology for flue gas carbon dioxide recovery and steam in power plant. *Energy Conversion and Management*, Volume 36, pp. 397-400.

- Mimura, T. et al., 1997. Development of energy saving technology for flue gas carbon dioxide recovery in power plant by chemical absorption method and steam system. *Energy Conversion and Management*, Volume 38, pp. 57-62.
- Mimura, T. et al., 1998. Kinetics of Reaction Between Carbon Dioxide and Sterically Hindered Amines for Carbon Dioxide Recovery from Power Plant Flue Gases. *Chemical Engineering Communications*, Volume 170, pp. 245-260.
- Mock, B., Evans, L. B. & Chen, C. -C., 1986. Thermodynamic Representation of Phase Equilibria of Mixed-solvent Electrolyte Systems. *American Institute of Chemical Engineers*, Volume 32, pp. 1655-1664.
- Monlau, F. et al., 2013. Enhancement of methane production from sunflower oil cakes by dilute acid pretreatment. *Applied Energy*, Volume 102, pp. 1105-1113.
- Monteiro, J. G.-S. et al., 2013. VLE data and modelling of aqueous N,N-diethylethanolamine (DEEA) solutions. *International Journal of Greenhouse Gas Control Volume*, Volume 19, pp. 432-440.
- Moore, W. J. & Hummel, D. O., 1986. *Physikalische Chemie*. Berlin, New York: Walter de Gruyter.
- Mottet, A. et al., 2013. New fractionation for a better bioaccessibility description of particulate organic matter in a modified ADM1 model. *Chemical Engineering Journal*, Volume 228, pp. 871-881.
- Mu, S. J. et al., 2008. Anaerobic digestion model No. 1 based distributed parameter model of anaerobic reactor: I. model development. *Bioresource Technology*, 99(9), pp. 3665-3675.
- Myint, M., Nirmalakhandan, N. & Speece, R. E., 2007. Anaerobic fermentation of cattle manure: modelling of hydrolysis and acidogenesis. *Water Research*, 41(2), pp. 323-332.
- Naumann, C. & Bassler, R., 1993. *Die Chemische Untersuchung von Futtermitteln*. Darmstadt: VDLUFA-Verlag.
- Nelder, J. A. & Mead, R., 1965. A simple Method for Function Minimization. *Computer Journal*, Volume 7, pp. 308-313.
- NETZSCH GmbH & Co. Holding KG, 2007. *Artifacts in data curves Service Trouble shooting - getting the best from your DSC, TG, STA*. s.l.:International Customer Service Training.

New Jersey Department of Health, 2008. *Right to Know; Hazardous Substance Fact Sheet: 2-(2-Aminoethoxy)Ethanol*. [Online]

Available at: <http://nj.gov/health/eoh/rtkweb/documents/fs/0073.pdf>

[Accessed 16 05 2014].

Nielsen, H. B. & Angelidaki, I., 2008. Strategies for optimizing recovery of the biogas process following ammonia inhibition. *Bioresour. Technol.*, Volume 99, pp. 7995-8001.

Nopens, I. et al., 2009. An ASM/ADM model interface for dynamic plant-wide simulation. *Water Research*, 43(7), pp. 1913-1923.

Novak, J. P., Matous, J. & Pick, J., 1987. *Liquid - Liquid Equilibria*. Amsterdam: Elsevier.

Ntaikou, I., Gavala, H. N. & Lyberatos, G., 2010. Application of a modified Anaerobic Digestion Model 1 version for fermentative production from sweet sorghum extract by *Ruminococcus albus*. *International Journal of Hydrogen Energy*, 35(8), pp. 3423-3432.

Pacheco, M. A., Kaganoi, S. & Rochelle, G. T., 2000. CO<sub>2</sub> Absorption into Aqueous Mixture of Diglycolamine and Methyldiethanolamine. *Chemical Engineering Science*, Volume 55, pp. 5125-5140.

Palatsi, J. et al., 2010. Long-chain fatty acids inhibition and adaptation process in anaerobic thermophilic digestion: Batch tests, microbial community structure and mathematical modelling. *Bioresour. Technol.*, 10(7), pp. 2243-2251.

Parker, W. J., 2005. Application of the ADM1 model to advanced anaerobic digestion. *Bioresour. Technol.*, 96(16), pp. 1832-1842.

Park, M. K. & Sandall, O. C., 2001. Solubility of Carbon Dioxide and Nitrous Oxide in 50 mass % Methyldiethanolamine. *Journal of Chemical Engineering Data*, Volume 46, pp. 166-168.

Peng, D. -Y. & Robinson, D. B., 1976. A New Two-Constant Equation of State. *Industrial and Engineering Chemical Fundamentals*, Volume 15, pp. 59-64.

Pinsent, B. R., Pearson, L. & Roughton, F. J., 1956. The Kinetics of Combination of Carbon Dioxide with Hydrogen Ions. *Transactions of the Faraday Society*, Volume 52, pp. 1512-1520.

Pinto, D. D. et al., 2013. eNRTL Parameter Fitting Procedure for Blended Amine Systems: MDEA-PZ Case study. *Energy Procedia*, Volume 37, pp. 1613-1620.

- Pitzer, K. S., 1980. Electrolytes. From dilute solutions to fused salts. *Journal of American Chemical Society*, Volume 102, pp. 2902-2906.
- Polka, H. M., 1993. *Experimentelle Bestimmung und Berechnung von Dampf-Fluessigs-Gleichgewichten fuer Systeme mit starken Elektrolyten*. Oldenburg: Thesis. University of Oldenburg.
- Puyol, D., Sanz, J. L., Rodriguez, J. J. & Mohedano, A. F., 2012. Inhibition of methanogenesis by chlorophenols: a kinetic approach. *New Biotechnology*, 30(1), pp. 51-61.
- Ramachandran, S. et al., 2007. Oil cakes and their biotechnological applications - A review. *Bioresource Technology*, Volume 98, pp. 2000-2009.
- Ramirez, I. et al., 2009a. Modified ADM1 disintegration/hydrolysis structures for modelling batch thermophilic anaerobic digestion of thermally pretreated waste activated sludge. *Water Research*, 43(14), pp. 3479-3492.
- Ramirez, I., Volcke, E. I., Rajinikanth, R. & Steyer, J.-P., 2009b. Modeling microbial diversity in anaerobic digestion through an extended ADM1 model. *Water Research*, 43(11), pp. 2787-2800.
- Rawat, J., Rao, P. V. & Choudary, N. V., 2011. *Controlling corrosion in amine treatment units*, s.l.: Digital Refining, Crambeth Allen Media LLP..
- Redlich, O. & Kwong, J. N., 1949. On the Thermodynamics of Solutions. V. An Equation of State. Fugacities of Gaseous Solutions. *Chemical Reviews*, 44(1), pp. 233-244.
- Reher, S., 2003. *Kraftstoffe aus Biogas - Technik, Qualitaet.*. Braunschweig, s.n.
- Renon, H. & Prausnitz, J. M., 1968. Local Compositions in Thermodynamic Excess Functions for Liquid Mixtures. *American Institute of Chemical Engineers*, Volume 41, pp. 135-144.
- Rieger, C. & Weiland, P., 2006. Prozessstoerungen fruehzeitig erkennen. *Biogas Journal*, Volume 4, pp. 18-20.
- Rivas-Garcia, P., Botello-Alvarez, J. E., Estrada-Baltazar, A. & Navarrete-Bolanos, J. L., 2013. Numerical study of microbial population dynamics in anaerobic digestion through the Anaerobic Digestion Model No. 1 (ADM1). *Chemical Engineering Journal*, Volume 228, pp. 87-92.

Robinson, R. A. & Stokes, R. H., 1970. *Electrolyte solutions*. 2nd ed. London: Butterworth and Co..

Rochelle, G. T., 2009. Amine scrubbing for CO<sub>2</sub> capture. *Science*, Volume 325, pp. 1652-1654.

Rojas, C. et al., 2010. *Simulationsunterstuetzte Prozessfuehrung von Biogasanlagen*. Nuernberg, Dechema Gessellschaft fuer Chemische Technik. Posterbeitrag und Abstract, DECHEMA-Tagung: Bioprozessorientiertes Anlagendesign. Dechema Gesellschaft fuer Chemische Technik., pp. 108-109.

Schimada, T., Zilles, J., Raskin, L. & Morgenroth, E., 2007. Carbohydrate storage in anaerobic sequencing batch reactors. *Water Research*, 41(20), pp. 4721-4729.

Schmack, D. & Nusko, R., 2006. *Biogas in Brennstoffzellen - in fuenf Jahren serienreif?*. [Online]

Available at: [http://www.erneuerbarenergien.de/0604/s\\_59-61.pdf](http://www.erneuerbarenergien.de/0604/s_59-61.pdf)

Schoen, M., 2009. *Numerical Modelling of Anaerobic Digestion Processes in Agricultural Biogas Plants*. Innsbruck: PhD Dissertation, University Innsbruck.

Schoen, M. et al., 2009. Population dynamics at digester overload conditions. *Bioresource Technology*, 100(23), pp. 5648-5655.

Shi, X. -S. et al., 2014. Modeling of the methane production and pH value during the anaerobic co-digestion of dairy manure and spent mushroom substrate. *Chemical Engineering Journal*, 224(15), pp. 258-263.

Sigma-Aldrich Co. LLC, 2012a. *Safety Data Sheet in accordance to Regulation (EC) No. 1907/2006: 2-(Ethylamino)ethanol*. [Online]

Available at: [www.sigma-aldrich.com](http://www.sigma-aldrich.com)

[Accessed 14 05 2014].

Sigma-Aldrich Co. LLC, 2012b. *Safety Data Sheet in accordance to Regulation (EC) No. 1907/2006: Diethanolamine (CAs No. 111-42-2)*. [Online]

Available at: [www.sigma-aldrich.com](http://www.sigma-aldrich.com)

[Accessed 14 05 2014].

Sigma-Aldrich Co. LLC, 2013a. *Safety Data Sheet in accordance to Regulation (EC) No. 1907/2006: 2-(2-Aminoethoxy)ethanol (CAS No. 929-06-6)*. [Online]

Available at: [www.sigma-aldrich.com](http://www.sigma-aldrich.com)

[Accessed 14 05 2014].

Sigma-Aldrich Co. LLC, 2013b. *Safety Data Sheet in accordance to Regulation (EC) No. 1907/2006: Methanol (CAS No. 67-56-1)*. [Online]

Available at: [www.sigma-aldrich.com](http://www.sigma-aldrich.com)

[Accessed 14 05 2014].

Sigma-Aldrich Co. LLC, 2014. *Safety Data Sheet in accordance to Regulation (EC) No. 1907/2006: Ethanolamine (CAS No. 141-43-5)*. [Online]

Available at: [www.sigma-aldrich.com](http://www.sigma-aldrich.com)

[Accessed 14 05 2014].

Silkenbaeumer, D., Rumpf, B. & Lichtenthaler, R. N., 1998. Solubility of Carbon Dioxide in Aqueous Solutions of 2-Amino-2-methyl-1-propanol and N-Methyldiethanolamine and Their Mixtures in Temperature Range from 313 to 353 K and Pressure up to 2.7 MPa. *Industrial and Engineering Chemical Research*, Volume 37, pp. 3133-3141.

Silva, F. et al., 2009. Modelling of anaerobic treatment of evaporator condensate (EC) from a sulphite pulp mill using the IWA anaerobic digestion model No. 1 (ADM1). *Chemical Engineering Journal*, 148(2-3), pp. 319-326.

Simoni, L. D., Chapeaux, A., Brennecke, J. F. & Stadtherr, M. A., 2009. Assymmetric Framework for Predicting Liquid-Liquid Equilibrium of Ionic Liquid-Mixed-Solvent Systems. 2. Prediction of Ternary Systems. *Industrial & Engineering Chemical Research*, 48(15), pp. 7257-7265.

Simoni, L. D. et al., 2010. Measurement and Prediction of Vapor-Liquid Equilibrium of Aqueous 1-Ethyl-3-methylimidazolium-Based Ionic Liquid Systems. *Industrial & Engineering Chemical Research*, 49(8), pp. 3893-3901.

Simoni, L. D., Lin, Y., Brennecke, J. F. & Stadtherr, M. A., 2007. Reliable computation of binary parameters in activity coefficient models of liquid-liquid equilibrium. *Fluid Phase Equilibria*, 255(2), pp. 138-146.

Simoni, L. D., Lin, Y., Brennecke, J. F. & Stadtherr, M. A., 2008. Modeling Liquid-Liquid Equilibrium of Ionic Liquid Systems with NRTL, Electrolyte-NRTL, and UNIQUAC. *Industrial & Engineering Chemical Research*, 47(1), pp. 256-272.

Soave, G., 1972. Equilibrium constants from a modified Redlich-Kwong equation of state. *Chemical Engineering Science*, 27(6), pp. 1197-1203.

- Souza, T. S. et al., 2013a. ADM1 calibration using BMP tests for modelling the effect of autohydrolysis pretreatment on the performance of continuous sludge digesters. *Water Research*, 47(9), pp. 3244-3254.
- Souza, T. S. et al., 2013b. Thermal pretreatment and hydraulic retention time in continuous digesters feed with sewage sludge: Assessment using the ADM1. *Bioresource Technology*, Volume 148, pp. 317-324.
- Staubmann, R. et al., 1997. Biogas production from *Jatropha curcas* press-cake. *Applied Biochemistry and Biotechnology*, Volume 63-65, pp. 457-467.
- St-Pierre, N., 2013. *Farm and Dairy*. [Online]  
Available at: <http://www.farmanddairy.com/top-stories/how-often-should-you-test-forages/49821.html>  
[Accessed 22 03 2014].
- Suda, T., Iwaki, T. & Mimura, T., 1996. Facile Determination of Dissolved Species in CO<sub>2</sub> - Amine - H<sub>2</sub>O System by NMR Spectroscopy. *Chemistry Letters*, Volume 25, pp. 777-778.
- Sun, S., Wang, J. & Li, Z., 2012. Solubility and Self-Consistent Modeling of Aniline Hydrochloride in H-Mg-Na-Ca-Al-Cl-H<sub>2</sub>O System at the Temperature Range of 288-348K. *Industrial & Engineering Chemical Research*, 51(9), pp. 3783-3790.
- Sutar, P. N., Jha, A., Vaidya, P. D. & Kenig, E. Y., 2012. Secondary amines for CO<sub>2</sub> capture: A Kinetic investigation using N-ethylmonoethanolamine. *Chemical Engineering Journal*, Volume 207-208, pp. 718-724.
- Thamsirioj, T. & Murphy, J. D., 2011. Modelling mono-digestion of grass silage on a 2-stage CSTR anaerobic digester using ADM1. *Bioresource Technology*, 102(2), pp. 948-959.
- The MathWorks, Inc., 2011. *MATLAB(R) - Optimization Toolbox(TM) 6, User's Guide*, Natick, MA, USA: The MathWorks, Inc.
- The Norwegian Activities Regulation (PSA), 2010. *Regulations relating to conducting petroleum activities (the activities regulation). Chapter XI emissions and discharges to the external environment*. s.l.:s.n.
- Thermodynamics Research Center, 2014. *ThermoDataEngine*, Boulder: National Institute of Standards and Technology, NIST Thermophysical Properties Division (638).

- Tian, P., Ning, P., Cao, H. & Li, Z., 2012. Determination and Modeling of Solubility for  $\text{CaSO}_4 \cdot 2\text{H}_2\text{O}$ - $\text{NH}_4(+)$ - $\text{Cl}(-)$ - $\text{SO}_4(2-)$ - $\text{NO}_3(-)$ - $\text{H}_2$  System. *Journal of Chemical Engineering Data*, 57(12), pp. 3664-3671.
- Vaidya, P. D. & Kenig, E. Y., 2007. Absorption of  $\text{CO}_2$  into aqueous blends of alkanolamines prepared from renewable resources. *Chemical Engineering Science*, Volume 62, pp. 7344-7350.
- van der Waals, J. D., 1873. *Over de Continuïteit van den Gasen Vloeistofoestand*, Thesis. Leiden: University of Leiden.
- van Soest, P. J. & Wine, R. H., 1967. Use of detergents in the analysis of fibrous feeds IV. Determination of plant cell-wall constituents.. *Journal of Association of Official Analytical Chemists*, 50(1), pp. 50-59.
- Vavilin, V. A., Fernandez, B., Palatsi, J. & Flotats, X., 2008. Hydrolysis kinetics in anaerobic degradation of particulate organic material: an overview. *Waste Management*, Volume 28, pp. 939-951.
- Vavilin, V. A. et al., 1997. Modelling methanogenesis during anaerobic conversion of complex organic matter at low temperatures. *Water Science Technology*, Volume 36, pp. 531-538.
- Vavilin, V. A. et al., 1998. Modelling low-temperature methane production from cattle manure by an acclimated microbial community. *Bioresource Technology*, Volume 63, pp. 159-171.
- Verein Deutscher Ingenieure (VDI), 2006. *Fermentation of organic material. Characterization of the substrate, sampling, collection of material data, fermentation tests*, Duesseldorf: Verein Deutscher Ingenieure.
- Wang, J., Sun, S. & Li, Z., 2011. Modeling of Solid-Liquid Equilibrium for the  $[\text{HAE}]\text{-Cl-MgCl}_2\text{-H}_2\text{O}$ . *Industrial & Engineering Chemical Research*, 50(13), pp. 8314-8322.
- Weiland, P., 2006. Biomass Digestion in Agriculture: A Successful Pathway for the Energy Production and Waste Treatment in Germany. *Engineering Life Science*, Volume 6, pp. 302-309.
- Wett, B., Eladawy, A. & Ogurek, M., 2006. Description of nitrogen incorporation and release in ADM1. *Water Science & Technology*, 54(4), pp. 67-76.
- Wett, B., Phothilangka, P. & Eladawy, A., 2010. Systematic comparison of mechanical and thermal sludge disintegration technologies. *Waste Management*, 30(6), pp. 1057-1062.

- Wett, B. et al., 2007. Model based design of an agricultural biogas plant: application of Anaerobic Digestion Model No.1 for an improved four chamber scheme. *Water Science Technology*, 55(10), pp. 21-28.
- Wichern, M. et al., 2009. Monofermentation of grass silage under mesophilic conditions: measurements and mathematical modelling with ADM1. *Bioresource Technology*, 100(4), pp. 1675-1681.
- Wichern, M. et al., 2008. Investigations and mathematical simulation on decentralized anaerobic treatment of agricultural substrates from livestock farming. *Water Science & Technology*, 58(1), pp. 67-72.
- Wikimedia, 2011. *Wikiquote: Albert Schweitzer*. [Online] Available at: [http://en.wikiquote.org/wiki/Talk:Albert\\_Schweitzer](http://en.wikiquote.org/wiki/Talk:Albert_Schweitzer) [Accessed 29 3 2014].
- Winter, J., 1985. Mikrobiologische Grundlagen der anaeroben Schlammfäulung. *Wasser-Abwasser*, 126(2), pp. 51-56.
- Xiao, X., Sheng, G.-P., Mu, Y. & Yu, H.-Q., 2013. A modelling approach to describe ZVI-based anaerobic system. *Water Research*, 47(16), pp. 6007-6013.
- Yan, Y. & Chen, C. -C., 2010. Thermodynamic modeling of CO<sub>2</sub> solubility in aqueous solutions of NaCl and Na<sub>2</sub>SO<sub>4</sub>. *The Journal of Supercritical Fluids*, Volume 55, pp. 623-634.
- Yan, Y. & Chen, C. -C., 2011. Thermodynamic representation of the NaCl + Na<sub>2</sub>SO<sub>4</sub> + H<sub>2</sub>O system with electrolyte NRTL model. *Fluid Phase Equilibria*, 306(2), pp. 149-161.
- Yasui, H., Goel, R., Li, Y. Y. & Noike, T., 2008. Modified ADM1 structure for modelling municipal primary sludge hydrolysis. *Water Research*, 42(1-2), pp. 249-259.
- Yuan, X.-Z. et al., 2014. Modelling anaerobic digestion of blue algae: Stoichiometric coefficients of amino acids acidogenesis and thermodynamics analysis. *Water Research*, 49(1), pp. 113-123.
- Yu, L. et al., 2013. Multiphase modelling of setting and suspension in anaerobic digester. *Applied Energy*, Volume 111, pp. 28-39.
- Yu, L. et al., 2012. Experimental and modelling study of a two-stage pilot scale high solid anaerobic digester system. *Bioresource Technology*, Volume 124, pp. 8-17.

- Zaher, U. et al., 2007. Transformers for interfacing anaerobic digestion models to pre- and post-treatment processes in a plant - wide modelling context. *Environmental Modelling & Software*, 22(1), pp. 40-58.
- Zaher, U. et al., 2009. GISCOD: General Integrated Solid Waste Co- Digestion model. *Water Research*, 43(10), pp. 2717-2727.
- Zhang, L., Guo, Y., Deng, D. & Ge, Y., 2013. Experimental Measurement and Modeling of Ternary Vapor - Liquid Equilibrium for Water+1-Propanol+1-Butyl-3-methylimidazolium Chloride. *Journal of Chemical Engineering Data*, 58(1), pp. 43-47.
- Zhang, Y. & Chen, C. -C., 2011. Thermodynamic Modeling for CO<sub>2</sub> Absorption in Aqueous MDEA Solutions with Electrolyte NRTL Model. *Industrial & Engineering Chemical Research*, 50(1), pp. 163-175.
- Zhang, Y., Que, H. & Chen, C. -C., 2011. Thermodynamic modelling for CO<sub>2</sub> absorption in aqueous MEA solution with electrolyte NRTL model. *Fluid Phase Equilibria*, Volume 311, pp. 67-75.
- Zhou, H., Loeffler, D. & Kranert, M., 2011. Model-based predictions of anaerobic digestion of agricultural substrates for biogas production. *Bioresource Technology*, 102(23), pp. 10819-10828.
- Zonta, Z., Alves, M. M., Flotats, X. & Palatsi, J., 2013. Modelling inhibitory effects of long chain fatty acids in the anaerobic digestion process. *Water Research*, 47(3), pp. 1369-1380.

## 9. Appendix

### 9.1. Appendix A

The Peterson matrix form of ADM1, along with variables, coefficients, and abbreviation from Schoen (Schoen, 2009):

- Chart a “*describes ADM1 matrix for soluble components (physico-chemical rate equations not included; Batstone et al., 2002a)*” (Schoen, 2009)
- Chart b “*ADM1 matrix for particulate components (physico-chemical rate equations not included; Batstone et al., 2002a)*” (Schoen, 2009)
- Chart c “*ADM1 matrix for acid-base reactions and for liquid-gas reactions as implemented in Matlab/SIMBA*” (Schoen, 2009)
- Chart d “*ADM1 stoichiometric parameters as implemented in Matlab/SIMBA*” (Schoen, 2009)
- Chart e “*ADM1 kinetic parameters as implemented in Matlab/SIMBA*” (Schoen, 2009)

Component i	1	2	3	4	5	6	7	8	9	10	11	12	Rate ( $\rho_i$ , kg COD·m <sup>-3</sup> ·d <sup>-1</sup> )
j Process	$S_{su}$	$S_{aa}$	$S_{fa}$	$S_{va}$	$S_{bu}$	$S_{pro}$	$S_{ac}$	$S_{hg}$	$S_{mg}$	$S_{ic}$	$S_{ni}$	$S_i$	
1 Disintegration												$f_{s,i} \cdot X_c$	$k_{dis} \cdot X_c$
2 Hydrolysis carbohydrates	1												$k_{hyd,ch} \cdot X_{ch}$
3 Hydrolysis of proteins		1											$k_{hyd,pr} \cdot X_{pr}$
4 Hydrolysis of lipids	$1-f_{fa,i}$		$f_{fa,i}$										$k_{hyd,l} \cdot X_{li}$
5 Uptake of sugars	-1				$(1-Y_{su}) \cdot f_{bu,su}$	$(1-Y_{su}) \cdot f_{pr,su}$	$(1-Y_{su}) \cdot f_{ac,su}$	$(1-Y_{su}) \cdot f_{hg,su}$		$-\sum_{i=1,2,11-24} C_i \cdot v_{i,5}$	$-(Y_{su}) \cdot N_{bac}$		$k_{m,su} \cdot \frac{S_{su}}{K_s + S_{su}} \cdot X_{su} \cdot I_1$
6 Uptake of amino acids		-1		$(1-Y_{aa}) \cdot f_{va,aa}$	$(1-Y_{aa}) \cdot f_{bu,aa}$	$(1-Y_{aa}) \cdot f_{pro,aa}$	$(1-Y_{aa}) \cdot f_{ac,aa}$	$(1-Y_{aa}) \cdot f_{hg,aa}$		$-\sum_{i=1,2,11-24} C_i \cdot v_{i,6}$	$N_{aa} - (Y_{aa}) \cdot N_{bac}$		$k_{m,aa} \cdot \frac{S_{aa}}{K_s + S_{aa}} \cdot X_{aa} \cdot I_1$
7 Uptake of LCFA			-1				$(1-Y_{fa}) \cdot 0.7$	$(1-Y_{fa}) \cdot 0.3$			$-(Y_{fa}) \cdot N_{bac}$		$k_{m,fa} \cdot \frac{S_{fa}}{K_s + S_{fa}} \cdot X_{fa} \cdot I_2$
8 Uptake of valerate				-1		$(1-Y_{va}) \cdot 0.54$	$(1-Y_{va}) \cdot 0.31$	$(1-Y_{va}) \cdot 0.15$			$-(Y_{va}) \cdot N_{bac}$		$k_{m,va} \cdot \frac{S_{va}}{K_s + S_{va}} \cdot X_{va} \cdot \frac{1}{1 + S_{bu}/S_{va}} \cdot I_2$
9 Uptake of butyrate					-1		$(1-Y_{bu}) \cdot 0.8$	$(1-Y_{bu}) \cdot 0.2$			$-(Y_{bu}) \cdot N_{bac}$		$k_{m,bu} \cdot \frac{S_{bu}}{K_s + S_{bu}} \cdot X_{bu} \cdot \frac{1}{1 + S_{fa}/S_{bu}} \cdot I_2$
10 Uptake of propionate						-1	$(1-Y_{pro}) \cdot 0.57$	$(1-Y_{pro}) \cdot 0.43$		$-\sum_{i=1,2,11-24} C_i \cdot v_{i,10}$	$-(Y_{pro}) \cdot N_{bac}$		$k_{m,pro} \cdot \frac{S_{pro}}{K_s + S_{pro}} \cdot X_{pro} \cdot I_2$
11 Uptake of acetate							-1		$(1-Y_{ac})$	$-\sum_{i=1,2,11-24} C_i \cdot v_{i,11}$	$-(Y_{ac}) \cdot N_{bac}$		$k_{m,ac} \cdot \frac{S_{ac}}{K_s + S_{ac}} \cdot X_{ac} \cdot I_3$
12 Uptake of hydrogen								-1	$(1-Y_{hg})$	$-\sum_{i=1,2,11-24} C_i \cdot v_{i,12}$	$-(Y_{hg}) \cdot N_{bac}$		$k_{m,hg} \cdot \frac{S_{hg}}{K_s + S_{hg}} \cdot X_{hg} \cdot I_1$
13 Decay of Xsu													$k_{dec,xsu} \cdot X_{su}$
14 Decay of Xaa													$k_{dec,xaa} \cdot X_{aa}$
15 Decay of Xfa													$k_{dec,xfa} \cdot X_{fa}$
16 Decay of Xc4													$k_{dec,xc4} \cdot X_{c4}$
17 Decay of Xpro													$k_{dec,xpro} \cdot X_{pro}$
18 Decay of Xac													$k_{dec,xac} \cdot X_{ac}$
19 Decay of Xh2													$k_{dec,xh2} \cdot X_{h2}$

a).

Monosaccharides	Amino acids	Long chain fatty acids	Total valerate	Total butyrate	Total propionate	Total acetate	Hydrogen gas	Methane gas	Inorganic carbon	Inorganic nitrogen	Soluble inerts	Inhibition factors: $I_1 = \frac{1}{1 + N_{i,im}}$ $I_2 = \frac{1}{1 + N_{i,im} \cdot I_2}$ $I_3 = \frac{1}{1 + N_{i,im} \cdot N_{H3,Xac}}$
[kgCOD·m <sup>-3</sup> ]	[kmoleC·m <sup>-3</sup> ]	[kmoleN·m <sup>-3</sup> ]	[kgCOD·m <sup>-3</sup> ]									

Component i	13	14	15	16	17	18	19	20	21	22	23	24	Rate ( $\rho_i$ , kg COD·m <sup>-3</sup> ·d <sup>-1</sup> )
j Process	$X_{su}$	$X_{ch}$	$X_{pr}$	$X_{ll}$	$X_{su}$	$X_{aa}$	$X_{fa}$	$X_{c4}$	$X_{pro}$	$X_{ac}$	$X_{h2}$	$X_i$	
1 Disintegration	-1	$f_{ch,xc}$	$f_{pr,xc}$	$f_{ll,xc}$								$f_{d,xc}$	$k_{dis} \cdot X_c$
2 Hydrolysis carbohydrates		-1											$k_{hyd,ch} \cdot X_{ch}$
3 Hydrolysis of proteins			-1										$k_{hyd,pr} \cdot X_{pr}$
4 Hydrolysis of lipids				-1									$k_{hyd,ll} \cdot X_{ll}$
5 Uptake of sugars					$Y_{su}$								$K_{m,su} \cdot \frac{S_{su}}{K_s + S} \cdot X_{su} \cdot I_1$
6 Uptake of amino acids						$Y_{aa}$							$K_{m,aa} \cdot \frac{S_{aa}}{K_s + S_{aa}} \cdot X_{aa} \cdot I_1$
7 Uptake of LCFA							$Y_{fa}$						$K_{m,fa} \cdot \frac{S_{fa}}{K_s + S_{fa}} \cdot X_{fa} \cdot I_2$
8 Uptake of valerate								$Y_{c4}$					$K_{m,c4} \cdot \frac{S_{va}}{K_s + S_{va}} \cdot X_{c4} \cdot \frac{1}{1 + S_{bu}/S_{va}} \cdot I_2$
9 Uptake of butyrate								$Y_{c4}$					$K_{m,c4} \cdot \frac{S_{bu}}{K_s + S_{bu}} \cdot X_{c4} \cdot \frac{1}{1 + S_{va}/S_{bu}} \cdot I_2$
10 Uptake of propionate									$Y_{pro}$				$K_{m,pr} \cdot \frac{S_{pro}}{K_s + S_{pro}} \cdot X_{pro} \cdot I_2$
11 Uptake of acetate										$Y_{ac}$			$K_{m,ac} \cdot \frac{S_{ac}}{K_s + S_{ac}} \cdot X_{ac} \cdot I_3$
12 Uptake of hydrogen											$Y_{h2}$		$K_{m,h2} \cdot \frac{S_{h2}}{K_s + S_{h2}} \cdot X_{h2} \cdot I_1$
13 Decay of Xsu	1				-1								$k_{dec,Xsu} \cdot X_{su}$
14 Decay of Xaa	1					-1							$k_{dec,Xaa} \cdot X_{aa}$
15 Decay of Xfa	1						-1						$k_{dec,Xfa} \cdot X_{fa}$
16 Decay of Xc4	1							-1					$k_{dec,Xc4} \cdot X_{c4}$
17 Decay of Xpro	1								-1				$k_{dec,Xpro} \cdot X_{pro}$
18 Decay of Xac	1									-1			$k_{dec,Xac} \cdot X_{ac}$
19 Decay of Xh2	1										-1		$k_{dec,Xh2} \cdot X_{h2}$

[kgCOD·m<sup>-3</sup>]

Composites	Carbohydrates	Proteins	Lipids	Sugar degraders	Amino acid degraders	LCFA degraders	Valerate and butyrate degraders	Propionate degraders	Acetate degraders	Hydrogen degraders	Particulate inerts	Inhibition factors:
												$I_1 = \rho_{H_2,lim}$ $I_2 = \rho_{H_2,lim} \cdot h_2$ $I_3 = \rho_{H_2,lim} \cdot h_{H_2,Xac}$

b).

Component i	8	9	10	25	26	27	28	29	30	31	32	33	34	35	36	Rate (p, kg COD·m <sup>-3</sup> ·d <sup>-1</sup> )
j	S <sub>h2</sub>	S <sub>ch4</sub>	S <sub>ic</sub>	S <sub>cat</sub>	S <sub>an</sub>	S <sub>va</sub>	S <sub>bu</sub>	S <sub>pro</sub>	S <sub>ac</sub>	S <sub>hco3</sub>	S <sub>nh4</sub>	pi <sub>sh2</sub>	pi <sub>sch4</sub>	pi <sub>sco2</sub>	P <sub>total</sub>	
A4	valerate acid-base					-1										$k_{A\_Bva} \cdot (S_{va} - S_{va} - K_{pva} \cdot (S_{va} - S_{va}))$
A5	butyrate acid-base						-1									$k_{A\_Bbu} \cdot (S_{bu} - S_{bu} - K_{pbu} \cdot (S_{bu} - S_{bu}))$
A6	propionate acid-base							-1								$k_{A\_Bpr} \cdot (S_{pr} - S_{pr} - K_{ppr} \cdot (S_{pr} - S_{pr}))$
A7	acetate acid-base								-1							$k_{A\_Bac} \cdot (S_{ac} - S_{ac} - K_{pac} \cdot (S_{ac} - S_{ac}))$
A10	inorg. carbon acid-base									-1						$k_{A\_Bco2} \cdot (S_{hco3} - S_{h} - K_{pco2} \cdot S_{co2})$
A11	inorg. nitrogen acid-base										-1					$k_{A\_Bin} \cdot (S_{nh3} - S_{n} - K_{pin} \cdot S_{nh4})$
ppSh2		$-V_{gas}/V$										$RT/(16/1000)$			$RT/(16/1000)$	$k_{i\_a_{h2}} \cdot (S_{h2} - pi_{sh2} \cdot (16/1000) / RT / (K_{h_{h2}})) \cdot V / V_{gas}$
ppSch4			$-V_{gas}/V$										$RT/(64/1000)$		$RT/(64/1000)$	$k_{i\_a_{ch4}} \cdot (S_{ch4} - pi_{sch4} \cdot (64/1000) / RT / (K_{h_{ch4}})) \cdot V / V_{gas}$
ppSco2				$-V_{gas}/V$										$RT/(1/1000)$	$RT/(1/1000)$	$k_{i\_a_{co2}} \cdot (S_{co2} - pi_{sco2} \cdot (1/1000) / RT / (K_{h_{co2}})) \cdot V / V_{gas}$
ppTotal												$pi_{sh2}/p_{total}$	$pi_{sch4}/p_{total}$	$pi_{sco2}/p_{total}$	-1	$k_p \cdot (P_{total} - P_{atm}) \cdot V / V_{gas}$

c).

Name	Description	Unit
fSI_XC	Soluble inerts from composites	-
fXI_XC	Particulate inerts from composites	-
fCH_XC	Carbonhydrates from composites	-
fPR_XC	Proteins from composites	-
fLI_XC	Lipids from composites	-
N_Xc	Nitrogen content composites	k mole N kg COD <sup>-1</sup>
N_I	Nitrogen content inerts	k mole N kg COD <sup>-1</sup>
N_aa	Nitrogen content in amino acids and proteins	k mole N kg COD <sup>-1</sup>
N_XB	Nitrogen content in biomass	k mole N kg COD <sup>-1</sup>
C_Xc	Carbon content composites	k mole C kg COD <sup>-1</sup>
C_SI	Carbon content soluble inerts	k mole C kg COD <sup>-1</sup>
C_Xch	Carbon content carbohydrates	k mole C kg COD <sup>-1</sup>
C_Xpr	Carbon content proteins	k mole C kg COD <sup>-1</sup>
C_Xli	Carbon content lipids	k mole C kg COD <sup>-1</sup>
C_XI	Carbon content particulate inerts	k mole C kg COD <sup>-1</sup>
C_su	Carbon content sugars	k mole C kg COD <sup>-1</sup>
C_aa	Carbon content amino acids	k mole C kg COD <sup>-1</sup>
C_Sfa	Carbon content fatty acids	k mole C kg COD <sup>-1</sup>
C_Sbu	Carbon content butyrate	k mole C kg COD <sup>-1</sup>
C_Spro	Carbon content propionate	k mole C kg COD <sup>-1</sup>
C_Sac	Carbon content acetate	k mole C kg COD <sup>-1</sup>
C_XB	Carbon content biomass	k mole C kg COD <sup>-1</sup>
C_Sva	Carbon content valerate	k mole C kg COD <sup>-1</sup>
C_Sch4	Carbon content methane	k mole C kg COD <sup>-1</sup>
fFA_Xli	fraction fatty acids from lipids	kg COD kg COD <sup>-1</sup>
fBU_SU	fraction butyrate from sugars	kg COD kg COD <sup>-1</sup>
fBU_AA	fraction butyrate from amino acids	kg COD kg COD <sup>-1</sup>
fPRO_SU	fraction propionate from sugars	kg COD kg COD <sup>-1</sup>
fPRO_AA	fraction propionate amino acids	kg COD kg COD <sup>-1</sup>
fPRO_VA	fraction propionate valerate	kg COD kg COD <sup>-1</sup>
fAC_SU	fraction acetate from sugars	kg COD kg COD <sup>-1</sup>
fAC_AA	fraction acetate amino acids	kg COD kg COD <sup>-1</sup>
fVA_AA	fraction valerate from amino acids	kg COD kg COD <sup>-1</sup>
fH2_SU	fraction hydrogen from sugars	kg COD kg COD <sup>-1</sup>
fH2_AA	fraction hydrogen from amino acids	kg COD kg COD <sup>-1</sup>
fH2_FA	fraction hydrogen from fatty acids	kg COD kg COD <sup>-1</sup>
fH2_VA	fraction hydrogen from valerate	kg COD kg COD <sup>-1</sup>
fH2_BU	fraction hydrogen from butyrate	kg COD kg COD <sup>-1</sup>
fH2_PRO	fraction hydrogen from propionate	kg COD kg COD <sup>-1</sup>

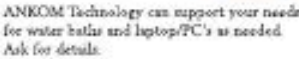
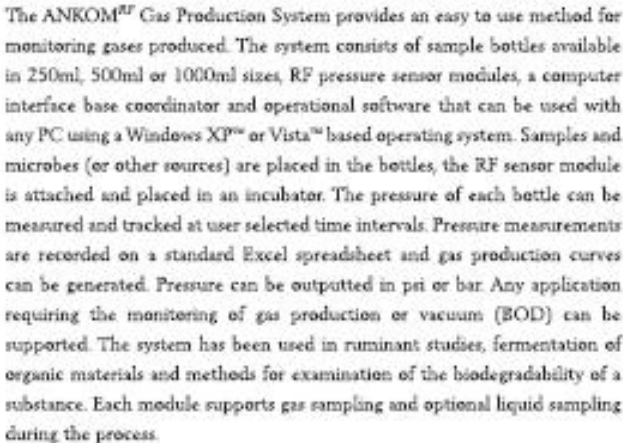
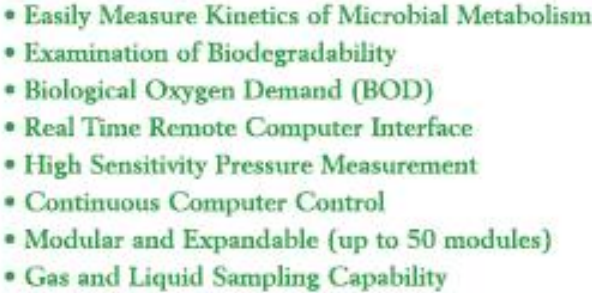
d).

Name	Description	Unit	Name	Description	Unit
kdis	disintegration rate	d <sup>-1</sup>	kdec_Xaa	decay rate amino acids	d <sup>-1</sup>
khyd_ch	Hydrolysis rate carbohydrates	d <sup>-1</sup>	kdec_Xfa	decay rate fatty acids	d <sup>-1</sup>
khyd_pr	hydrolysis rate propionate	d <sup>-1</sup>	kdec_Xc4	decay rate butyrate and valerate	d <sup>-1</sup>
khyd_li	hydrolysis rate lipids	d <sup>-1</sup>	kdec_Xpro	decay rate propionate	d <sup>-1</sup>
Ysu	Yield uptake sugars	kgCOD_X kgCOD_S <sup>-1</sup>	kdec_Xac	decay rate acetate	d <sup>-1</sup>
Yaa	Yield uptake amino acids	kgCOD_X kgCOD_S <sup>-1</sup>	kdec_Xh2	decay rate hydrogen	d <sup>-1</sup>
Yfa	Yield uptake LCFA	kgCOD_X kgCOD_S <sup>-1</sup>	kA_Bva	valerate rate coefficient for acid-base	k mole d <sup>-1</sup>
Yc4	Yield uptake of buterate and valerate	kgCOD_X kgCOD_S <sup>-1</sup>	kA_Bbu	butyrate rate coefficient for acid-base	k mole d <sup>-1</sup>
Ypro	Yield uptake propionate	kgCOD_X kgCOD_S <sup>-1</sup>	kA_Bpro	propionate rate coefficient for acid-base	k mole d <sup>-1</sup>
Yac	Yield uptake acetate	kgCOD_X kgCOD_S <sup>-1</sup>	kA_Bac	acetate rate coefficient for acid-base	k mole d <sup>-1</sup>
Yh2	Yield uptake hydrogen	kgCOD_X kgCOD_S <sup>-1</sup>	kA_Bco2	CO2 rate coefficient for acid-base	k mole d <sup>-1</sup>
KS_su	half saturation coefficient sugars	kg COD m <sup>-3</sup>	kA_Bin	inorganic nitrogen rate coefficient for acid-base	k mole d <sup>-1</sup>
KS_aa	half saturation coefficient amino acids	kg COD m <sup>-3</sup>	Kw	water acid-base equilibrium constant	k mole m <sup>-1</sup>
KS_fa	half saturation coefficient fatty acids	kg COD m <sup>-3</sup>	Kava	valerate acid-base equilibrium constant	k mole m <sup>-1</sup>
KS_c4	half. sat. coeff. valerate and butyrate	kg COD m <sup>-3</sup>	Kabu	butyrate acid-base equilibrium constant	k mole m <sup>-1</sup>
KS_pro	half sat. coeff. propionate	kg COD m <sup>-3</sup>	Kapro	propionate acid-base equilibrium constant	k mole m <sup>-1</sup>
KS_ac	half sat. coeff. acetate	kg COD m <sup>-3</sup>	Kaac	acetate acid-base equilibrium constant	k mole m <sup>-1</sup>
KI_NH3	half. sat. coeff. NH3 in p11	k mole N m <sup>-3</sup>	Kaco2	CO2 acid-base equilibrium constant	k mole m <sup>-1</sup>
KS_IN	half saturation coefficient inorganic N	k mole N m <sup>-3</sup>	Kain	inorganic nitrogen acid-base equilibrium constant	k mole m <sup>-1</sup>
KI_H2_fa	half sat. coeff. H2 for p7	kg COD m <sup>-3</sup>	klaH2	dynamic gas-liquid transfer coefficient	d <sup>-1</sup>
KI_H2_c4	half. sat. coeff. H2 for p8,9	kg COD m <sup>-3</sup>	klaCH4	dynamic gas-liquid transfer coefficient	d <sup>-1</sup>
KS_h2	half sat. coeff. H2 for p12	kg COD m <sup>-3</sup>	klaCO2	dynamic gas-liquid transfer coefficient	d <sup>-1</sup>
KI_H2_pro	half sat. coeff. H2 in p10	kg COD m <sup>-3</sup>	KH_CO2	Henry constant	mol bar <sup>-1</sup> m <sup>-3</sup>
km_su	max uptake rate sugars	kgCOD_S kgCOD_X <sup>-1</sup> d <sup>-1</sup>	KH_CH4	Henry constant	mol bar <sup>-1</sup> m <sup>-3</sup>
km_aa	max. uptake rate amino acids	kgCOD_S kgCOD_X <sup>-1</sup> d <sup>-1</sup>	KH_H2	Henry constant	mol bar <sup>-1</sup> m <sup>-3</sup>
km_fa	max. uptake rate fatty acids	kgCOD_S kgCOD_X <sup>-1</sup> d <sup>-1</sup>	pHUL_a	upper pH limit for p5..10	-
km_c4	max. uptake rate valerate and butyrate	kgCOD_S kgCOD_X <sup>-1</sup> d <sup>-1</sup>	pHLL_a	lower pH limit for p5..10	-
km_pro	max. uptake rate propionate	kgCOD_S kgCOD_X <sup>-1</sup> d <sup>-1</sup>	pHUL_ac	upper pH limit p11	-
km_ac	max. uptake rate acetate	kgCOD_S kgCOD_X <sup>-1</sup> d <sup>-1</sup>	pHLL_ac	lower pH limit for p11	-
km_h2	max. uptake rate hydrogen	kgCOD_S kgCOD_X <sup>-1</sup> d <sup>-1</sup>	pHUL_h2	upper pH limit p12	-
kdec_Xsu	decay rate sugars	d <sup>-1</sup>	pHLL_h2	lower pH limit p12	-

e).

## 9.2. Appendix B

Further information about ANKOM's system, together with example of calculation.



*Helping To Feed The World!*

## Specifications

**Easy Data Conversion to Gas Production Curves**

**2-Way RF Communication**

**RF Data Collection up to 100'**

**Low Cost Starter Kit Available!**

RF sensors communicate with a computer (not included) to capture data based on user selected parameters.

The program allows individual settings for each sample jar, to include: frequency of pressure readings, pressure release points and length of experiment.

The system provides constant feedback on outgoing pressure readings and more.

### Product Specifications:

**Measuring Principle:**  
 Manometric

**Cumulative Pressure Range:**  
 -10.0 to 500.0 psi  
 (bar equivalent included)

**Accuracy:**  
 ± 1% of measured value

**Resolution:** ± 0.04

**Module Height:**

w/250ml bottle	20.3 cm
w/500ml bottle	24.1 cm
w/1000ml bottle	29.1 cm

**Diameter (without bottle):** 7.2 cm

**Jar Capacity:**  
 250ml, 500ml and  
 1000ml available

**PC Link:** Radio Frequency

## Helping To Feed The World!

ANKOM Technology is the developer of Filter Bag Technology (FBT) used around the world for fiber and fat analysis. With customers in over 85 countries, ANKOM has a reputation for quality and innovation. Constantly seeking to develop better methods for time-consuming analytical methods, ANKOM Technology focuses on customers' needs. We offer instruments, chemicals and other ancillary products to support fiber studies, crude fat extraction, total fat extraction, in vitro and in situ research and more. We work hard to keep costs low with quality and service high.



ANKOM Technology  
 2052 O'Neil Rd.  
 Macedon, NY 14502

Phone: (315) 986 - 8090  
 Fax: (315) 986 - 8091  
 E-mail: [gsp1@ankom.com](mailto:gsp1@ankom.com)

## Anhang D

### Umrechnung des Drucks in die Gasmenge

#### Berechnung des Gasvolumens in ml bei 39 °C über den Druck, gemessen in psi

Das während der Fermentation gebildete Gas führt zu einer Druckerhöhung, gemessen in psi oder mbar. Diese Erhöhung des Gasdrucks kann in ml Gas konvertiert werden, unter Anwendung der folgenden Gasgleichung (Im Beispiel erfolgt die Druckerfassung in psi).

Der gemessene Gasdruck kann in Mol Gas unter Anwendung der "Idealen" Gasgleichung umgewandelt werden, und dann als Milliliter (ml) Gas unter Verwendung des "Avogadro" Gesetzes berechnet werden.

#### "Ideale" Gasgleichung

$$n = p (V / RT)$$

n = gebildete Gasmenge in Mol (mol)

p = Druck in Kilopascal (kPa)

V = Kopfraumvolumen der Glasflasche in Liter (L)

T = Temperatur in Kelvin (K)

R = Gaskonstante ( 8,314472 L · kPa · K<sup>-1</sup> · mol<sup>-1</sup> )

#### Gesetz von Avogadro

Bei Anwendung des Avogadro Gesetzes wird der atmosphärische Druck in psi gemessen (1 psi = 6,894757293 Kilopascal), 1 Mol sind 22,4 l bei 0 ° C bzw. 1 Mol sind 25,6 l bei 39 ° C (312 Kelvin).

Die in Mol gemessene Gasmenge wird wie folgt in ml umgerechnet:

$$\text{gebildete Gasmenge in ml} = n \cdot 25,6 \cdot 1000$$

#### Beispiel:

Der gemessene Gesamtdruck ist 10 psi bei 39 °C

Die Glasflasche hat ein Volumen von 250 ml

Die Menge Probe/Lösung/Puffer sind zusammen 150 ml je Glasflasche

Das Kopfraumvolumen in den Glasflaschen ist dann 250ml – 150ml = 0,1 L

$$p = 10 \text{ psi} \cdot 6,894757293 \text{ kPa} = 68,94757293 \text{ kPa}$$

$$V = 0,1 \text{ L}$$

$$R = 8,314472 \text{ L} \cdot \text{kPa} \cdot \text{K}^{-1} \cdot \text{mol}^{-1}$$

$$T = 273 \text{ °K} + 39 \text{ °C} = 312 \text{ °K}$$

$$n = p (V / RT)$$

$$n = 68,94757293 \text{ kPa} (0,1 \text{ L} / (8,314472 \text{ L} \cdot \text{kPa} \cdot \text{K}^{-1} \cdot \text{mol}^{-1} \cdot 312 \text{ °K}))$$

$$n = 0,002657845 \text{ mol}$$

$$\text{gebildete Gasmenge in ml} = 0,002657845 \text{ mol} \cdot 25,6 \text{ L/mol} \cdot 1000 \text{ mL}$$

$$\text{gebildete Gasmenge in ml} = 68,040842 \text{ ml}$$

### 9.3. Appendix C

Anaerobic Digestion Model No. 1 (ADM1) was transferred from SIMBA<sup>®</sup> Simulation Software to the MATLAB R2006b by author. In this part the script from MATLAB is presented, where the ADM1xp is implemented together with the optimization software. In addition to that, values of the all parameters used for the simulation are included. Starting from part A the modified version of the code is presented, which was used for determination of the common hydrolysis constants (CHC), and an individual kinetic constant for disintegration phase for 6 substrates simultaneously.

- A. Code starting the ADM1xp normally (not in the optimization mode) via `init_myadm.m`, and giving the starting values for the kinetic constants for disintegration and hydrolysis phases (*KK*)

```
global ZeitSpanne;

reader = xlsread('expdata');

ZeitSpanne = reader(:,1)';
CumData = reader(:,2);

KK(1) = 1.4283;
KK(2) = 0.8385;
KK(3) = 0.0138;
KK(4) = 0.0021;

gas = init_myadm(KK);
```

- B. This part delivers the general data (e.g. reactor volume) and fractions for the main m.file: `myadm_ode.m`

```
function cumgas = init_myadm(KinKonstanten)
    clear t;
    clear Xo;
    clear X;
    clear qgas;
    global qgas;
    global kdis;           %disintegration rate    1/d
    global khyd_ch;       %Hydrolysis rate carbohydrates 1/d
    global khyd_pr;       %hydrolysis rate propionate 1/d
    global khyd_li;       %hydrolysis rate lipids 1/d
    global ZeitSpanne;
    global CumData;
    global AdjustmentMin;
    global AdjustmentMax;

    % General Datat (global)
    global T;
    global pext;
    global V;
```

```

global Vgas;
global kp;
global RT;
global NQ;
global pH;
global Kw;

% Fixed kincetic constants
%kdis = 0.5;
%khyd_ch = 10;
%khyd_pr = 10;
%khyd_li = 10;

% Transfer Optimization Data
kdis = KinKonstanten(1); %disintegration rate 1/d
khyd_ch = KinKonstanten(2); %Hydrolysis rate carbohydrates 1/d
khyd_pr = KinKonstanten(3); %hydrolysis rate propionate 1/d
khyd_li = KinKonstanten(4); %hydrolysis rate lipids 1/d

% Transfer Optimization Data end

Xo = zeros(1,33);

% General Data
T = 37; %Temperatur in °C
pext = 1.04 ; %external total pressure in bar
V = 500; %Tank volume liquid phase (m3)
Vgas = 600; %Gas volume in tank (m3)
kp = 10000; % Proportional control constant in m3/(m3*d)
RT = 8.314510 * 1E-5* (273.15+T); % in bar * m^3/ mol
NQ = 100000/(8.3145 * 273.15); % Norm cubic meter in mol/m3
pH = 7;

% General data end;

% Initialization
gas = 0;
ch4 = 0;
h2= 0;
co2 = 0;

% Initialization end

% Fractions
Xo(1) = 0.012; %Suu, monosaccarides kg COD/m3
Xo(2) = 0.0053; %Saa, amino acids kg COD/m3
Xo(3) = 0.1; %Sfa, total LCFA kg COD/m3
Xo(4) = 0.01; %Sva , valeric acid + valerate kg COD/m3
Xo(5) = 0.014; %Sbu , butyric acid +bytyrate kg COD/m3
Xo(6) = 0.0168; %Spro , propionic acid + propionate kg COD/m3
Xo(7) = 0.1785; %Sac , acetic acid + acetate kg COD/m3
Xo(8) = 0.24E-07; %Sh2,hydrogen kg COD/m3
Xo(9) = 0.048; %Sch4,methane kg COD/m3
Xo(10) = 0.09; %carbon dioxide k mole C/m3
Xo(11) = 0.17013; %Snh4, Ammonium k mol N/m3
Xo(12) = 5.53; %SI soluble inerts kg COD/m3
Xo(13) = 4.88; %Xc, composite kg COD/m3
Xo(14) = 0.055307; %Xch, carbohydrates kg COD/m3
Xo(15) = 0.055; %Xpr, proteins kg COD/m3

```

```

    Xo(16) = 0.083; %Xli, lipids kg COD/m3
    Xo(17) = 0.855; %Xsu, Biomass Sugar degraders kg COD/m3
    Xo(18) = 0.637; %Xaa, Biomass amino acids degraders kg COD/m3
    Xo(19) = 0.67; %Xfa, Biomass LCFA degraders kg COD/m3
    Xo(20) = 0.283; %Xc4, Biomass valerate, butyrate degraders kg
COD/m3
    Xo(21) = 0.13559; %Xpro, Biomass propionate degraders kg COD/m3
    Xo(22) = 0.9; %Xac, Biomass acetate degraders kg COD/m3
    Xo(23) = 0.43; %Xh2, Biomass hydrogen degraders kg COD/m3
    Xo(24) = 45; %XI, particulate inerts kg COD/m3
    Xo(25) = 10; %Xp, Particulate products arising from biomass
decay kg COD/m^3
    Xo(26) = 0.039126; % Scat k mol/m3
    Xo(27) = 0.178460; % San k mol/m3
    Xo(28) = 0.01; %Sva_, valerate kg COD/m3
    Xo(29) = 0.014; %Sbu_, Butyrate kg COD/m3
    Xo(30) = 0.016; %Spro_, propionate kg COD/m3
    Xo(31) = 0.177; %Sac_, acetate kg COD/m3
    Xo(32) = 0.083; %Shco3, bicarbonate k mole C/m3
    Xo(33) = 0.00378; %Snh3, Ammonia kmol N/m3
    Xo(34) = 0; %h2, Partial pressure of Sh2 bar
    Xo(35) = 0; %piSch4, Partial pressure of Sch4 bar
    Xo(36) = 0; %piSco2 Partial pressure of Sco2 bar
    Xo(37) = 1.0; %pTOTAL

% Fractions end

tspan = ZeitSpanne;
options = odeset('RelTol',1e-3,'AbsTol',1e-6);
[t,X] = odel5s(@myadm_ode,tspan,Xo,options);

for z = 1:length(X(:,1))
    gas(end+1) = kp*(X(z,37)-pext)/RT/NQ*V;
    ch4(end+1) = (X(z,35)/X(z,37))*gas(length(gas));
    h2(end+1) = (X(z,34)/X(z,37))*gas(length(gas));
    co2(end+1) = (X(z,36)/X(z,37))*gas(length(gas));
end

ch4 = ch4';
h2 = h2';
co2 = co2';
ch4 = ch4(2:end);
h2 = h2(2:end);
co2 = co2(2:end);
rate = [t ch4 h2 co2];

% numerical integration
rch4 = cumtrapz(t,ch4);
rh2 = cumtrapz(t,h2);
rco2 = cumtrapz(t,co2);
rgesamt = rch4+rh2+rco2;
diffges = ch4+h2+co2;

%cumgas = [t rgesamt X];
%cumgas = [t diffges ch4 h2 co2 ];
cumgas = [t rgesamt];

return

```

### C. The main body of the ADM1:

```
function [adm_dt] = myadm_ode(t, fractions)
global qgas;

% General Datat (global)
global T;
global pext;
global V;
global Vgas;
global kp;
global RT;
global NQ;
global pH;
global Kw;

% Kinetic constants are declared as global variables and defined in the
% calling function

global kdis;           %disintegration rate 1/d
global khyd_ch;       %Hydrolysis rate carbohydrates 1/d
global khyd_pr;       %hydrolysis rate propionate 1/d
global khyd_li;       %hydrolysis rate lipids 1/d

Ssu = fractions(1); %monosaccarides kg COD/m3
Saa = fractions(2); %amino acids kg COD/m3
Sfa = fractions(3); %total LCFA kg COD/m3
Sva = fractions(4); %valeric acid + valerate kg COD/m3
Sbu = fractions(5); %butyric acid +butyrate kg COD/m3
Spro = fractions(6); %propionic acid + propionate kg COD/m3
Sac = fractions(7); %acetic acid + acetate kg COD/m3
Sh2 = fractions(8); %hydrogen kg COD/m3
Sch4 = fractions(9); %methane kg COD/m3
Sco2 = fractions(10); %carbon dioxide k mole C/m3
Snh4 = fractions(11); %Ammonium k mol N/m3
SI = fractions(12); %soluble inerts kg COD/m3
Xc = fractions(13); %composite kg COD/m3
Xch = fractions(14); %carbohydrates kg COD/m3
Xpr = fractions(15); %proteins kg COD/m3
Xli = fractions(16); %lipids kg COD/m3
Xsu = fractions(17); %Biomass Sugar degraders kg COD/m3
Xaa = fractions(18); %Biomass amino acids degraders kg COD/m3
Xfa = fractions(19); %Biomass LCFA degraders kg COD/m3
Xc4 = fractions(20); %Biomass valerate, butyrate degraders kg COD/m3
Xpro = fractions(21); %Biomass propionate degraders kg COD/m3
Xac = fractions(22); %Biomass acetate degraders kg COD/m3
Xh2 = fractions(23); %Biomass hydrogen degraders kg COD/m3
XI = fractions(24); %particulate inerts kg COD/m3
Xp = fractions(25); %Particulate products arising from biomass decay kg
COD/m^3
Scat = fractions(26); %cations k mol/m3
San = fractions(27); %Anions k mol/m3
Sva_ = fractions(28); %valerate kg COD/m3
Sbu_ = fractions(29); %Butyrate kg COD/m3
Spro_ = fractions(30); %propionate kg COD/m3
Sac_ = fractions(31); %acetate kg COD/m3
Shco3 = fractions(32); %bicarbonate k mole C/m3
Snh3= fractions(33); %Ammonia kmol N/m3
piSh2 = fractions(34); %Partial pressure of Sh2 bar
```

```

piSch4= fractions(35); %Partial pressure of Sch4 bar
piSco2= fractions(36); %Partial pressure of Sco2 bar
pTOTAL= fractions(37); %Sum of all partial pressures bar
% Define Parameters (parameters which can be found in the parameter file
% read by simba
% needs to be changed for each substrate !
% includes as well the parameters for optimization

fSI_XC= 0.1; %fraction SI from XC -
dummy_fXI_XC = 0.210; %- -
%fCH_XC = 0.711; %fraction Xch from XC -
fCH_XC = 0.54; %fraction Xch from XC -
fPR_XC = 0.211;
fLI_XC = 0.04; %fraction Xli from XC -
fXP_XC= 0.05; %fraction Xp from XC -
N_Xc = 0.0376/14; %N content Xc k mole N/kg COD
N_I = 0.06/14; %Nitrogen content inerts k mole N/kg COD
N_aa = 0.098/14; %N content proteins k mole N/kg COD
C_Xc = 0.03; %C content Xc k mole C/kg COD
C_SI = 0.03; %C content SI k mole C/kg COD
C_Xch = 0.0313; %C content Xch k mole C/kg COD
C_Xpr = 0.03; %C content Xpr k mole C/kg COD
C_Xli = 0.022; %C content Xli k mole C/ kg COD
C_XI = 0.03; %C content XI k mole C/ kg COD
dummy_C_su = 0.313; %equal to C_Xch -
dummy_Caa = 0.03; %equal to C_Xpr -
fFA_Xli = 0.95; %fraction Sfa from Xli -
C_Sfa = 0.0217; %Carbon content Sfa k mole C/kg COD
fH2_SU = 0.19; %- -
fBU_SU = 0.13; %- -
fPRO_SU = 0.27; %- -
dummy_fAC_SU = 0.41; %residual to 1 -
N_XB = 0.08/14; %N content Biomass k mole N/kg CSB
C_Sbu = 0.025; %C content Sbu k mole C/kg COD
C_Spro = 0.0268; %C content Spro k mole C/kg COD
C_Sac = 0.0313; %C content Sac k mole C/kg COD
C_XB = 0.0313; %C content biomass k mole C/kg COD
Ysu = 0.1; %Yield uptake sugars -
fH2_AA = 0.06; %- -
fVA_AA = 0.23; %- -
fBU_AA = 0.26; %- -
fPRO_AA = 0.05; %- -
dummy_fAC_AA = 0.4; %residual to 1 -
C_Sva = 0.024; %C content Sva k mole C / kg COD
Yaa = 0.08; %Yield uptake amino acids -
fH2_FA = 0.3; %- -
Yfa = 0.06; %Yield uptake LCFA -
fH2_VA = 0.15; %- -
fPRO_VA = 0.54; %- -
fH2_BU = 0.2; %- -
Yc4 = 0.06; %Yield uptake of buterate and valerate -
fH2_PRO = 0.43; %- -
Ypro = 0.04; %Yield uptake propionate -
C_Sch4 = 0.0156; %C content Sch4 k mole C/kg COD
Yac = 0.05; %Yield uptake acetate -
Yh2 = 0.06; %Yield uptake hydrogen -
KS_IN = 1.00E-04; %half saturation coefficient inorganic N k mole
N/m3
km_su = 30; %Uptake rate sugars 1/d
KS_su = 0.5; %half saturation constant substate kg COD/m3
pHUL_a = 5.5; %upper pH limit for p5..10 -

```

```

pHLL_a = 4; %lower pH limit for p5..10 -
km_aa = 50; %max. uptake rate amino acids 1/d
KS_aa = 0.3; %half saturation coefficient amino acids kg COD/
m3
km_fa = 6; %max. uptake rate Sfa 1/d
KS_fa = 0.4; %half saturation coeff. Sfa kg COD/m3
KI_H2_fa = 5.00E-06; %half sat. coeff. H2 for p7 kg COD/m3
km_c4 = 20; %max. uptake rate valerate and butyrate 1/d
KS_c4 = 0.2; %half. sat. coeff. valerate and butyrate kg
COD/m3
KI_H2_c4 = 1.00E-05; %half. sat. coeff. H2 for p8,9 kg COD/m3
km_pro= 13; %max. uptake rate propionate 1/d
KS_pro = 0.1; %half sat. coeff. propionate kg COD/m3
KI_H2_pro = 3.50E-06; %half sat. coeff. H2 in p10 kg COD/m3
km_ac = 8; %max. uptake rate acetate 1/d
KS_ac = 0.15; %half sat. coeff. acetate kg COD/m3
KI_NH3 = 0.0018; %half. sat. coeff. NH3 in p11 k mole N/m3
pHUL_ac = 7; %upper pH limit p11 -
pHLL_ac = 6; %lower pH limit for p11 -
km_h2 = 35; %max. uptake rate hydrogen -
KS_h2 = 7.00E-06; %half sat. coeff. H2 for p12 kg COD/m3
pHUL_h2 = 6; %upper pH limit p12 -
pHLL_h2 = 5; %lower pH limit p12 -
kdec_Xsu = 0.02; %decay rate Xsu 1/d
kdec_Xaa = 0.02; %decay rate Xaa 1/d
kdec_Xfa = 0.02; %decay rate Xfa 1/d
kdec_Xc4 = 0.02; %decay rate Xc4 1/d
kdec_Xpro = 0.02; %decay rate Xpro 1/d
kdec_Xac = 0.02; %decay rate Xac 1/d
kdec_Xh2 = 0.02; %decay rate Xh2 1/d
Kw = 2.08E-14; % - -
Kava = 1.38E-05; %*10^-4.86;% k mole /m3
Kabu = 1.51E-05; %*10^-4.82;% -
Kapro = 1.32E-05; %*10^-4.88;% -
Kaac = 1.74E-05; %*10^-4.76;% -
Kaco2 = 4.94e-7; %*10^-6.35*exp(7646/(8.3145)*(1/(298.15) -
1/(273.15+T))), 10^-6.35*exp(7646/(R*100)*(1/Tbase - 1/T)) -
Kain = 1.11e-9; %*10^-9.25*exp(51965/(8.3145)*(1/(298.15) -
1/(273.15+T))), 10^-9.25*exp(51965/(R*100)*(1/Tbase - 1/T)) -
kA_Bva = 1.00E+08; %rate coefficient for acid-base (valerate) k
mole/d
kA_Bbu = 1.00E+08; %- -
kA_Bpro = 1.00E+08; %- -
kA_Bac = 1.00E+08; %- -
kA_Bco2 = 1.00E+08; %- -
kA_Bin = 1.00E+08; %- -
klaH2 = 200; %- -
klaCH4 = 200; %- -
klaCO2 = 200; %- -
KH_CO2 = 1/(0.0271*0.08314*(T+273.15)); %Henry constant mol/bar m^3
KH_CH4= 1/(0.00116*0.08314*(T+273.15)); %Henry constant mol/bar m^3
KH_H2 = 1/((7.38E-04)*0.08314*(T+273.15)); %Henry constant mol/bar m^3
C_Xp = 0.03; %C content of XP k mole C/ kg COD
N_Xp = (0.06/14); %N content of Xp k mole N/kg COD
fP = 0.08; %Fraction of biomass leading to particulate
products -

fXI_XC = (1-fSI_XC-fCH_XC-fPR_XC-fLI_XC-fXP_XC);
%fraction XI from XC -
fCO2_XC = (C_Xc - fSI_XC*C_SI - fCH_XC*C_Xch - fPR_XC*C_Xpr -fLI_XC*C_Xli -
fXI_XC*C_XI-fXP_XC*C_Xp); %- -

```

```

fSIN_XC      =      (N_Xc-fSI_XC*N_I-fPR_XC*N_aa-fXI_XC*N_I-fXP_XC*N_Xp);
%NH3+NH4 fraction from XC -
fCO2_Xli     =      (C_Xli      -      fFA_Xli*C_Sfa      -      (1-fFA_Xli)*C_Xch);
%Inorganic C fraction hydolysis Xli -
fAC_SU       =      (1-fH2_SU-fBU_SU-fPRO_SU);
fCO2_SU      =      (C_Xch-(fBU_SU*C_Sbu+fPRO_SU*C_Spro+fAC_SU*C_Sac)*(1-Ysu)      -
Ysu*C_XB);
fAC_AA       =      (1-fH2_AA-fVA_AA-fBU_AA-fPRO_AA);
fCO2_AA      =      (C_Xpr-
(fVA_AA*C_Sva+fBU_AA*C_Sbu+fPRO_AA*C_Spro+fAC_AA*C_Sac)*(1-Yaa)      -
Yaa*C_XB);
fAC_FA       =      (1.0-fH2_FA);
fCO2_FA      =      (C_Sfa-fAC_FA*C_Sac*(1-Yfa)-Yfa*C_XB);
fAC_VA       =      (1-fPRO_VA-fH2_VA);
fCO2_VA      =      (C_Sva-(fPRO_VA*C_Spro + fAC_VA*C_Sac)*(1-Yc4) - Yc4*C_XB);
fAC_BU       =      (1-fH2_BU);
fCO2_BU      =      (C_Sbu-fAC_BU*C_Sac*(1-Yc4)-Yc4*C_XB);
fAC_PRO      =      (1-fH2_PRO);
fCO2_PRO     =      (C_Spro-fAC_PRO*C_Sac*(1-Ypro)-Ypro*C_XB);
fCO2_AC      =      (C_Sac-(1-Yac)*C_Sch4-Yac*C_XB);
fCO2_H2      =      (-1*(1-Yh2)*C_Sch4-Yh2*C_XB);
pfac_h       =      ((Scat)+(Snh4)-(Shco3)-((Sac_)/64)-((Spro_)/112)-((Sbu_)/160)-
((Sva_)/208)-(San));
SH           =      (((-1)*(pfac_h)/2) + 0.5*(pfac_h*pfac_h + 4*Kw)^0.5);
Iin          =      ((Snh4+Snh3)/(Snh4+Snh3+KS_IN));
I_NH3        =      (KI_NH3/(KI_NH3+Snh3));
I_H2_c4      =      (KI_H2_c4/(KI_H2_c4 + Sh2));
KI_H_a       =      (10^(-1*(pHUL_a+pHLL_a)/2));
IpH_a        =      (KI_H_a^2/(SH^2+KI_H_a^2));
KI_H_h2      =      (10^(-1*(pHUL_h2+pHLL_h2)/2));
IpH_h2       =      ((KI_H_h2)^3/(SH^3+(KI_H_h2)^3));
KI_H_AC      =      (10^(-1*(pHUL_ac+pHLL_ac)/2));
IpH_ac       =      (KI_H_AC^3/(SH^3+KI_H_AC^3));
fCH_XB       =      (fCH_XC/(fCH_XC+fPR_XC+fLI_XC)*(1-fP));
%Fraction Xsu from biomass arising by decay -
fPR_XB       =      (fPR_XC/(fCH_XC+fPR_XC+fLI_XC)*(1-fP));
%Fraction Xpr from biomass arising by decay -
fLI_XB       =      (fLI_XC/(fCH_XC+fPR_XC+fLI_XC)*(1-fP));
%Fraction Xli from biomass arising by decay -
fSIN_XB      =      (N_XB-fP*N_Xp-fPR_XB*N_aa);
fCO2_XB      =      (C_XB-fP*C_Xp-fCH_XB*C_Xch-fPR_XB*C_Xpr-fLI_XB*C_Xli);
Qgas         =      kp*(pTOTAL-pext)/(RT*NQ)*V;

% Fraction: Ssu (monosaccarides)

dSsu         =      + (1) * (khyd_ch*Xch) + ((1-fFA_Xli)) * (khyd_li*Xli) + (-1) *
(km_su*Ssu/(KS_su+Ssu)*Xsu*Iin*IpH_a);

% Fraction: Saa (amino acids)
dSaa         =      + (1) * (khyd_pr*Xpr) + (-1) *
(km_aa*Saa/(KS_aa+Saa)*Xaa*Iin*IpH_a);

% Fraction: Sfa (total LCFA)
dSfa         =      + (fFA_Xli) * (khyd_li*Xli) + (-1) *
(km_fa*Sfa/(KS_fa+Sfa)*Xfa*Iin*KI_H2_fa/(KI_H2_fa + Sh2)*IpH_a);

% Fraction: Sva (valeric acid + valerate)
dSva         =      + ((1-Yaa)*fVA_AA) * (km_aa*Saa/(KS_aa+Saa)*Xaa*Iin*IpH_a) + (-1)
* (km_c4*Sva/(KS_c4+Sva)*Xc4*Sva/(Sva+Sbu+0.000001)*Iin*I_H2_c4*IpH_a);

```

```

% Fraction: Sbu (butyric acid + butyrate)
dSbu = + ((1-Ysu)*fBU_SU) * (km_su*Ssu/(KS_su+Ssu)*Xsu*Iin*IpH_a) + ((1-
Yaa)*fBU_AA) * (km_aa*Saa/(KS_aa+Saa)*Xaa*Iin*IpH_a) + (-1) *
(km_c4*Sbu/(KS_c4+Sbu)*Xc4*Sbu/(Sbu+Sva+0.000001)*Iin*I_H2_c4*IpH_a);

% Fraction: Spro (propionic acid + propionate)
dSpro = + ((1-Ysu)*fPRO_SU) * (km_su*Ssu/(KS_su+Ssu)*Xsu*Iin*IpH_a) +
((1-Yaa)*fPRO_AA) * (km_aa*Saa/(KS_aa+Saa)*Xaa*Iin*IpH_a) + ((1-
Yc4)*fPRO_VA) *
(km_c4*Sva/(KS_c4+Sva)*Xc4*Sva/(Sva+Sbu+0.000001)*Iin*I_H2_c4*IpH_a) + (-1)
* (km_pro*Spro/(KS_pro+Spro)*Xpro*Iin*KI_H2_pro/(KI_H2_pro + Sh2)*IpH_a);

% Fraction: Sac (acetic acid + acetate)
dSac = + ((1-Ysu)*fAC_SU) * (km_su*Ssu/(KS_su+Ssu)*Xsu*Iin*IpH_a) + ((1-
Yaa)*fAC_AA) * (km_aa*Saa/(KS_aa+Saa)*Xaa*Iin*IpH_a) + ((1-Yfa)*fAC_FA) *
(km_fa*Sfa/(KS_fa+Sfa)*Xfa*Iin*KI_H2_fa/(KI_H2_fa + Sh2)*IpH_a) + ((1-
Yc4)*fAC_VA) *
(km_c4*Sva/(KS_c4+Sva)*Xc4*Sva/(Sva+Sbu+0.000001)*Iin*I_H2_c4*IpH_a) + ((1-
Yc4)*fAC_BU) *
(km_c4*Sbu/(KS_c4+Sbu)*Xc4*Sbu/(Sbu+Sva+0.000001)*Iin*I_H2_c4*IpH_a) + ((1-
Ypro)*fAC_PRO) * (km_pro*Spro/(KS_pro+Spro)*Xpro*Iin*KI_H2_pro/(KI_H2_pro +
Sh2)*IpH_a) + (-1) * (km_ac*Sac/(KS_ac+Sac)*Xac*Iin*I_NH3*IpH_ac);

% Fraction: Sh2 (hydrogen)
dSh2 = + ((1-Ysu)*fH2_SU) * (km_su*Ssu/(KS_su+Ssu)*Xsu*Iin*IpH_a) + ((1-
Yaa)*fH2_AA) * (km_aa*Saa/(KS_aa+Saa)*Xaa*Iin*IpH_a) + ((1-Yfa)*fH2_FA) *
(km_fa*Sfa/(KS_fa+Sfa)*Xfa*Iin*KI_H2_fa/(KI_H2_fa + Sh2)*IpH_a) + ((1-
Yc4)*fH2_VA) *
(km_c4*Sva/(KS_c4+Sva)*Xc4*Sva/(Sva+Sbu+0.000001)*Iin*I_H2_c4*IpH_a) + ((1-
Yc4)*fH2_BU) *
(km_c4*Sbu/(KS_c4+Sbu)*Xc4*Sbu/(Sbu+Sva+0.000001)*Iin*I_H2_c4*IpH_a) + ((1-
Ypro)*fH2_PRO) * (km_pro*Spro/(KS_pro+Spro)*Xpro*Iin*KI_H2_pro/(KI_H2_pro +
Sh2)*IpH_a) + (-1) * (km_h2*Sh2/(KS_h2+Sh2)*Xh2*Iin*IpH_h2) + (-1*Vgas/V) *
((klaH2) * (Sh2-piSh2*(16/1000)/RT/(KH_H2)) * V/Vgas);

% Fraction: Sch4 (methane)
dSch4 = + ((1-Yac)) * (km_ac*Sac/(KS_ac+Sac)*Xac*Iin*I_NH3*IpH_ac) + ((1-
Yh2)) * (km_h2*Sh2/(KS_h2+Sh2)*Xh2*Iin*IpH_h2) + (-1*Vgas/V) *
((klaCH4) * (Sch4-piSch4*(64/1000)/RT/(KH_CH4)) * V/Vgas);

% Fraction: Sco2 (carbon dioxide)
dSco2 = + (fCO2_XC) * (kdis*Xc) + (fCO2_Xli) * (khyd_li*Xli) + (fCO2_SU)
*
(km_su*Ssu/(KS_su+Ssu)*Xsu*Iin*IpH_a) + (fCO2_AA) *
(km_aa*Saa/(KS_aa+Saa)*Xaa*Iin*IpH_a) + (fCO2_FA) *
(km_fa*Sfa/(KS_fa+Sfa)*Xfa*Iin*KI_H2_fa/(KI_H2_fa + Sh2)*IpH_a) + (fCO2_VA)
*
(km_c4*Sva/(KS_c4+Sva)*Xc4*Sva/(Sva+Sbu+0.000001)*Iin*I_H2_c4*IpH_a) +
(fCO2_BU) *
(km_c4*Sbu/(KS_c4+Sbu)*Xc4*Sbu/(Sbu+Sva+0.000001)*Iin*I_H2_c4*IpH_a) +
(fCO2_PRO) * (km_pro*Spro/(KS_pro+Spro)*Xpro*Iin*KI_H2_pro/(KI_H2_pro +
Sh2)*IpH_a) + (fCO2_AC) * (km_ac*Sac/(KS_ac+Sac)*Xac*Iin*I_NH3*IpH_ac) +
(fCO2_H2) * (km_h2*Sh2/(KS_h2+Sh2)*Xh2*Iin*IpH_h2) + (fCO2_XB) *
(kdec_Xsu*Xsu) + (fCO2_XB) * (kdec_Xaa*Xaa) + (fCO2_XB) * (kdec_Xfa*Xfa) +
(fCO2_XB) * (kdec_Xc4*Xc4) + (fCO2_XB) * (kdec_Xpro*Xpro) + (fCO2_XB) *
(kdec_Xac*Xac) + (fCO2_XB) * (kdec_Xh2*Xh2) + (1) * (kA_Bco2*(Shco3*SH-
Kaco2*Sco2)) + (-1*Vgas/V) * ((klaCO2) * (Sco2-
piSco2*(1/1000)/RT/(KH_CO2)) * V/Vgas);

% Fraction: Snh4 (Ammonium)
dSnh4 = + (fSIN_XC) * (kdis*Xc) + (-1*Ysu*N_XB) *
(km_su*Ssu/(KS_su+Ssu)*Xsu*Iin*IpH_a) + (N_aa-Yaa*N_XB) *

```

```

(km_aa*Saa/(KS_aa+Saa)*Xaa*Iin*IpH_a) + (-1*Yfa*N_XB) *
(km_fa*Sfa/(KS_fa+Sfa)*Xfa*Iin*KI_H2_fa/(KI_H2_fa + Sh2)*IpH_a) + (-
1*Yc4*N_XB) *
(km_c4*Sva/(KS_c4+Sva)*Xc4*Sva/(Sva+Sbu+0.000001)*Iin*I_H2_c4*IpH_a) + (-
1*Yc4*N_XB) *
(km_c4*Sbu/(KS_c4+Sbu)*Xc4*Sbu/(Sbu+Sva+0.000001)*Iin*I_H2_c4*IpH_a) + (-
1*Ypro*N_XB) * (km_pro*Spro/(KS_pro+Spro)*Xpro*Iin*KI_H2_pro/(KI_H2_pro +
Sh2)*IpH_a) + (-1*Yac*N_XB) * (km_ac*Sac/(KS_ac+Sac)*Xac*Iin*I_NH3*IpH_ac)
+ (-1*Yh2*N_XB) * (km_h2*Sh2/(KS_h2+Sh2)*Xh2*Iin*IpH_h2) + (fSIN_XB) *
(kdec_Xsu*Xsu) + (fSIN_XB) * (kdec_Xaa*Xaa) + (fSIN_XB) * (kdec_Xfa*Xfa) +
(fSIN_XB) * (kdec_Xc4*Xc4) + (fSIN_XB) * (kdec_Xpro*Xpro) + (fSIN_XB) *
(kdec_Xac*Xac) + (fSIN_XB) * (kdec_Xh2*Xh2) + (1) * (kA_Bin*(Snh3*SH-
Kain*Snh4));

% Fraction: SI (soluble inerts)
dSI = + (fSI_XC) * (kdis*Xc);

% Fraction: Xc (composite)
dXc = + (-1) * (kdis*Xc) + (1) * (kdec_Xsu*Xsu) + (1) * (kdec_Xaa*Xaa) +
(1) * (kdec_Xfa*Xfa) + (1) * (kdec_Xc4*Xc4) + (1) * (kdec_Xpro*Xpro) + (1)
* (kdec_Xac*Xac) + (1) * (kdec_Xh2*Xh2);

% Fraction: Xch (carbohydrates)
dXch = + (fCH_XC) * (kdis*Xc) + (-1) * (khyd_ch*Xch);

% Fraction: Xpr (proteins)
dXpr = + (fPR_XC) * (kdis*Xc) + (-1) * (khyd_pr*Xpr);

% Fraction: Xli (lipids)
dXli = + (fLI_XC) * (kdis*Xc) + (-1) * (khyd_li*Xli);

% Fraction: Xsu (Biomass Sugar degraders)
dXsu = + (Ysu) * (km_su*Ssu/(KS_su+Ssu)*Xsu*Iin*IpH_a) + (-1) *
(kdec_Xsu*Xsu);

% Fraction: Xaa (Biomass amino acids degraders)
dXaa = + (Yaa) * (km_aa*Saa/(KS_aa+Saa)*Xaa*Iin*IpH_a) + (-1) *
(kdec_Xaa*Xaa);

% Fraction: Xfa (Biomass LCFA degraders)
dXfa = + (Yfa) * (km_fa*Sfa/(KS_fa+Sfa)*Xfa*Iin*KI_H2_fa/(KI_H2_fa +
Sh2)*IpH_a) + (-1) * (kdec_Xfa*Xfa);

% Fraction: Xc4 (Biomass valerate, butyrate degraders)
dXc4 = + (Yc4) * (km_c4*Sva/(KS_c4+Sva)*Xc4*Sva/(Sva+Sbu+0.000001)*Iin*I_H2_c4*IpH_a) +
(Yc4) * (km_c4*Sbu/(KS_c4+Sbu)*Xc4*Sbu/(Sbu+Sva+0.000001)*Iin*I_H2_c4*IpH_a) + (-1)
* (kdec_Xc4*Xc4);

% Fraction: Xpro (Biomass propionate degraders)
dXpro = + (Ypro) * (km_pro*Spro/(KS_pro+Spro)*Xpro*Iin*KI_H2_pro/(KI_H2_pro +
Sh2)*IpH_a) + (-
1) * (kdec_Xpro*Xpro);

% Fraction: Xac (Biomass acetate degraders)
dXac = + (Yac) * (km_ac*Sac/(KS_ac+Sac)*Xac*Iin*I_NH3*IpH_ac) + (-1) *
(kdec_Xac*Xac);

```

```

% Fraction: Xh2 (Biomass hydrogen degraders)
dXh2 =      + (Yh2) * (km_h2*Sh2/(KS_h2+Sh2)*Xh2*Iin*IpH_h2) + (-1) *
(kdec_Xh2*Xh2);

% Fraction: XI (particulate inerts)
dXI =      + (fXI_XC) * (kdis*Xc);

% Fraction: Xp (Particulate products arising from biomass decay)
dXp =      + (fXP_XC) * (kdis*Xc) + (fP) * (kdec_Xsu*Xsu) + (fP) *
(kdec_Xaa*Xaa) + (fP) * (kdec_Xfa*Xfa) + (fP) * (kdec_Xc4*Xc4) + (fP) *
(kdec_Xpro*Xpro) + (fP) * (kdec_Xac*Xac) + (fP) * (kdec_Xh2*Xh2);

% Fraction: Scat (cations)
dScat = 0;

% Fraction: San (Anions)
dSan = 0;

% Fraction: Sva_ (Valerate)
dSva_ =      + (-1) * (kA_Bva*(Sva_*SH-Kava*(Sva-Sva_)));

% Fraction: Sbu_ (Butyrate)
dSbu_ =      + (-1) * (kA_Bbu*(Sbu_*SH-Kabu*(Sbu-Sbu_)));

% Fraction: Spro_ (propionate)
dSpro_ =      + (-1) * (kA_Bpro*(Spro_*SH-Kapro*(Spro-Spro_)));

% Fraction: Sac_ (acetate)
dSac_ =      + (-1) * (kA_Bac*(Sac_*SH-Kaac*(Sac-Sac_)));

% Fraction: Shco3 (bicarbonate)
dShco3 =      + (-1) * (kA_Bco2*(Shco3*SH-Kaco2*Sco2));

% Fraction: Snh3 (Ammonia)
dSnh3 =      + (-1) * (kA_Bin*(Snh3*SH-Kain*Snh4));

% Fraction: piSh2 (Partial pressure of Sh2)
dpiSh2 =      + (RT/(16/1000)) * ((klaH2)*(Sh2-
piSh2*(16/1000)/RT/(KH_H2))*V/Vgas) + (0-piSh2/pTOTAL) * (kp*(pTOTAL-
pext)*V/Vgas);

% Fraction: piSch4 (Partial pressure of Sch4)
dpiSch4 =      + (RT/(64/1000)) * ((klaCH4)*(Sch4-
piSch4*(64/1000)/RT/(KH_CH4))*V/Vgas) + (0-piSch4/pTOTAL) * (kp*(pTOTAL-
pext)*V/Vgas);

% Fraction: piSco2 (Partial pressure of Sco2)
dpiSco2 =      + (RT/(1/1000)) * ((klaCO2)*(Sco2-
piSco2*(1/1000)/RT/(KH_CO2))*V/Vgas) + (0-piSco2/pTOTAL) * (kp*(pTOTAL-
pext)*V/Vgas);

% Fraction: pTOTAL (Sum of all partial pressures)
dpTotal =      + (RT/(16/1000)) * ((klaH2)*(Sh2-
piSh2*(16/1000)/RT/(KH_H2))*V/Vgas) + (RT/(64/1000)) * ((klaCH4)*(Sch4-

```

```

piSch4*(64/1000)/RT/(KH_CH4))*V/Vgas) + (RT/(1/1000)) * ((klaCO2)*(Sco2-
piSco2*(1/1000)/RT/(KH_CO2))*V/Vgas) + (-1) * (kp*(pTOTAL-pext))*V/Vgas);

```

```

% differential equations need to be transferred to a vector;

```

```

% Fraction: Ssu (monosaccharides)
adm_dt(1) = dSsu;

```

```

% Fraction: Saa (amino acids)
adm_dt(2) = dSaa;

```

```

% Fraction: Sfa (total LCFA)
adm_dt(3) =dSfa;

```

```

% Fraction: Sva (valeric acid + valerate)
adm_dt(4) = dSva;

```

```

% Fraction: Sbu (butyric acid +butyrate)
adm_dt(5) = dSbu ;

```

```

% Fraction: Spro (propionic acid + propionate)
adm_dt(6) = dSpro ;

```

```

% Fraction: Sac (acetic acid + acetate)
adm_dt(7) = dSac ;

```

```

% Fraction: Sh2 (hydrogen)
adm_dt(8) = dSh2 ;

```

```

% Fraction: Sch4 (methane)
adm_dt(9) = dSch4;

```

```

% Fraction: Sco2 (carbon dioxide)
adm_dt(10 ) =dSco2;

```

```

% Fraction: Snh4 (Ammonium)
adm_dt(11) =dSnh4;

```

```

% Fraction: SI (soluble inerts)
adm_dt(12) =dSI;

```

```

% Fraction: Xc (composite)
adm_dt(13) =dXc;

```

```

% Fraction: Xch (carbohydrates)
adm_dt(14) =dXch;

```

```

% Fraction: Xpr (proteins)
adm_dt(15) =dXpr;

```

```

% Fraction: Xli(lipds)
adm_dt(16) = dXli;

```

```

% Fraction: Xsu (Biomass Sugar degraders)
adm_dt(17) = dXsu;

```

```

% Fraction: Xaa (Biomass amino acids degraders)

```

```

adm_dt(18) = dXaa;

% Fraction: Xfa (Biomass LCFA degraders)
adm_dt(19) = dXfa;

% Fraction: Xc4 (Biomass valerate, butyrate degraders)
adm_dt(20) = dXc4;

% Fraction: Xpro (Biomass propionate degraders)
adm_dt(21) = dXpro;

% Fraction: Xac (Biomass acetate degraders)
adm_dt(22) = dXac ;

% Fraction: Xh2 (Biomass hydrogen degraders)
adm_dt(23) = dXh2;

% Fraction: XI (particulate inerts)
adm_dt(24) = dXI;

% Fraction: Xp (Particulate products arising from biomass decay)
adm_dt(25) = dXp;

% Fraction: Scat (cations)
adm_dt(26) = dScat;

% Fraction: San (Anions)
adm_dt(27) = dSan;

% Fraction: Sva_ (Valerate)
adm_dt(28) = dSva_;

% Fraction: Sbu_ (Butyrate)
adm_dt(29) = dSbu_;

% Fraction: Spro_ (propionate)
adm_dt(30) = dSpro_ ;

% Fraction: Sac_ (acetate)
adm_dt(31) = dSac_ ;

% Fraction: Shco3 (bicarbonate)
adm_dt(32) = dShco3 ;

% Fraction: Snh3 (Ammonia)
adm_dt(33) = dSnh3 ;

% Fraction: piSh2 (Partial pressure of Sh2)
adm_dt(34) = dpiSh2;

% Fraction: piSch4 (Partial pressure of Sch4)
adm_dt(35) = dpiSch4;

% Fraction: piSco2 (Partial pressure of Sco2)
adm_dt(36) = dpiSco2;

% Fraction: pTOTAL (Sum of all partial pressures)

```

```

adm_dt(37) = dpTotal;

    %transpose adm_dt so it is a column vector
adm_dt= adm_dt';

qgas(end+1) = Qgas;

return

```

#### D. File initializing the optimization tool:

```

clear all;
global CumData;
global ZeitSpanne;
global kminvalue;
global kmaxvalue;
global AdjustmentMin;
global AdjustmentMax;
global WeightFactor;

reader = xlsread('expdata');
ZeitSpanne = reader(:,1)';
CumData = reader(:,2);
WeightFactor = reader(:,3);

kminvalue = 0.001;
kmaxvalue = 11;
AdjustmentMin = 0.1;
AdjustmentMax = 1;

KK(1) = 1.4283;
KK(2) = 0.8385;
KK(3) = 0.0138;
KK(4) = 0.0021;

```

#### E. Optimization tool, which starts init\_myadm.m file

```

function fehler = optimierer(KK)
    global CumData;
    global ZeitSpanne;
    global kminvalue;
    global kmaxvalue;
    global AdjustmentMin;
    global AdjustmentMax;
    global WeightFactor;

    for j=1:length(KK-1)
        if ((KK(j) > kmaxvalue))
            fehler = 1e10;
            return;
        end
        if ((KK(j) < kminvalue))
            fehler = 1e10;
            return;
        end
    end
    erg = init_myadm(KK);

```

```

fehler = 0;
for t = 1:length(ZeitSpanne)
    fehler = fehler+(abs(CumData(t)-erg(t,2))*WeightFactor(t));
end

```

- F. Code starting the ADM1xp normally (not in the optimization mode) via `init_myadm.m`, during the determination of the CHC's and individual  $k_{Dis}$  and giving the starting values for the kinetic constants for disintegration and hydrolysis phases ( $KK$ ). Additionally required here are values for composite fraction ( $X_C$ ), composition of the composite fraction (lipids, carbohydrates, and proteins content), together with dimensions of the reactor.

```

%clear all;

global ZeitSpanne;
global CumData;
reader = xlsread('expdata');
reader2 = xlsread('inputdata');

ZeitSpanne = reader(:,1)';
CumData = reader(:,6);

KD = 10.1197;
KK(1) = 0.554;
KK(2) = 0.1592;
KK(3) = 0.0089;
Xc = reader2 (1,5);
Ch = reader2 (2,5);
Pr = reader2 (3,5);
Li = reader2 (4,5);
VL = 500; %dimension of the reactor: liquid phase
VG = 600; %dimension of the reactor: vapour phase

gas = init_myadm(KK,KD,Xc,Ch,Pr,Li,VL,VG);

```

- G. This part is modified file is modified version of the `init_myadm.m`, which delivers the general data (and fractions for the main m.file: `myadm_ode.m`)

```

function cumgas = init_myadm(KK,KD,Xc,Ch,Pr,Li,VL,VG)
%clear all;
clear t;
clear Xo;
clear X;
clear qgas;
global qgas;
global kdis;           %disintegration rate    1/d
global khyd_ch;       %Hydrolysis rate carbohydrates 1/d
global khyd_pr;       %hydrolysis rate propionate 1/d
global khyd_li;       %hydrolysis rate lipids 1/d
global ZeitSpanne;

```

```

global Chh;
global Prr;
global Lii;
global CumData;
%global Xc;

% General Datat (global)
global T;
global pext;
global V;
global Vgas;
global kp;
global RT;
global NQ;
global pH;
global Kw;

% Transfer Optimization Data
kdis      = KD;           %disintegration rate 1/d
khyd_ch   = KK(1);       %Hydrolysis rate carbohydrates 1/d
khyd_pr   = KK(2);       %hydrolysis rate propionate 1/d
khyd_li   = KK(3);       %hydrolysis rate lipids 1/d
Chh = Ch;
Prr = Pr;
Lii = Li;
% MyAdjustment = KinKonstanten(5);
% Transfer Optimization Data end

Xo = zeros(1,33);

% General Data
T = 37;           %Temperatur in °C
pext = 1.04 ; %external total pressure in bar
V = VL;          %Tank volume liquid phase (m3)
Vgas = VG;       %Gas volume in tank (m3)
kp = 10000;      % Proportional control constant in m3/(m3*d)
RT = 8.314510 * 1E-5* (273.15+T); % in bar * m^3/ mol
NQ = 100000/(8.3145 * 273.15); % Norm cubic meter in mol/m3
pH = 7;
% General data end;

% Initialization
gas = 0;
ch4 = 0;
h2= 0;
co2 = 0;

% Initialization end

% Fractions
Xo(1) = 0.012;           %Suu, monosaccharides kg COD/m3
Xo(2) = 0.0053;         %Saa, amino acids kg COD/m3
Xo(3) = 0.1;           %Sfa, total LCFA kg COD/m3
Xo(4) = 0.01;          %Sva , valeric acid + valerate kg COD/m3
Xo(5) = 0.014;         %Sbu , butyric acid +butyrate kg COD/m3
Xo(6) = 0.0168;        %Spro , propionic acid + propionate kg COD/m3
Xo(7) = 0.1785;        %Sac , acetic acid + acetate kg COD/m3
Xo(8) = 0.24E-07;      %Sh2,hydrogen kg COD/m3
Xo(9) = 0.048;         %Sch4,methane kg COD/m3
Xo(10) = 0.09;         %carbon dioxide k mole C/m3

```

```

Xo(11) = 0.17013; %Snh4, Ammonium k mol N/m3
Xo(12) = 5.53; %SI soluble inerts kg COD/m3
Xo(13) = Xc; %Xc, composite kg COD/m3
Xo(14) = 0.055307; %Xch, carbohydrates kg COD/m3
Xo(15) = 0.055; %Xpr, proteins kg COD/m3
Xo(16) = 0.083; %Xli, lipids kg COD/m3
Xo(17) = 0.855; %Xsu, Biomass Sugar degraders kg COD/m3
Xo(18) = 0.637; %Xaa, Biomass amino acids degraders kg COD/m3
Xo(19) = 0.67; %Xfa, Biomass LCFA degraders kg COD/m3
Xo(20) = 0.283;%Xc4, Biomass valerate, butyrate degraders kg COD/m3
Xo(21) = 0.13559; %Xpro, Biomass propionate degraders kg COD/m3
Xo(22) = 0.9; %Xac, Biomass acetate degraders kg COD/m3
Xo(23) = 0.43; %Xh2, Biomass hydrogen degraders kg COD/m3
Xo(24) = 45; %XI, particulate inerts kg COD/m3
Xo(25) = 10; %Xp, Particulate products arising from biomass decay
kg COD/m^3
Xo(26) = 0.039126; % Scat k mol/m3
Xo(27) = 0.178460; % San k mol/m3
Xo(28) = 0.01; %Sva_, valerate kg COD/m3
Xo(29) = 0.014; %Sbu_, Butyrate kg COD/m3
Xo(30) = 0.016; %Spro_, propionate kg COD/m3
Xo(31) = 0.177; %Sac_, acetate kg COD/m3
Xo(32) = 0.083; %Shco3, bicarbonate k mole C/m3
Xo(33) = 0.00378; %Snh3, Ammonia kmol N/m3
Xo(34) = 0; %h2, Partial pressure of Sh2 bar
Xo(35) = 0; %piSch4, Partial pressure of Sch4 bar
Xo(36) = 0; %piSco2 Partial pressure of Sco2 bar
Xo(37) = 1.0; %pTOTAL

% Fractions end

tspan = ZeitSpanne;
options = odeset('RelTol',1e-3,'AbsTol',1e-6);
%[t,X] = ode15s(@myadm_ode,tspan,Xo,Chh,Prr,Lii,options);
[t,X] = ode15s(@myadm_ode,tspan,Xo,options);

for z = 1:length(X(:,1))
    gas(end+1) = kp*(X(z,37)-pext)/RT/NQ*V;
    ch4(end+1) = (X(z,35)/X(z,37))*gas(length(gas));
    h2(end+1) = (X(z,34)/X(z,37))*gas(length(gas));
    co2(end+1) = (X(z,36)/X(z,37))*gas(length(gas));

end

ch4 = ch4';
h2 = h2';
co2 = co2';
ch4 = ch4(2:end);
h2 = h2(2:end);
co2 = co2(2:end);
rate = [t ch4 h2 co2];

% numerical integration
rch4 = cumtrapz(t,ch4);
rh2 = cumtrapz(t,h2);
rco2 = cumtrapz(t,co2);
rgesamt = rch4+rh2+rco2;
diffges = ch4+h2+co2;

```

```

%cumgas = [t rgesamt X];
%cumgas = [t diffges ch4 h2 co2 ];
cumgas = [t rgesamt];

```

```
return
```

## H. The main body of the ADM1, modified to determine the CHC.

```

function [adm_dt] = myadm_ode(t,fractions)

global qgas;

% General Datat (global)
global T;
global pext;
global V;
global Vgas;
global kp;
global RT;
global NQ;
global pH;
global Kw;

% Kinetic constants are declared as global variables and defined in the
% calling function

global kdis;           %disintegration rate 1/d
global khyd_ch;       %Hydrolysis rate carbohydrates 1/d
global khyd_pr;       %hydrolysis rate propionate 1/d
global khyd_li;       %hydrolysis rate lipids 1/d
global Chh;
global Prr;
global Lii;

Ssu = fractions(1); %monosaccarides kg COD/m3
Saa = fractions(2); %amino acids kg COD/m3
Sfa = fractions(3); %total LCFA kg COD/m3
Sva = fractions(4); %valeric acid + valerate kg COD/m3
Sbu = fractions(5); %butyric acid +butyrate kg COD/m3
Spro = fractions(6); %propionic acid + propionate kg COD/m3
Sac = fractions(7); %acetic acid + acetate kg COD/m3
Sh2 = fractions(8); %hydrogen kg COD/m3
Sch4 = fractions(9); %methane kg COD/m3
Sco2 = fractions(10); %carbon dioxide k mole C/m3
Snh4 = fractions(11); %Ammonium k mol N/m3
SI = fractions(12); %soluble inerts kg COD/m3
Xc = fractions(13); %composite kg COD/m3
Xch = fractions(14); %carbohydrates kg COD/m3
Xpr = fractions(15); %proteins kg COD/m3
Xli = fractions(16); %lipids kg COD/m3
Xsu = fractions(17); %Biomass Sugar degraders kg COD/m3
Xaa = fractions(18); %Biomass amino acids degraders kg COD/m3
Xfa = fractions(19); %Biomass LCFA degraders kg COD/m3
Xc4 = fractions(20); %Biomass valerate, butyrate degraders kg COD/m3
Xpro = fractions(21); %Biomass propionate degraders kg COD/m3
Xac = fractions(22); %Biomass acetate degraders kg COD/m3
Xh2 = fractions(23); %Biomass hydrogen degraders kg COD/m3
XI = fractions(24); %particulate inerts kg COD/m3

```

```

Xp = fractions(25); %Particulate products arising from biomass decay
kg COD/m^3
Scat = fractions(26); %cations k mol/m3
San = fractions(27); %Anions k mol/m3
Sva_ = fractions(28); %valerate kg COD/m3
Sbu_ = fractions(29); %Butyrate kg COD/m3
Spr_ = fractions(30); %propionate kg COD/m3
Sac_ = fractions(31); %acetate kg COD/m3
Shco3 = fractions(32); %bicarbonate k mole C/m3
Snh3= fractions(33); %Ammonia kmol N/m3
piSh2 = fractions(34); %Partial pressure of Sh2 bar
piSch4= fractions(35); %Partial pressure of Sch4 bar
piSco2= fractions(36); %Partial pressure of Sco2 bar
pTOTAL= fractions(37); %Sum of all partial pressures bar

% Define Parameters (parameters which can be found in the parameter file
% read by simba
% needs to be changed for each substrate !
% includes as well the parameters for optimization

fSI_XC= 0.1; %fraction SI from XC -
dummy_fXI_XC = 0.210; %- -
fCH_XC = Chh; %fraction Xch from XC -
fPR_XC = Prr;
fLI_XC = Lii; %fraction Xli from XC -
(...)

```

The rest of the code myadm\_ode.m is unchanged.

#### I. File initializing the optimization tool, modified for CHC determination:

```

clear all;
global ZeitSpanne;
global kminvalue;
global kmaxvalue;
global KD;
global KD1;
global KD2;
global KD3;
global KD4;
global KD5;
global KD6;
global KD7;
global reader;
global reader2;

reader = xlsread('expdata');
reader2 = xlsread('inputdata');
ZeitSpanne = reader(:,1)';

kminvalue = 0.001;
kmaxvalue = 11;

KD = 0.4;
KK(1) = 0.25;
KK(2) = 0.2;
KK(3) = 0.1;

options = optimset('TolFun',1e-6,'Display','iter','MaxIter',25);

```

```
erg = fminsearch(@optimierer,KK,options);
```

#### J. Modified optimization tool for CHC determination, which starts init\_myadm.m file:

```
function globalfehler = optimierer(KK,KD)
    global ZeitSpanne;
    global kminvalue;
    global kmaxvalue;
    global blad;
    global KD;
    global reader;
    global reader2;
    global KD1;
    global KD2;
    global KD3;
    global KD4;
    global KD5;
    global KD6;
    global KD7;

    for j=1:length(KK-1)
        if ((KK(j) > kmaxvalue))
            globalfehler = 1e10;
            return;
        end
        if ((KK(j) < kminvalue))
            globalfehler = 1e10;
            return;
        end
    end

options = optimset('TolFun',1e-6,'Display','iter','MaxIter',15);
erg2 = fminsearch(@optimiererA,KD,options);
function fehler = optimiererA(KD)

CumData1 = reader(:,2);
Xc = reader2 (1,1);
Ch = reader2(2,1);
Pr = reader2(3,1);
Li = reader2(4,1);
VL = 500;
VG = 600;
for j=1:length(KD-1)
    if ((KD(j) > kmaxvalue))
        fehler = 1e10;
        return;
    end

    if ((KD(j) < kminvalue))
        fehler = 1e10;
        return;
    end

end

erg2 = init_myadm(KK,KD,Xc,Ch,Pr,Li,VL,VG);
fehler = 0;

for t = 1:length(ZeitSpanne)
    fehler = fehler+(abs(CumData1(t)-erg2(t,2)));
```

```

end

blad1 = fehler;
KD1=KD;
end

options = optimset('TolFun',1e-6,'Display','iter','MaxIter',15);
erg3 = fminsearch(@optimiererB,KD,options);
function fehler = optimiererB(KD)

CumData2 = reader(:,3);
Xc = reader2 (1,2);
Ch = reader2(2,2);
Pr = reader2(3,2);
Li = reader2(4,2);
VL = 500;
VG = 600;

for j=1:length(KD-1)
if ((KD(j) > kmaxvalue))
fehler = 1e10;
return;
end

if ((KD(j) < kminvalue))
fehler = 1e10;
return;
end

end

erg3 = init_myadm(KK,KD,Xc,Ch,Pr,Li,VL,VG);
fehler = 0;
for t = 1:length(ZeitSpanne)
fehler = fehler+(abs(CumData2(t)-erg3(t,2)));
end

blad2 = fehler;
KD2=KD;

end

options = optimset('TolFun',1e-6,'Display','iter','MaxIter',15);
erg4 = fminsearch(@optimiererC,KD,options);
function fehler = optimiererC(KD)

CumData3 = reader(:,4);
Xc = reader2 (1,3);
Ch = reader2(2,3);
Pr = reader2(3,3);
Li = reader2(4,3);
VL = 500;
VG = 600;
for j=1:length(KD-1)
if ((KD(j) > kmaxvalue))
fehler = 1e10;
return;

end

if ((KD(j) < kminvalue))

```

```

fehler = 1e10;
return;
end

end

erg4 = init_myadm(KK,KD,Xc,Ch,Pr,Li,VL,VG);
fehler = 0;
for t = 1:length(ZeitSpanne)
fehler = fehler+(abs(CumData3(t)-erg4(t,2)));
end

blad3 = fehler;
KD3=KD;

end

options = optimset('TolFun',1e-6,'Display','iter','MaxIter',15);
erg5 = fminsearch(@optimiererD,KD,options);
function fehler = optimiererD(KD)
CumData4 = reader(:,5);
Xc = reader2(1,4);
Ch = reader2(2,4);
Pr = reader2(3,4);
Li = reader2(4,4);
VL = 500;
VG = 600;

for j=1:length(KD-1)
if ((KD(j) > kmaxvalue))
fehler = 1e10;
return;

end

if ((KD(j) < kminvalue))
fehler = 1e10;
return;
end

end

erg5 = init_myadm(KK,KD,Xc,Ch,Pr,Li,VL,VG);
fehler = 0;
for t = 1:length(ZeitSpanne)
fehler = fehler+(abs(CumData4(t)-erg5(t,2)));

end

blad4 = fehler;
KD4=KD;
end

options = optimset('TolFun',1e-6,'Display','iter','MaxIter',15);
erg6 = fminsearch(@optimiererE,KD,options);
function fehler = optimiererE(KD)
CumData5 = reader(:,6);
Xc = reader2(1,5);
Ch = reader2(2,5);
Pr = reader2(3,5);

```

```

Li = reader2(4,5);
VL = 500;
VG = 600;
for j=1:length(KD-1)
if ((KD(j) > kmaxvalue))
fehler = 1e10;
return;

end

if ((KD(j) < kminvalue))
fehler = 1e10;
return;
end

end

erg6 = init_myadm(KK,KD,Xc,Ch,Pr,Li,VL,VG);
fehler = 0;
for t = 1:length(ZeitSpanne)
fehler = fehler+(abs(CumData5(t)-erg6(t,2)));
end

blad5 = fehler;
KD5=KD;
options = optimset('TolFun',1e-6,'Display','iter','MaxIter',15);
erg7 = fminsearch(@optimiererF,KD,options);
function fehler = optimiererF(KD)
CumData6 = reader(:,7);
Xc = reader2 (1,6);
Ch = reader2(2,6);
Pr = reader2(3,6);
Li = reader2(4,6);
VL = 500;
VG = 600;
for j=1:length(KD-1)
if ((KD(j) > kmaxvalue))
fehler = 1e10;
return;

end

if ((KD(j) < kminvalue))
fehler = 1e10;
return;
end

end

erg7 = init_myadm(KK,KD,Xc,Ch,Pr,Li,VL,VG);
fehler = 0;
for t = 1:length(ZeitSpanne)
fehler = fehler+(abs(CumData6(t)-erg7(t,2)));

end

blad6 = fehler;
KD6=KD;

end

```

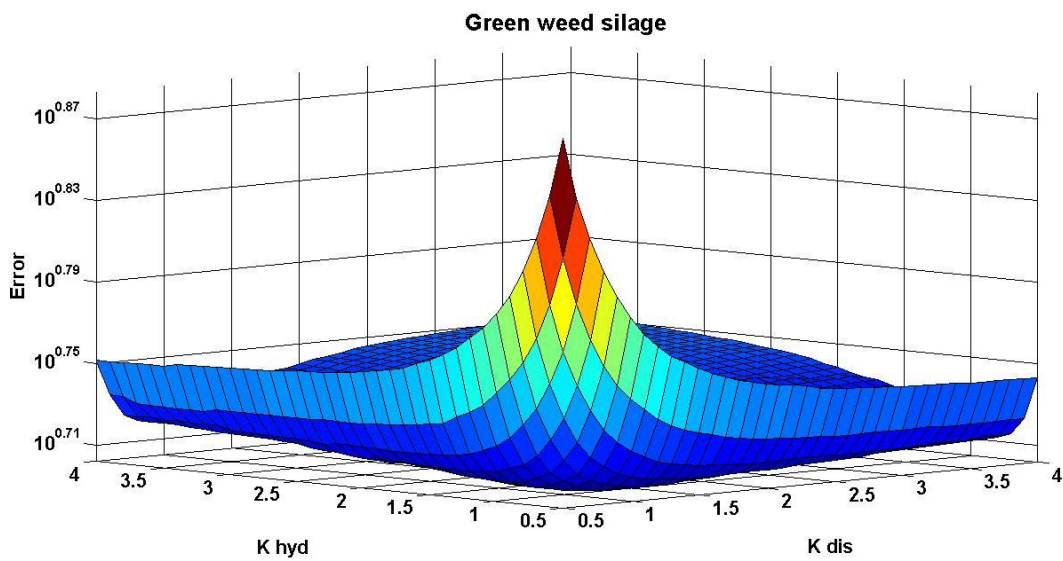
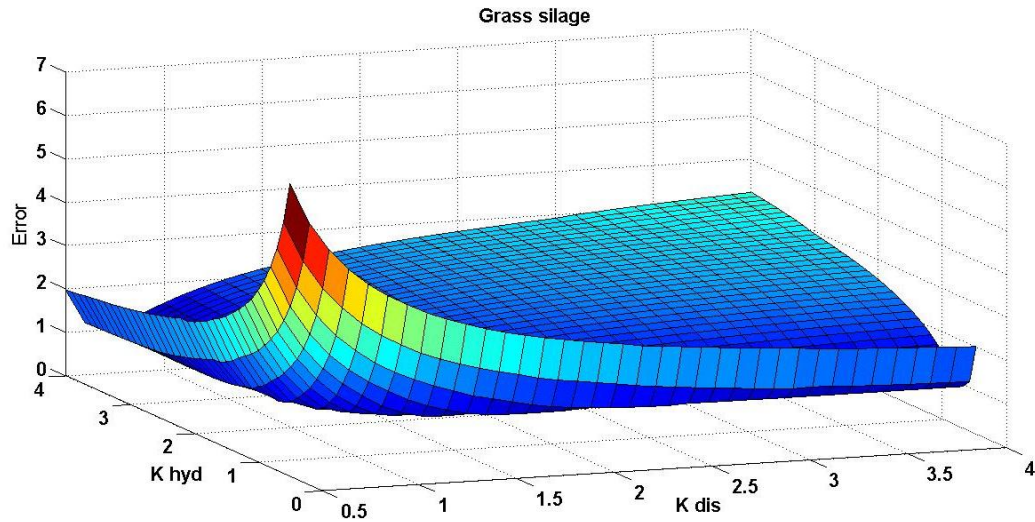
```

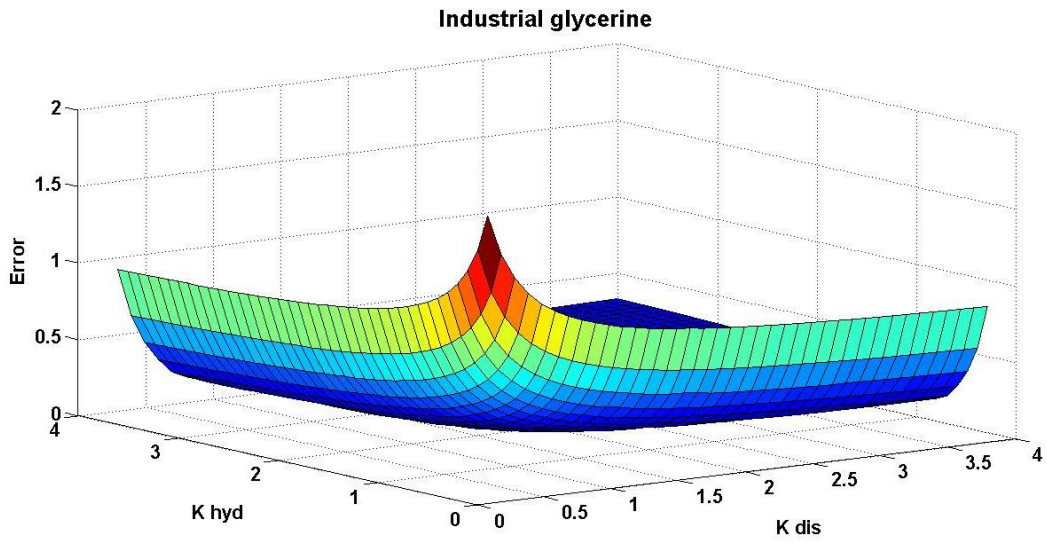
options = optimset('TolFun',1e-6,'Display','iter','MaxIter',15);
erg8 = fminsearch(@optimiererG,KD,options);
function fehler = optimiererG(KD)
CumData7 = reader(:,8);
Xc = reader2(1,7);
Ch = reader2(2,7);
Pr = reader2(3,7);
Li = reader2(4,7);
VL = 500;
VG = 600;
for j=1:length(KD-1)
if ((KD(j) > kmaxvalue))
fehler = 1e10;
return;
end
if ((KD(j) < kminvalue))
fehler = 1e10;
return;
end
end
erg8 = init_myadm(KK,KD,Xc,Ch,Pr,Li,VL,VG);
fehler = 0;
for t = 1:length(ZeitSpanne)
fehler = fehler+(abs(CumData7(t)-erg8(t,2)));
end
blad7 = fehler;
KD7=KD;
end
for t = 1:length(ZeitSpanne)
globalfehler = blad1+blad2+blad3+blad4+blad5+blad6+blad7;
end
end

```

#### 9.4. Appendix D

Disintegration ( $k_{dis}$ ) and hydrolysis ( $k_{hyd}$ ) kinetic constants sensitivity analysis for grass silage, green weed silage and industrial glycerine, where the lowest error represents the best correlation between simulated and experimental results.





Name Piotr Biernacki  
 E-Mail Piotr.Biernacki@hs-emden-leer.de  
 Geburtsdatum 20.05.1985  
 Geburtsort Breslau (Wroclaw), Polen  
 Nationalität Polnisch  
 Familienstand verheiratet



## Bildung

**Seit IV 2014 Carl von Ossietzky Universität Oldenburg**  
*Fakultät* V – Mathematik und Naturwissenschaften  
*Institut* Institut für Chemie  
*Abschluss* Promotion (Dr. rer. nat)

**X 2009 – VII 2010 Universität Breslau von Umwelt- und Biowissenschaften, Polen**  
*Studiengang* Gesundheit und Sicherheit-Verwaltung  
*Abschluss* Aufbau-Studium

**IX 2007 – XI 2008 De Montfort University, Leicester, Großbritannien**  
*Studiengang* MSc. Umwelttechnik und Management  
*Abschluss* MSc. mit Auszeichnung

**X 2003 – X 2008 Technische Universität Breslau, Polen**  
*(Politechnikwa Wroclawska)*  
*Studiengang* Umwelttechnik/ Umweltschutz  
*Abschluss* Master in Ingenieurwesen

## Erfahrung

**Seit X 2013 Hochschule Emden/Leer (Technologietransfer)**  
 Gründungs-Koordinator

**IX 2010 – X 2013 Hochschule Emden/Leer (EUTEC Institute)**  
 Wissenschaftlichen Mitarbeiter BMBF Projekt:  
 „Öko-effiziente Herstellung von Biomethan“

**XI 2008 – VIII 2010 Hewlett Packard Global e-Business Operations (Breslau, Polen)**  
 Marketing-Abteilung  
 Marketing fonds analyst und Marketing intelligence analyst  
 erfolgreich Kaizen Projekt ( für ISO 9001)

**VII 2007 KGHM PM S.A. Tailings Management Division (Rudna, Polen)**  
 Praktikum: Abfallwirtschaft

**VII 2006 Stadt Klodzko, Polen**  
 Praktikum: Kläranlage, Wasserversorgung Netzwerk, Trinkwasser